Department of Mineral and Petroleum Resources

RECORD 2001/9

ARCHAEAN GEOLOGY OF THE EAST PILBARA GRANITE–GREENSTONE TERRANE WESTERN AUSTRALIA — A FIELD GUIDE

by M. J. Van Kranendonk, A. H. Hickman, I. R. Williams, and W. Nijman

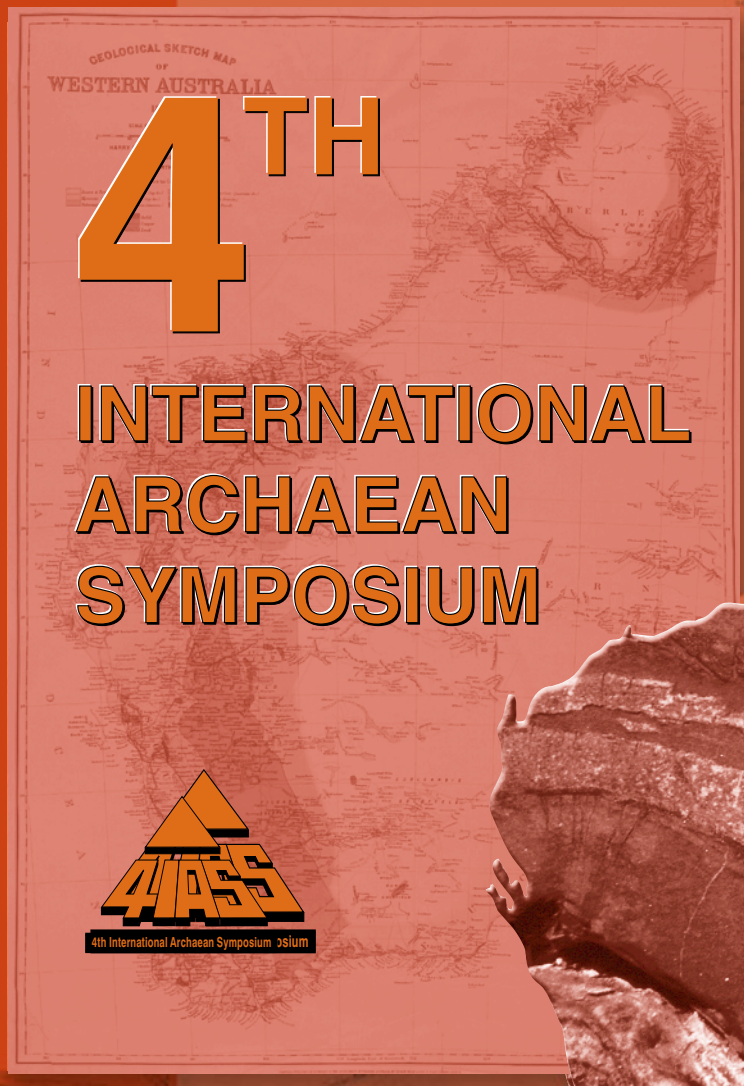

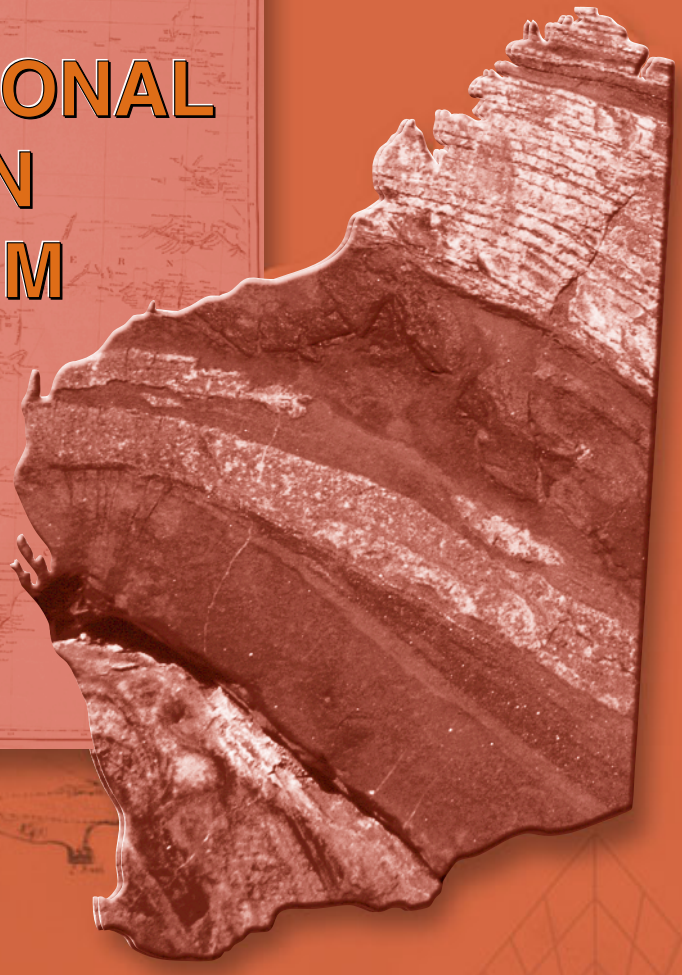

Geological Survey of Western Australia

GEOLOGICAL SURVEY OF WESTERN AUSTRALIA

Record 2001/9

ARCHAEAN GEOLOGY OF THE EAST PILBARA GRANITE–GREENSTONE TERRANE, WESTERN AUSTRALIA — A FIELD GUIDE

by

M. J. Van Kranendonk[1], A. H. Hickman[1], I. R. Williams[1], and W. Nijman[2]

[1] Geological Survey of Western Australia
[2] University of Utrecht, The Netherlands

Perth 2001

MINISTER FOR STATE DEVELOPMENT
The Hon. Clive Brown MLA

DIRECTOR GENERAL
DEPARTMENT OF MINERAL AND PETROLEUM RESOURCES
Jim Limerick

DIRECTOR, GEOLOGICAL SURVEY OF WESTERN AUSTRALIA
Tim Griffin

Notice to users of this guide:
This field guide is one of a series published by the Geological Survey of Western Australia (GSWA) for excursions conducted as part of the 4th International Archaean Symposium, held in Perth on 24–28 September 2001. Authorship of these guides included contributors from AGSO, CSIRO, tertiary academic institutions, and mineral exploration companies, as well as GSWA. Editing of manuscripts was restricted to bringing them into GSWA house style. The scientific content of each guide, and the drafting of the figures, was the responsibility of the authors.

REFERENCE
The recommended reference for this publication is:
VAN KRANENDONK, M. J., HICKMAN, A. H., WILLIAMS, I. R., and NIJMAN, W., 2001, Archaean geology of the East Pilbara Granite–Greenstone Terrane, Western Australia — a field guide: Western Australia Geological Survey, Record 2001/9, 134p.

National Library of Australia Card Number and ISBN 0 7307 5697 1

Grid references in this publication refer to either the Geocentric Datum of Australia 1994 (GDA94), with locations referenced using Map Grid Australia (MGA) coordinates, Zones 50 and 51, or the Australian Geodetic Datum 1984 (AGD84), with locations referenced using Australian Map Grid (AMG) coordinates, Zones 50 and 51. All locations are quoted to at least the nearest 100 m.

Printed by Optima Digital Copy, Perth, Western Australia

Published 2001 by Geological Survey of Western Australia

Copies available from:
Information Centre
Department of Mineral and Petroleum Resources
100 Plain Street
EAST PERTH, WESTERN AUSTRALIA 6004
Telephone: (08) 9222 3459 Facsimile: (08) 9222 3444
This and other publications of the Geological Survey of Western Australia are available online through dme.bookshop at www.dme.wa.gov.au

Contents

Plates

Figures

Tables

Record 2001/9
East Pilbara Excursion

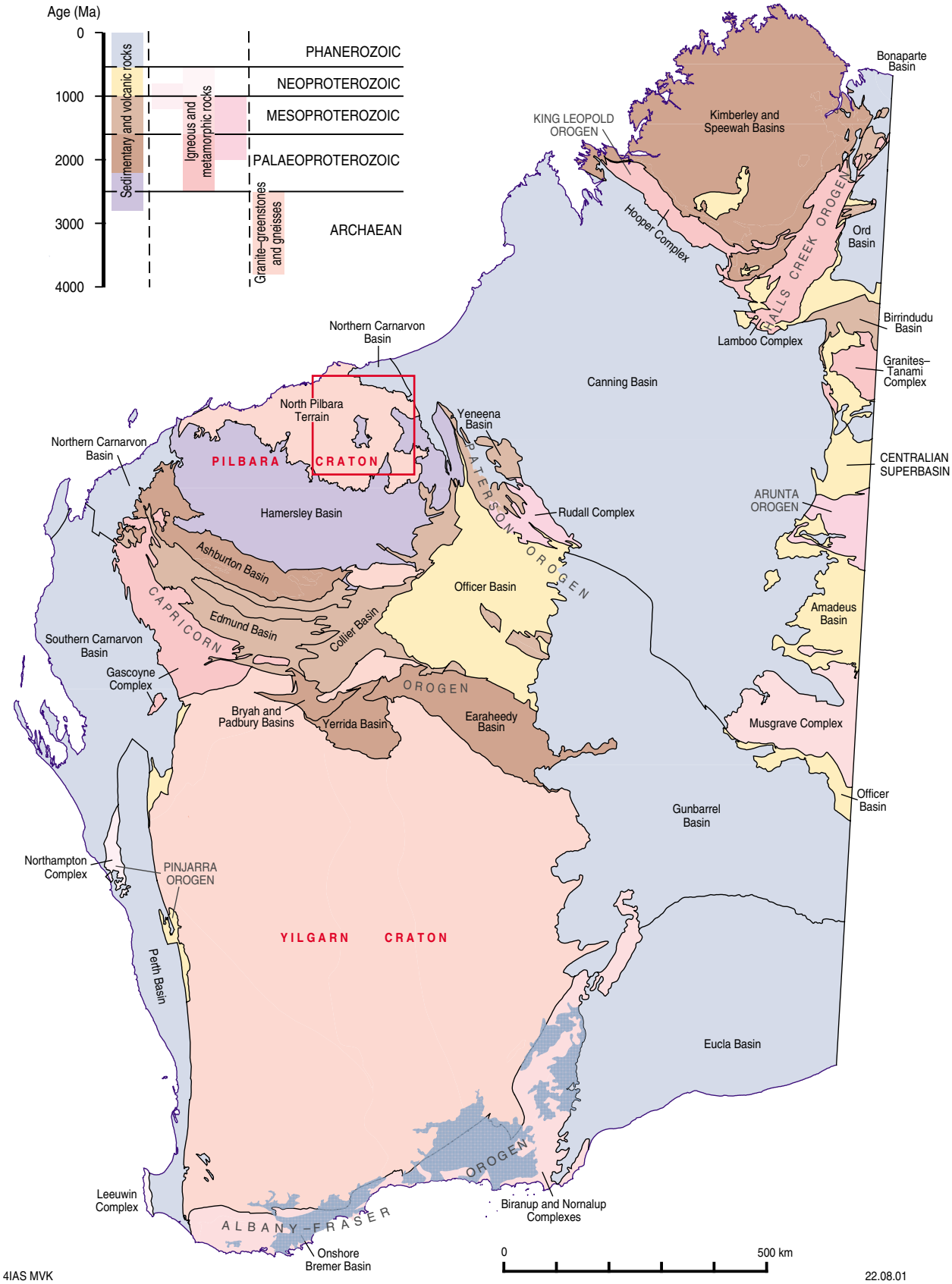

Archaean geology of the East Pilbara Granite–Greenstone Terrane, Western Australia — a field guide

by

M. J. Van Kranendonk[1], A. H. Hickman[1], I. R. Williams[1], and W. Nijman[2]

Introduction

In the 11 years since the Third International Archaean Symposium in 1990, a significant amount of new geological mapping and associated geochronology, geochemistry, geophysics, metallogeny, and isotopic analyses have been undertaken in the Archaean granite–greenstone basement rocks of the North Pilbara Terrain of the Pilbara Craton of Western Australia (see **Terminology** below). The research has been conducted by various groups, including mineral exploration companies, the University of Western Australia, the University of Utrecht in the Netherlands, the University of Newcastle in New South Wales, and the Geological Survey of Western Australia (GSWA) in conjunction with the Australian Geological Survey Organisation (AGSO) as part of a National Geoscience Mapping Accord (NGMA) project established in 1994.

The result is a much more detailed understanding of greenstone stratigraphy and the component elements of granitoid complexes. Geochronological studies in the East Pilbara Granite–Greenstone Terrane have provided more than 117 high-precision sensitive high-resolution ion microprobe (SHRIMP) and conventional U–Pb dates on zircon and baddeleyite, in addition to dozens of Ar–Ar and Pb–Pb dates. The new age data alone have greatly increased our knowledge of the age and distribution of volcanic and plutonic events, and the timing of deformation and mineralization events, compared with what was known in 1990, and has led to numerous refinements of previous models. Thus it is timely to present a review of the geology of the terrain and an excursion through some of the oldest, best preserved rocks on Earth.

Terminology

The Pilbara Craton in the northwestern part of Western Australia is an ovoid area, covering about 600 × 400 km, comprising a crystalline basement of late to early Archaean granitoid rocks and greenstones (3720–2850 Ma) overlain by a weakly deformed and metamorphosed, 2775–2450 Ma cover succession of volcanic and sedimentary rocks known as the Mount Bruce Supergroup, deposited in the Hamersley Basin (Griffin, 1990; inset of Fig. 1). The basement rocks outcrop as inliers, the largest of which is in the northern part of the craton. This area was previously referred to as either the 'Pilbara Block' (Hickman, 1983) or the 'North Pilbara granite–greenstone

[1] Geological Survey of Western Australia
[2] Institute of Earth Sciences, University of Utrecht, The Netherlands

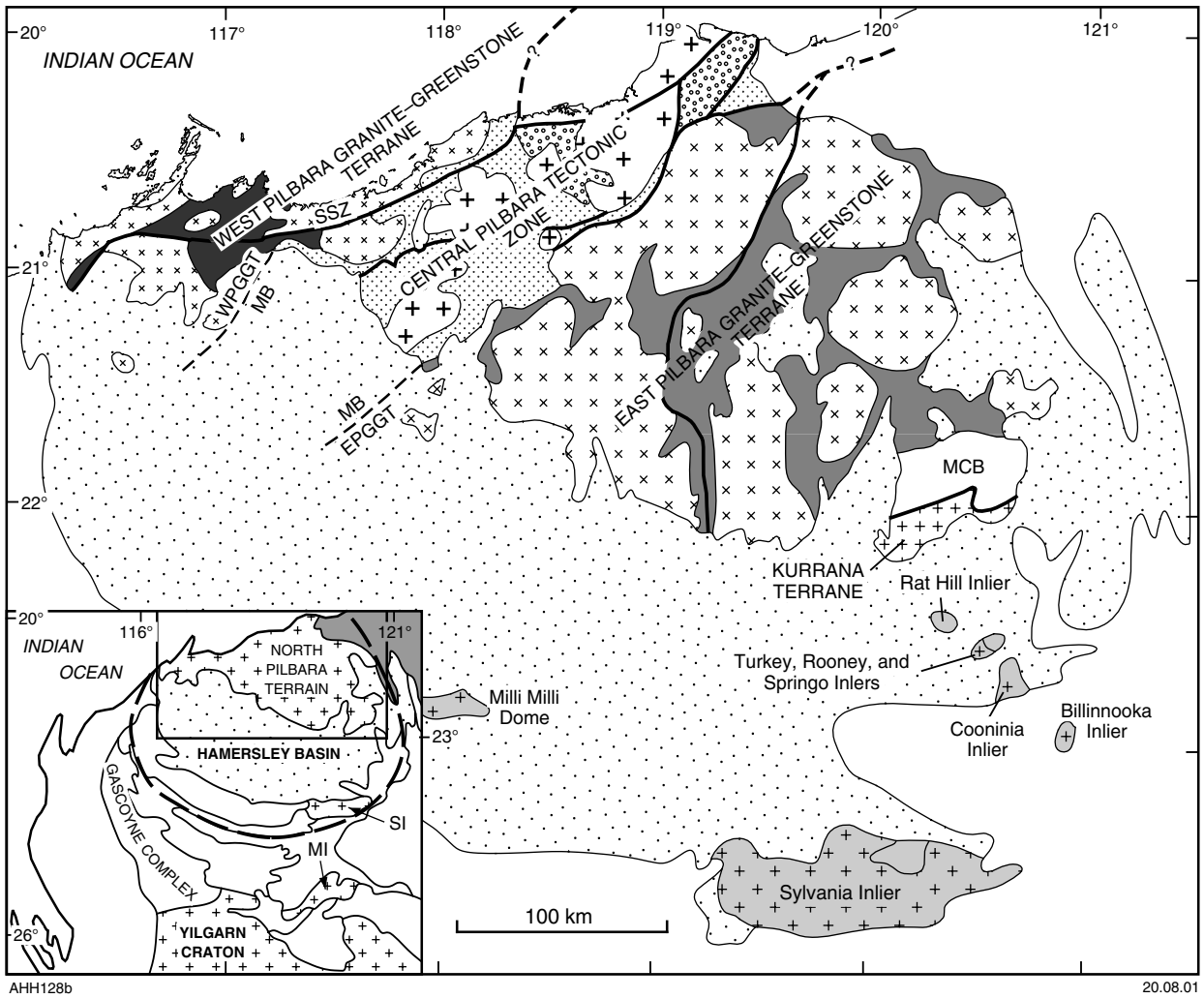

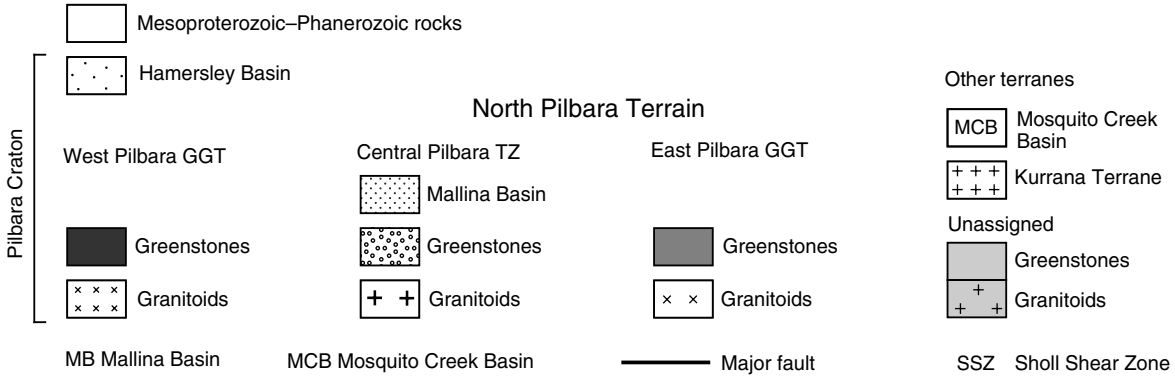

Figure 1. Regional geological setting of the East Pilbara Granite–Greenstone Terrane within the Pilbara Craton. Inset shows the position of the Pilbara Craton in Western Australia (heavy dashed line)

terrane' (Griffin, 1990), but new data from the NGMA project indicates that it is composed of three granite–greenstone terranes, each with a distinct stratigraphy and unique geochronological and structural histories, that are separated by sedimentary basins formed in active tectonic zones. As a result, the exposed basement area in the northern part of the Pilbara Craton is here referred to as the North Pilbara Terrain*, and is subdivided into five lithotectonic elements (Fig. 1; Van Kranendonk et al., in prep.):

1. The East Pilbara Granite–Greenstone Terrane (EPGGT) represents the ancient nucleus of the Pilbara Craton, with primary crust formation between c. 3515 and 3240 Ma. It was built on remnants of older sialic crust as old as 3720 Ma, and affected by successive events to 2850 Ma.
2. The c. 3280–2920 Ma West Pilbara Granite–Greenstone Terrane (WPGGT) is described in the accompanying excursion guide GSWA Record 2001/16 by Hickman et al. (2001).
3. The intervening, c. 3010–2940 Ma Mallina Basin includes a dominantly volcanic succession on the western margin (including the Whim Creek and Bookingarra Groups) and a dominantly clastic sedimentary succession in the remainder of the basin (Constantine Sandstone and Mallina Formation of the De Grey Group), which were deposited during three pulses of intracontinental rifting and intruded by granitoid rocks and deformed at c. 2950–2930 Ma (Hickman et al., 2001).
4. The Kurrana Terrane is present in the far southeast, but very little is known about it (Tyler et al., 1992).
5. The undated Mosquito Creek Basin, between the Kurrana Terrane and the EPGGT, consists of dominantly clastic sedimentary rocks deposited between c. 3310 and 2850 Ma.

Comprehensive overviews of the geology of the North Pilbara Terrain can be found in Hickman (1983, 1984, 1990). Alternative interpretations are presented by Krapez (1993), Krapez and Eisenlohr (1998), and Blewett (2000). The detailed summary of the geology of the East Pilbara Granite–Greenstone Terrane, which is the focus of this excursion guidebook, is based on a recent summary of the North Pilbara Terrain by Van Kranendonk et al. (in prep.). This summary is largely based on mapping, geochronology, geophysics, and geochemistry undertaken since 1994 as part of the NGMA project, but additional information has been obtained from published and unpublished data that are referenced throughout the text. The evolution of the Mount Bruce Supergroup is outside the scope of this summary, but detailed studies have been undertaken by Blake (1993) and Thorne and Trendall (2001). It must be stressed that the tectonic models presented herein are the result of work in progress, and will be tested through further studies based on mapping and geochronology conducted through to 2003.

Previous interpretations of the rocks of the North Pilbara Terrain

The recent increase in data has spawned numerous tectonic models for the North Pilbara Terrain that, as with the debate on Archaean tectonics in general (e.g. de Wit, 1998, vs Hamilton, 1998), are divided into two end-member views: those viewing deformation as the result of so-called 'vertical tectonics' or partial convective overturn of the crust driven by granitoid diapirism, versus those invoking modern plate-tectonic analogues, including the generation of magmatic arcs through subduction processes, and horizontal compression due to terrane accretion and plate convergence. These models are reviewed and discussed in detail, following an overview of the geology of the EPGGT.

* In this Record, 'terrain' refers to a geographical area, whereas 'terrane' is used to indicate a distinct geological element.

Based on reconnaissance geological mapping during the 1970s, Hickman (1975, 1983, 1984) provided a regional lithostratigraphic interpretation of the 'Pilbara Block' as a single granite–greenstone terrain with a regionally coherent greenstone stratigraphy and with deformation as the result of essentially solid-state granitoid diapirism. Without precise geochronology, stratigraphic correlations between greenstone belts were supported by either physical continuity or by similarity of lithological successions. This led to the conclusions that (a) a relatively uniform lithostratigraphic succession is present in greenstone belts of the east Pilbara, and (b) the lower, dominantly volcanic part of the greenstone succession (Warrawoona Group) in the east Pilbara is also preserved in the west. Subsequent geochronology has shown that the second conclusion was incorrect (Horwitz and Pidgeon, 1993; Hickman, 1997; Nelson, 1997, 1998; Smith et al., 1998), and that greenstones of the EPGGT are more laterally variable than previously envisaged (Vearncombe et al., 1995; Morant, 1998; Van Kranendonk and Morant, 1998; Williams, 1999).

During the 1980s, individual research projects in parts of the EPGGT resulted in differing interpretations of stratigraphy and structural geology. Objections to the regional lithostratigraphic interpretation arose as a result of locally observed lateral stratigraphic variations (Barley, 1981), and from interpretations of structural duplication due to horizontal tectonics (Bickle et al., 1985; Boulter et al., 1987). Since these early studies, the operation of horizontal tectonics in various parts of the North Pilbara Terrain has been advocated by several workers (Ohta et al., 1996; Zegers et al., 1996; Kiyokawa and Taira, 1998; van Haaften and White, 1998). Several other studies have documented evidence in support of diapiric evolution in the EPGGT (Collins, 1989; Collins et al., 1998; Van Kranendonk and Collins, in prep.), interrupted by a period of sinistral transpression at c. 2940 Ma (Van Kranendonk and Collins, 1998; Zegers et al., 1998).

Partly in response to the interpretations of horizontal tectonics, Horwitz and Krapez (1991) attempted to apply sequence stratigraphy to the greenstone successions of the North Pilbara Terrain. In a much more detailed account, Krapez (1993) interpreted that much of the stratigraphic succession has been tectonically repeated and intercalated, some units might be allochthonous, and several tectono-stratigraphic cycles might be present. He erected a sequence stratigraphic model based on the concept of global tectonic cycles, and then attempted to fit observational and isotopic data into this model. The North Pilbara Terrain was divided into five tectono-stratigraphic domains separated by northeast-trending lineaments, following Krapez and Barley (1987). These lineaments were stated to 'form the dominant structural fabric of the Pilbara Block, and have a long history of development and reactivation'. Krapez (1993) concluded that lithostratigraphic correlation across such domain boundaries, or even between structural belts, had to be supported by precise radiometric dating.

Krapez and Eisenlohr (1998) further developed the sequence stratigraphic model, recognizing two 'Megacycle Sets' spanning 3500–2775 Ma, which they divided into four 'Megacycles' each of 190–175 m.y. duration. Each 'Megacycle' was inferred to contain a 'Megasequence', that could be divided into supersequences or basins. Krapez and Eisenlohr (1998) reiterated that the 'domain boundaries' had a long history of development and reactivation, but admitted that evidence for any pre-3000 Ma history was only 'cryptic, and related to interpreted stratigraphic patterns'. Van Kranendonk and Collins (1998) showed that the stratigraphy was continuous across one of the proposed domain boundaries in the EPGGT (Lalla Rookh strike-slip orogen of Eriksson et al., 1994) and that it represented a late zone of intracontinental transpression.

Smith et al. (1998) presented geochronological data in support of two lithotectonic domains within the WPGGT, separated by the sinistral Sholl Shear Zone. They used this data to develop a model of late Archaean continental growth involving the tectonic

accretion of outboard island arcs and other continental-scale fragments onto the EPGGT. Barley (1997) summarized the evolution of the Pilbara Craton in terms of westerly continental growth through accretion, based on the modern plate-tectonic style.

Results of the NGMA program have shown that previous interpretations for the whole of the North Pilbara Terrain, involving either craton-wide correlations of lithostratigraphy (Hickman, 1983) or a solely uniformitarian tectonic accretion model (e.g. Krapez, 1993; Barley, 1997), were not applicable. Instead, Van Kranendonk (1998a) suggested that the Pilbara Craton evolved through three stages, as follows:

- Stage 1 — construction of the east Pilbara crust from c. 3515 to 3400 Ma;
- Stage 2 — partial convective overturn of the east Pilbara crust from c. 3325 to 3240 Ma;
- Stage 3 — microplate and arc-accretion tectonics across the WPGGT from c. 3130 to 2940 Ma.

This theme was developed in more detail, and somewhat modified in relation to the WPGGT, by Van Kranendonk et al. (in prep.) who presented a three-stage history involving non-uniformitarian development of a crustal nucleus in the EPGGT from >3700 to c. 3350 Ma (see **Early Archaean tectonic evolution**), followed by plume-generated rifting at c. 3320–3240 Ma (see **Middle Archaean tectonic evolution**), and the onset of microplate tectonics flanking the nucleus thereafter (see **Late Archaean tectonic evolution**).

East Pilbara Granite-Greenstone Terrane

Lithotectonic elements

The East Pilbara Granite–Greenstone Terrane is one of Earth's best exposed, most complete record of early to late Archaean crustal evolution. It is underlain by groups of well preserved volcanic and sedimentary rocks (greenstones) deposited between c. 3515 and 3240 Ma, in addition to younger, dominantly sedimentary, greenstone successions, and numerous suites of granitoid rocks varying in composition from trondhjemite through to monzogranite that were emplaced between c. 3576 and 2850 Ma (Fig. 2). The terrane is host to a variety of mineral deposit types and styles that have been exploited since the late nineteenth century, with gold being the most important commodity mined at the start of the twentieth century.

The EPGGT is characterized by large, ovoid (35–120 km-diameter) granitoid complexes (Griffin, 1990; formerly 'batholiths' of Hickman, 1983) flanked by curviplanar belts of commonly steeply dipping volcano-sedimentary rocks collectively referred to as greenstones (Fig. 2). Greenstones were deposited in five intrusion- or unconformity-bound groups over 575 m.y. from 3515 to 2940 Ma, with the bulk of crust having formed between c. 3490 and 3340 Ma during deposition of the dominantly mafic volcanic Warrawoona Group and intrusion of a synvolcanic tonalite–trondhjemite–granodiorite (TTG) sill complex. Final cratonization at c. 2850 Ma followed several intervening volcano-plutonic events, the details of which are outlined below.

The lithotectonic nomenclature used herein and displayed on Figure 2 modifies that used by Hickman (1983, insert on Plate 1) as discussed by Van Kranendonk (1998b). Hickman (1983, 1984) showed that granitoid complexes commonly formed domes, and greenstones formed synclinal belts. Van Kranendonk (1998b) noted that some greenstone belts were monoclines (e.g. Western Shaw greenstone belt, 11 on Fig. 2), and confirmed the existence of greenstone domes (e.g. Panorama greenstone belt of the North Pole Dome, 7 on Fig. 2; Fig. 3) previously recognized by Hickman (1975,

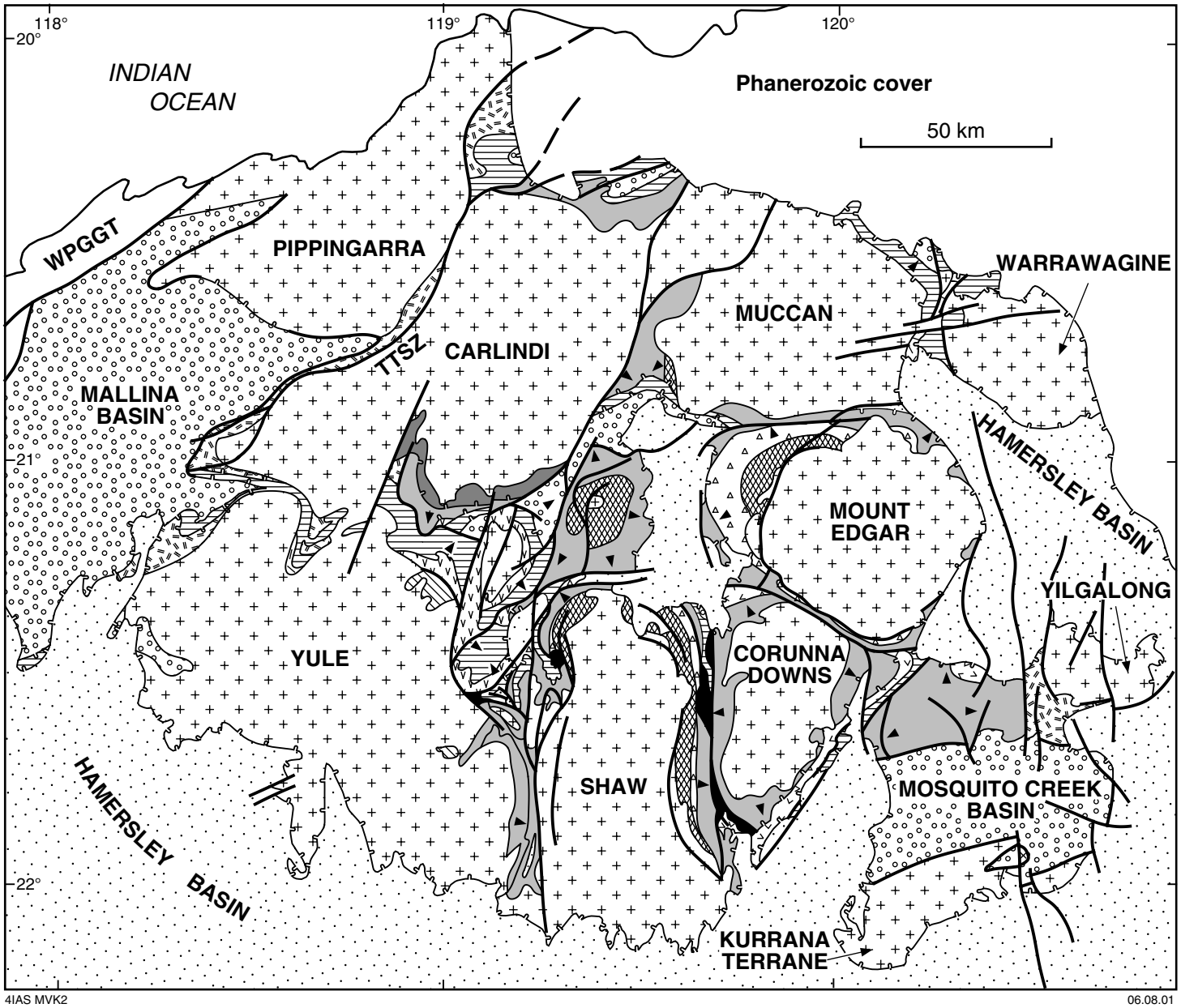
a)
118°
119°
120°
20°
21°
22°
INDIAN
OCEAN
Phanerozoic cover
50 km
WPGGT
PIPPINGARRA
WARRAWAGINE
MUCCAN
TTSZ
CARLINDI
MALLINA
BASIN
HAMERSLEY BASIN
MOUNT
EDGAR
YILGALONG
YULE
CORUNNA
DOWNS
SHAW
MOSQUITO CREEK
BASIN
HAMERSLEY BASIN
KURRANA
TERRANE
4IAS MVK2
06.08.01

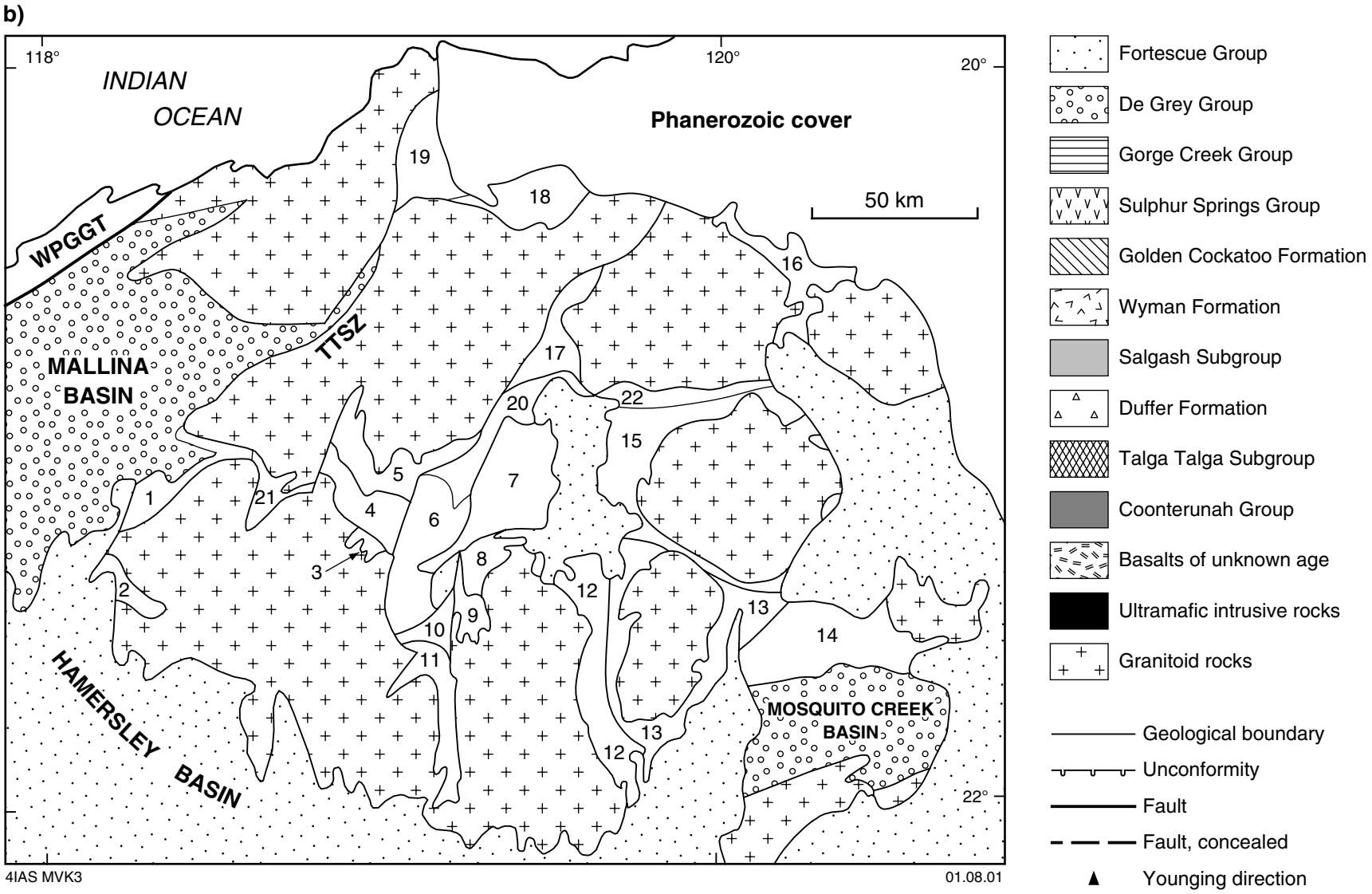

Figure 2. Simplified geological maps of the East Pilbara Granite–Greenstone Terrane: a) Granitoid complexes are labelled in bold upper case. WPGGT = West Pilbara Granite–Greenstone Terrane; TTSZ = Tabba Tabba Shear Zone; b) Greenstone belts are labelled as follows: 1. Pilbara Well, 2. Cheearra, 3. Abydos, 4. Pincunah, 5. East Strelley, 6. Soanesville, 7. Panorama, 8. North Shaw, 11. Western Shaw, 12. Coongan, 13. Kelly, 14. McPhee–Elsie, 15. Marble Bar, 16. Shay Gap, 17. Warralong, 18. Goldsworthy, 19. Ord Range, 20. Lalla Rookh, 21. Wodgina, 22. Doolena Gap. Greenstone complexes are labelled as follows: 9. Emerald Mine, 10. Tambina

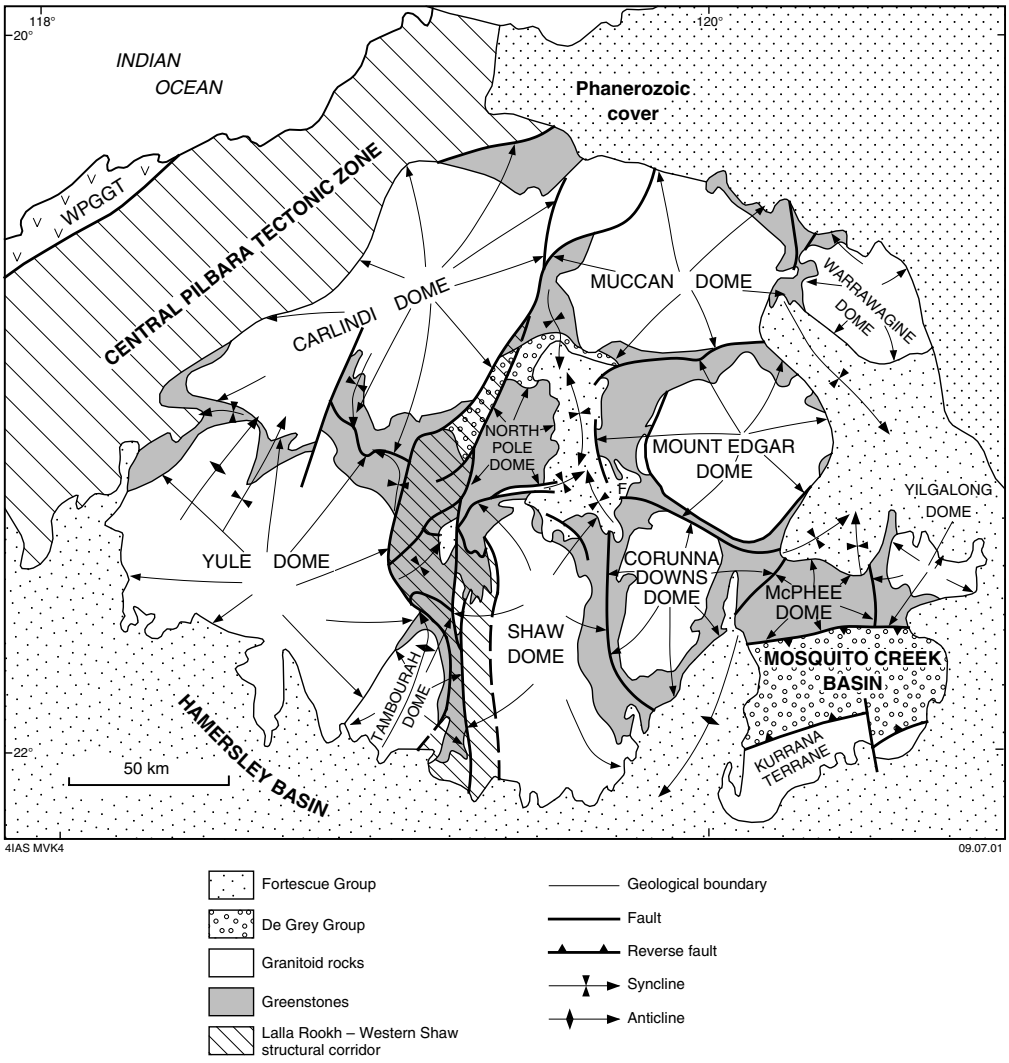

Figure 3. Schematic map of large-scale structures of the East Pilbara Granite–Greenstone Terrane. The named granitoid-cored domes formed throughout the development of the terrane. The sinistral transpressional Lalla Rookh – Western Shaw structural corridor formed at c. 2940 Ma as a result of compression across the Central Pilbara Tectonic Zone, and was coeval with deposition of the De Grey Group in the Lalla Rookh Synclinorium

1983). In the North Shaw area, Van Kranendonk (1998b) could not correlate the greenstone stratigraphy across the faulted axes of some synclines. As a result, he proposed that structural domes include both granitoid rocks and attached greenstones and showed that adjacent domes were separated by faults within greenstones that he referred to as ring faults (Fig. 3).

Van Kranendonk (1998b) defined greenstone belts as relatively well preserved tracts of commonly coherent greenstone stratigraphy bounded by faults, intrusive or sheared intrusive contacts (or both) with granitoid complexes, or unconformities with older supracrustal rocks and, locally, with granitoid rocks (e.g. Buick et al., 1995; Dawes et al., 1995). This terminology differs from that used by Hickman (1983) in which greenstone belts were commonly linear belts of greenstones bounded by granitoid contacts, regional unconformities, or major faults equivalent to domain boundaries. Greenstone complexes, as defined by Van Kranendonk (1998b), are areas of high structural complexity in which a coherent stratigraphy is commonly lacking and faulting or shearing (or both) is common.

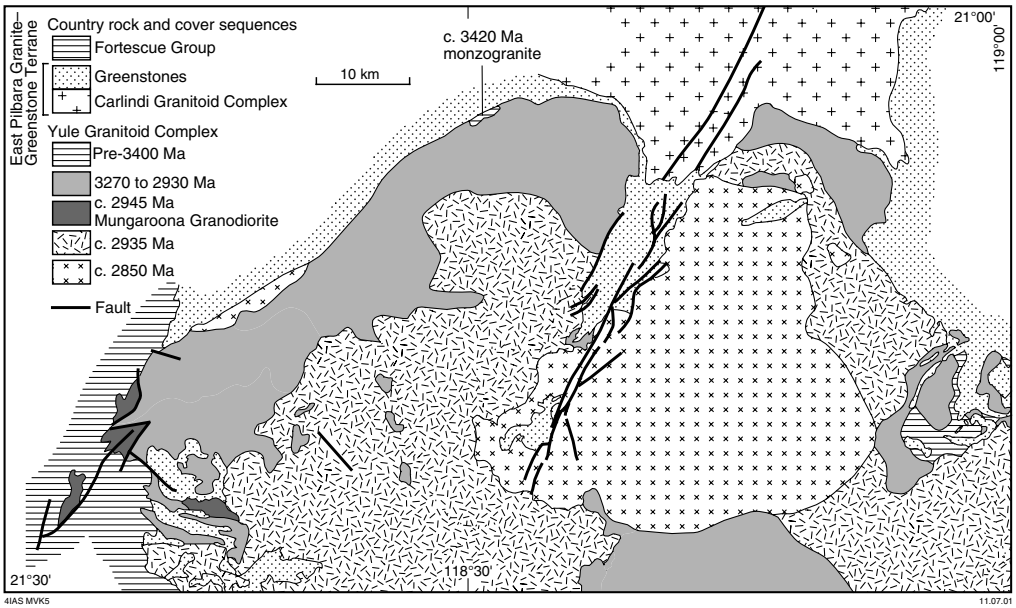

Figure 4. Geology of the northwestern part of the Yule Granitoid Complex, showing a typical example of how successive generations of granites were emplaced into the core of the granitoid complex, pushing older phases out to the margins (adapted from Champion and Smithies, 2000)

The domical granitoid complexes are multicomponent bodies that evolved parallel with deposition of felsic volcanic components of the greenstones (Hickman, 1984; Williams and Collins, 1990; Barley and Pickard, 1999). Similar-aged suites of plutonic rocks are present in many individual complexes. This, combined with structural and gravity data, suggests that the complexes link up at depth beneath intervening synclinal greenstone keels and thus represent structural domes of a continuous, mid-crustal granitoid layer (Hickman, 1984; Wellman, 2000). Early, more-sodic components (c. 3490–3410 Ma) were emplaced as a sheeted sill complex into the Warrawoona Group and older crustal remnants. They are preserved principally around the outer margins of granitoid complexes, pushed up and out by successive generations of more-potassic components that were emplaced into the cores of progressively amplifying domes at punctuated intervals throughout the history of the terrane, as exemplified by the Yule Granitoid Complex (Fig. 4).

Lithostratigraphy

The Pilbara Supergroup of the EPGGT is divided into five volcano-sedimentary groups and two additional formations that include, from base to top (Figs 2 and 5):

- the c. 3515 Ma Coonterunah Group;
- the c. 3490–3350 Ma Warrawoona Group;
- the c. 3325–3308 Ma Wyman Formation;
- the c. 3255–3235 Ma Sulphur Springs Group;
- the possibly diachronous Gorge Creek Group, part of which is c. 3235 Ma;
- the c. 3000–2940 Ma De Grey Group.

The undated Golden Cockatoo Formation is a local component of the succession preserved in the Yule Granitoid Complex and probably related to the Sulphur Springs Group.

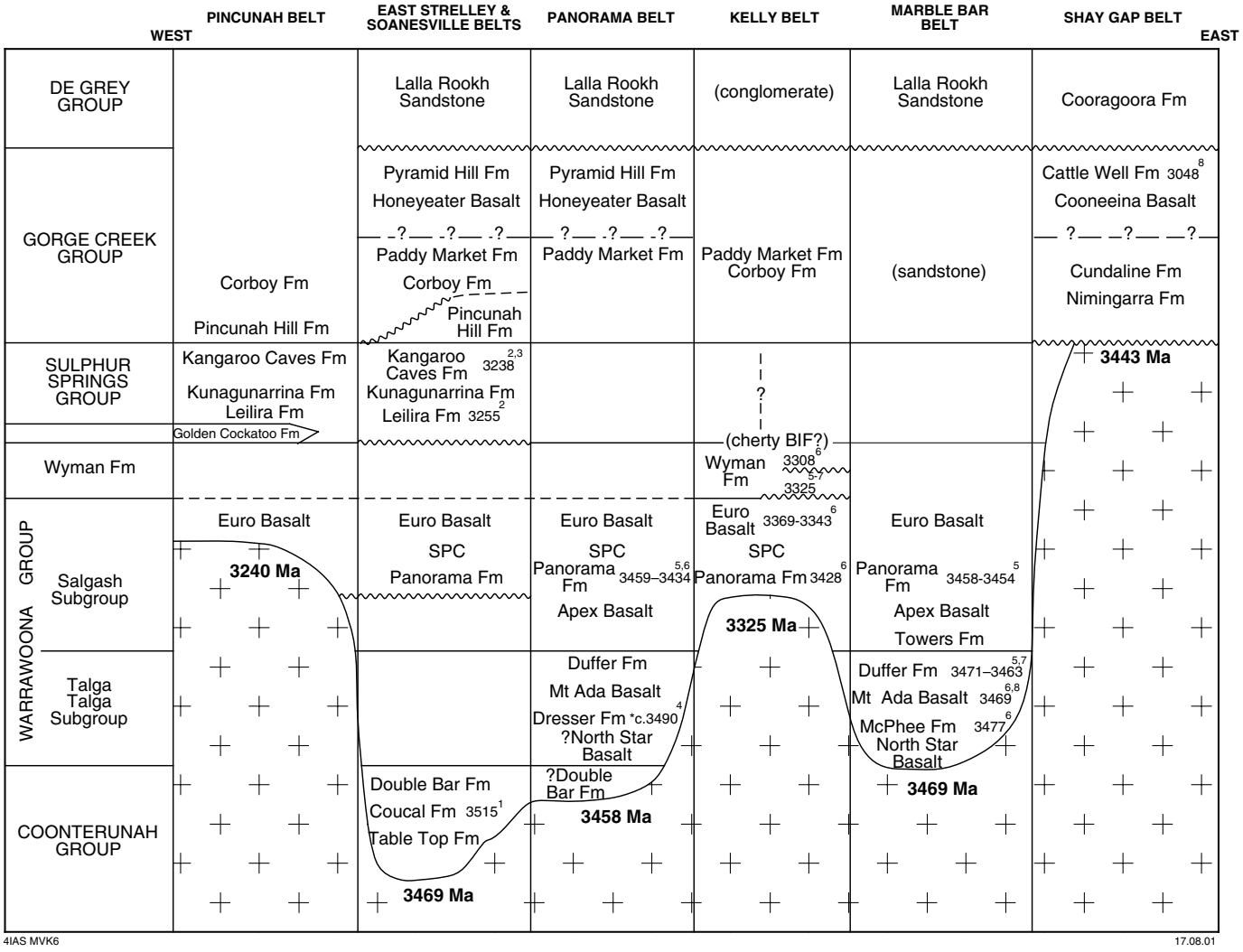

Figure 5. Schematic stratigraphic profiles of greenstone belts across the East Pilbara Granite–Greenstone Terrane. See Figure 2 for locations of greenstone belts (SPC = Strelley Pool Chert; Fm = Formation; BIF = banded iron-formation). Age data are U–Pb zircon ages except those labelled with a * which are Pb–Pb isochron ages on galena. Superscript numbers are references: 1. Buick et al. (1995); 2. Brauhart (1999); 3. Thorpe, R., 1999, Geological Survey of Canada, written comm.; 4. Thorpe et al. (1992b); 5. Thorpe et al. (1992a); 6. Nelson (1998); 7. Nelson (in prep.); 8. Nelson (1999)

Coonterunah Group

The Coonterunah Group (Buick et al., 1995; defined by Van Kranendonk and Morant, 1998; Van Kranendonk, 2000a) is a 5.9 km-thick succession of dominantly tholeiitic basalt and subordinate intermediate to felsic volcanic rocks distributed around the southern flank of, and intruded by, the Carlindi Granitoid Complex (Fig. 2). This group was identified on the basis of a local high-angle unconformity with the upper part of the Warrawoona Group and an 'old' age of 3515 ± 3 Ma (Buick et al., 1995). Two Ar–Ar dates of c. 3500 Ma on hornblende from amphibolite-facies metabasalts in the Panorama and Coongan greenstone belts (Davids et al., 1997; Zegers et al., 1999) suggest that the Coonterunah Group may be more widespread than presently recognized (Fig. 6). Geochemical data indicate significant contamination of Coonterunah Group basalts by older sialic crust, a conclusion that precludes their deposition in a mid-ocean ridge setting (Green et al., 2000).

Warrawoona Group

Hickman (1977, 1983, 1990) originally subdivided the lithostratigraphy of the Warrawoona Group into two major basaltic divisions: the lower Talga Talga Subgroup and the overlying Salgash Subgroup (Table 1). These were separated by the c. 3470 Ma felsic volcanic Duffer Formation and overlain by the c. 3325 Ma Wyman Formation, neither of which was included in the subgroups (age data from Thorpe et al., 1992a, and McNaughton et al., 1993). Thick units of layered chert from different greenstone belts were placed within the Towers Formation at the base of the Salgash Subgroup and used in craton-wide stratigraphic correlations (Hickman, 1983, 1990). Since then, additional geochronology and detailed mapping have shown the need for some changes to this scheme (Table 1).

Firstly, the basal part of the c. 3474–3463 Ma Duffer Formation is locally interbedded with, and the same age as, the upper part of the Mount Ada Basalt, indicating the need for inclusion of the Duffer Formation in the Talga Talga Subgroup (age data from Thorpe et al., 1992a; McNaughton et al., 1993; Nelson 1999, 2000, in prep.).

Secondly, geochronology since 1983 has established that various chert–basalt assemblages of the EPGGT, previously correlated as the Towers Formation (Hickman, 1983), instead belong to three separate, compositionally distinct units (Van Kranendonk, 2000a). The oldest of these is the stromatolitic chert–barite unit of the Dresser Formation in the Panorama greenstone belt, which may be as old as c. 3490 Ma (age from Thorpe et al., 1992b; stratigraphic nomenclature from Van Kranendonk and Morant, 1998). Slightly younger is the c. 3460 chert–basalt succession of the Towers Formation in the Marble Bar greenstone belt, which includes the Marble Bar Chert Member (Hickman, 1983). The youngest unit, at 3426 Ma, is the Strelley Pool Chert which is now recognized across most of the EPGGT (SPC in Fig. 5; name after Lowe, 1983 and Van Kranendonk and Morant, 1998; age data from Nelson, 1998, 2000, in prep.).

The type area of the Talga Talga Subgroup is in the Marble Bar greenstone belt, where several age dates show that it is a coherent, right-way-up succession, rather than a downward-younging tectonic assemblage as suggested by van Haaften and White (1998; Figs 5 and 7; Thorpe et al., 1992a; McNaughton et al., 1993; Nelson, 1999, 2000, in prep.; Van Kranendonk, 1999b, 2000b; Van Kranendonk et al., 2001). The basal contact of this subgroup is everywhere an intrusive one with synvolcanic or younger granitoid rocks. The Warrawoona Group has an average thickness of about 12 km in this area, with the bulk deposited over only about 25–30 m.y. at rates of accumulation comparable to that in modern oceanic plateaus.

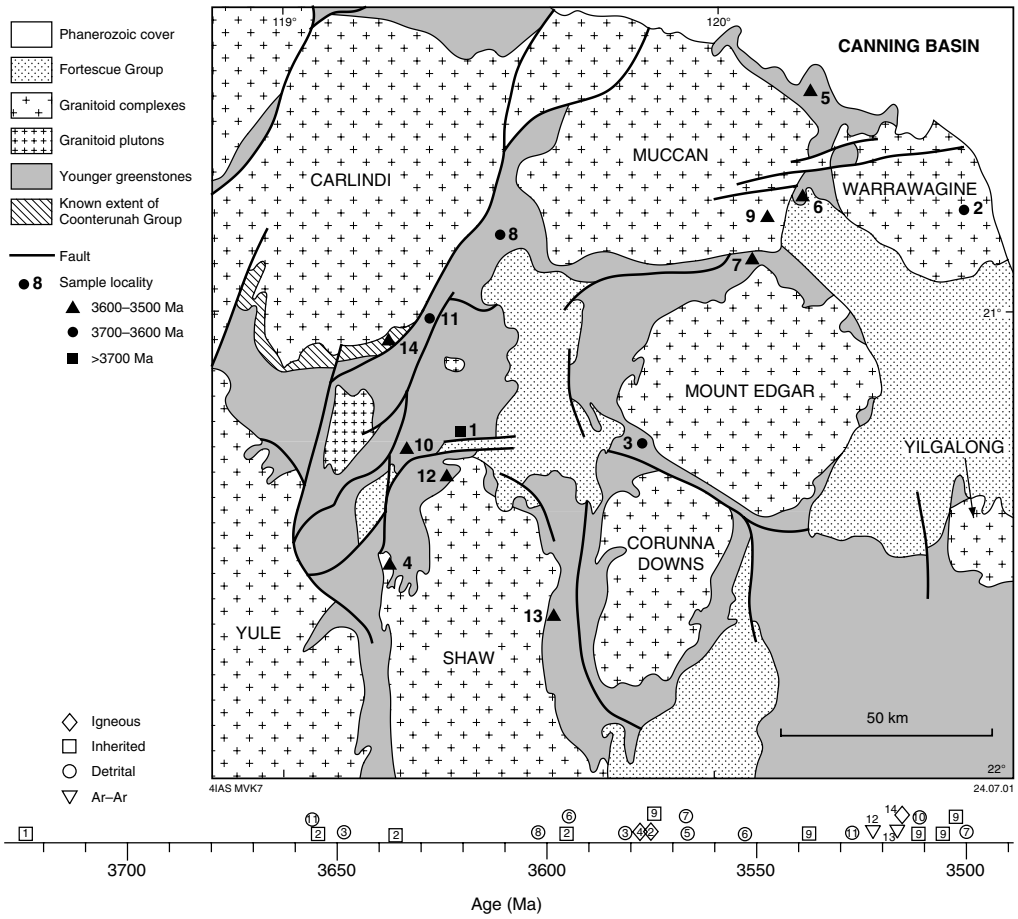

Figure 6. Location and time line of samples with U–Pb zircon evidence of ancient crust in the East Pilbara Granite–Greenstone Terrane. Numbers refer to sources: 1. Thorpe et al. (1992a); 2. Nelson (1999, sample 142870); 3. Collins, W. J., 1996, University of Newcastle (written comm.); 4. McNaughton et al. (1998); 5. Nelson (1998, sample 143996); 6. Nelson (1998, sample 143995); 7. Nelson (1998, sample 143994); 8. Nelson (1998, sample 142836); 9. Nelson (1998, sample 142828); 10. Buick et al. (1995, sample 94001); 11. Nelson (2000, sample 142951); 12. Zegers et al. (1999); 13. Davids et al. (1997); 14. Buick et al. (1995, sample 70601)

Table 1. Revised stratigraphic nomenclature of the Warrawoona Group

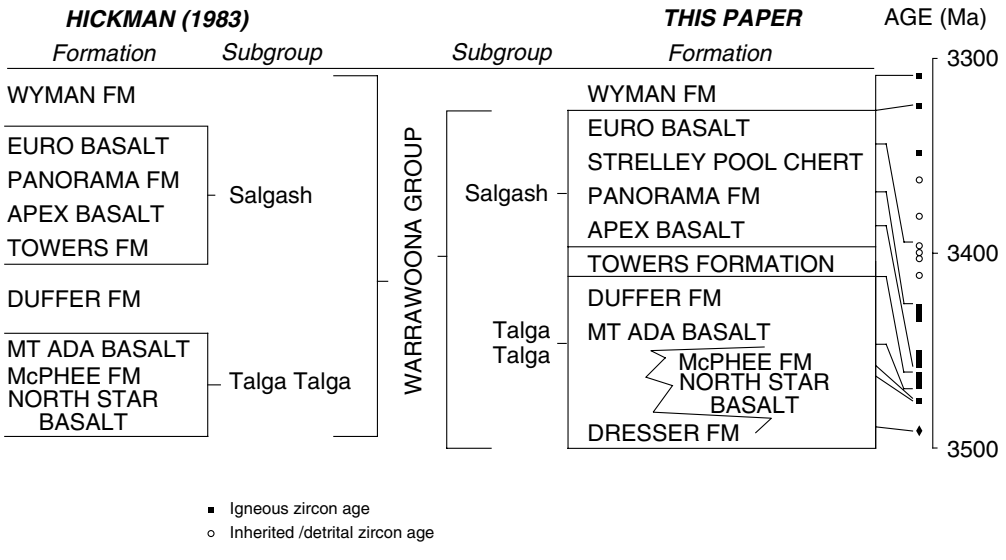

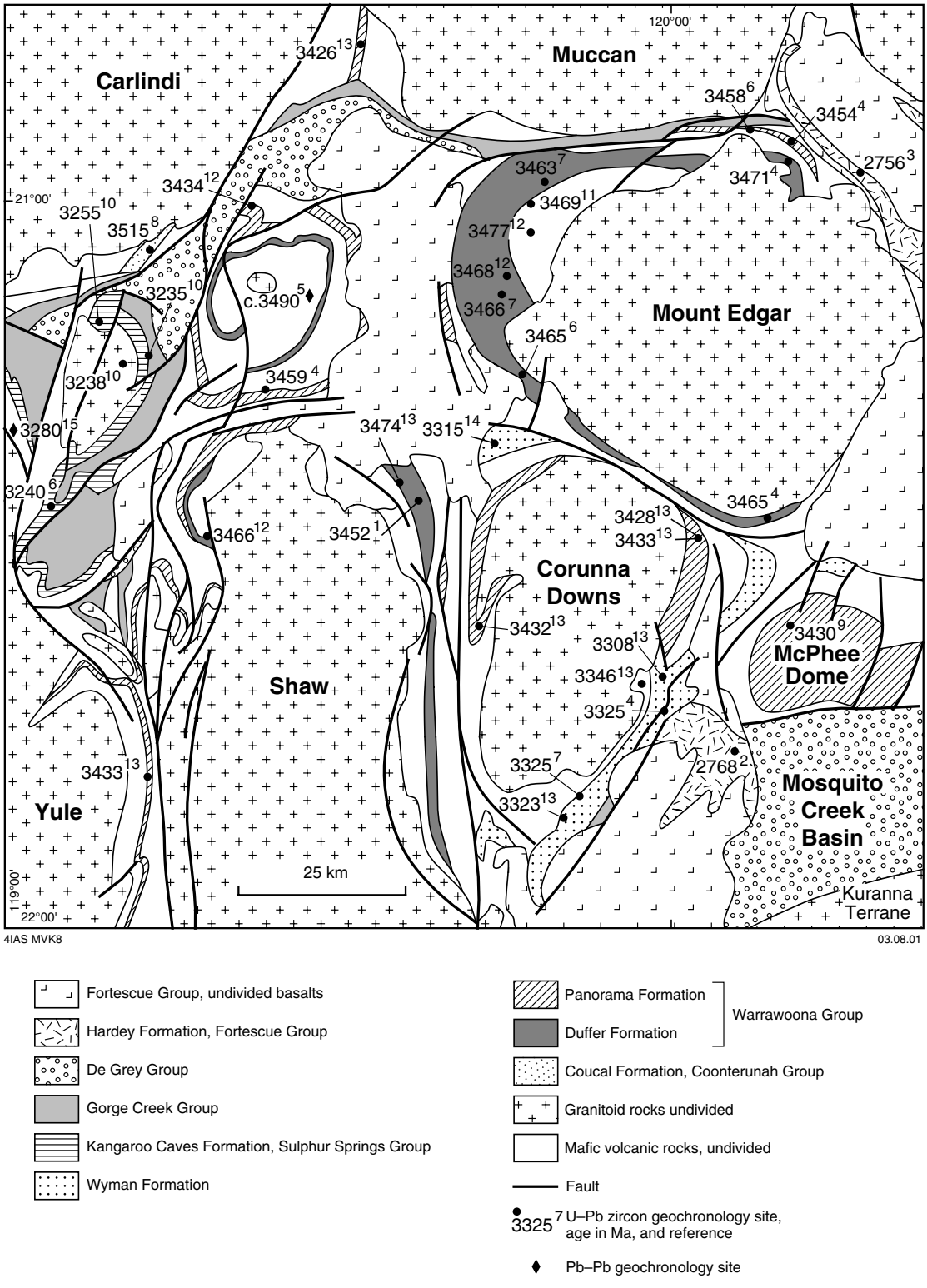

Figure 7. U–Pb zircon and Pb–Pb age data for felsic volcanic units across the East Pilbara Granite–Greenstone Terrane. Sources: 1. Pidgeon (1978); 2. Pidgeon (1984); 3. Arndt et al. (1991); 4. Thorpe et al. (1992a); 5. Thorpe et al. (1992b); 6. Thorpe, R., 1999, Geological Survey of Canada (written comm.); 7. McNaughton et al. (1993); 8. Buick et al. (1995); 9. Barley et al. (1998); 10. Brauhart (1999); 11. Nelson (1999); 12. Nelson (2000); 13. Nelson (in prep.); 14. Age cited in Barley and Pickard (1999); 15. Morant, P., 1998, Sipa Resources NL (written comm.)

In the Panorama greenstone belt, the lower part of the Talga Talga Subgroup includes the c. 3490 Ma Dresser Formation, a unit with up to five beds of stromatolitic, carbonate- and sulfate-bearing chert interbedded with pillow basalt (Nijman et al., 1998a, 1999a; Van Kranendonk, 2000a; age from Thorpe et al., 1992b). Although it was previously thought that these cherts were deposited through evaporative precipitation in a quiet marine environment (e.g. Groves et al., 1981; Buick and Dunlop, 1990), more recent studies have shown that they were deposited from hydrothermal fluids during lacco-caldera formation (Nijman et al., 1998a, 1999a; Van Kranendonk, in prep. a). It is unknown whether unnamed basaltic rocks beneath the Dresser Formation belong to the North Star Basalt, or if they correlate with the Coonterunah Group.

In the Marble Bar greenstone belt, Hickman (1983) defined the Towers Formation to include interbedded komatiitic basalt, pillowed tholeiitic basalt, and jaspilitic chert. These rocks lie immediately above the Duffer Formation and are interpreted to represent a transitional unit from the Talga Talga Subgroup to the Salgash Subgroup, with the Marble Bar Chert Member representing the last remnant activity of Duffer Formation felsic volcanism, and the komatiitic basalts representing the onset of ultramafic–mafic volcanism of the overlying Apex Basalt. In other areas, this transitional unit is absent and the Apex Basalt lies directly on the Duffer Formation (Williams, 1999). Locally, the Panorama Formation may lie directly on the Duffer Formation (DiMarco and Lowe, 1989; Van Kranendonk, 1999a), and this has recently been confirmed by geochronology in the Coongan greenstone belt (Nelson, D. R., 2001, written comm.).

The felsic volcanic Panorama Formation has now been identified in all greenstone belts across the EPGGT (Figs 5 and 7). It is a dominantly rhyolitic succession of massive, volcaniclastic rocks up to 1.5 km thick in its type area in the Panorama greenstone belt (DiMarco and Lowe, 1989; Van Kranendonk, 2000a), but varies along strike to volcaniclastic quartzite a few metres thick in some belts. Stratigraphic variations suggest that it was erupted from several volcanic sources, including the vent of the Panorama volcano that is exposed in cross section in the northern part of the Panorama greenstone belt, where synvolcanic carbonate degassing has been recognized (Van Kranendonk, 2000a, in prep. a). The formation has been dated at 3459–3452 Ma in the southern part of the Panorama greenstone belt and northern part of the Marble Bar greenstone belt, whereas elsewhere, rocks assigned to the upper part of the formation have been dated at 3434–3428 Ma (Figs 5 and 7; Thorpe et al., 1992a; Nelson, 1998, 2000, in prep.). Cullers et al. (1993) presented geochemical evidence that the lower part of the Panorama Formation was derived from melting of eclogite, in contrast to the Duffer Formation which was derived through fractional crystallization from basaltic parents.

The Strelley Pool Chert (Lowe, 1983) conformably overlies the Panorama Formation and contains distinctive stratigraphic elements that can be correlated across a distance of 130 km across most of the EPGGT (Fig. 5). The chert is commonly composed of a lower unit of pervasively silicified, stromatolitic carbonate–silica laminites, and an overlying unit of clastic sedimentary rocks (Lowe, 1983; Hoffman et al., 1999; Van Kranendonk, 2000a, in prep. b). Laminites in the North Pole Dome were deposited in shallow-water conditions from hydrothermal precipitates during the waning stages of Panorama Formation volcanism. The laminites were probably deposited in one or more alkaline caldera lakes that were fed by hot springs. Overlying clastic sedimentary rocks are interpreted to have been deposited during caldera collapse prior to the onset of renewed mafic volcanism (Van Kranendonk, 1999b, in prep. a,b). Although the chert has not been directly dated, epithermal gold mineralization dated at c. 3400 ± 10 Ma from the North Pole Dome (Thorpe et al., 1992b) probably formed from the same

hydrothermal system that deposited the chert. This age has also been obtained from zircon overgrowths and diatexite melt fractions in the Shaw Granitoid Complex (Zegers, 1996; Van Kranendonk, unpublished data) and from detrital zircons in some Gorge Creek Group sedimentary rocks (Nelson, 1998).

The Euro Basalt conformably overlies the Strelley Pool Chert or Panorama Formation across the EPGGT. It is a thick unit (up to 9.4 km in the southwestern extension of the Panorama greenstone belt; Van Kranendonk, 2000a) of dominantly basaltic volcanic rocks interbedded with numerous thin cherts. Typically, the Euro Basalt contains a basal unit, less than 3 km thick, of komatiitic basalt, which is overlain by tholeiitic basalt and interbedded komatiitic basalt (e.g. Glikson et al., 1986; Van Kranendonk and Hickman, 2000). Direct evidence for the age of the Euro Basalt is limited to zircon data from a silicified felsic tuff close to the top of the formation. Combined with detrital zircon populations in younger rocks, these data suggest essentially continuous deposition of the Euro Basalt from c. 3395 to 3346 Ma (Table 1; Nelson, 1998, 1999).

A characteristic and significant feature of the whole Warrawoona Group is the common presence of interflow chert beds at intervals from 100 to 1000 m. Buick and Barnes (1984) showed that the cherts represent a variety of silicified precursor lithologies (e.g. flowtop breccias, tuffs, carbonates). More recent work has shown that the silica was leached from underlying volcanic rocks by circulating hydrothermal fluids that were expelled onto the surface from swarms of conduits now represented by the chert dykes (Nijman et al., 1998a, 1999a; Brauhart, 1999; Van Kranendonk, in prep. a,b). This hydrothermal circulation resulted in pervasive hydrothermal alteration (argillic–phyllic and carbonate) of the underlying volcanic rocks (e.g. Glikson and Hickman, 1981; Van Kranendonk, in prep. a).

Wyman Formation

The 3325–3308 Ma, rhyolitic Wyman Formation is present in the Kelly greenstone belt around the coeval Corunna Downs Granitoid Complex, and is correlated with rhyolite in the northern part of the McPhee Dome (Figs 2, 5, and 7; Pidgeon, 1984; McNaughton et al., 1993; Barley and Pickard, 1999; Nelson, 2000, in prep.). This 500–1100 m-thick formation lies conformably on the Euro Basalt in the northwestern and northeastern parts of the belt, but rests unconformably on folded rocks of the Euro Basalt in the southeast. Thus, it is regarded as younger than the Warrawoona Group (Fig. 5; Hickman, 1983). The top of the formation is commonly defined by either a fault or an unconformity with younger rocks, but in the McPhee Dome, the top of the Wyman Formation includes stromatolitic chert fed by hydrothermal black chert.

Golden Cockatoo Formation

The Golden Cockatoo Formation is a highly folded sequence of amphibolite-facies quartzite, pelite, rhyolite, and banded iron-formation (BIF) that is found only within the northeastern part of the Yule Granitoid Complex (Figs 2 and 5; Van Kranendonk and Morant, 1998; Van Kranendonk, 1999a, 2000a, in prep. c). In the Abydos belt, these rocks are deformed into a small-scale dome-and-basin pattern and intruded by synkinematic granitoid rocks dated at c. 3240 Ma (M. Van Kranendonk, unpublished U–Pb SHRIMP data). In the small outlier to the south, preliminary mapping data suggests that these rocks were deposited unconformably on c. 3450 Ma orthogneiss. Although the age of these rocks is unknown, they are tentatively interpreted as a basal formation to the Sulphur Springs Group.

Sulphur Springs Group

The Sulphur Springs Group (Van Kranendonk and Morant, 1998; Van Kranendonk, 2000a) is a succession of dominantly volcanic rocks in the western part of the EPGGT (in the Soanesville, Pincunah, East Strelley, and Warralong greenstone belts), that may underlie much of the Pilbara Well belt (Fig. 2). The group was previously divided into four formations, but new map and geochemical data suggest that the lowermost Six Mile Creek Formation is part of the underlying Euro Basalt.

The Leilira Formation, herein defined as those rocks at the base of the Sulphur Springs Group, is composed of lithic wacke, felsic volcaniclastic sandstone, tuff, and dacite. It unconformably overlies the Euro Basalt in the southwestern extension of the Panorama belt and in the East Strelley belt (Fig. 2; Van Kranendonk, 1999a, 2000a). A maximum age for deposition of this formation is c. 3255 Ma, based on a SHRIMP age of detrital zircons (R. Buick, cited in Brauhart, 1999). However, Pb–Pb dates of c. 3280 Ma for sulfide mineralization from small felsic intrusions near the base of the group suggest a possibly older maximum age of deposition (Morant, P., 1998, Sipa Resources Ltd., written comm.). Conformably overlying rocks of the Kunagunarrina Formation include komatiite, high-Mg basalt, and chert. The type section of this unit is 2.4 km thick in the Pincunah belt. These rocks have distinctive, strongly light rare-earth element (LREE) depleted profiles, with ε_{Nd} values of between +3.2 to –2.3 (on the depleted-mantle evolution curve), becoming more negative up the stratigraphic section (Van Kranendonk, M., unpublished data), indicating progressive crustal contamination. Conformably overlying this formation is the Kangaroo Caves Formation, comprising up to 1.5 km of basalt–andesite to rhyolitic volcanic rocks and chert (Vearncombe et al., 1998; Brauhart, 1999; Van Kranendonk, 2000a). Felsic volcanism was coeval with emplacement of the Strelley Granite laccolith, both of which have been dated at c. 3238 Ma (Brauhart, 1999).

Intrusion of the synvolcanic Strelley Granite laccolith drove hydrothermal circulation that silicified a unit of fine-grained epiclastic sediments at the top of the group and developed several zinc–copper volcanic-hosted massive sulfide (VHMS) deposits spaced at regular intervals around the granite (Morant, 1998; Vearncombe et al., 1995, 1998; Brauhart et al., 1998; Brauhart, 1999; Van Kranendonk, 2000a). The intermediate to felsic volcanic rocks of the Kangaroo Caves Formation have more-fractionated LREE profiles, and ε_{Nd} values are consistently between –1 and –0.3.

Gorge Creek Group

The Gorge Creek Group is an extensive, but as yet undated, component of many greenstone belts across the EPGGT (Figs 2 and 5). Van Kranendonk and Morant (1998) and Williams (1999) provided a revised stratigraphy for the Soanesville and Shay Gap greenstone belts (Fig. 5). The group lies conformably to unconformably on a variety of older rocks including Warrawoona Group basalts, the Sulphur Springs Group, and granitoid rocks (Dawes et al., 1995; Williams, 1999; Van Kranendonk, 2000a). The group is characterized by thick BIF with locally economic concentrations of iron ore, chert, ferruginous shale, and clastic sedimentary rocks, but basaltic rocks are also included. M. Van Kranendonk interprets the lower formations (Soanesville Subgroup) in the western part of the EPGGT to be related to the Sulphur Springs Group magmatic event, as they disconformably overlie relict topography of the Sulphur Springs Group and have been affected by alteration related to mineralization at Sulphur Springs (Hill, 1997; Vearncombe et al., 1998). The slightly younger Pb–Pb ages of c. 3220 Ma from the Sulphur Springs mineralization may date the age of deposition of these lower sedimentary rocks. Where the Sulphur Springs Group is absent, age constraints on the basal formations of the Gorge Creek Group are limited, with the maximum age constrained only by the ages of underlying units such as the Wyman Formation.

Higher in the Gorge Creek Group, across what may represent a significant time gap, are the Honeyeater and Cooneeina Basalts. Although these mafic rocks are conformable on the Paddy Market Formation in the Soanesville greenstone belt, they lie unconformably on correlative rocks in the northern part of the Marble Bar greenstone belt in the Coppin Gap Syncline (Williams, 1999). The basalts were accompanied by the intrusion of thick, locally differentiated, ultramafic and mafic sills (e.g. Dalton Suite; Van Kranendonk and Morant, 1998; Van Kranendonk, 2000a) hosting platinum group element (PGE) minerals and nickel sulfides. This mafic magmatism may have occurred at c. 3070 Ma, the age of Pb–Pb model ages on some galenas from the c. 3240 Ma Sulphur Springs deposit (Huston, D. L., 2000, written comm.). The basaltic rocks are disconformably overlain by felsic tuffs, tuffaceous sandstones, and ferruginous shales of the Cattle Well and Pyramid Hill Formations (Williams, 1999; Van Kranendonk, 2000a), the former being younger than c. 3048 Ma (Nelson, 1999). These data suggest that the basaltic–felsic volcaniclastic association near the top of the Gorge Creek Group may represent a separate magmatic event and, although a direct cause of this magmatism is unknown, it may relate to events commencing in the WPGGT (see **Late Archaean tectonic evolution**). Since the c. 3048 Ma age of the Cattle Well Formation is a maximum depositional age, this does not preclude correlation between at least some of the east Pilbara BIFs and the Cleaverville Formation in the western part of the EPGGT and in the WPGGT. However, as noted above, there is indirect evidence that basal iron formations of the Gorge Creek group in the EPGGT are significantly older than the Cleaverville Formation.

De Grey Group

Scattered, isolated synclinoria of coarse clastic rocks belonging to the De Grey Group are present across the EPGGT (Fig. 2). The largest of these is the Lalla Rookh Synclinorium, located along strike northeast of the Soanesville greenstone belt, and deposited in a fault-bounded basin (Krapez, 1984) during intracontinental sinistral transpression at c. 2940 Ma (Van Kranendonk and Collins, 1998). In the Shay Gap greenstone belt, volcaniclastic tuff of the Cattle Well Formation at the base of the group has yielded a maximum age of deposition of c. 3048 Ma (Nelson, 1999; Williams, 1999).

Granitoid complexes

Nine ovoid, domical granitoid complexes are present in the EPGGT (Fig. 2). These form structural domes with commonly outward dipping margins, although some are locally overturned. The contacts of granitoid complexes vary from being locally intrusive (e.g. all contacts of the Corunna Downs, northern Shaw, southern Carlindi, and northeastern Mount Edgar Granitoid Complexes), or the locus of shearing (e.g. southwestern Mount Edgar, and western and eastern Shaw Granitoid Complexes), to an unconformity with younger supracrustal rocks (e.g. Shay Gap greenstone belt: Dawes et al., 1995). Although granitoid complexes have simple outlines, they are characterized by complex and even chaotic internal geometries (Van Kranendonk and Collins, in prep.). Older components are commonly preserved along the margins of the complexes, whereas successively younger phases occupy the cores (Fig. 4). In the Yule and Mount Edgar Granitoid Complexes, roof pendants of amphibolite and orthogneiss form trains of enclaves separating lobes of younger granitoid rocks. Along the margins of other granitoid complexes, particularly the Corunna Downs and Shaw Granitoid Complexes, complex folds analogous to those found around salt diapirs are present (Van Kranendonk, 1997; Van Kranendonk and Collins, in prep.).

All mapped granitoid complexes, except Warrawagine, contain gneissic to foliated remnants of tonalite–trondhjemite–granodiorite (TTG) dated between c. 3500 and 3410 Ma, in addition to suites of younger components including those dated at 3321–3303, 3252–3242, c. 2935, and c. 2850 Ma. The complexes contain varying proportions of components of different ages, as shown in Table 2. Of particular significance is the large volume of c. 3490–3410 TTG in the Shaw Granitoid Complex, the c. 3315 Ma granite in the Corunna Downs Granitoid Complex, the typically young age of the Yule, Carlindi, and Pippingarra Granitoid Complexes in the east, and the presence of c. 3575 Ma gneisses in the Warrawagine Granitoid Complex (Williams, 2000). Plutonic phases coincide with episodes of felsic volcanism (Williams and Collins, 1990; Thorpe et al., 1992a; Barley and Pickard, 1999; Brauhart, 1999), and are separated by large gaps between felsic plutonic–volcanic events (e.g. the 300 m.y. gap between c. 3240 and 2940 Ma).

The early TTG suite is silicic and sodic and derived from high-pressure melting of a mafic source. Bickle et al. (1983, 1993) compared the TTG suite favourably with modern calc-alkaline, subduction-related arc suites, whereas Smithies (2000) showed that the compositions are incompatible with an origin from slab melting in a modern-style steep subduction setting. Rather, he suggested that TTGs were more likely to be generated by melting of lower mafic crust — an interpretation in part supported by geochemical evidence presented by Bickle et al. (1993), who showed that at least some

Table 2. Estimated volume and age of components in granitoid complexes of the East Pilbara Granite–Greenstone Terrane

Age (Ma)	YULE	CARLINDI	SHAW	CORUNNA DOWNS	MT EDGAR	MUCCAN (eastern one third)	WARRAWAGINE
2800	10%	?	15%		?1%		
2900	75%	?	15%				
3000							
3100							
3200							
Kangaroo Caves Fm	~10%				20%	20%	20–30%
3300							
Wyman Fm				95%	50%	10%	60%
3400							
Panorama Fm	~5%		70%	5%		70%	?10–20%
Duffer Fm		?			30%		
>3500							1%

4IAS MVK75 01.08.01

of the North Shaw Suite was derived from melting of crustal sources older than 3600 Ma. Bickle et al. (1989) and Collins (1993) showed that younger granitoid suites were derived through progressive episodes of melting and recycling of the TTG suite.

Distribution of ancient crust

Indications of older crust in the EPGGT were first detected from Sm–Nd studies of Warrawoona Group volcanic rocks, which returned model ages of 3560 ± 32 Ma (Hamilton et al., 1981) and 3712 ± 98 Ma (Gruau et al., 1987). Inherited and detrital zircon studies on a variety of different host rocks support the presence of ancient sialic crust across the EPGGT (Fig. 6). The oldest date of >3724 Ma is from a xenocrystic zircon from the Panorama Formation in the Panorama belt (1 on Fig. 6; Thorpe et al., 1992a). The oldest dated rock is an inclusion of tightly folded, gneissic tonalite from the Warrawagine Granitoid Complex, which yielded zircon populations at 3655 ± 6, 3637 ± 12, 3595 ± 4, and 3576 ± 6 Ma (the probable igneous age), in addition to populations with typical Warrawoona Group ages (2 on Fig. 6; Nelson, 1999). The rest of the zircon data indicate peak crust-formation times at c. 3650, c. 3575, and c. 3530–3500 Ma. The T_{DM} model ages from c. 3450 Ma TTG from the Carlindi, Warrawagine, and Yule Granitoid Complexes fall in the range c. 3700 to 3564 Ma (GSWA, unpublished data). Samarium–neodymium data from c. 3490–3470 Ma TTG of the North Shaw Suite indicate contamination by, and in part derivation from, older crustal sources to 3700 Ma (Bickle et al., 1993). The presence of c. 3650 and c. 3580 Ma detrital zircons in a quartzite from the Apex Basalt (Collins, W. J., 2001, University of Newcastle, written comm.) indicate that parts of the ancient sialic crust were exposed by c. 3460 Ma.

Deformation

There are two types of regional-scale structures in the EPGGT (Fig. 3): a dome-and-basin pattern of granitoid-cored domes and intervening synclinal tracts of greenstones that evolved over the entire history of the craton; and structures within the Lalla Rookh – Western Shaw structural corridor (LWSC) that formed during a discrete event of sinistral transpressional at c. 2940 Ma (Van Kranendonk and Collins, 1998).

General characteristics of the dome-and-basin pattern are that the margins of granitoid complexes commonly have steeply dipping foliations that are parallel to, and pass across, contacts with greenstones (Hickman, 1984). Adjacent greenstones are metamorphosed under amphibolite to greenschist facies in contact metamorphic aureoles. Farther away from granitoid contacts, greenstones are still commonly steeply dipping, but unaffected by penetrative foliations. This probably reflects either a decrease in temperature and strain away from the granitoid heat source, or a younger age of deposition of the stratigraphically higher rocks, or both. Apart from being able to say that the foliations must be younger than their host rocks, it is difficult to constrain the precise age of these structures since many of the host rocks have yet to be dated or the metamorphic minerals defining them have been largely reset by successive generations of intrusive granitoid phases or other regional events (or both). In fact, attempts at Ar–Ar dating of foliated metamorphic minerals around the Shaw Granitoid Complex (Davids et al., 1997; Zegers et al., 1999) have indicated a long history of heating and cooling that can be interpreted as relating to the progressive, commonly coaxial development of the dome-and-basin structures (see **Middle Archaean tectonic evolution**). As a result, it is commonly difficult to ascribe a particular set of structures to a precise time interval, and thus some structures have been grouped together in broad categories. Blewett (2000) presented a different interpretation of the structural evolution of the North Pilbara Terrain.

D_1 deformation

The earliest recognized structures span a period from c. 3490 to 3410 Ma and are broadly lumped together as D_1 deformation structures. These include the local development of synvolcanic, listric, normal growth faults in the Dresser Formation (Nijman et al., 1998a, 1999a; Van Kranendonk and Hickman, 2000), Duffer Formation (Zegers et al., 1996), and Panorama Formation (Nijman et al., 1998b, 1999b). Faults in the Dresser Formation are filled by hydrothermal chert–barite veins and were interpreted to have formed as a result of caldera collapse during intrusion of a subvolcanic laccolith (Van Kranendonk, in prep. a). Zegers et al. (1996) presented a different model for the origin of extensional faults in the Duffer Formation and associated structures (but see **Evidence for thrusting** below).

The D_1 deformation also caused tilting of the Coonterunah Group and Talga Talga Subgroup away from the cores of synvolcanic granitoids; this occurred prior to deposition of the Panorama Formation and Apex Basalt respectively (Hickman, 1983; Van Kranendonk, 2000a). DiMarco and Lowe (1989) argued that these structures probably formed as a result of granitoid intrusion and doming during episodes of felsic volcanism. Local D_1 folds were also developed in the Coonterunah Group, and their geometry is consistent with formation during gravitational sliding off the rising Carlindi Granitoid Complex (Van Kranendonk and Collins, 1998), as proposed for folds with a similar geometry, but different age, adjacent to the Mount Edgar Granitoid Complex (Collins, 1989).

Gneissic fabrics were developed in >3450 Ma protoliths of the Shaw Granitoid Complex between c. 3450 and 3400 Ma, as evidenced by the fact that homogeneous, weakly foliated granitoid rocks dated at c. 3430 Ma contain xenoliths of migmatitic orthogneiss. Gneissification was the result of partial melting of TTG protoliths and lit-par-lit injection of resultant leucogranite during synmagmatic doming (Van Kranendonk and Hickman, 2000). Partial melting in the Shaw Granitoid Complex continued to c. 3400 Ma as determined from zircon ages on melt veins and diatexite (Van Kranendonk, 2000a). A similar age of 3410 ± 7 Ma was obtained for partial melting of >3600 Ma gneiss from the Warrawagine Granitoid Complex (Nelson, 1999).

Bickle et al. (1980, 1985) described D_1 isoclinal folds and medium-pressure metamorphic assemblages from the northwestern Shaw area, which they interpreted as early recumbent folds formed during an Alpine-style thrusting event that predated granitoid doming. Zegers et al. (1996) suggested that this occurred prior to metamorphic core-complex development of the Shaw Granitoid Complex at c. 3470 Ma. However, it is now known that these folds affect rocks of the <3235 Ma Gorge Creek Group and that they are coaxial, and thus probably coeval, with structures developed at c. 2940 Ma, as described below.

D_2 deformation

D_2 structures accompanied deposition of the felsic volcanic Wyman Formation and intrusion of related granitoid rocks at c. 3325–3308 Ma across the eastern part of the EPGGT, but most notably in the Corunna Downs and Mount Edgar Granitoid Complexes (Fig. 8). Collins (1989) and Collins et al. (1998) documented a set of structures within and around the Mount Edgar Granitoid Complex related to diapirism. These structures include a 1–3 km-wide, horseshoe-shaped shear zone within the southwestern margin of the complex that has granite-side-up displacement indictors, across which uplift of the granitoid complex was achieved. This shear zone gradually dies out to the northwest and northeast in undeformed, synkinematic granites emplaced into greenstones at a high level and locally associated with porphyry copper–

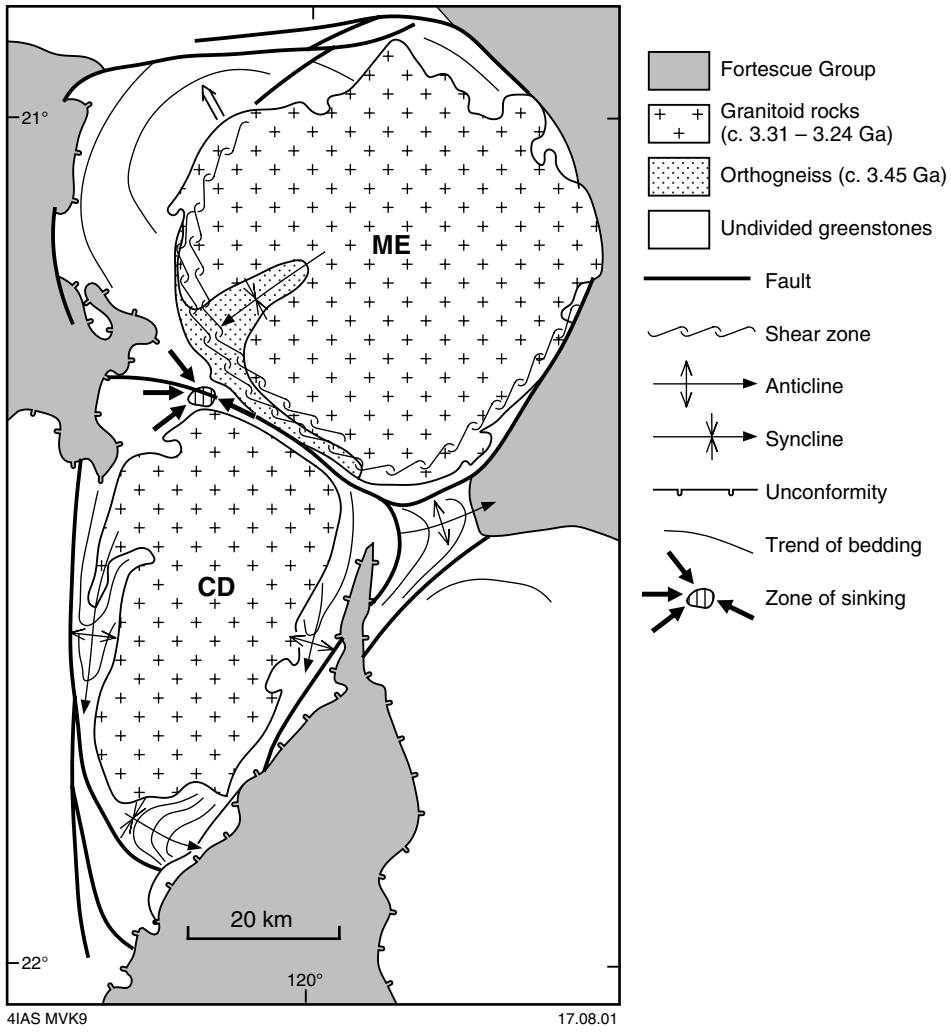

Figure 8. Simplified sketch map of the geology around the Mount Edgar (ME) and Corunna Downs (CD) Granitoid Complexes, showing the main structures generated by granitoid diapirism (see text for discussion). Open arrow denotes area of recumbent folding of greenstones in the McPhee Reward area generated by gravitational sliding to the northwest, off the rising granitoid complex described by Collins (1989). Zone of sinking between the granitoid complexes denotes area of vertical L-tectonites as described in the text (after Collins et al., 1998)

molybdenum mineralization. Associated ring faults in the flanking greenstones accommodated sinking of the greenstones as well as later exhumation of marginal components adjacent to granitoid complexes (Collins and Van Kranendonk, 1999). A synformal roof pendant of greenstones and c. 3450 Ma gneisses within the complex formed during diapiric emplacement of two domical lobes of synkinematic, c. 3300 Ma granite. In the McPhee Formation of the adjacent Marble Bar greenstone belt, a set of tight, asymmetrical folds that verge away from the Mount Edgar Granitoid Complex formed as a result of gravitational sliding of greenstones off the rising dome (Collins, 1989). Greenstones in the Warrawoona Syncline were deformed into a zone of sinking between the coeval Mount Edgar and Corunna Downs Granitoid Complexes, which is characterized by a core of intense vertical stretching. Collins and Gray (1990) presented geochronological evidence that doming of the Mount Edgar Granitoid Complex was largely completed by c. 3200 Ma.

The progressive, commonly coaxial nature of folding of the greenstones during granitoid doming is documented by the fold style in the far southern part of the Kelly greenstone belt, immediately south of the Corunna Downs Granitoid Complex (Fig. 9). This fold developed incrementally throughout deposition of the Wyman Formation, since upper units dated at 3308 Ma rest unconformably on moderately folded lower units of the formation dated at 3325 Ma, which themselves rest on more tightly folded rocks of the Euro Basalt. This fold is one of three contemporaneous, hook-shaped folds that formed around the Corunna Downs Granitoid Complex (Fig. 9). The westernmost of these tight folds is cored by a syntectonic granite with a minimum age of c. 3270 Ma (Rb–Sr isochron: Cooper et al., 1982), which is almost certainly part of the c. 3315 Ma felsic igneous complex recognized by Barley and Pickard (1999). The hook-shaped folds are bound by a ring fault surrounding the Corunna Downs Granitoid Complex. Such hook-shaped folds and ring faults are characteristic of salt diapirs (Jackson et al., 1990) and are a key piece of evidence supporting the diapir hypothesis (Van Kranendonk and Collins, in prep.). Note that some of the tilting in this area occurred after deposition of the Gorge Creek, De Grey, and Fortescue Groups, as all these rocks are tilted away from the granitoid complex; this is a feature common to other domes.

D_3 deformation

D_3 structures formed in the western part of the EPGGT during eruption of the Sulphur Springs Group and widespread granite intrusion at c. 3240 Ma. In the Soanesville greenstone belt, intrusion of the Strelley Granite resulted in a suite of synvolcanic growth faults in the Kangaroo Caves Formation that were sites of hydrothermal venting and massive sulfide deposition (Vearncombe et al., 1998). Late caldera collapse resulted in renewed faulting and deposition of an olistostrome breccia with synsedimentary folds (Van Kranendonk, 2000a). Intrusion of the Strelley Granite and deposition of the Kangaroo Caves Formation was accompanied by dome-and-basin folding and granite intrusion in the northeastern part of the Yule Granitoid Complex, including the Tambourah Dome. Van Kranendonk (1997) showed that this dome-and-basin pattern has the same hook-shaped folds and ring faults characteristic of diapiric emplacement of the Corunna Downs Granitoid Complex. Doming was accompanied by amphibolite-facies contact metamorphism of the Western Shaw greenstone belt (Wijbrans and McDougall, 1987). Deposition of the Gorge Creek Group occurred during the late stages of doming, in basins between granitoid complexes affected by horst and graben faults (Wilhelmij and Dunlop, 1984). In the northern Marble Bar greenstone belt, deposition of the Gorge Creek Group spanned a change from extensional to compressional structures (Nijman et al., 1998b, 1999b). Depocentre shifts were interpreted by these authors to be due to differential doming of adjacent granitoid complexes, whereas subsequent compressional faults were interpreted as the result of either regional thrusting or folding between granitoid complexes (or both).

D_4 deformation

At c. 2940 Ma, D_4 deformation produced the northerly striking Lalla Rookh – Western Shaw structural corridor (LWSC), and was accompanied by deposition of the coarse clastic De Grey Group in a trough developed in advance of the north-moving Strelley Granite and associated greenstones (Figs 10 and 11: Van Kranendonk and Collins, 1998). The LWSC is characterized by large, northeasterly–southwesterly trending folds, north- to northwest-striking sinistral faults and shear zones, and northeast-striking dextral faults, that collectively indicate a northwest–southeast direction of maximum compression (Fig. 10). The two strands of the Mulgandinnah Shear Zone formed along the western margin of the Shaw Granitoid Complex at this time (Van Kranendonk and Collins, 1998;

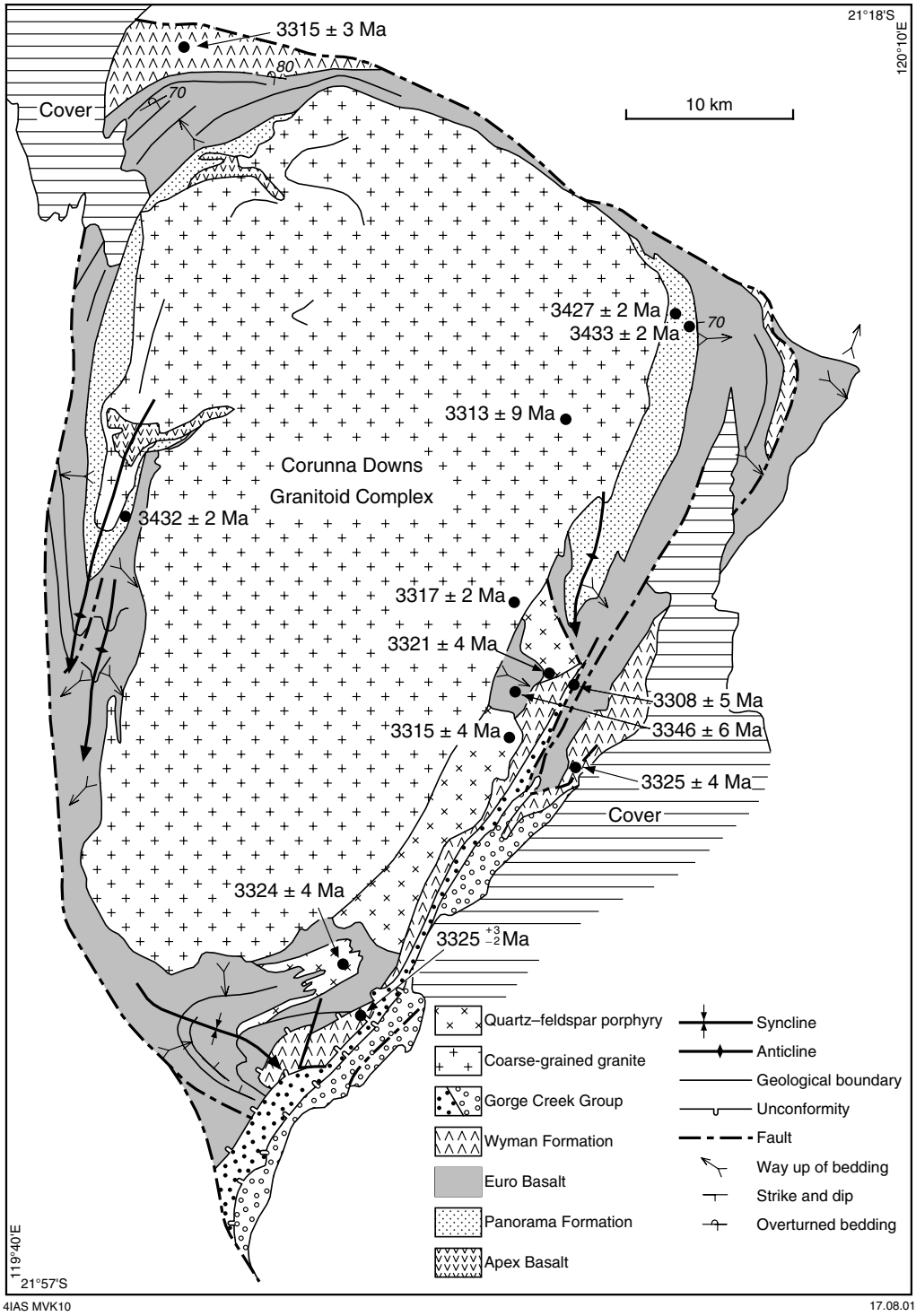

Figure 9. Simplified geological map of the Kelly greenstone belt and interpreted diapiric structures around the Corunna Downs Granitoid Complex. Note the three hook-shaped folds within the bounding ring fault. Note also the progressive development of the southernmost fold, as evidenced by successive unconformities between the >3325 Ma Euro Basalt, the 3325–3315 Ma Wyman Formation, and the basal unit of the c. 3308 Ma 'Gorge Creek Group'. Age data from Thorpe et al. (1992a), McNaughton et al. (1993), Barley and Pickard (1999), and Nelson (2000, in prep.)

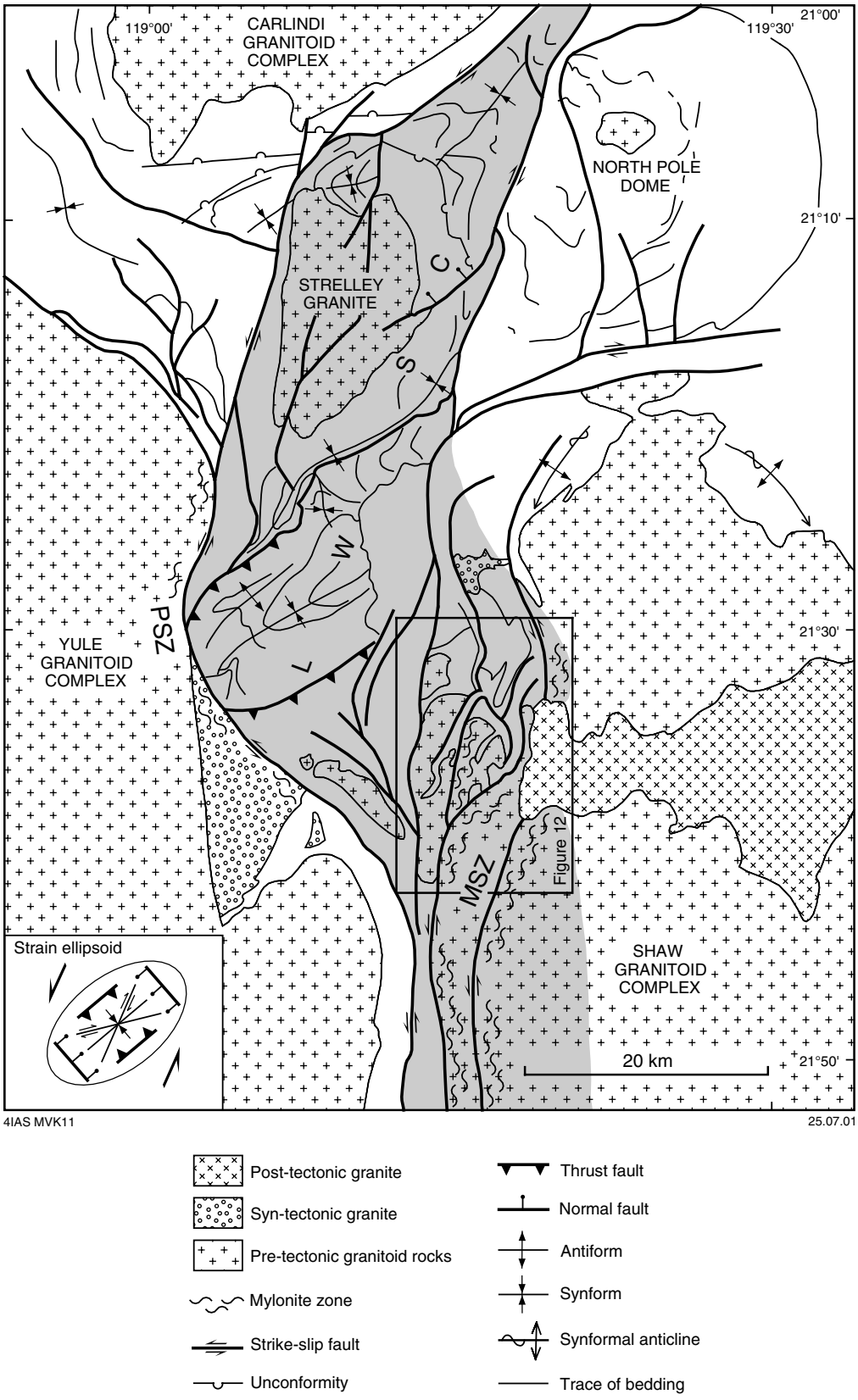

Figure 10. Principal D_4 structures in the Lalla Rookh – Western Shaw structural corridor, formed at c. 2940 Ma as a result of northwest–southeast compression (see inset). Note that northeast-trending folds within the Lalla Rookh – Western Shaw structural corridor are bound by, and do not affect, the western and eastern boundary faults of the system, indicating coeval formation during sinistral wrenching (MSZ= Mulgandinnah Shear Zone, PSZ = Pulcunnah Shear Zone; modified from Van Kranendonk and Collins, 1998)

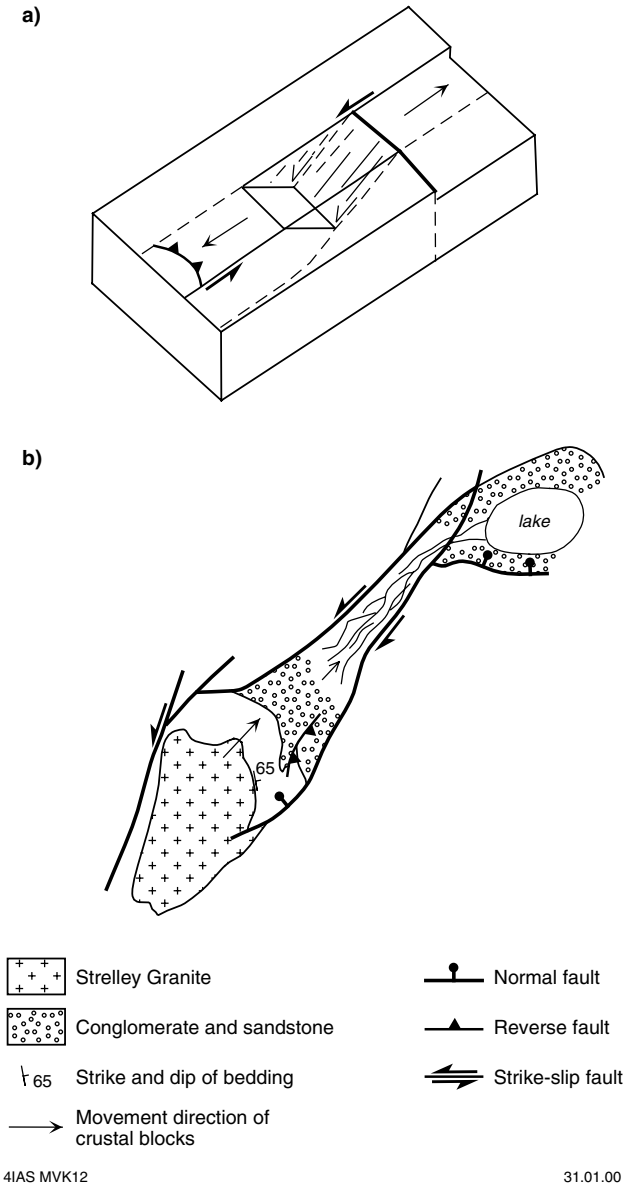

Figure 11. Proposed models for the evolution of the Lalla Rookh Synclinorium: a) sinistral strike-slip pull-apart model (Krapez, 1984); b) small trough developed in advance of the northerly moving Strelley Granite and associated supracrustal rocks, bound by sinistral and dextral faults; modified from Van Kranendonk and Collins (1998)

Zegers et al., 1998). Linear fabric elements within it are colinear with lineations and fold axes in the area of tight folds and locally overturned stratigraphy described by Bickle et al. (1980, 1985) and ascribed by these authors to Alpine-style thrusting. However, Van Kranendonk (1997) showed that these folds formed after, not before, granitoid doming and suggested that they were the products of constriction within a restraining bend between stepped splays of the Mulgandinnah Shear Zone (Fig. 12). Although it represents a significant zone of translation and was responsible for exhumation and tilting of the Strelley Granite and flanking greenstones, stratigraphic links across the LWSC show that it is an entirely intracontinental structure and not the site of terrane accretion as proposed by Krapez (1993; Van Kranendonk and Collins, 1998).

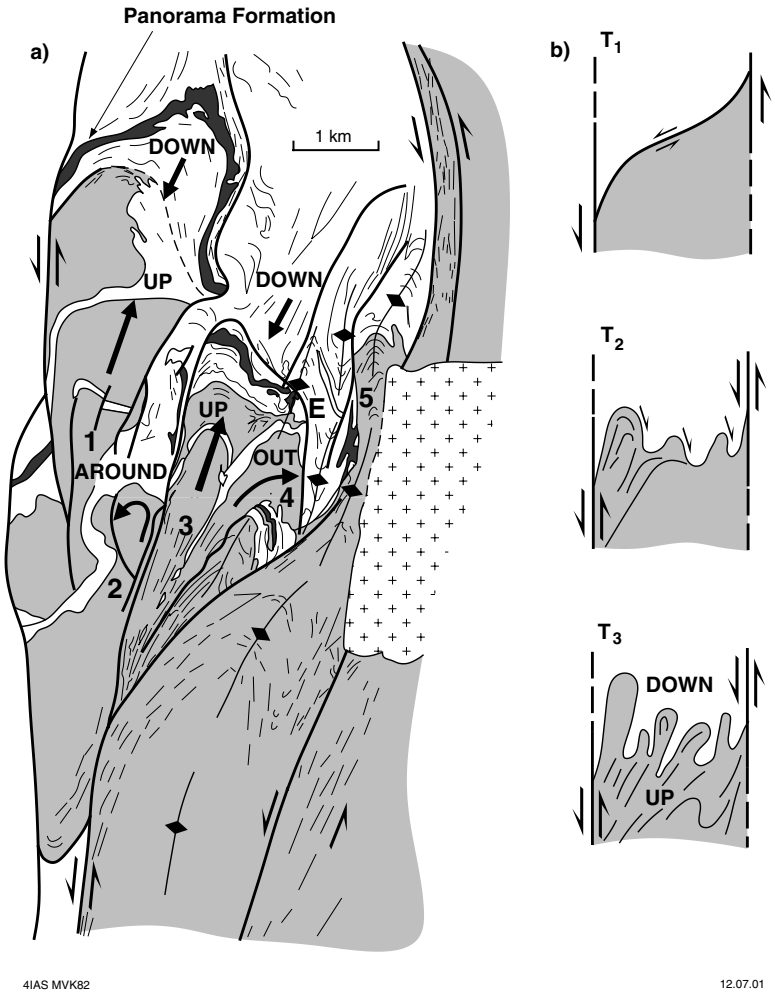

Figure 12. a) Geological sketch map of the folded granitoid lobes in the northwestern Shaw area, showing the principal structures and sense of displacement of the granitoid lobes during D_4 deformation (see Fig. 10 for location). Numbers 1–5 refer to folded granitoid lobes as discussed in the text; shaded area = deformed granitoid rocks; unpatterned areas = greenstones; + pattern = post-tectonic Cooglegong Monzogranite;
b) Schematic development of the folded granitoid lobes as a result of compression within a restraining bend between stepped splays of the Mulgandinnah Shear Zone. T_1–T_3 are interpreted time slices during progressive sinistral shearing at c. 2940 Ma

The D_4 deformation also caused amplification of the Tambourah Dome, low-grade metamorphism of adjacent greenstones (Wijbrans and McDougall, 1987), and development of a north-northeasterly striking quartz foliation across the Yule and Shaw Granitoid Complexes. Synkinematic monzogranite plutonism was widespread across the western part of the EPGGT at this time (Nelson, 1998, 2000), but is unknown east of the Shaw Granitoid Complex.

D_5 deformation

Sinistral shearing on north northeast-striking zones affected the northwestern part of the EPGGT at c. 2890 Ma and was accompanied by gold mineralization in the Mount York and Lynas Districts (Neumayr et al., 1993.). Deformation of the EPGGT was

largely completed by 2850 Ma, which was the time of emplacement of large, undeformed tin–tantalum-bearing granites into the cores of granitoid complexes across the terrane (Hickman, 1983; Nelson, 1998; Kinny, 2000).

D_6 deformation

The predominantly basaltic volcanic rocks of the c. 2775–2630 Ma Fortescue Group (Hamersley Basin), that unconformably overlie the older dome-and-basin pattern of the EPGGT across an angular erosional unconformity, record a late component of granitoid doming. Although the bulk of deformation of the basement rocks was completed prior to Fortescue Group deposition, the group is only preserved in synclinal outliers between domical granitoid complexes (Fig. 2: Hickman, 1984). The Marble Bar Sub-basin preserves evidence that doming occurred during deposition of the Fortescue Group. This is seen by an angular unconformity between rocks of the c. 2772 Ma Mount Roe Basalt (age data from Arndt et al., 1991; Wingate, 1999) that were tightly folded in a syncline between the Shaw and North Pole Domes, and the overlying, gently dipping Hardey Formation and younger formations (Van Kranendonk, 2000a). Palaeocurrent data from the Hardey Formation in this area document transport of sand detritus radially inwards to the basin centre (Blake, 1993), which is situated over a triple-point zone of sinking greenstones between rising granitoid domes. A felsic sill and related epiclastic volcanic suite in the Hardey Formation dated as 2756 ± 8 Ma (Arndt et al., 1991; Williams, 1999) provide a minimum age estimate for this late component of doming.

Metamorphism

Metamorphic mineral assemblages in greenstones show a common decrease in temperature away from granitoid complexes, from lower amphibolite facies adjacent to granitoid complexes to greenschist and prehnite–pumpellyite facies throughout most of the upper part of the Warrawoona Group, the Wyman Formation, and the Sulphur Springs and Gorge Creek Groups, to very low temperature (anchizone) metamorphism of the De Grey and Fortescue Groups. Two-pyroxene granulite remnants have been recorded in amphibolite xenoliths in the Shaw and Yule Granitoid Complexes (Van Kranendonk, 2000a).

Moderately high pressure estimates of about 6 kb were obtained from kyanite-bearing felsic schists in two areas of tightly folded greenstones immediately adjacent to granitoid complexes, including the Emerald Mine greenstone complex adjacent to the northwestern margin of the Shaw Granitoid Complex (Bickle et al., 1985) and the southern part of the Marble Bar greenstone belt adjacent to the southwestern margin of the Mount Edgar Granitoid Complex (Delor et al., 1991). The geology and metamorphic mineral assemblages of the Emerald Mine greenstone complex along the northwestern margin of the Shaw Granitoid Complex were used to support Alpine-style thrusting, whereas a thermal anomaly associated with the granitoid complex was unexplained. An alternative model for the development of kyanite-bearing assemblages in these two areas was presented by Collins and Van Kranendonk (1999), who suggested that greenstone burial in these areas occurred during partial convective overturn of the upper and middle crust. A model whereby this could have occurred is shown in Figure 13.

Amphibolite-facies metamorphism of the Western Shaw greenstone belt was dated at c. 3234 Ma, and greenschist-facies metamorphism at c. 2950 Ma (Wijbrans and McDougall, 1987). Elsewhere, extensive Ar–Ar dating of metamorphic amphiboles in greenstones indicate a range of ages throughout the tectonic evolution of the EPGGT,

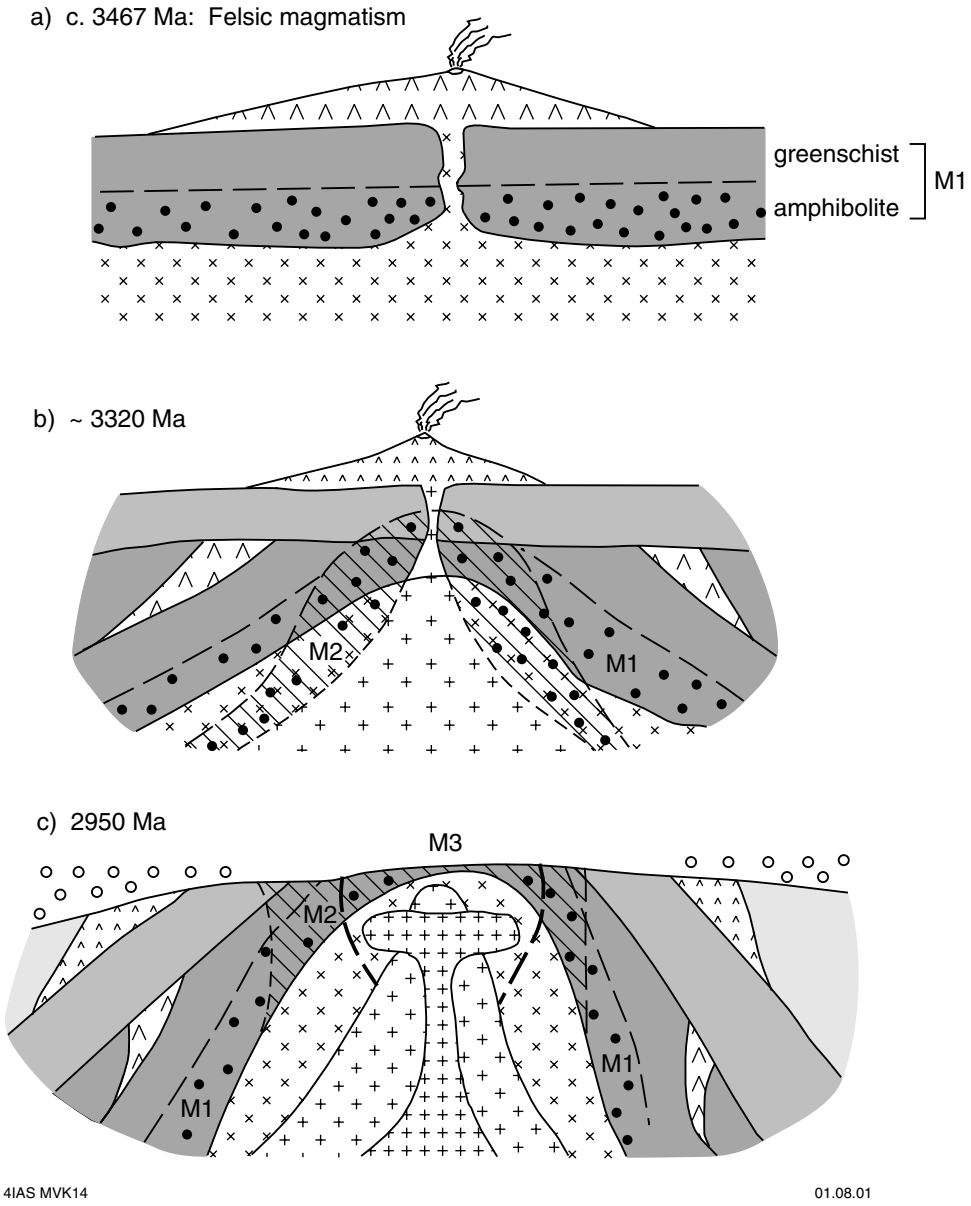

Figure 13. Model for the metamorphic development of the East Pilbara Granite–Greenstone Terrane:
a) the onset of metamorphism of the lowermost greenstones is associated with the emplacement of felsic magmas at c. 3467 Ma;
b) and c) show intervals in the punctuated evolution of the dome-and-syncline geometry, in which thermal aureoles are superimposed on parts of the metamorphic assemblages in the lower greenstones, and cause the initial metamorphism of younger greenstones. Synchronous doming of granitoid complexes with granite emplacement causes an overlap in the areas of amphibolite-facies contact-metamorphic aureoles through time. Doming leads to the deposition of wedges of greenstones, resulting in the preservation of thick stratigraphic sections in syncline cores that have never experienced high-grade metamorphism

including end-member dates similar to those of the Coonterunah and Fortescue Groups (Davids et al., 1997; Zegers et al., 1999). Much of the rest of the Ar–Ar data shows that greenstones adjacent to granitoid complexes cooled over the protracted development of the terrane, even during times of no known geological activity. This suggests that granitoid complexes were long-lived conduits for the release of conductive heat from the lower crust and mantle.

Early Archaean tectonic evolution (>3700–3300 Ma)

Hickman (1984) listed several types of geological evidence in favour of granitoid diapirism in the North Pilbara Terrain, and this has been supported by more-detailed studies in the EPGGT (Collins, 1989; Williams and Collins, 1990; Collins et al., 1998; Collins and Van Kranendonk, 1999; Van Kranendonk and Collins, in prep.). However, the presence of local complications in greenstone stratigraphy, overturned bedding, reverse faults, and linear deformation zones in the EPGGT has been used by several authors to invoke regional thrust-accretion models for early crust formation in the EPGGT (Bickle et al., 1985; Boulter et al., 1987; Krapez, 1993; Zegers et al., 1996; Barley, 1997).

Data obtained from recent mapping and geochronology allows certain constraints to be placed on these competing hypotheses of crust formation. Significant in this regard is that all volcanic rocks in the EPGGT, even the oldest, show geochemical evidence for contamination by sialic crust (e.g. Green et al., 2000) and this precludes crust formation in a mid-ocean ridge setting as proposed for the stratigraphically similar and contemporaneous Barberton greenstone belt of South Africa (de Wit et al., 1992). Geochemical data from the c. 3470 Ma TTG suite show that it, too, was generated from melting of, or was contaminated by, older crust (Bickle et al., 1993). Detrital and inherited zircon data from samples across the EPGGT indicate that this ancient crust was widespread (Fig. 6).

Also significant is that the upper part of the felsic volcanic Panorama Formation is now recognized across most greenstone belts of the EPGGT, indicating crustal coherence by c. 3430 Ma. Correlation of this unit and younger groups across the EPGGT shows that structures identified as domain boundaries by Krapez (1993) do not represent significant tectonic features during crust formation in part of the North Pilbara Terrain, but instead are late, relatively minor fault zones.

Evidence that the low-grade greenstone-dominated upper crust of the EPGGT was up to 12 km thick by the end of Panorama Formation deposition (c. 3430 Ma; Van Kranendonk, 2000b), and locally up to 19 km thick after deposition of the Euro Basalt (prior to 3325 Ma), suggests a thick volcanic crust. If the thicknesses of the middle granitoid crust and the lower crust are added to this estimate, then the total crustal thickness may have been in the order of 50 km by this time (e.g. Bickle et al., 1985; Van Kranendonk, 1999b).

In addition to the above, any model that attempts to explain the early tectonic evolution of the EPGGT must account for the following:

- the essentially continuous and autochthonous nature of volcanism over about 220 m.y., from c. 3530 to 3310 Ma;
- the repeated development of ultramafic to felsic volcanic cycles;
- deposition of shallow-water sediments (including stromatolitic units) between c. 3490 and 3420 Ma;
- the widespread generation of TTG magmas at c. 3490–3400 Ma;
- the dome-and-basin architecture of the terrane;
- the regional contact-style and low metamorphic grade of greenstones, as well as the anomalous areas of higher metamorphic grade.

The EPGGT has an almost completely hidden early geological history that is distinct from any other part of the North Pilbara Terrain, commencing at c. 3724 Ma and continuing to c. 3515 Ma, the age of the oldest exposed supracrustal rocks. At least some of this crust was sialic, but it also included gabbroic anorthosite (McNaughton et al., 1988). Xenocrystic and detrital zircon information suggests that continuous crust formation commenced at c. 3530 Ma (Fig. 6) and was completed over about 220 m.y.,

from c. 3530 to 3310 Ma. This stage is represented by the Coonterunah and Warrawoona Groups and consisted of the eruption of large volumes of compositionally homogeneous pillow lavas that were interspersed with episodes of felsic magmatism and predominantly chemical sedimentation in quiet, shallow-water conditions. During this period, felsic volcanism was coeval with the emplacement of granitoid rocks as subvolcanic sills and plutons (Thorpe et al., 1992a; Barley and Pickard, 1999). The lateral continuity of units in these groups over hundreds of kilometres suggests deposition on a tectonically inactive volcanic plain. Such environments in the modern tectonic model are present only in back-arc basins or above mantle plumes on oceanic plateaus or continental flood-basalt provinces. Considering that crustal plates were probably much smaller in the early Archaean (if present) and convection was much faster, then the 220 m.y. duration of volcanism in the EPGGT, combined with the presence of interspersed felsic volcanic horizons, precludes formation in a back-arc setting.

Was an oceanic or continental plateau the tectonic setting of crust formation from c. 3530 to 3310 Ma? A generalized stratigraphic section of the dominant Warrawoona Group shows that it is composed of repeated ultramafic – felsic volcanic cycles that range in duration from 9 to 63 m.y. (Fig. 14). This duration is consistent with estimates for the duration of mantle plume events (cf. Campbell et al., 1989), and this, combined with the stratigraphic data, is used as evidence to suggest that the early Pilbara crust formed from the successive eruption of melts derived from repeated magmatic underplating events that probably resulted from the decompression melting of rising mantle plumes. Although earlier cycles may have occurred in the Coonterunah Group, the end of the first volcanic cycle at the base of the Warrawoona Group is interpreted to include tholeiitic basalts and dolerites of the North Star Basalt capped by a thin unit of interbedded felsic schist and chert of the McPhee Formation. Overlying this is the next volcanic cycle that commenced with carbonate-altered peridotitic komatiites that have either been included in the McPhee Formation (Marble Bar greenstone belt) or in a correlated unit (Hickman, 1983) below the Mount Ada Basalt in the Coongan greenstone belt. This unit is up to 1 km thick and passes up into a thick basalt unit that differentiates further up-section into andesite, dacite, and local rhyolite of the Duffer Formation. The combined thickness of the Mount Ada Basalt and Duffer Formation is up to 10 km in the Marble Bar greenstone belt. This is capped by grey-and-white banded chert and jaspilitic chert of the Towers Formation that was deposited from hydrothermal precipitates at the close of this magmatic cycle (Van Kranendonk, in prep. a). This cycle was completed in only 6 m.y., but accounts for an average 6 km of stratigraphy in the Marble Bar greenstone belt (Hickman, 1983). In the Marble Bar greenstone belt, chert from the underlying cycle is interbedded with peridotitic komatiites of the Apex Basalt, representing the onset of the next magmatic cycle, that are locally more than 500 m thick in the Warrawoona Syncline. These rocks grade up into a 2 km-thick unit of relatively homogeneous basalt (Apex Basalt) that is capped by felsic volcanic rocks and hydrothermally precipitated chert, here of the Panorama Formation and Strelley Pool Chert.

The Euro Basalt and Wyman Formation represent a fourth cycle that took 100 m.y. to complete. Basal peridotitic komatiites and high-Mg basalts in this formation are up to 3 km thick (Van Kranendonk, 2000a). Geochemical analyses of the Euro Basalt (Glikson and Hickman, 1981; Glikson et al., 1986) show that it is composed of several cycles of alternating high-magnesian and tholeiitic basalt (Van Kranendonk and Hickman, 2000), similar to the pattern of basalts erupted from mantle plumes (Campbell et al., 1989).

In apparent conflict with an oceanic plateau setting, however, is the composition of felsic rocks of the Duffer Formation and TTG sill complex that have commonly

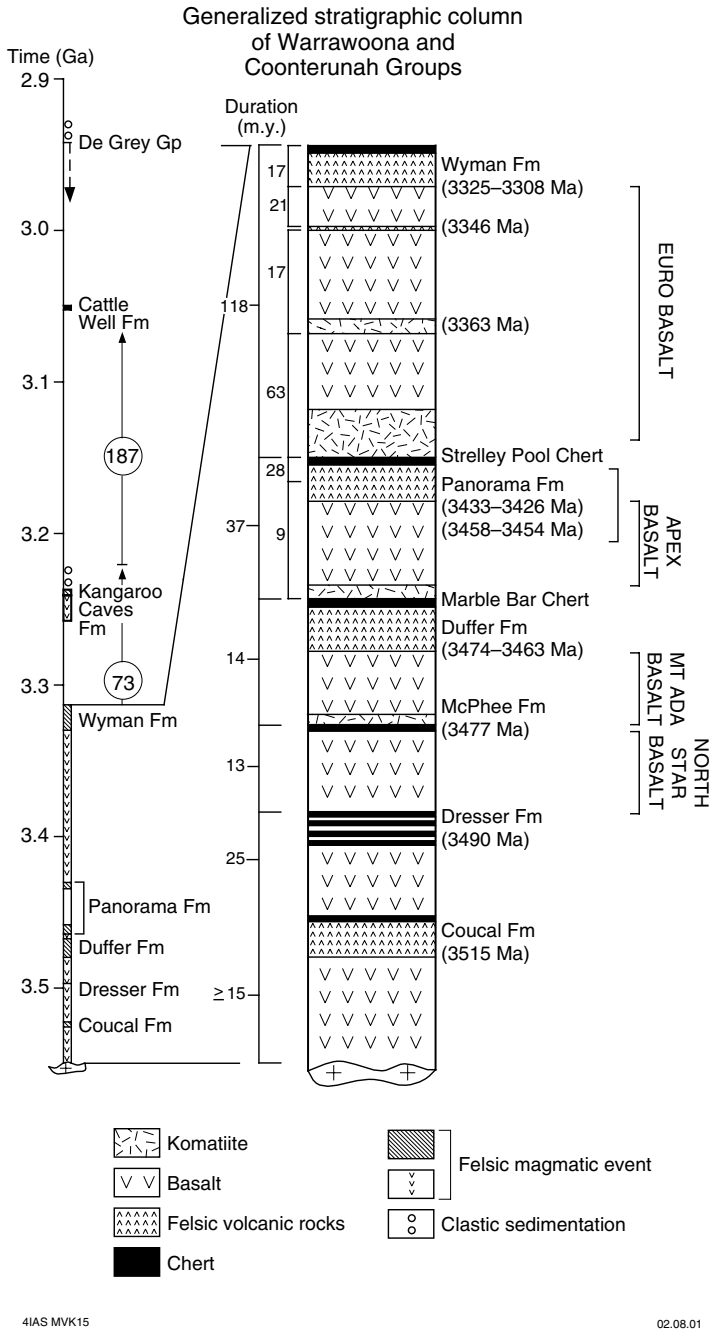

Figure 14. Schematic composite stratigraphic section of the Warrawoona and Coonterunah Groups. Time line on the left shows the duration of episodes of magmatism. Circled numbers refer to the duration of magmatic events, in millions of years

been interpreted as the products of arc magmatism (Bickle et al., 1993; Barley et al., 1998). An important new view on the origin of these rocks was presented by Smithies (2000), who showed that Archaean TTG differ from Phanerozoic arc magmas and are more likely to be melts of hydrated lower mafic crust. All that is required to generate Archaean TTG with characteristic high La/Yb ratios are depths great enough for melting of basalt to be within the stability field of garnet or hornblende (or both). These conditions are met if the Pilbara crust was 55 km thick or more, which is within the range of thickness of the EPGGT estimated by Bickle et al. (1985) and Van Kranendonk

(2000b). Glikson et al. (1987) suggested a crustal origin for Pilbara TTG and associated felsic volcanism, as did DiMarco and Lowe (1989) for the Panorama Formation. A similar origin has been suggested for a tonalite batholith exposed at the base of a Phanerozoic oceanic plateau on the island of Aruba in the Caribbean (White et al., 1999). A crustal origin for TTG in the EPGGT is supported by the fact that magmas were emplaced over a roughly circular area 220 km in diameter (vs modern arcs which are linear and 50–100 km wide) and that the duration of magmatism was 200 m.y. (compared with modern arc segments that last only about 10 m.y.). The rapid accumulation rate of the Warrawoona Group and the evidence for pervasive alteration of these basalts by hydrothermal circulation suggests the possibility that TTG's were generated by melting of hydrated basalts at the base of a rapidly accumulated volcanic pile. This accords well with the plume model for the generation of upper-crustal greenstones, erupted onto older continental crust.

Felsic volcanic rocks were erupted from the TTG sill complex through point sources now occupied by domical granitoid complexes, and this occurred at slightly different times in different places from scattered volcanic vents developed over synvolcanic laccoliths. A classic example of this is in the North Pole Dome, where the undeformed, high-level North Pole Monzogranite is dated as the same age as rhyolite of the Panorama Formation (Thorpe et al., 1992a). Emplacement of subvolcanic laccoliths and deeper level sills caused synvolcanic doming of overlying rocks and of the surface (e.g. Barley et al., 1979; DiMarco and Lowe, 1989). A similar situation occurred during emplacement of the younger, but geometrically identical, Strelley Granite of the Soanesville greenstone belt (Van Kranendonk, 2000a). Synvolcanic doming associated with granite emplacement can account for all of the observed D_1 deformation in the EPGGT, up to c. 3400 Ma. This point-source release of heat and felsic magmas to the surface initiated positive perturbations in the upper contact of the mid-crustal TTG sill complex, and it is these perturbations that were later amplified into domical granitoid complexes as a result of partial convective overturn of the crust during successive tectono-thermal events (Fig. 15; see below).

Evidence for thrusting

Despite the apparent simplicity of the regional map pattern, the complex structural geology of local areas has led to several regional models invoking horizontal thrust-accretion processes. Specifically, the question under debate regards the presence and significance of early thrusting in Pilbara crustal evolution.

Van Haaften and White (1998) suggested that a set of bedding-parallel shears in the Marble Bar greenstone belt were responsible for tectonic thickening and inversion of greenstone stratigraphy. Van Kranendonk et al. (2001) contested the geometrical and geochronological database on which this was founded. Furthermore, mapping and geochronology by A. H. Hickman confirmed that the greenstones represent an autochthonous succession at least 12 km thick (age dates in Nelson, 2000; Van Kranendonk, 2000b).

Bickle et al. (1985) presented evidence in support of Alpine-style thrusting for an area of complex folds, overturned bedding, and anomalously high pressure (kyanite-grade, pressure estimated at 6 kb) metamorphism in the northwestern Shaw area. In the proposed model, thrusting and recumbent isoclinal folding were interpreted to pre-date doming of the Shaw Granitoid Complex and to be responsible for the high-grade metamorphism. A thermal anomaly associated with the granitoid complex was not explained, and the authors admitted several other problems with the model. Zegers et al. (1996) proposed that the Shaw Granitoid Complex formed as a core complex at 3470 Ma, following, and resulting from, the period of thrusting documented by Bickle

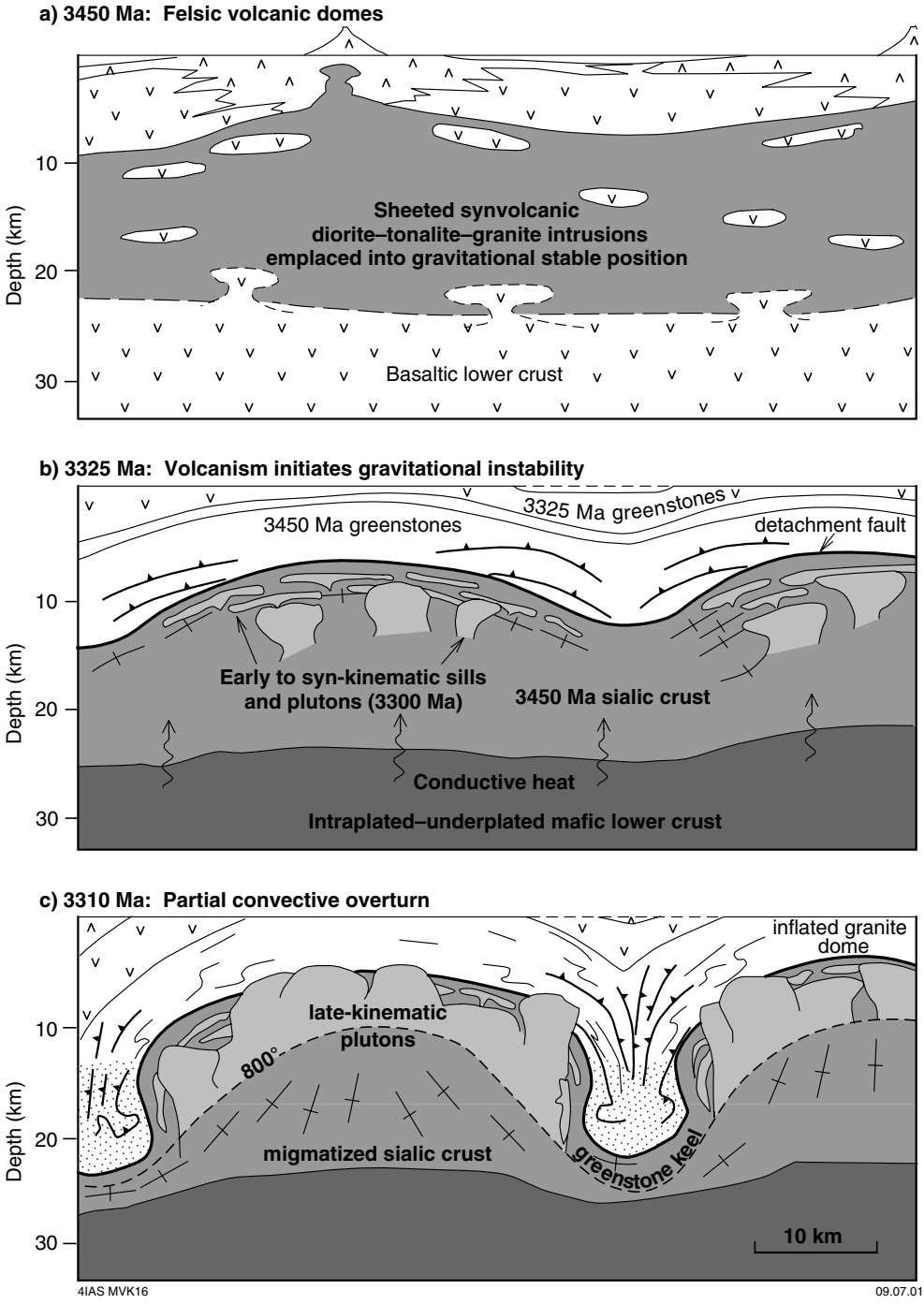

Figure 15. Schematic model of partial convective overturn for the eastern part of the East Pilbara Granite–Greenstone Terrane:
a) at c. 3450 Ma, a sheeted sill complex of tonalite–trondhjemite–granodiorite magmas was emplaced into a gravitationally stable position within older greenstones. Coeval eruption of the Duffer Formation from point sources resulted in volcanic domes over synvolcanic laccoliths;
b) deposition of the thick Euro Basalt generated a gravitationally unstable crustal configuration. Destabilization was caused by a discrete thermal event starting at 3325 Ma. Domal reactivation of older felsic volcanic centres commenced at this time, coeval with eruption of the felsic volcanic Wyman Formation;
c) the main period of partial convective overturn of the crust was coeval with voluminous granitoid plutonism in two pulses, at c. 3310 Ma and at c. 3240 Ma (modified from Collins et al., 1998)

et al. (1985). In this model, the Split Rock Shear Zone along the eastern margin of the Shaw Granitoid Complex was extended across the northern margin of the complex and interpreted to represent the detachment fault between the developing metamorphic core zone and the cover sequence.

There are, however, several problems with these models. Detailed mapping has shown that the proposed northern part of the Split Rock Shear Zone (Zegers et al., 1996) does not exist (Van Kranendonk, 1999a, 2000a; see **Day 7, Introduction** and **Locality 7.4**). Also, the large-scale folds and medium-pressure metamorphic assemblages in the northwestern Shaw area affect the c. 3430 Ma South Daltons Pluton (age from McNaughton et al., 1993) as well as rocks of the <3235 Ma Gorge Creek Group (Van Kranendonk, in prep. c) and thus cannot be related to crustal thickening at >3470 Ma, as suggested. Instead, the fold axes are shown to be colinear with metamorphic mineral lineations in the c. 2940 Ma Mulgandinnah Shear Zone, and a model has been presented whereby these structures formed as a flower structure due to localized compression in a restraining bend between stepped strands of the shear zone at this time (Fig. 12; Van Kranendonk and Collins, 1995; Van Kranendonk, 1997). This much younger age is also probably coeval with the formation of the Split Rock Shear Zone, based on ages of synkinematic amphiboles from the zone (Davids et al., 1997; Zegers et al., 1999).

The presence of reverse faults in rocks of the Gorge Creek Group in the Coppin Gap area of the Marble Bar greenstone belt, which Nijman et al. (1998b, 1999b) ascribed to '…regional thrusting and interbatholith folding', is consistent with constriction of bed-length as greenstones were deformed into synclines between pairs of granitoid diapirs (cf. Dixon and Summers, 1983). Deposition of the Gorge Creek Group across a transition from extensional to compressional structures is consistent with progressive diapirism, whereby cover rocks are initially extended as they shed off the top of the rising dome, and then constricted in tight synclines between domes (cf. Chardon et al., 1996; Collins et al., 1998).

Middle Archaean tectonic evolution (c. 3280–3020 Ma)

3325–3308 Ma: Partial convective overturn

After c. 3420 Ma, the EPGGT was destabilized by the eruption of up to 9 km stratigraphic thickness of the Euro Basalt. The eruption of this dense greenstone lid over the more buoyant mid-crustal TTG sill complex, combined with the probable addition of conductive heat (?from underplated magmas) below, caused widespread partial melting of TTG at two distinct periods including c. 3325 Ma in the eastern part of the EPGGT, and at c. 3240 Ma across the western, northern, and northeastern parts of the EPGGT. The resultant granitic melts (Collins, 1993) migrated up the pre-existing perturbations in the TTG sill complex and were emplaced as little-deformed plutons into the cores of rising granitoid complexes during partial convective overturn of the crust (Collins, 1989; Williams and Collins, 1990; Collins et al., 1998; Van Kranendonk and Collins, in prep.).

Perhaps the most persuasive argument in favour of partial crustal overturn is the regional map pattern of domical granitoid complexes flanked by circular tracts of greenstones that have been affected by contact metamorphism (Fig. 3; Hickman, 1984; Van Kranendonk and Collins, in prep.). However, the diapir hypothesis is also supported by the autochthonous nature of successive groups in progressively deepening synclines, and by the repeated intrusion of successively younger phases of granitoid rocks into the cores of progressively evolving granitoid domes (Figs 4 and 15). A late component of this deformation is exemplified by the distribution of the Fortescue Group, which

is preserved in synclinal outliers over older synclines in greenstones between granitoid domes (see Fig. 2). In this model, the development of the dome-and-basin architecture occurred during periods of coeval granitoid plutonism and felsic volcanism at punctuated intervals over the entire evolution of the EPGGT, with distinct episodes at c. 3450, 3310, 3240, 2930, and c. 2760 Ma (Fig. 15; Hickman, 1984; Collins et al., 1998) and with different domes attaining their maximum heights at different times (Fig. 16). Contact metamorphism of greenstones occurred along the margins of progressively more steeply inclined granitoid domes at punctuated intervals throughout the protracted history of the region (Fig. 13), and the diapir model convincingly explains the localized presence of medium-pressure, kyanite-bearing metamorphic assemblages adjacent to some granitoid complexes (Collins and Van Kranendonk, 1999). These domes acted as conduits for the escape of heat from the mantle and lower crust to the surface through conduction, and in this light, the domes may be viewed as very long lived crustal-scale 'boils' (e.g. Hickman, 1984).

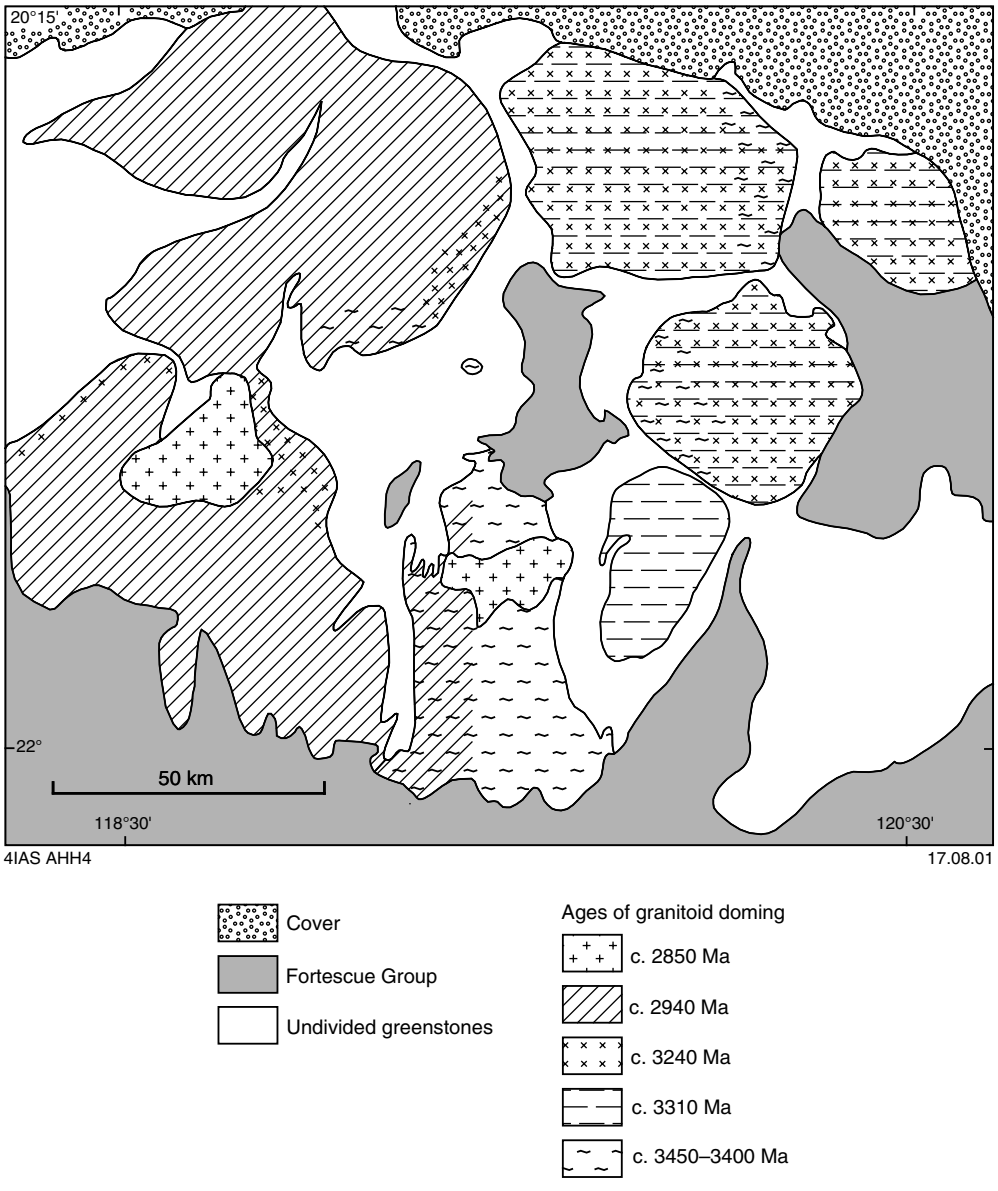

Figure 16. Diagrammatic sketch showing the ages of major doming episodes in each of the granitoid complexes. Note the prevalence of c. 2940 Ma doming in the western complexes

3280–3220 Ma: Plume-generated rifting

From about 3280 Ma, the WPGGT evolved over the same time interval as the EPGGT (Table 3). Events with common ages between the two terranes include:

- deposition of the c. 3270–3250 Ma Roebourne Group and coeval intrusion of the Karratha Granodiorite in the Karratha domain of the WPGGT; synchronous with deposition of the Sulphur Springs Group in the EPGGT, possibly from c. 3280 Ma, but definitely from c. 3255–3235 Ma;
- granitoid plutonism across the northern part of the EPGGT from 3252 to 3242 Ma;
- a 3236 Ma detrital zircon from the basal Cleaverville Formation of the Cleaverville domain;
- granite plutonism at c. 3236 Ma in the Cherratta Granitoid Complex south of the Sholl Shear Zone in the WPGGT.

Although a back-arc setting has been proposed for the felsic volcanic rocks and associated VHMS mineralization of the Kangaroo Caves Formation of the Sulphur Springs Group (Vearncombe et al., 1998; Vearncombe and Kerrich, 1999; Brauhart, 1999), the upward progression in the group from ultramafic to felsic volcanic rocks is atypical of such a setting, as are the large volume of silicic volcanic rocks and the unconformable lower contact of the group with older basement. An alternative hypothesis is that the Sulphur Springs Group represents the products of a mantle plume erupted beneath, and contaminated by, continental crust of the EPGGT, in a manner similar to that described for other Archaean greenstone belts (cf. Dostal and Mueller, 1997; Tomlinson et al., 1999; Zhou et al., 2000). This model is based on a close similarity between the composition of Sulphur Springs Group komatiites and ultramafic–mafic magmas erupted in Phanerozoic oceanic plateaus formed over mantle plumes (cf. Arndt et al., 1997), but differs from the latter in that the Sulphur Springs Group plume magmas became significantly contaminated up-section by sialic basement (as indicated by unpublished GSWA data). The lower komatiites were generated from the plume core, whereas basalts were generated from entrained upper mantle or mantle melted by the plume (cf. Campbell et al., 1989). The more silicic Kangaroo Caves Formation represents the more fractionated or highly contaminated part of the suite (or both), the latter supported by $T_{(2\text{-stage})}$ model ages of between 3507 and 3459 Ma (Brauhart, 1999). The almost within-plate geochemistry of the Strelley Granite (Brauhart, 1999) can be rationalized with evidence for melting of the TTG basement in the adjacent Yule Granitoid Complex (Van Kranendonk, 1997). Significant heat was imparted across the EPGGT by this magmatic event, as evidenced by widespread melting of the mid-crustal TTG sill complex at this time, to produce new granitoid intrusions in the Yule, Muccan, Warrawagine and Mount Edgar Granitoid Complexes. Granite intrusion was accompanied by doming (Van Kranendonk and Collins, 1998; Nelson, 1998, 1999) and contact metamorphism (Wijbrans and McDougall, 1987).

Significantly, the Roebourne Group overlaps in age with the Sulphur Springs Group and yields Nd T_{DM} model ages that overlap with the Warrawoona Group of the EPGGT, suggesting that the Roebourne Group may be underlain by EPGGT crust or mantle or both (Sun and Hickman, 1998). If so, it is possible that the Karratha domain in the WPGGT is the preserved part of a rifted fragment of the EPGGT (Hickman et al., 2001).

3160–2945 Ma

Geochronology on the crustal evolution of the North Pilbara Terrain between 3160 and 2945 Ma is currently largely restricted to data obtained from the WPGGT and Mallina Basin (Table 3), and these data are documented and interpreted in an accompanying excursion guide (Hickman et al., 2001). In the EPGGT, events during this period appear to have been limited to intrusion of c. 3160 Ma granitoids along the eastern margin of

Table 3. Middle to Late Archaean geological history of the North Pilbara Terrain

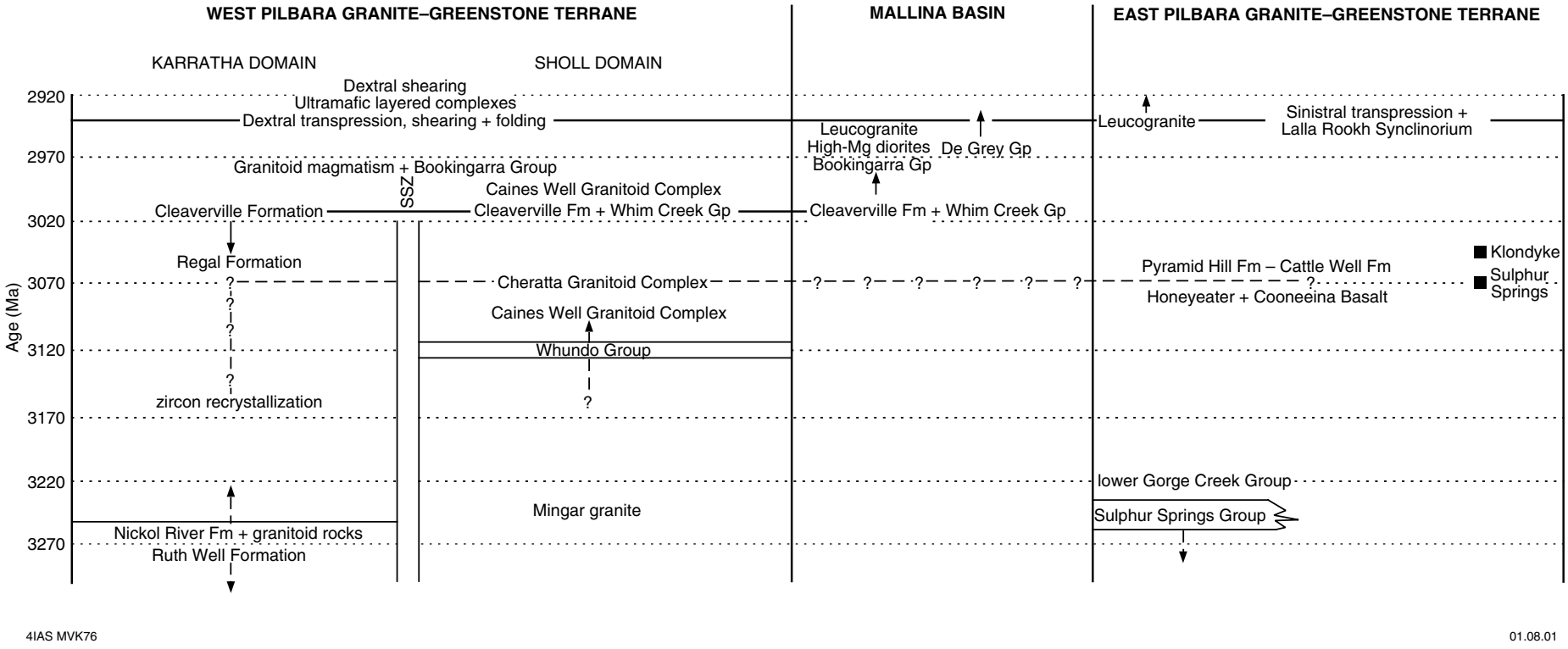

what later developed into the Mallina Basin, and continued deposition of the Gorge Creek Group, including deposition of the Cleaverville Formation.

Late Archaean tectonic evolution

2945–2920 Ma: Compression

Rifting changed to compression across the Mallina Basin at c. 2945 Ma, causing renewed sedimentation, widespread monzogranite plutonism, and the extensive development of northeasterly-trending structures across the Central Pilbara Tectonic Zone (CPTZ). These D_4 structures also continue into the western part of the EPGGT, where they consist of north-northeasterly trending folds across the Yule Granitoid Complex (e.g. Wodgina Syncline, Tambourah Dome) and structures within the sinistral transpressional Lalla Rookh – Western Shaw structural corridor (Table 3; Van Kranendonk and Collins, 1998; Zegers et al., 1998). Deposition of the coarse-clastic De Grey Group in the Lalla Rookh Basin was synchronous with, and resultant from, sinistral transpression. Deformation and sediment deposition was accompanied, and followed, by monzogranite magmatism between 2941 and 2931 Ma in the CPTZ. This magmatism forms part of a more regional magmatic event that also affects the eastern half of the WPGGT and western half of the EPGGT. Monzogranite magmatism is most voluminous immediately adjacent to the CPTZ, and decreases in volume and age eastwards into the EPGGT where it was emplaced between 2936 and 2919 Ma. As mentioned above, Van Kranendonk and Collins (1998) and Van Kranendonk (2000a) documented stratigraphic links across the LWSC that show it is an entirely intracontinental structure and not the site of terrane accretion as proposed by Krapez (1993).

Dextral offset across the Sholl Shear Zone (WPGGT) and sinistral offset across the LWSC indicates a northwest–southeast orientation of σ_1 at this time (Van Kranendonk and Collins, 1998). The synchronous deposition of coarse clastic rocks on either side of the Yule Granitoid Complex and emplacement of voluminous granitoid magmas in the core of the complex suggests a linked evolution of these events. A possible model for such linked evolution follows on from the scenario illustrated in Figure 17a, whereby the effects of the broad thermal anomaly at c. 2955 Ma caused partial melting of the lower crust. These melts migrated up through the crust and were emplaced as granitoid plutons at higher structural levels. Granite emplacement caused domal amplification of the Yule Granitoid Complex (Fig. 17b) and was accompanied by erosion of the top of the dome. Uplift and erosion was accompanied by deposition of coarse clastic sedimentary rocks in flanking basins. Northerly directed transport of the older greenstone cover into the Wodgina Syncline and flanking synclinal greenstone belts was accommodated by dextral and sinistral shearing on the western and eastern flanks of the dome respectively (Fig. 17b).

2920–2850 Ma: Compression in the southeast

At c. 2920–2850 Ma, the EPGGT was affected by shearing with associated gold mineralization, and by tin–tantalum bearing granite plutonism. We speculate that this event was due to shortening across the Mosquito Creek Basin. This finalized the formation of the North Pilbara Terrain, although the pre-existing dome-and-basin geometry of the EPGGT, as well as many faults throughout the CPTZ and WPGGT, was subsequently reactivated during and after deposition of the Fortescue Group.

a) Stage 1: Mantle upwelling and lithospheric extension
Deposition of Whim Creek Group and lower Mallina Basin

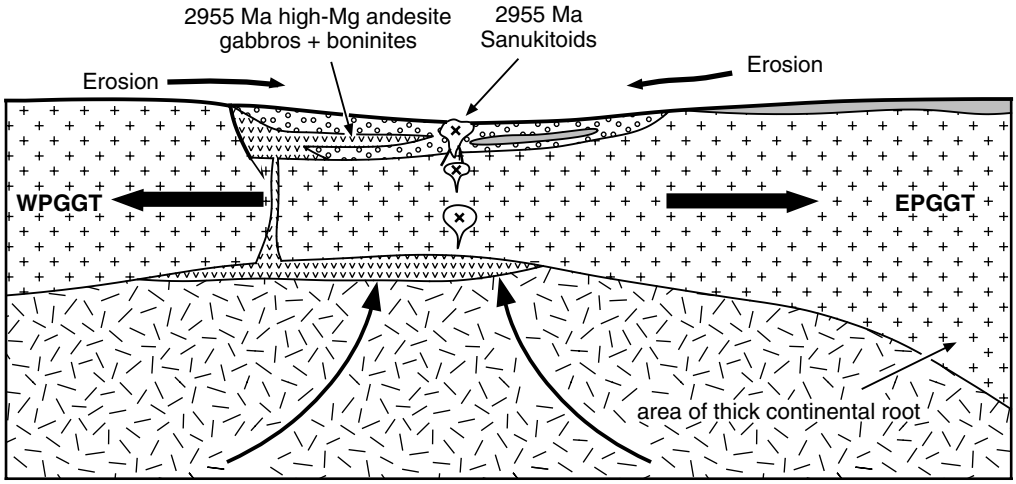

b) Stage 2: Doming of Yule Granitoid Complex and deformation of adjacent greenstones (c. 2940 Ma)

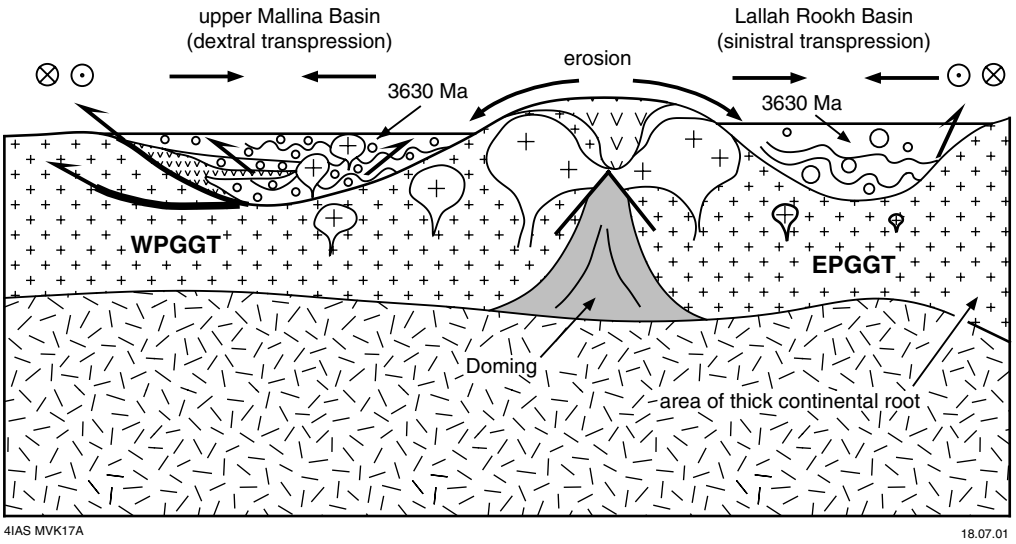

Figure 17. Schematic evolution of the central Pilbara region: a) mantle upwelling and extension at c. 2970–2955 Ma resulted in the formation of the Mallina Basin and intrusion of sanukitoid magmas; b) further heating caused widespread melting of pre-existing granitoid crust and doming of the Yule Granitoid Complex at c. 2940 Ma. Uplift of the complex resulted in erosion and deposition of clastic sedimentary rocks in the flanking Mallina and Lalla Rookh Basins; note that both basins contain c. 3630 Ma detrital zircons. Doming of granitoid rocks was accompanied by shortening across the synkinematic basins, with dextral transpression in the west and sinistral compression in the east (Lalla Rookh – Western Shaw structural corridor).

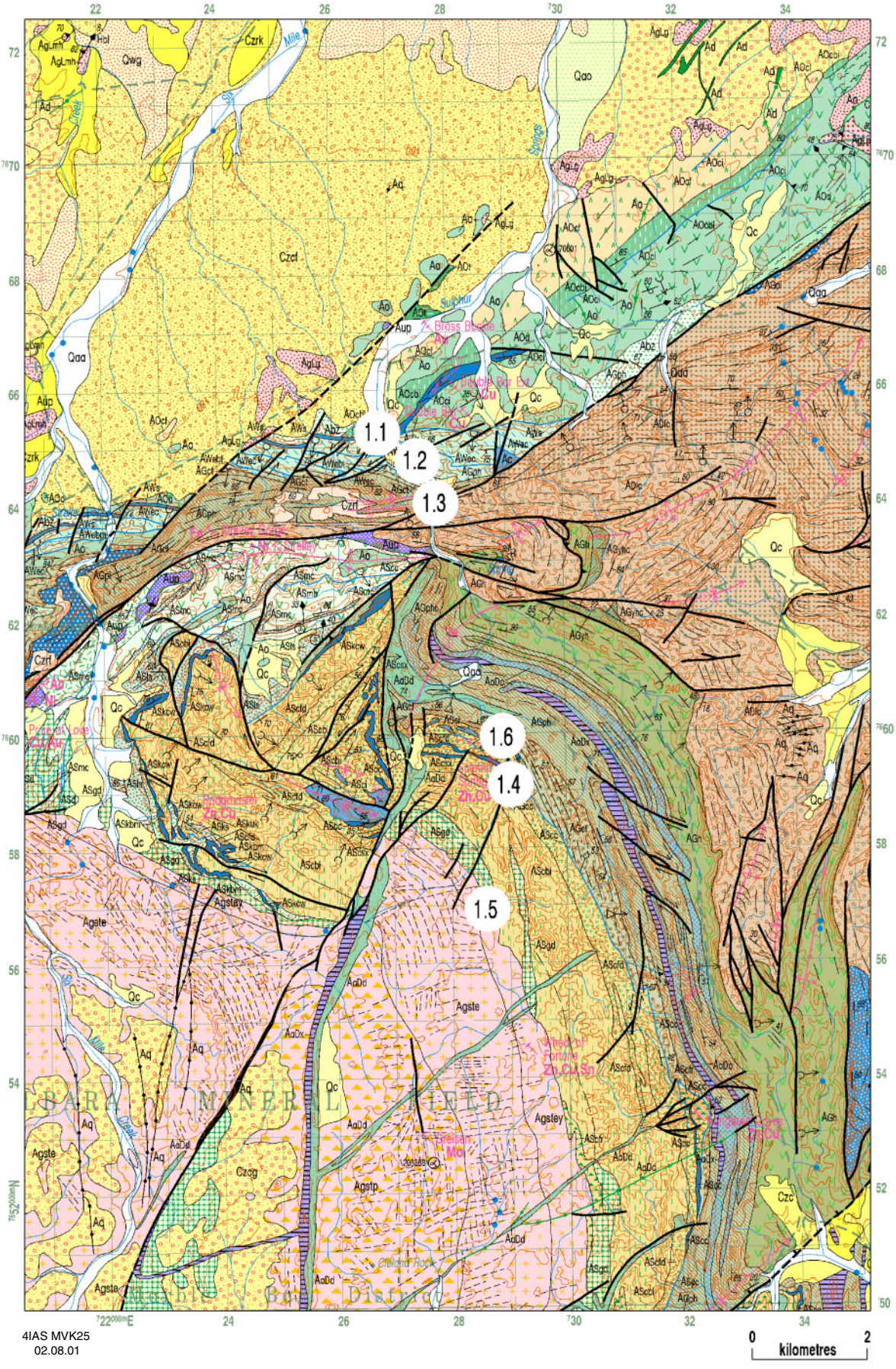

Figure 18. Portion of the North Shaw 1:100 000 sheet (Van Kranendonk, 1999a) showing the excursion localities for Day 1

Excursion localities

Day 1: Stratigraphy of the East Strelley and Soanesville greenstone belts

by M. J. Van Kranendonk (Geological Survey of Western Australia)

During the first day, the characteristic lithostratigraphy of the Pilbara Supergroup will be examined, including the c. 3515 Ma Coonterunah Group, its unconformable contact with overlying rocks of the upper part of the Warrawoona Group (3430 Ma Strelley Pool Chert and Euro Basalt), the upper part of the c. 3240 Ma Sulphur Springs Group, the Gorge Creek Group (between c. 3240 and 2940 Ma), and the c. 2940 Ma De Grey Group. The excursion localities for Day 1 are on the NORTH SHAW* 1:100 000 sheet and shown in Figure 18.

Locality 1.1: Angular unconformity between the Strelley Pool Chert and the Coonterunah Group (NORTH SHAW, AMG 726800E 7665200N)

From Port Hedland Airport: turn right and drive east on the North West Coastal Highway for 37 km, then turn right onto Highway 138 towards Marble Bar and proceed for 54.3 km. Just past a cattle grid, about 100 m before the Shaw River crossing, turn right on to a dirt track that leads to the Lalla Rookh mine and beyond (unsigned). Stop to put in the hubs and engage four-wheel drive. Drive along the track for about 32.8 km, at which point you will have a good view of the range of orange-brown hills that rise in front of you, which are underlain by coarse sandstones and conglomerates of the c. 2940 Ma Lalla Rookh Sandstone of the De Grey Group, the youngest succession of the Pilbara Supergroup. Unexposed at the foot of the linear range extending for almost as far as you can see in either direction is the northeast–southwest striking fault that forms the western boundary to the c. 2940 Ma Lalla Rookh – Western Shaw structural corridor of sinistral transpression. Continue driving for 19 km, past the defunct Lalla Rookh gold mine on the left, and turn sharp left at a fork in the track towards the base of the range. Continue for a further 1.3 km to the base of the range. Park in the creekbed, on the right side of the track at the foot of a prominent east–west ridge.

Low total strain in this part of the East Strelley greenstone belt has resulted in excellent preservation of the oldest recognized angular unconformity in the world between northeast-striking, slightly overturned volcanic and interbedded volcaniclastic rocks of the c. 3515 Ma Coonterunah Group, and the overlying, easterly–westerly striking c. 3430 Ma Strelley Pool Chert of the Warrawoona Group (Fig. 19; Buick et al., 1995). At this locality we will observe D_1 folds in the Coonterunah Group, the angular unconformity at the base of the Strelley Pool Chert, and textural features of the Strelley Pool Chert.

On the north-facing hillslope are two, 2 m-thick units of black-and-white layered cherty metasediment interbedded with fractured, but otherwise featureless, metavolcanic rocks belonging to the Coucal Formation of the Coonterunah Group. Rare graded bedding within the cherts are consistent with pillow facing directions from elsewhere in the group indicating that the rocks are slightly overturned and face to the southeast. The eastern cherty unit forms a planar, subvertical ridge that strikes towards the base of the east–west striking, subvertical Strelley Pool Chert. The eastern cherty unit formed an 18 m-high palaeoridge during deposition of the Strelley Pool Chert and is cut by

* Capitalized names refer to standard 1:100 000 map sheets.

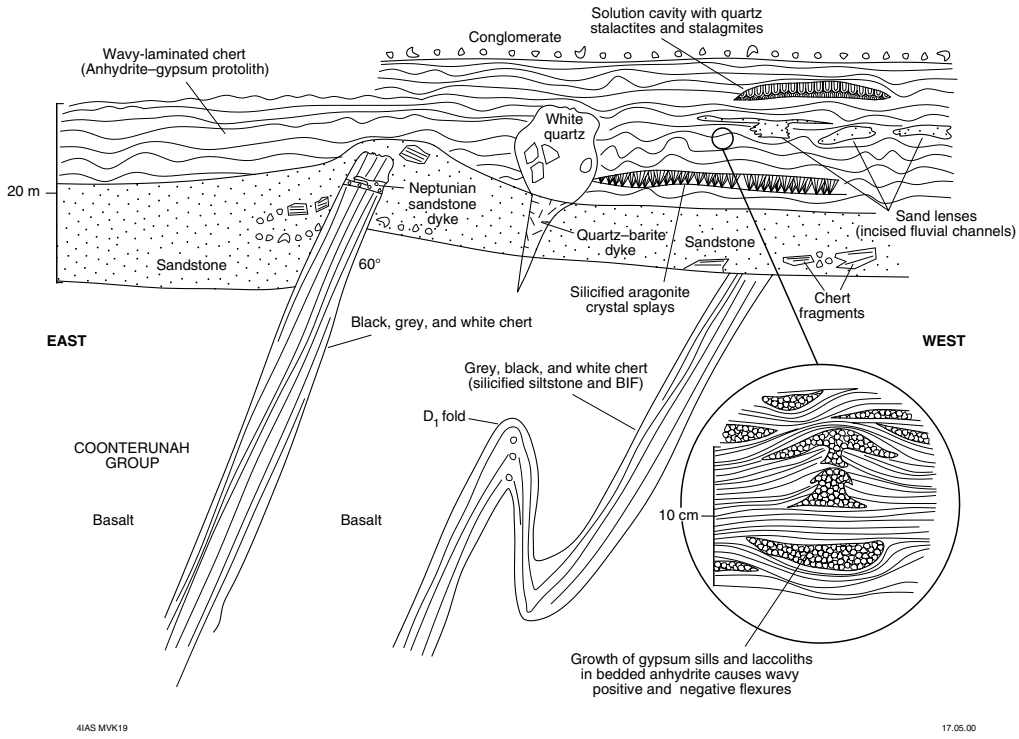

Figure 19. Sketch, looking south, of the unconformity beneath the Strelley Pool Chert at Locality 1.1

Neptunian sandstone dykes at the top of the cherty unit and flanked by small palaeovalleys filled by conglomeratic lags and quartz sandstone beds. The western cherty unit of the Coonterunah Group is folded into a tight 'Z'-shaped asymmetric D_1 fold midway up the hill. The eastern hinge of this fold snapped during buckling and is marked by breccia, whereas the western hinge of the fold is a ductile structure. The western limb of the folded cherty unit can be traced up the side of the hill to the base of the Strelley Pool Chert where bedding is sharply truncated by the basal sandstone and conglomerate of the Strelley Pool Chert. The presence of angular boulders and cobbles of the cherty metasedimentary rock in basal quartzite of the Strelley Pool Chert west of the unit indicates that water flowed 'downstream' to the west at this time.

The D_1 folds in the cherts are not present in rocks of the overlying Strelley Pool Chert and younger formations, and thus are interpreted to be older than c. 3430 Ma, which is the estimated age of the Strelley Pool Chert. Back-rotation of the subvertical Strelley Pool Chert to horizontal indicates that the D_1 folds formed on shallow-plunging axes (Fig. 20). Fold asymmetry indicates translation of the Coonterunah Group to the east, away from the c. 3484–3468 Ma Carlindie Granitoid Complex, which underlies the plains to the north (Buick et al., 1995; Nelson, 1998). The fold asymmetry is consistent with lateral gravitational collapse of greenstones from off the Carlindie Granitoid Complex during doming.

The Strelley Pool Chert is a 10–30 m-thick succession of characteristically white and grey layered chert that. Bedding dips 70–80° to the south and cuts at a high angle across bedding that strikes northeasterly in the underlying Coonterunah Group. At this locality, the Strelley Pool Chert comprises basal quartzite with subordinate conglomerate, an intermediate unit of thinly bedded and commonly wavy-laminated chert of problematic origin, and an upper unit of conglomerate. Along strike to the west, in places, the siliceous laminites pass gradationally into patches of relict carbonate

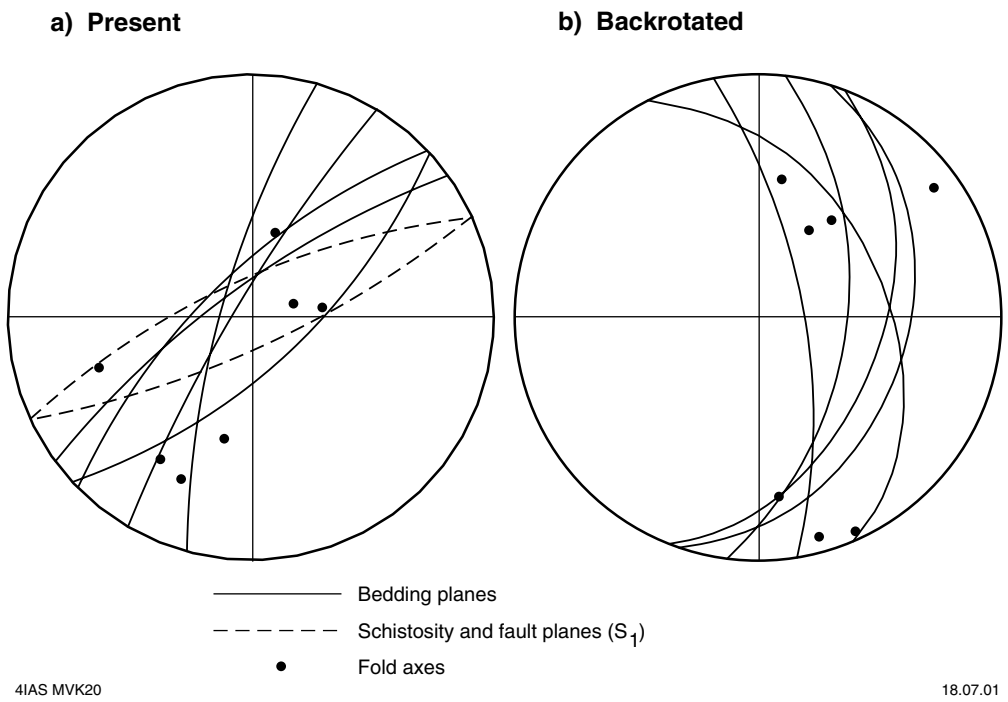

Figure 20. Equal area stereoplots of structural data from the Coonterunah Group beneath the unconformity of the Strelley Pool Chert at Locality 1.1: a) measured fabric elements; b) bedding planes and fold axes of (a), backrotated 90° to the north about an east–west axis, reflecting restoration of the subvertically dipping unconformity beneath the Strelley Pool Chert to the horizontal. Note the moderate easterly dip of bedding and the shallow plunge of fold axes

laminite, which contain identical textures as those in silicified counterparts. Lowe (1983) suggested that the basal quartzite was deposited in a high-energy, shallow-water environment, an interpretation supported by the presence of an erosional pothole at the base of the unit along strike to the west (Fig. 21). The laminites were interpreted as a regressive succession of subaqueous wavy laminate, stromatolitic and evaporitic rocks, and intraformational detrital units deposited under intermittent to predominantly exposed conditions. The upper conglomerate was interpreted as a progradational sequence of a volcaniclastic alluvial fringe. Lowe (1983) suggested that silicification may have occurred long after deposition, during or after a karstic event of carbonate dissolution, although there is evidence that some, if not all, silicification must have occurred during, or soon after, deposition of the sediment because an intrusive quartz–barite dyke in the chert does not penetrate into the overlying volcanic rocks (Fig. 19). Silicification was accompanied by quartz–sericite alteration of metabasalts immediately underlying the Strelley Pool Chert (Fig. 22).

Along the ridge of Strelley Pool Chert at this locality, one can see several distinctive textures that give clues to the origin of the wavy-laminated chert. The wavy-laminated chert is composed of variable amounts of fine-grained, well-laminated grey material with irregular layers and lenses of coarser grained, nonlaminated white material (both now silica). It is not clear whether the wavy flexures in these cherts locally represent stromatolites (Lowe, 1983, 1994), but in this area the presence of positive *and* negative flexures in the laminated cherts indicate that they are not stromatolites (this is in contrast to other parts of the chert, where positively flexed conical stromatolites have been documented by Hoffman et al., 1999). A clue to the origin of the wavy laminations may be obtained from detailed inspection of the distribution of the white material in

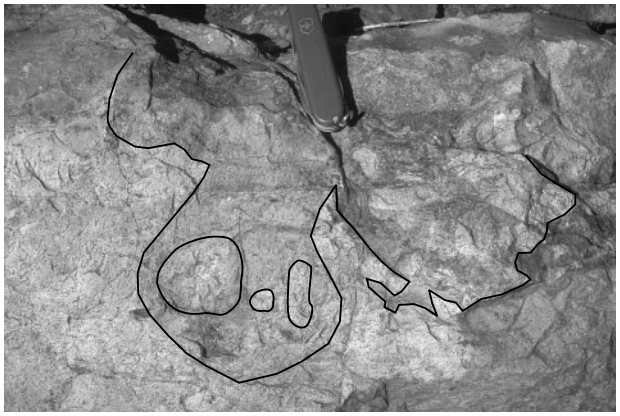

4IAS MVK137 02.08.01

Figure 21. Photograph of the unconformity between the Strelley Pool Chert and the Coonterunah Group at Strelley Pool, showing a pothole developed in underlying silicified and altered metabasalt of the Coonterunah Group. The pothole is filled by quartz sandstone of the base of the Strelley Pool Chert and by scouring pebbles of silicified metabasalt (outlined)

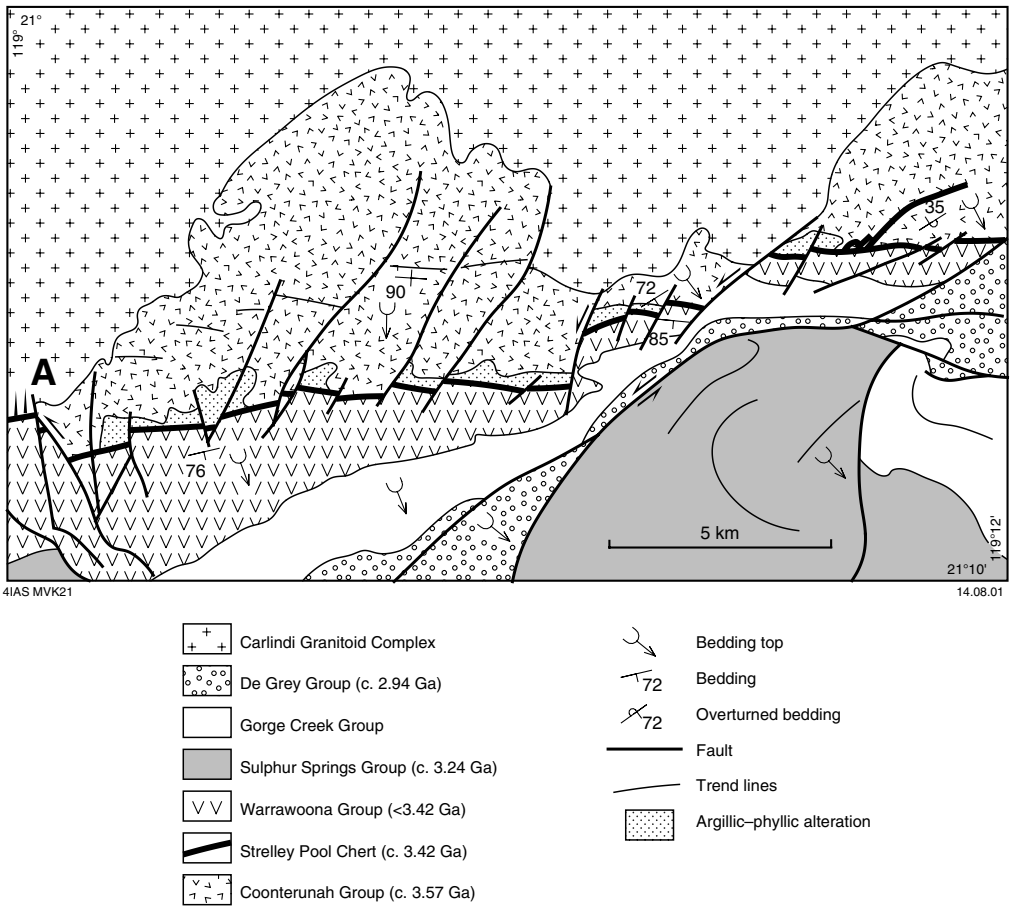

Figure 22. Simplified geological map of the Strelley Pool Chert in the East Strelley greenstone belt, showing the zone of underlying argillic–phyllic alteration, and the position of hydrothermal chert feeder dykes at A

the cherts. As one proceeds along the ridge, it may be observed that the bulk of the rock is composed of finely laminated grey material and that the proportion of white material varies. Where the white material increases, there is an increase in the degree of waviness of laminations in the rock. The white material forms sills and small laccoliths in the grey material that prised open and expanded the bedding, and thereby caused the flexing (inset of Fig. 19). The preferred interpretation of the origin of these wavy textures is that the transition from grey laminated material to white featureless material represents a diagenetic change from anhydrite to gypsum, accompanied by a volume increase and a resultant flexing of original bedding.

Locality 1.2: Pillowed high-Mg basalt of the Euro Basalt, Warrawoona Group (North Shaw, AMG 727400E 7664700N)

Return to the track and turn right, southward. Proceed for 1 km to a low outcrop on the right.

Weakly flattened pillow basalts of the Euro Basalt, Warrawoona Group, are well exposed on the west bank of Sulphur Springs Creek at this locality. These pale-brown-weathering, high-Mg basalts (MgO = 5–10 wt%) dip at 85° to the north, but show good evidence of facing to the south and are thus slightly overturned. Pillows show chilled vesicular margins, variolitic cores, and interpillow hyaloclastite breccia. The pillows are slightly carbonate altered, which is visible in the interpillow hyaloclastite breccia as recessive-weathering, medium-brown material.

Geochemistry

Glikson et al. (1986; samples 69946–69964) presented a geochemical transect through the Euro Basalt about 13 km west of this locality. Major- and trace-element data indicate vertical changes in mafic magma composition within three flow units (Fig. 23). The most striking of these changes occurs in the lower unit, in which MgO, Al_2O_3 and Ni all decrease upward and then become replenished again, almost to initial values. All three units show a saddle-shaped pattern of initial MgO depletion and then enrichment, and this is accompanied by changes in FeO_{total} (decreasing towards the top in the upper two cycles) and Al_2O_3. Such changes may reflect successive pulses of magma replenishment during eruption, and intervening fractional crystallization.

Locality 1.3: Banded iron-formation of the Paddy Market Formation, Gorge Creek Group; Lalla Rookh – Western Shaw Fault; Lalla Rookh Sandstone (North Shaw, AMG 727800E 7664100N)

Continue south along the track for about 750 m to Locality 1.3.

Representative red and black BIF of the Paddy Market Formation, Gorge Creek Group, is well exposed in this small roadside outcrop and is representative of the rocks that form the high dark-red hills to the west.

About 25 m farther south, and partway up the slope, is an exposure of the curviplanar western boundary fault of the Lalla Rookh - Western Shaw structural corridor of sinistral D_4 (c. 2940 Ma) transpression that transects the EPGGT for a distance of more than 150 km in a north–south direction (Fig. 10; Van Kranendonk and Collins, 1998). Here the fault is a brittle structure, about 5 m wide, trending about 233°, and dipping 30–60° to the northwest. It is composed of silicified fault breccia, fractured Lalla Rookh Sandstone of the De Grey Group, and lumps of massive ironstone derived from the Paddy Market Formation.

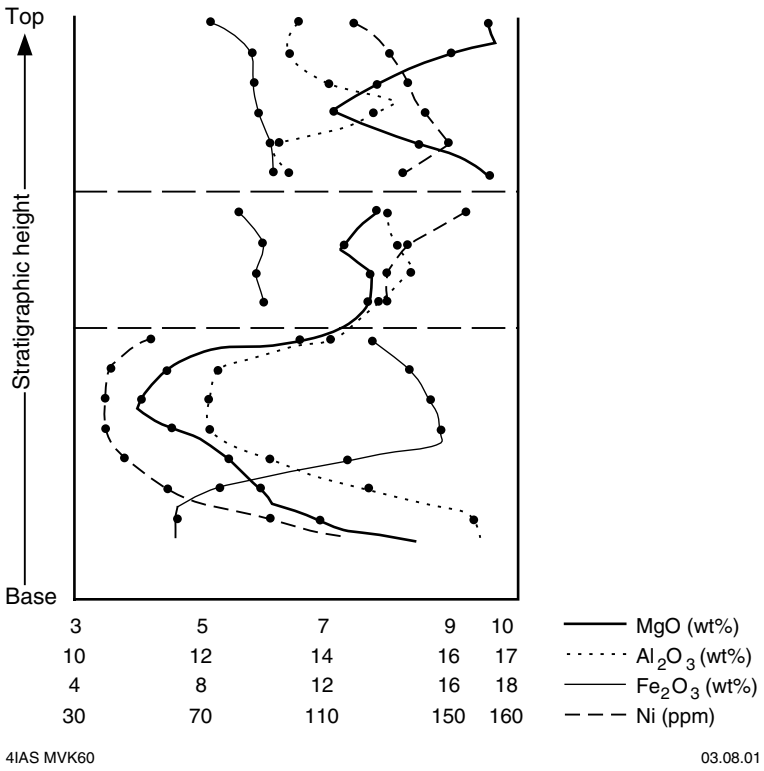

Figure 23. Changes in geochemical composition of the Euro Basalt in the East Strelley greenstone belt (data from Glikson et al., 1986)

Continuing south along the side of the creek, one passes through a tilted, but little-deformed part of the Lalla Rookh Sandstone. This is a synorogenic clastic succession of coarse feldspathic sandstone and polymictic conglomerate, deposited during the northerly translation of the Strelley Granite and associated supracrustal rocks during regional D_4 sinistral transpression. The subvertically dipping rocks include weakly foliated sandstones proximal to the fault, but these pass into undeformed pebble to cobble conglomerate about 30 m farther south. Clasts include quartzite, black chert, banded mudstone, BIF, and felsic volcanic rocks.

Krapez (1984, 1993) proposed a strike-slip pull-apart model for the Lalla Rookh Sandstone in the Lalla Rookh Synclinorium, in which fault displacement was inferred to have been transferred from the northwestern boundary to the southeastern boundary across a transfer fault located either beneath the basin or to the southwest where a thrust fault was inferred (Fig. 11a). However, detailed mapping in this region has failed to locate evidence of this thrust fault (Van Kranendonk, 1999a, 2000a). Furthermore, Van Kranendonk and Collins (1998) noted that the northwestern fault continues for a great distance to the south and the southeastern fault has an oblique, north-side-down and dextral sense of displacement and is not continuous to the northeast as required by the pull-apart model. Instead, based on the regional pattern of D_3 structures throughout the LWSC, Van Kranendonk and Collins (1998) proposed that the Lalla Rookh Sandstone was deposited initially over a much larger area and then concentrated in a trough in advance of the north-moving Strelley Granite, bound by strike-slip faults with opposite senses of relative displacement (Fig. 11b).

Note: By this point, after travelling a total of 1.5 km from Locality 1.1, you will have traversed through four unconformity-bound groups that span 575 m.y. (3515–

2940 Ma), or slightly more than the entire Phanerozoic era! This succession is typical of many Archaean granite–greenstone terranes, and documents progressive cratonization, from marine pillow basalts with high-Mg compositions, to BIF and shale, to intra-continental sandstone and conglomerate.

Locality 1.4: Flow-banded, vesicular rhyolite and marker chert, Kangaroo Caves Formation, Sulphur Springs Group (North Shaw, AMG 728800E 7659500N)

Continue south along the track. At 1.5 km, notice the shallow-dipping beds of the Lalla Rookh Sandstone to the east. At 1.7 km, look right at the cliffs of folded BIF of the Gorge Creek Group. Continue for a further 700 m (2.4 km cumulative) to the creek and turn right. Proceed for 1.7 km until you just exit the creek and then turn right. Continue for 2.6 km and notice, as you drive by, dark-weathering outcrops of tholeiitic basalt–andesite forming the base of the c. 3240 Ma Kangaroo Caves Formation of the Sulphur Springs Group. Proceed a further 1.5 km south and take the left fork. ***Engage low four-wheel drive — steep ascent follows****. Follow the track for 2.6 km to the top of the hill, keeping to the left at all forks. Park vehicles at the top of the hill, just before a low chert ridge at Locality 1.4.*

At this locality are flows, several metres thick, of highly vesicular rhyodacite of the c. 3240 Ma Kangaroo Caves Formation of the Sulphur Springs Group. The flows vary from those with macrospherulitic (and ?peperite) texture to others with well-developed flow banding defined by trains of 'folded' vesicles. In one flow-banded rhyolite, vesicles wrap concentrically around several quartz-filled gas vents up to 20 cm in diameter.

About 50 m to the north is a 20 m-thick unit of cherty silicified felsic tuff, which forms the top of the Sulphur Springs Group over much of the region. The chert is a millimetre-bedded tuff composed of grey felsic ash. Black chert layers represent intrusive sills emplaced during hydrothermal circulation driven by the heat of intrusion of the Strelley Granite laccolith, which was emplaced about 1.5 km below the sediment–water interface (Figs 24 and 25). The black chert sills were fed by veins emplaced along growth faults emanating up and radially out from the Strelley Granite (Vearncombe et al., 1998).

The Sulphur Springs gossan is about 600 m to the east, over the edge of a cliff. This is the largest of a group of five zinc–copper VHMS prospects at the base of the marker chert at the top of the Sulphur Springs Group, spaced at regular 5–7 km intervals around the Strelley Granite (Fig. 24). A sixth prospect, the Bernts prospect, is at the same stratigraphic level, but within the fault-bound Bernts deformation zone of folded, sheared, and brecciated rocks located between the Soanesville and Panorama greenstone belts to the east. The Cardinal and Jamesons prospects and Roadmaster mineral occurrence are about 1 km stratigraphically below the other prospects.

Since 1989, 50 000 m of diamond drilling and reverse circulation drilling by Sipa Resources has identified the following inferred and indicated resource estimates (Morant, 1998):

- Sulphur Springs: 2.8 Mt at 10.7% Zn and 0.6% Cu, and 2.5 Mt at 1.1% Zn and 4.0% Cu
- Kangaroo Caves: 1.7 Mt at 9.8% Zn and 0.6% Cu
- Bernts: 0.6 Mt at 7.8% Zn and 0.3% Cu.

The zinc–copper mineralization at Sulphur Springs is hosted within a 200 m-thick dacite sill immediately beneath the marker chert, within the marker chert itself, and rarely in the hangingwall rhyodacite (Morant, 1998). The mineralization is zoned, from

zinc rich within the marker chert to copper rich beneath the marker chert. The sulfide assemblage at Sulphur Springs and Kangaroo Caves comprises pyrite, low-iron sphalerite, chalcopyrite, and galena, with minor arsenopyrite and tennantite–arsenopyrite (Vearncombe, 1996; Morant, 1998; Vearncombe et al., 1998; Buick and Doepel, 1999). Well-preserved ore textures include dendritic, colloform, and botryoidal types that may have formed by open-space precipitation of sulfides (Vearncombe, 1996; Vearncombe et al., 1995, 1998). Vearncombe et al. (1995) considered that the development of some delicate sulfide textures, such as spherical pellets and stromatolitic types, were analogous to black-smoker sulfide chimneys developed at present-day submarine hydrothermal vents. Rasmussen (2000) described microbes from sulfides at Sulphur Springs.

Zinc–copper mineralization at the five main prospects around the Strelley Granite is spatially related to growth faults emanating from the granite (Fig. 24; Vearncombe et al., 1998). Mineralized prospects are surrounded by a zone of related feldspar-destructive chlorite–quartz alteration (Brauhart et al., 1998). Farther away from the

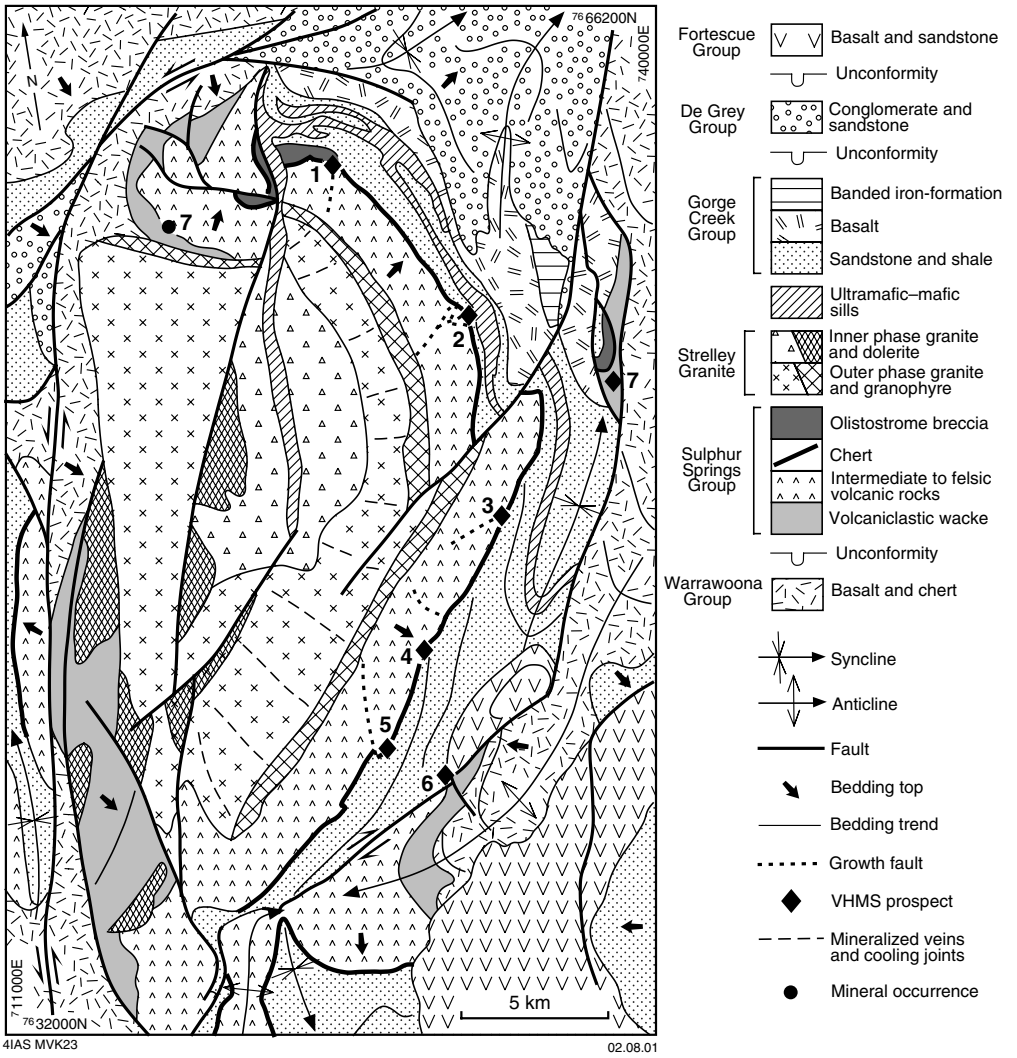

Figure 24. Simplified geological map of the Strelley Granite, showing volcanogenic massive sulfide prospects and the principal D_4 structures. Prospects: 1 = Sulphur Springs, 2 = Kangaroo Caves, 3 = Breakers, 4 = Man O'War, 5 = Anomaly 45, 6 = Jamesons. Mineral occurrence: 7 = Roadmaster

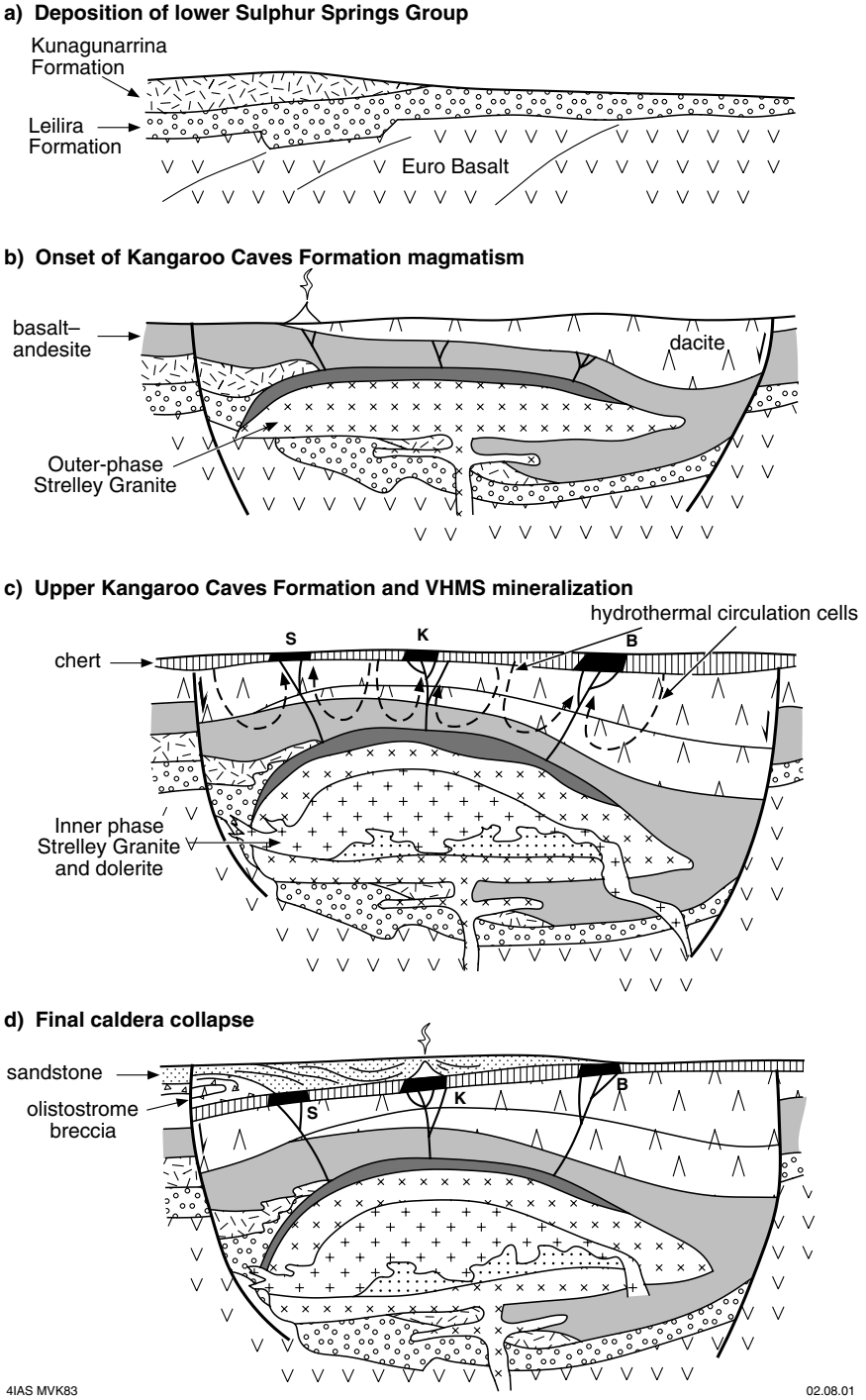

Figure 25. Schematic evolution of the Sulphur Springs Group and Strelley Granite: a) unconformable deposition of the lower part of the Sulphur Springs Group on the Euro Basalt; b) intrusion of the outer phase of the Strelley Granite with a granophyric carapace, and deposition of intermediate to felsic volcanic rocks in the lower part of the Kangaroo Caves Formation during the onset of block faulting. Note the asymmetrical tilting of older strata (south-side-down) and the resultant slightly discordant lower contact of the granite; c) intrusion of the inner phase of the Strelley Granite during continued block faulting and felsic volcanism. Extensive hydrothermal circulation cells are instigated during the late stage of magmatism, resulting in precipitation of massive sulfides beneath an impermeable marker chert unit of silicified epiclastic sediments; d) asymmetrical (north-side-down) late-stage caldera collapse results in deposition of an olistostrome breccia at Sulphur Springs (S) and coarse sandstone turbidites that onlap the marker chert between Sulphur Springs and a late volcanic dome at Kangaroo Caves (K; B = Breakers prospect)

mineralized prospects, sericite–quartz(–carbonate) and albite–carbonate(–pyrite) alteration facies have been recognized. Sulfide mineralization is in veins with greisen-altered margins in the outer phase of the Strelley Granite. Porphyry molybdenum in greisen has locally been observed near the top of the inner phase. These data indicate that the intrusion of the Strelley Granite caused extensive hydrothermal circulation that led to the deposition of the associated base metal mineralization (Vearncombe et al., 1998).

Geochronological and geochemical similarities between the Strelley Granite and felsic volcanic rocks of the Kangaroo Caves Formation (Vearncombe, 1996; Brauhart, 1999) indicate that the Strelley Granite was a synvolcanic laccolith during eruption of the Kangaroo Caves Formation. Such an inter-relationship between volcanism, granite-laccolith intrusion, and massive sulfide mineralization is characteristic of Archaean to Holocene volcanogenic massive sulfide deposits, although the Strelley Granite is unusually potassic and alkaline.

A model for the magmatic and structural development of the Kangaroo Caves Formation, Strelley Granite, and VHMS mineralization is presented in Figure 25. In this model, eruption of the basal mafic volcanic sequence was followed by intrusion of felsic subvolcanic sills near the top of the volcanic pile, beneath a carapace of volcaniclastic and epiclastic sediments. Intrusion of the outer phase of the Strelley Granite as a sill, only 1.5 km below the surface–water interface, initiated extensive hydrothermal circulation which caused leaching of metals from the volcanic sequence (Brauhart, 1999) and silicification of the sedimentary carapace to form an impermeable cap. This was followed by intrusion of the inner phase of the Strelley Granite and comagmatic dolerite, causing asymmetrical inflation of the sill into a sphenolith. Inflation was accommodated by the development of growth faults in the overlying volcanic sequence (Vearncombe et al., 1998), and of mineralized extension veins into the outer rind of the granite. Since the extension veins and growth faults are both mineralized, it is thought that the bulk of mineralization in the main prospects beneath the marker chert was deposited at this time.

Locality 1.5: Outer phase rind of the Strelley Granite laccolith, from microgranophyre to equigranular monzogranite (North Shaw, AMG 728700E 7656700N)

Drive east along the east track for about 600 m and take the right fork downhill for 2.05 km, back out the way you came. Turn left at the fork in the road and proceed for 900 m. Turn left at the fork in the road and then proceed for a further 2.4 km to Locality 1.5.

This short traverse to the west passes through the outermost, quench-textured rind of the c. 3240 Ma, synvolcanic Strelley Granite laccolith to the Kangaroo Caves Formation of the Sulphur Springs Group. The first outcrops contain a distinctive clotty texture consisting of centimetre-sized mafic clots in microgranophyre granite. The mafic clots represent either the original distribution of mafic minerals during quenching or the effects of chlorite–epidote alteration (or both). A few narrow, zoned greisen veins cut the granophyre. These are representative of a much more pervasive, and commonly thicker, suite of greisen veins that cut the outer phase of the granite.

Continuing south for about 500 m, there is a gradual transition into a medium-grained, high-silica monzogranite that is characterized by abundant, 1–2 mm, euhedral to subhedral quartz phenocrysts. Feldspars are weakly zoned, and petrographic examination of samples shows that the rock has a rapakivi texture (plagioclase rims on K-feldspar).

Locality 1.6: Synsedimentary slump folds in olistostrome breccia of the Kangaroo Caves Formation, and peperite textures at the margin of a dacite sill (North Shaw, AMG 728600E 7659800N)

Return to the vehicles, turn them around and retrace the track in, heading north for 2.4 km. Turn right, continue for 900 m and turn left back onto the main track. Follow the track out for 4.1 km and turn right. After 900 m, turn right onto the track along Sulphur Springs Creek and continue about 500 m. Locality 1.6 is a short walk away.

There are several features to see by walking up the two forks of the Sulphur Springs Creek at this locality. The area of interest lies within a unit of very coarse olistostrome breccia that overlies the marker chert at the top of the Kangaroo Caves Formation, over a strike length of about 4 km on either side of the Sulphur Springs gossan. At this locality the breccia reaches a maximum of 1 km in thickness. It contains blocks of underlying lithology (dacite, marker chert, rare massive sulfides) and a dismembered, folded unit of ferruginous shale or BIF (or both). Dacite and massive chert blocks may be up to house size, whereas well-bedded cherty layers may form panels up to 300 m long and tens of metres thick. Although largely unsorted, thick, crude bedding is locally developed in the breccia (Hill, 1997). In places, the crude bedding outlines slump folds at the decametre and outcrop scale.

At a larger scale, the entire breccia represents a sedimentary slump, facing east, with the fold outlined by a 5–10 m-thick unit of ferruginous shale – BIF, which was originally deformed into a recumbent, east-facing fold. The matrix to the breccia is a fine-grained grey rock composed of fine-grained quartz–sericite. In thin section, shards of quartz and devitrified rhyolite glass are observed, suggesting that the matrix to the breccia is a reworked (and locally welded) rhyolitic tuff (Van Kranendonk, 2000a). The fold hinge is occupied by a dacite sill with a peperitic rind that was emplaced during slumping.

At the first stop there are exposures showing the hinge of a large-scale fold of the thin unit of ferruginous shale – BIF within olistostrome breccia at the top of the Kangaroo Caves Formation. Along strike to the southwest, several minor folds may be observed. Just upstream, the olistostrome breccia may be observed cutting down into the ferruginous shale – BIF, demonstrating the erosive nature of the breccia. Around the corner of the stream to the right, and partway up a small cliff on the north bank, chaotic synsedimentary slump folds with thrust faults are developed in the ferruginous shale – BIF (Fig. 26).

About 100 m farther upstream in the bed of the creek there is an excellent exposure of the olistostrome breccia. The fresh rock is light grey and the unit here is not bedded. The matrix is host to numerous angular clasts of a variety of rocks, including a 40 cm-long clast of folded shale. Dacite blocks and chert are the most common clast type.

Return downstream, then turn right up the main branch of Sulphur Springs Creek.

This is the head of Sulphur Springs Creek, which cuts through the Sulphur Springs gossan, and it contains abundant limonite staining along its length. It was the discovery of sulfate encrustations in this creekbed by H. Wilhelmij in 1984 that led to the discovery of the Sulphur Springs gossan and subsequently to the numerous other gossans that have been explored by Sipa Resources. About 200 m upstream there are yellow sulfate crystals in the creekbed. Slightly further upstream on the right is a small, separate spring emanating from a drillhole that has delicately encrusted rocks with zoned white (outer), yellow, and green sulfate minerals.

4IAS MVK218 02.08.01

Figure 26. Synsedimentary slump folds in banded iron-formation in the olistostrome breccia at the top of the Sulphur Springs Group at the Sulphur Springs prospect, Locality 1.6

Fit and enthusiastic people are strongly recommended to continue upstream, past two steep ledges, to the contact between the marker chert and the underlying dacite, where large boulders with spectacular peperite textures are in the creek bed. Peperite here was formed along the contacts of hot felsic lava emplaced as sills into wet sediment.

Return to your vehicles, turn around and head out on the track. At the first fork (300 m), turn right. Continue for 900 m and turn left. Proceed a further 1.15 km and turn right into the Sipa Resources exploration camp where we will camp for the night.

Day 2: Geology of the North Pole Dome

by M. J. Van Kranendonk (Geological Survey of Western Australia) and W. Nijman (Utrecht University, The Netherlands)

All of Day 2 and the morning of Day 3 will be spent in the North Pole Dome, home of Earth's oldest fossil stromatolites that are present in two stratigraphically, mineralogically, and texturally distinct chert horizons: the c. 3490 Ma Dresser Formation and the c. 3430 Ma Strelley Pool Chert. We will investigate the depositional environment of these fossiliferous chert horizons and their relationships to swarms of hydrothermal chert (–carbonate– barite) veins and to volcanism. Except for Locality 2.4, which we wish to protect, the Localities for Day 2 and the morning of Day 3 are shown in Figure 27.

Overview of the North Pole Dome

The North Pole Dome is underlain by little-deformed, dominantly mafic volcanic rocks of the Warrawoona Group, which form the Panorama greenstone belt and are arranged in a broad dome around a central nucleus occupied by the 3459 ± 18 Ma North Pole Monzogranite (Fig. 28; age data from Thorpe et al., 1992a). Facing directions from pillows and graded bedding in volcaniclastic rocks indicate that all the rocks face away from the core of the dome in a radial pattern, although this pattern is slightly disrupted in the western half of the dome by the Antarctic Fault, a curviplanar post-Fortescue Group structure with west-side-down displacement (Van Kranendonk, 2000a). The dip of strata increases outwards from the core of the dome, from gentle dips of 40° to 80° at the outer edges of the dome where remnants of younger rocks of the Gorge Creek, De Grey, and Fortescue Groups are preserved. The rocks have been metamorphosed to lower greenschist to prehnite–pumpellyite facies, although a lower amphibolite-facies contact-metamorphic aureole is developed around the North Pole Monzogranite.

The majority of the Panorama greenstone belt is underlain by pillowed mafic volcanic rocks that vary from dominantly tholeiitic with N-MORB REE profiles, to some high-Mg basalts immediately overlying chert horizons at places throughout the succession. The stratigraphy of the greenstones has been slightly modified since the publication of the North Shaw 1:100 000 sheet, as follows. The oldest unit is an unnamed and undated metabasalt that surrounds the North Pole Monzogranite at the core of the dome. These basalts may represent either the lower parts of the Warrawoona Group (North Star Basalt?) or the upper part of the Coonterunah Group (Double Bar Formation), although it is possible that these are one and the same in any case. Overlying this are up to five stromatolitic chert–barite horizons interbedded with pillowed basalts, collectively referred to as the Dresser Formation (previously called the Towers Formation: Van Kranendonk and Morant, 1998; Nijman et al., 1998a, 1999a). Two Pb–Pb model ages on galena in barite of c. 3490 Ma (Thorpe et al., 1992b) are interpreted as the age of the formation. The stratiform chert–barite units were fed by a set of chert–barite dykes that were emplaced within, and immediately above, listric normal growth faults that were active during deposition of the cherts, as we will see at Localities 2.1 to 2.3 (Nijman et al., 1998a, 1999a; Van Kranendonk and Hickman, 2000; Van Kranendonk, in prep. a).

Above the Dresser Formation lie mafic volcanic rocks of the Mount Ada Basalt, and a thin felsic volcaniclastic chert previously called the Antarctic Creek Member (Van Kranendonk, 1999a, 2000a), but now interpreted to represent a distal facies of the Duffer Formation. Overlying this are up to 4 km of the Apex Basalt and this is capped by up to 1.3 km of felsic volcanic and volcaniclastic rocks of the Panorama Formation. A sample of massive rhyolite from the lower part of the Panorama Formation

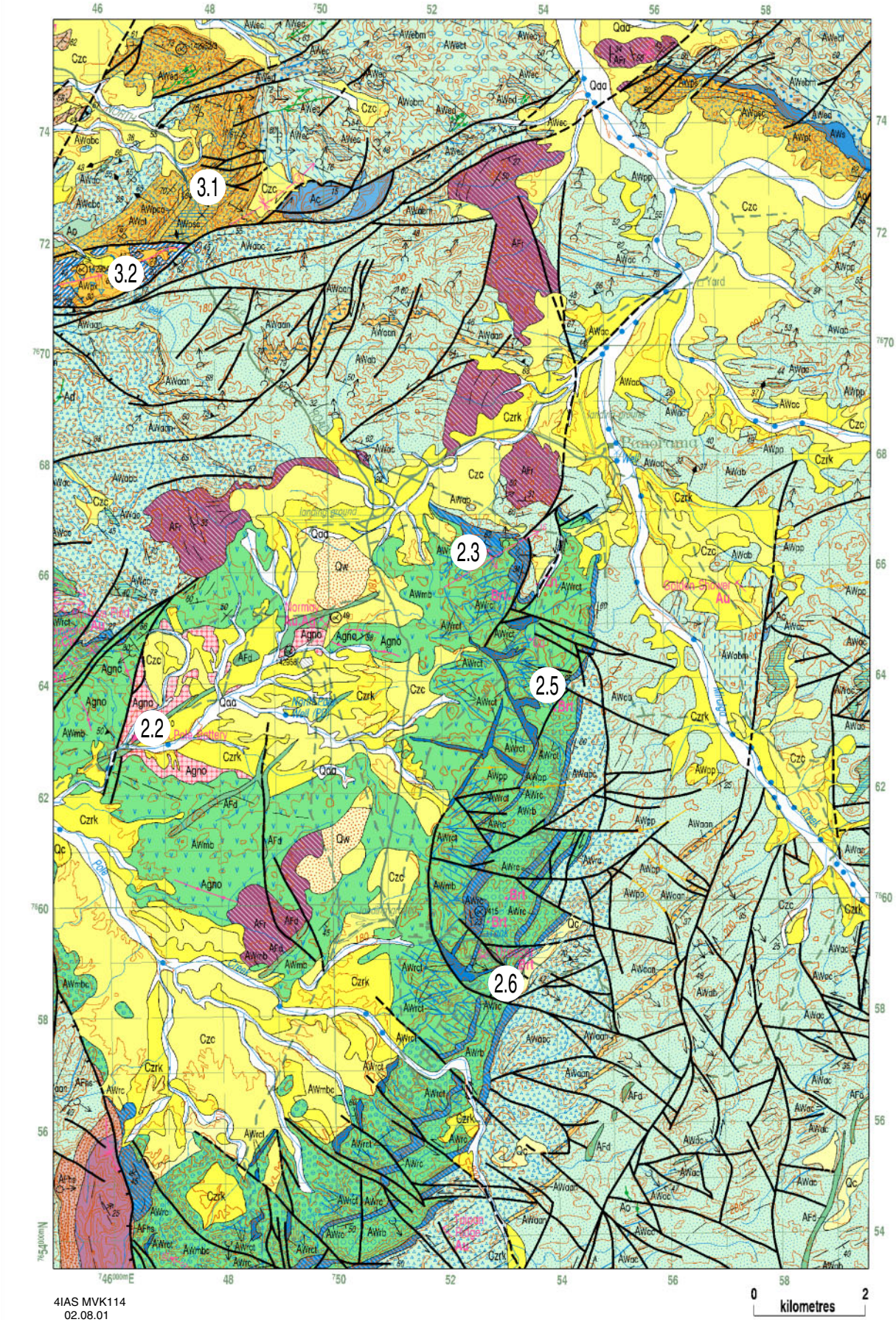

Figure 27. Portion of the North Shaw 1:100 000 sheet (Van Kranendonk, 1999a) showing the excursion localities for parts of Day 2 and Day 3

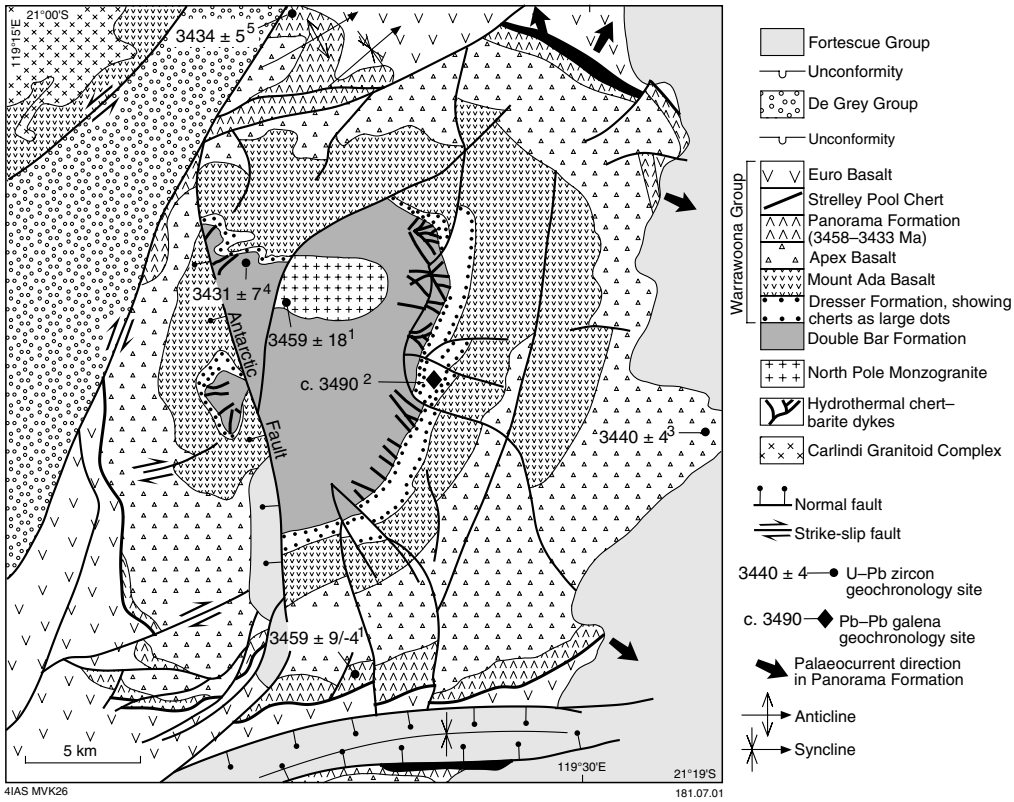

Figure 28. Sketch map of the North Pole Dome, showing the revised stratigraphy and geochronology sample sites. Age data from: 1. Thorpe et al. (1992a); 2. Thorpe et al. (1992b); 3. the Miralga Porphyry, a subvolcanic intrusion related to the Panorama Formation (Amelin et al., 2000); 4. the subvolcanic Breens Porphyry (Thorpe, R., 1992, Geological Survey of Canada, written comm., unpublished data,); 5. Nelson (2000)

in the southern part of the belt has been dated at 3458 ± 2 Ma, the same age as the North Pole Monzogranite (Thorpe et al., 1992a), indicating that the granite was emplaced as a synvolcanic laccolith into a cover sequence (similar to the emplacement of the Strelley Granite into its synvolcanic overburden some 220 m.y. later, as we saw on Day 1).

In the northwestern part of the Panorama belt is the Panorama volcano, comprising a felsic volcanic vent and flanking volcaniclastic apron of the Panorama Formation, which we will transect on Day 3 (Localities 3.1 and 3.2). Although the vent is preserved in plan view between fault splays in the hinge of an open D_3 syncline, the volcaniclastic apron is preserved in cross section around the hinge of a steeply plunging, east-facing D_3 anticline. A sample of bedded tuff with local pumice layers from the upper part of the volcaniclastic apron from this locality returned an age of 3434 ± 5 Ma (Fig. 28; Nelson, 2000; Van Kranendonk, 2000a). This area is of particular interest and significance in that it contains evidence of a magmatic source for carbonate in the volcano-sedimentary sequence, as described below.

Conformably overlying the Panorama Formation is the Strelley Pool Chert, which is the same unit seen at Locality 1.1 and containing a similar stratigraphy and with similar, distinctive conical stromatolites (e.g. Lowe, 1983; Hoffman et al., 1999). Overlying the chert is a thick succession of interbedded high-Mg and tholeiitic basalts and various cherts of the Euro Basalt, which reaches a maximum total thickness of 9.4 km in the southwestern extension of the North Pole Dome.

Locality 2.1: Trendall locality of the Strelley Pool Chert

Note: This is a locality of major geological significance. Hammering or sampling are not permitted.

This outcrop of the Strelley Pool Chert is the locality from which a sample of conical stromatolites was collected for the Western Australian Museum. A group of international stromatolite experts was invited to view the sample in situ prior to its removal, in order to gain their opinion on the biogenicity of the structures. The general opinion (except for one more cautious participant) was that the structures were undoubtedly biogenic, supporting the view presented by Hofmann et al. (1999). The sample collection and the views expressed by the experts formed the basis of an ABC television documentary on Earth's oldest life on the science program Quantum. The sample is housed at the museum in the Diamonds to Dinosaurs exhibit. In spite of the removal of this sample and subsequent damage of parts of the remaining outcrop by persons unknown, the outcrop remains a key locality for understanding the geological setting of ancient stromatolites.

A detailed map of the outcrop is presented in Figure 29. It contains three main rock assemblages, described in detail below, including:

- a lower succession composed of planar and stromatolitic laminites that are commonly silicified, but preserved as carbonate in one locality, and large areas of coarse crystal splays;
- an upper succession of coarse- to fine-grained clastic sedimentary rocks;
- a suite of black chert veins.

The rocks lie conformably on 1–2 m of jasper-pebble-bearing felsic volcaniclastic rocks of the Panorama Formation which, although not visible at this immediate locality, can be viewed some 150 m along strike. The volcaniclastic conglomerates and sandstones themselves lie on 20–30 m of golden-weathering, lineated and foliated quartz–feldspar schists derived from highly altered high-Mg basalts. This argillic–phyllic style of alteration is typical of basalts immediately beneath the Strelley Pool Chert here and in the East Strelley greenstone belt (e.g. Fig. 22) and characteristic of low-sulfur epithermal systems. The golden-weathering schists grade downward into moderately deformed, medium- to dark-brown weathering basalts of the Apex Basalt.

Planar-bedded and stromatolitic laminites

The areally dominant lithology in the lower part of the outcrop is planar-bedded, millimetre-scale laminite. Where silicified, the laminae are composed of recrystallized, polygonal microquartz that alternates from pale grey to pale creamy brown in colour. In areas of preserved carbonate, laminae are defined by couplets of dark-brown siderite–dolomite and polygonal microquartz. Commonly, the lower contacts of carbonate laminae with chert are sharp, whereas the upper contact of carbonate laminae with chert are more gradational, indicating that carbonate was the first component deposited in each couplet. In one area, cyclical bundles of 7–10 carbonate–chert couplets were observed (Fig. 30a). It may be observed at various places, that the original laminite material was composed of carbonate–chert, and that the bulk of these rocks have been silicified as a result of intrusion of black-chert veins, as described below.

Across the outcrop, planar laminite passes along strike into a texturally identical rock with a variety of structures formed by the growth of stromatolites (Hofmann et al., 1999). The dominant stromatolite morphology is that of stacked, commonly slightly elliptical cones (Fig. 30b). The cones initiate from a flat generation surface, may individually reach 20 cm in height, and form structures that extend upsection for anywhere from a few centimetres up to a metre in height. Individual bedding planes

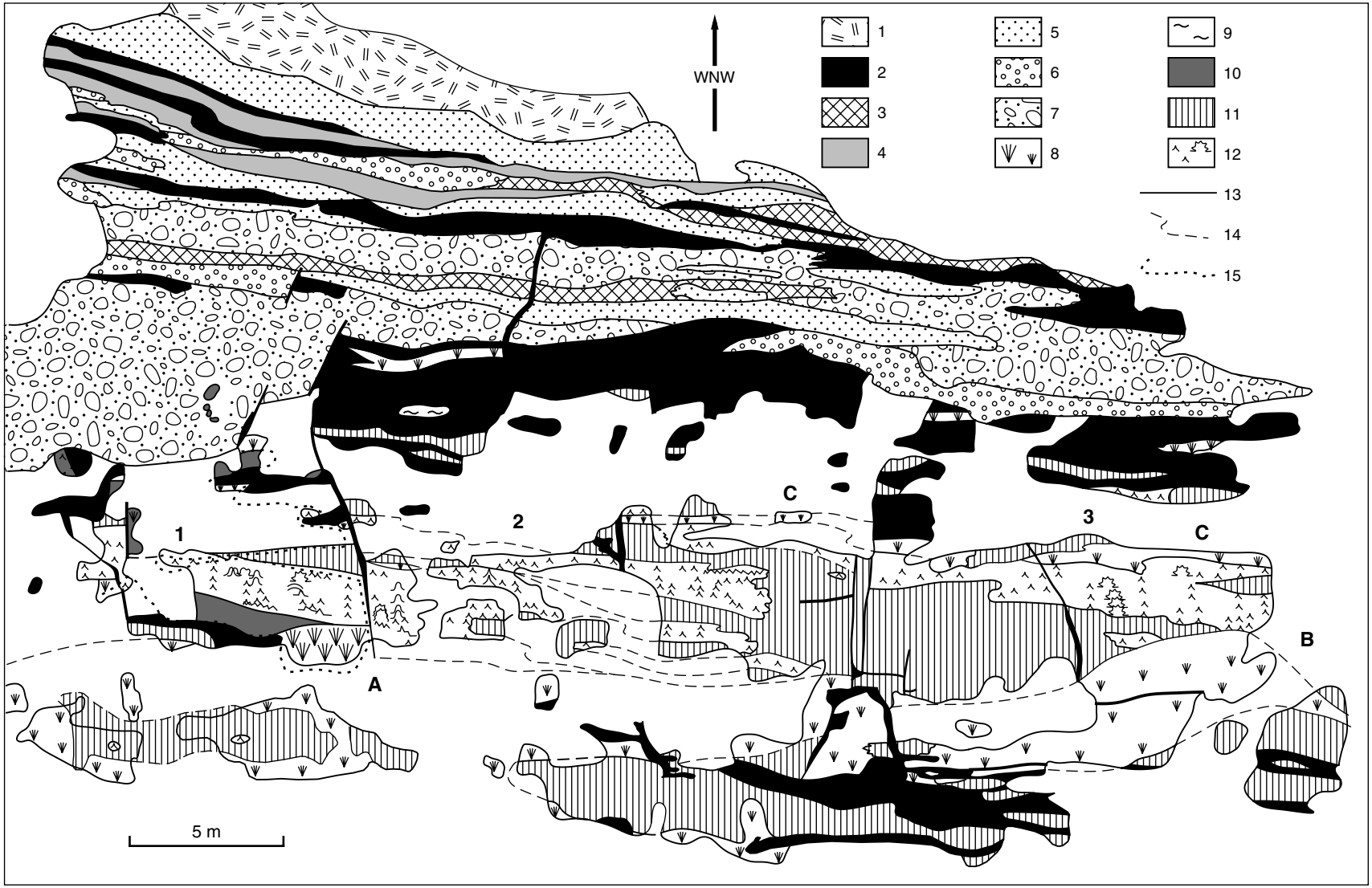

Figure 29. Geological map of the Strelley Pool Chert at the Trendall locality (Locality 2.1). Numbers refer to: 1. ophitic–subophitic basalt, 2. blue-black kerogenous chert, 3. rip-up mudstone conglomerate, 4. mudstone, 5. sandstone, 6. pebble conglomerate, 7. cobble to boulder conglomerate, 8. radiating crystal splays, 9. wavy carbonate laminite, 10. planar carbonate laminite, 11. siliceous planar laminite, 12. stromatolitic laminite, 13. geological contact, 14. interpreted geological contact, 15. limit of preserved carbonate; bold numbers 1–3 are stacked offset biostromes (after Van Kranendonk, in prep. b)

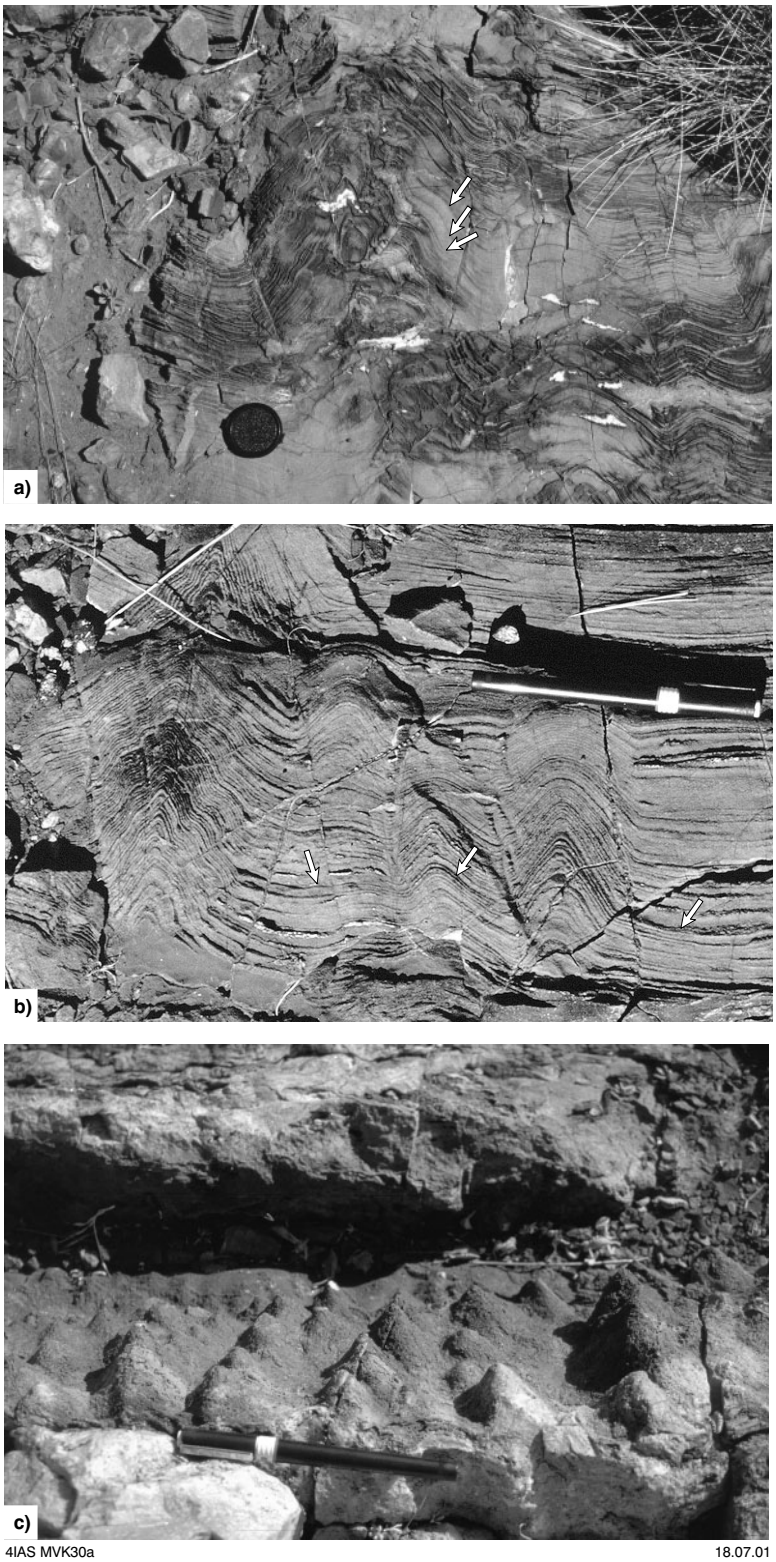

Figure 30. Outcrop features of the Strelley Pool Chert at the Trendall locality (Locality 2.1): a) cross sectional view of a large, weakly branching conical stromatolite and a smaller, cumulate stromatolite in smooth carbonate–chert laminite. Arrows denote cyclical bundling of carbonate–chert couplets; b) cross sectional view of conical stromatolites in carbonate–chert laminite. Note how individual laminae are continuous across all stromatolites. Note also the asymmetrical, longer limbs on the right-hand side of the cones, and the down-to-the-right stepping of individual laminae as denoted by the arrows; c) oblique view of a bedding plane with conical stromatolites in silicified laminite;

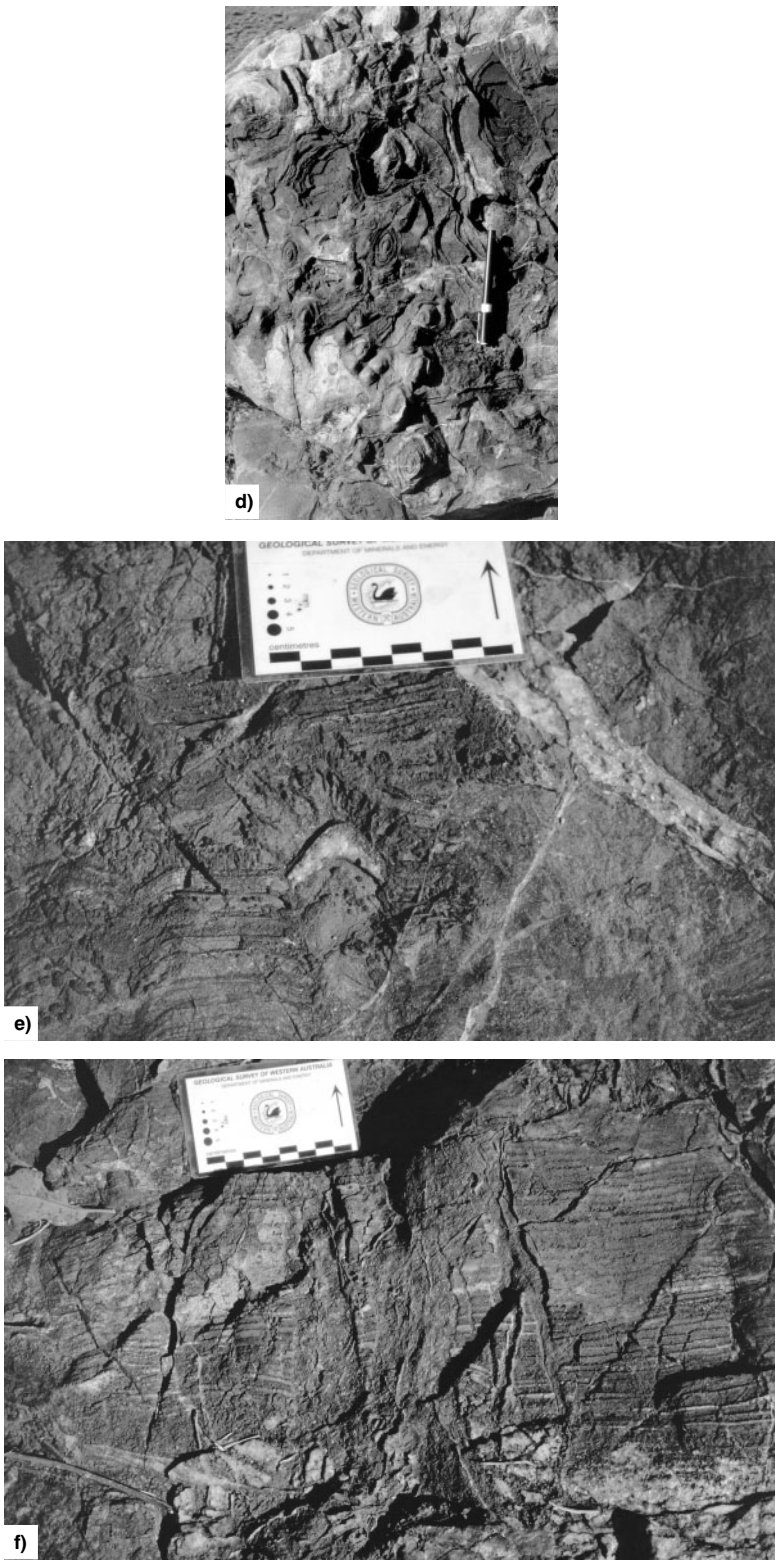

Figure 30. Outcrop features of the Strelley Pool Chert at the Trendall locality (Locality 2.1): d) plan view of a bedding-plane section through elliptical conical stromatolites in silicified laminite; e) cross-sectional view of a small conical stromatolite in carbonate–microquartz laminite that is capped by a small radiating set of crystals (?aragonite), at which level its growth was terminated, suggesting a prolonged period of exposure; f) veins of coarse-grained carbonate cutting planar bedded carbonate–microquartz couplets; (e) and (f) are from an outcrop of the Strelley Pool Chert, 1 km along strike from the Trendall locality

may contain many cones of similar dimension (e.g. Fig. 30c) or of varied size (Fig. 30d). Cross sectional views show that although the stromatolites are commonly symmetrical, many are asymmetrical, with consistently longer northern limbs than southern limbs (Fig. 30b; Hoffman et al., 1999), suggesting growth on a palaeoslope dipping 15° to the north. Conical stromatolites are characteristically elliptical in plan view (Figs 30c,d), being elongate down the dip of bedding, although this is not as a result of tectonic strain. It is thought that this shows the original shape of the stromatolites, possibly reflecting a preferred direction of water flow, such as occurs due to tidally induced flow at Shark Bay. A second stromatolite morphology consists of rounded, branching columns (Fig. 30a). Locally, these form isolated structures, but the majority of these types form on the flanks of large domical stromatolites with a maximum amplitude of 25 cm and a maximum height upsection of 1.2 m. Up to 10 small lateral branches have been observed on the flanks of the largest conical forms.

Areas of stromatolitic laminite define three stacked, offset biostromes (bold numbers 1–3 on Fig. 29) that dip to the north at an angle of up to 15° from the bedding. Each biostrome initiates at a black chert dyke and, like individual stromatolites, passes abruptly into planar-bedded laminite along strike downslope. The largest and most diverse assemblages of stromatolites are over a restricted area along strike away from the dykes, in a manner analogous with temperature-controlled variations in biota observed in recent hotsprings (cf. Jones et al., 1997; Farmer, 2000). In the southern biostrome (1 on Fig. 29), small conical forms in carbonate laminites are nearest to the southernmost of the chert dykes in the outcrop, and pass about 5 m downslope into large stromatolites with diverse morphology and complex branching forms. The middle biostrome (2 on Fig. 29) is the thickest of the three and characterized by large and diverse forms immediately adjacent to the chert dyke that separates carbonates from siliceous laminites in the southern-central part of the outcrop (A on Fig. 29). Downslope, the stromatolites become progressively smaller and end in planar laminites. The stratigraphically highest biostrome, in the northern part of the outcrop (3 on Fig. 29), contains fewer large forms than the other two, and these are about 17 m downslope from the central chert dyke.

Radiating crystal splays

Two textural types of straight to weakly radiating vertical crystal splays have been recognized. One type grew across planar-bedded and stromatolitic laminites, such as those that are throughout the lower part of the outcrop (below A on Fig. 29) and those about halfway up the succession in the northern part of the outcrop.

Another type includes the largest crystal splays (≥50 cm long) in which no trace of a previous bedding is evident. These include the coarse crystal splays in carbonate immediately adjacent to the black chert-pebble dyke that separates carbonate from siliceous laminites in the southern part of the outcrop (A on Fig. 29). Also included in this category are up to five sharp-bounded ‘beds’ of radiating crystal splays, 30 cm thick, that define a broad dome in the silicified northern part of the outcrop (B on Fig. 29). These crystal splay ‘beds’ are similar in appearance to beds of aragonite crystals deposited in recent travertine deposits at Lake Bogoria, Kenya in the African Rift Valley (see fig. 2d of Jones and Renaut, 1996). The development of these massive crystal splays is locally associated with termination of stromatolite growth, as shown, for example by a 20–80 cm-thick, massive layer of radiating crystal splays that overlies the main stromatolitic unit (C on Fig. 29). More specific evidence of this was observed at a smaller scale in a nearby outcrop, where a radiating crystal set grew on top of a single stromatolite column and terminated its growth (Fig. 30e). This is used to suggest that episodes of crystal splay growth may represent periods of subaerial exposure.

Although the original mineral species forming the crystal splays is unknown due to diagenetic silicification and carbonate alteration, preserved cross sections of some large silicified crystals are pseudohexagonal and thus the original crystals are thought to most likely have been aragonite.

It is important to emphasize that the crystal splays are unrelated to the development of stromatolitic morphology. The varieties of stromatolite morphology are all away from crystal splays and outlined by the millimetre-scale laminites that, elsewhere in the outcrop, are *overgrown* by the crystal splays.

Clastic member

Overlying the lower laminite member are clastic rocks that can be divided into five fining-up successions (Fig. 29). The basal conglomerate unit is very coarse grained, with subrounded boulders up to 40 cm in diameter. Blocks of layered and massive blue-black chert are the dominant clast lithology, but boulders of dark-brown carbonate, some with stromatolites, are locally common, and fragments of komatiitic basalt were observed 250 m along strike to the south. The basal conglomerate fills a 6.2 m-deep channel bound by normal faults, lined by black vein-chert, that extend partway into, but terminate within, the conglomerate. The presence of vein chert along the channel-forming faults and the abundance of chert clasts in the conglomerate suggest that some black-chert veining was synchronous with deposition of clastic succession. The clastic rocks are interpreted as a series of receding alluvial fans.

In one of the coarse sandy layers, stromatolitic mats have been observed, manifest as 2–5 mm-thick layers of blue-black chert. In thin section, the mats display good preservation of wavy laminite structure (Figs 31a,b). The outlines of some tube-like shapes in thin section views suggest that possible microfossils may be present. It is unknown how widespread or common these stromatolites are in the clastic succession, but they may be quite prevalent.

Trough cross-bedded sandstone and imbricate clasts from a conglomerate indicate a palaeocurrent direction towards 132°, or towards the core of the North Pole Dome, when bedding is rotated back to horizontal. Significantly, this is opposite to the palaeocurrent data from the underlying volcaniclastic rocks of the Panorama Formation, which were everywhere oriented away from the centre of the North Pole Dome, which formed a topographic high during Panorama Formation felsic volcanism (DiMarco and Lowe, 1989).

Overlying the clastic member is a medium-grained dolerite sill and pillow basalts of the Euro Basalt. In an outcrop about 1 km along strike, the dolerite sill is absent and the chert is overlain by five 10–30 cm-thick basalt flows before the pillow basalts.

Hydrothermal veins

A suite of black chert veins transects the outcrop and displays a variety of texture. Although some are massive black chert, others are zoned with a white quartz core, sometimes with euhedral quartz crystals filling void space. Other zoned veins contain massive black-chert margins and a core of pebble breccia derived through phreatomagmatic brecciation of host rocks. One massive sill displays a pseudoconglomeratic texture derived from nearly in situ breakup of the country rock during intrusion.

In addition to chert veins, carbonate veins have been observed cutting carbonate–chert laminite in outcrop about 1 km along strike (Fig. 30f), and carbonate alteration of some rocks and crystal splays has also been observed. Carbonate alteration largely

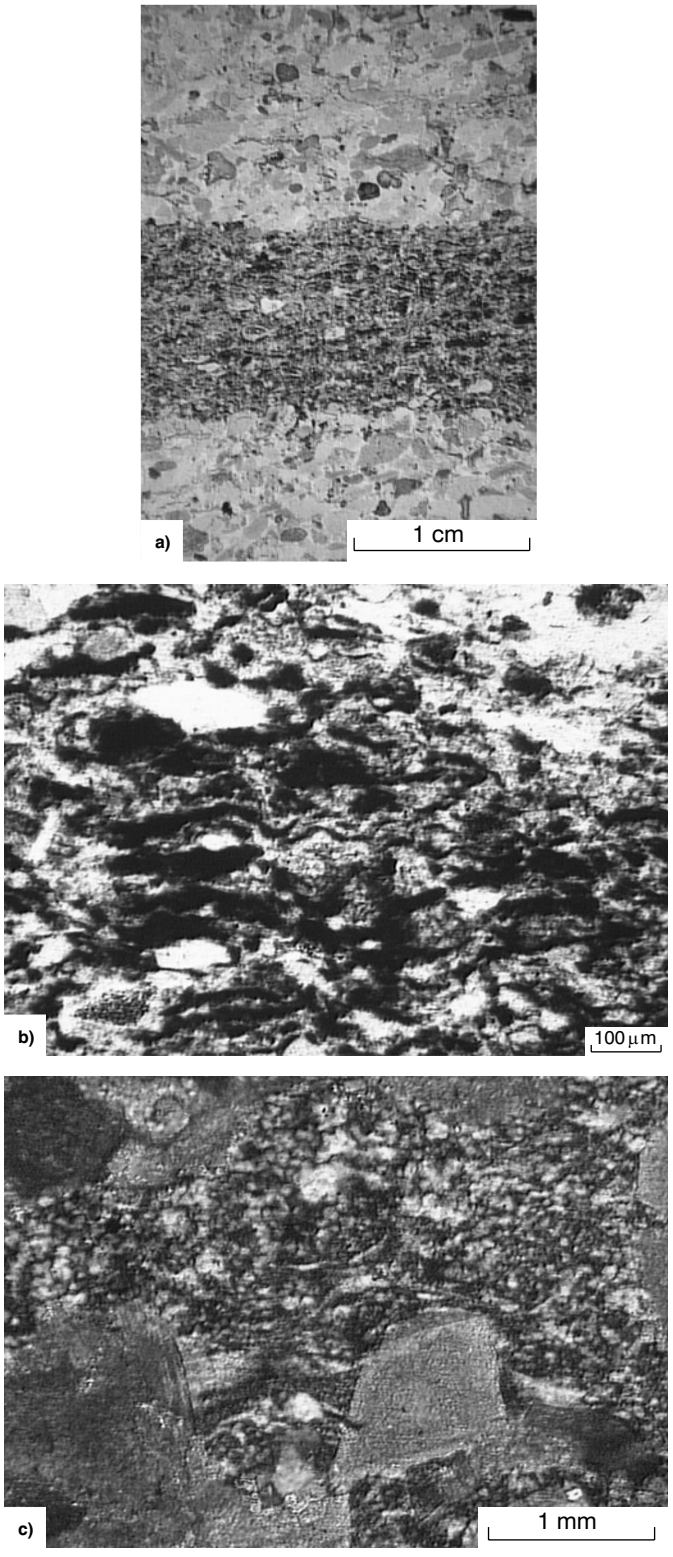

Figure 31. Thin sections of stromatolites and chert of the Strelley Pool Chert at the Trendall locality: a) a wavy-laminated stromatolite mat in coarse sandstone of the clastic member (plane polarized light); b) close-up of (a), showing wavy carbonaceous material of the stromatolite mat, and trapped sand grains; c) a pocket of polygonal microquartz (fine speckled pattern) and euhedral carbonate rhomb (light grey; cross polarized light). Note the curving pseudoperlitic texture of the quartz and the outer growth zone of the carbonate rhomb

occurred prior to silicification, although evidence of carbonate veining of chert is also locally observed. Outcrop evidence shows that the silicification of carbonate–chert laminites was directly a result of intrusion of the chert veins, as shown for example, by the chert vein at point A on Figure 29, which separates carbonate laminites from siliceous laminites. Additional examples of how the veins silicified the laminites can be observed throughout the outcrop.

Chert and carbonate veining was restricted in time to deposition of the Strelley Pool Chert, as these veins are neither above nor below the chert horizon. The presence of black chert and carbonate blocks in the lowest conglomerate unit of the clastic member indicates that the veining commenced prior to clastic deposition. The presence of black chert veins higher up in the clastic rocks indicates that chert veining continued throughout deposition of the clastic member.

Environment of deposition

Carbonate–chert laminae couplets are remarkably continuous across numerous conical and branching stromatolites over distances of several metres, and this is used to infer that the laminae are primary. The continuity of the delicate laminae indicates very quiet water conditions and contrasts sharply with laminations precipitated on stromatolites through evaporation from seawater in modern marine tidal environments (e.g. Shark Bay), which are highly irregular. Furthermore, the crystal growth splays suggest periodically exposed conditions.

The presence of chert and carbonate veins in the outcrop suggests that it may have been the veins that supplied the chert and carbonate precipitated in the laminites. The zoned nature of the chert veins with quartz crystals in some vein centres are suggestive of epithermal veins formed from circulating hydrothermal fluids. Thin section petrography of chert shows it was affected by perlitic cracks formed during cooling of a hot siliceous fluid (Fig. 31c; Van Kranendonk, in prep. b). A hydrothermal origin of the veins is also supported by the spatial association between large and diverse stromatolite assemblages and the chert veins and by the fact that the stromatolitic biostromes initiate at chert veins (thermophillic organisms).

An analogy for the environment of deposition is drawn with alkaline lakes in the East African Rift Valley where many features identical to those in the Strelley Pool Chert have been recorded. Similarities include, in particular, the presence of millimetre-scale carbonate–chert laminites and laminated stromatolites, a nearly identical geometry of a hydrothermal vein network, and beds of aragonite crystal splays (Casanova, 1986; Renaut and Jones, 1997).

Based on data from this area, the Strelley Pool Chert laminites are interpreted as having been deposited in an alkaline caldera lake that was fed by swarms of hotsprings. Hydrothermal circulation was driven by heat from the late-stage emplacement of the North Pole Monzogranite, at the close of eruptive volcanism (Fig. 32). Laccolith intrusion caused uplift of the surface into the photic zone and this allowed the growth of stromatolites. Stromatolites grew preferentially at, or downflow from, hydrothermal veins, many of which were emplaced within growth faults.

The microscale carbonate–chert couplets in the Strelley Pool Chert may be interpreted to reflect seasonal variations in the chemistry of the lake water as a result of changes in the amount of rainfall and insolation (Fig. 33; cf. Renaut and Jones, 1997). If the carbonate–chert couplets represent seasonal variations as argued above, then the presence of cyclical bundles of 7–10 couplets that form about 1 cm of bedding thickness seen in one area (Fig. 30a) may reflect variations in the amount of insolation at a 7–10-year timescale. Possible controls on insolation include features such as the current

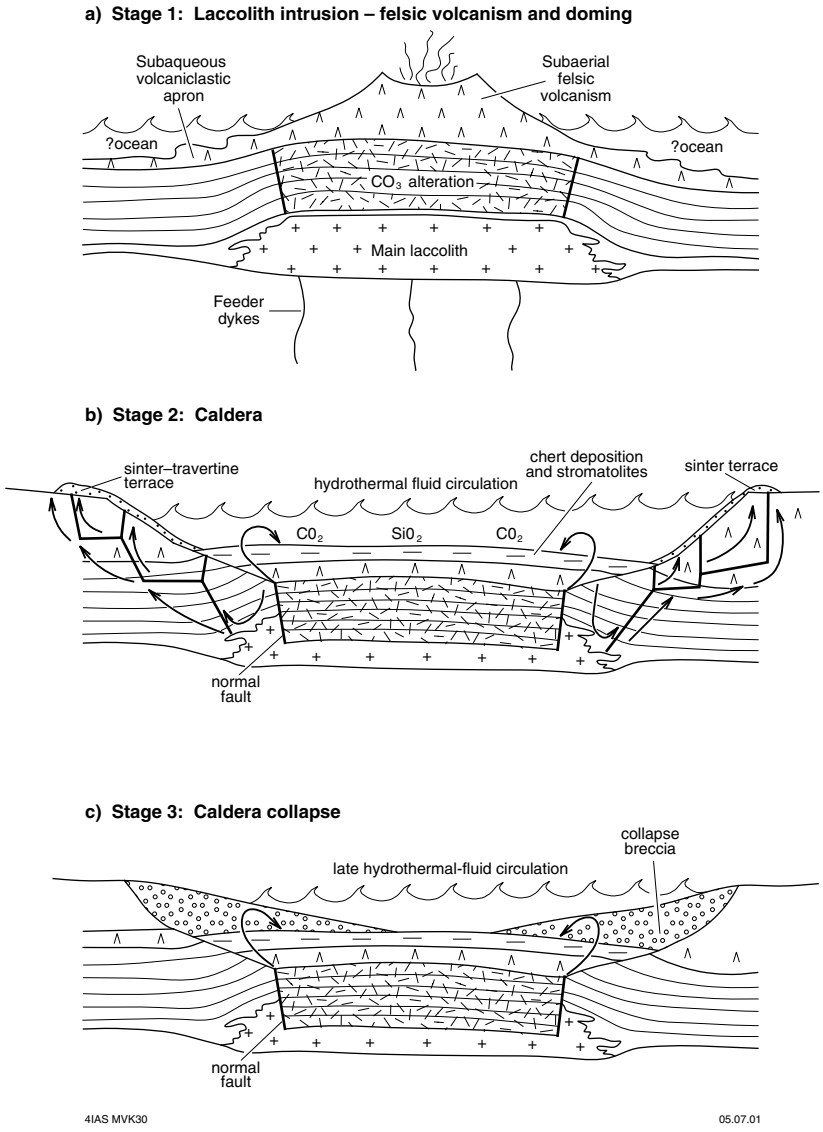

Figure 32. Schematic model, in cross section, showing the three interpreted stages in the deposition of the Panorama Formation and Strelley Pool Chert:
a) stage I — felsic magmatism results in the surface eruption of felsic volcanic rocks, emplacement of a subvolcanic laccolith, and volcanic doming;
b) stage II — waning of felsic magmatism, characterized by low-level hydrothermal circulation, volcanic degassing, and the formation of one or a nest of calderas. Precipitation of carbonate–silica laminites in, and marginal to, an alkaline caldera lake is accompanied or facilitated (or both) by stromatolite growth;
c) stage III — caldera collapse filled by proximal detritus transported on alluvial fans

11-year sunspot cycle that causes changes in the temperature of the troposphere, or possibly even an early type of a climatic El Niño.

The quiescent stage of hydrothermal circulation, chert precipitation, and stromatolite growth was terminated by deposition of the clastic member. The palaeocurrent data from this member suggests that the clastic rocks were deposited during the final stages of caldera collapse (Fig. 32c).

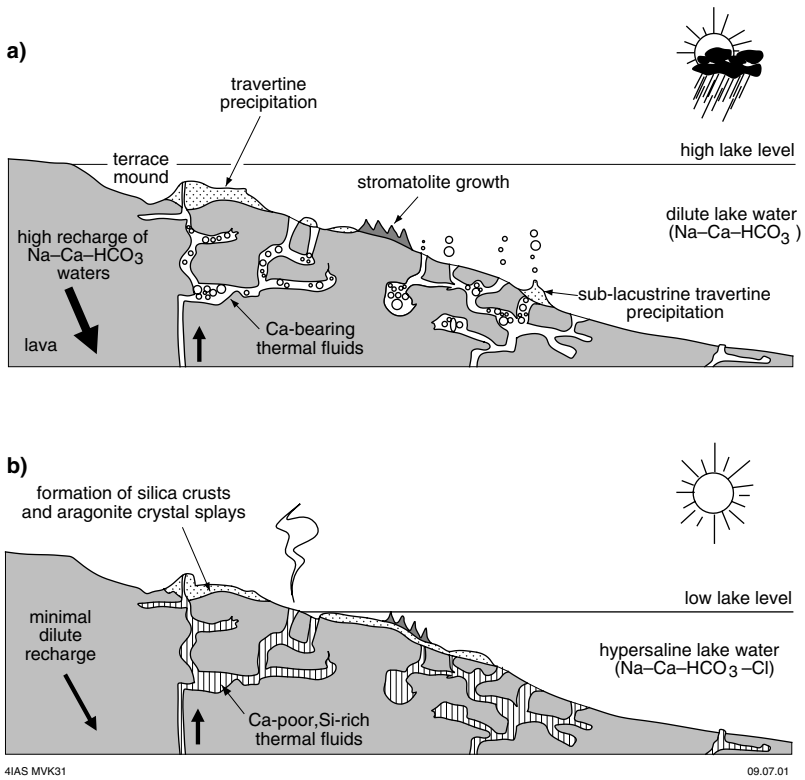

Figure 33. Schematic model, in cross section, showing how changes in lake water level due to seasonal variations in insolation can affect the chemistry of hotsprings and their precipitates (after Van Kranendonk (in prep. b); adapted from Renaut and Jones (1997, fig. 5):
a) the rainy season, with high lake levels, results in dilute lake water and intensive weathering of substrate with resultant calcium-rich thermal fluids and travertine precipitation;
b) low lake levels during the summer season causes hypersaline lake water, minimal dilute recharge of thermal waters, and precipitation of siliceous crusts and sinter

Locality 2.2: North Pole Monzogranite at the North Pole battery (NORTH SHAW, AMG 746500E 7663100N)

From the previous outcrop proceed for about 2.5 km to an old, rusted truck and the North Pole state battery.

Low outcrops of coarse-grained, undeformed granite of the North Pole Monzogranite at this locality have been dated at 3459 ± 18 Ma (Thorpe et al., 1992a). A more recent attempt to obtain a date with a smaller error failed due to lead loss in zircons, despite using a fresh sample obtained by blasting. In neither attempt were older xenocrysts identified. The monzogranite has a coarse-grained to weakly porphyritic texture, and miarolitic cavities have locally been observed, indicating crystallization under relatively shallow crustal conditions.

The North Pole battery and associated cyanide tanks at the hilltop were used in the processing of 400.52 oz of gold mined from the North Pole mining centre from 1899 to 1931, about 2 km to the northwest. The Breens Reward mine is an epithermal type, polymetallic deposit, with gold, copper, silver, and bismuth mineralization. It is associated with a small felsic intrusive porphyry dated at 3431 ± 7 Ma (Thorpe, R., 1992, Geological Survey of Canada, written comm.), the same age as the upper part of the Panorama Formation.

Locality 2.3: Hydrothermal chert–barite–Fe-gossan dyke and syngenetic chert–barite–Fe-gossan–sandstone strata, Dresser Formation (North Shaw, AMG 753000E 7666200N)

Continue on the track for 3.7 km, keeping left and following the main track until a T-junction at a cumulative distance of 5.75 km. Turn left, proceed for 1.25 km and take the right, less prominent fork in the road. Follow this track for 1.1 km and turn right onto a faint track. Head south on this track for about 600 m. Turn right where another small track joins at a high angle. Follow this track for about 2.0 km and turn left up a steep hill. At the top of the hill, do not go through the saddle, but turn left across the face of the hill to the next saddle and park the vehicle. Walk west along the base of the steep ridge for about 50 m to a ridge of chert–barite at Locality 2.3.

Note: Hammering or sampling are not permitted at this locality, as it lies within a proposed Geological Monument area.

At the next three localities, we examine the relationships between hydrothermal chert–barite dykes, bedded chert–barite, and stromatolite growth in the c. 3490 Ma Dresser Formation. Figure 34 shows the relationships between the chert–barite dykes and bedded chert units in the Barite Range and Localities 2.3 to 2.6.

At Locality 2.3, we can observe the relationships between a 2–10 m-wide chert–barite–Fe-gossan hydrothermal feeder dyke, striking north–south, and the basal, 20 m-thick unit of bedded chert–barite–Fe-gossan–sandstone of the Dresser Formation. The dyke cuts altered basaltic rocks beneath the bedded chert and is crudely zoned with white, grey, and massive black chert on the outer flanks, massive coarse-bladed barite in the middle, and a discontinuous zone of Fe-gossan in the core (Fig. 35a).

The bedded chert comprises layered white and blue-grey chert, with thin beds of jasper chert and poorly developed beds of BIF (Fig. 35a). Halfway up the unit, the chert is disconformably overlain by thick-bedded, coarse sandstone and fine conglomerate, which thickens dramatically from west to east across the upward projection of the dyke. This is consistent with the offset across small faults in the chert to the east, which indicate east-side-down normal faulting during sedimentation. The origin of the main grey-and-white layered chert at this locality is controversial. Buick and Dunlop (1990) suggested that much of the chert was originally a carbonate on the basis of carbonate rhombs scattered throughout much of the chert. However, an alternative possibility is that the rock is a primary chert precipitate in which there is a small amount of contained carbonate.

The zoned chert–barite dyke can be followed up to the base of the bedded chert–barite unit and farther up until about halfway through the lower parts of the unit, where it curls over and becomes parallel to bedding (Fig. 35b). At the transitional bend, the massive barite dyke develops a distinctly wavy lamination characteristic of textures in stromatolitic mats observed about 10 m along strike to the east in this outcrop and elsewhere throughout the unit. Immediately beneath the curl of the dyke is a stromatolitic mound of wavy-laminated barite, with a wedge of sandstone on the top, indicating that the mound was present during sedimentation. Similar features are present about 10 m along strike to the east, where three large domical stromatolites in wavy-laminated barite are draped by sandstone wedges (Fig. 36).

If time permits, continue east along the ridge, being careful of your footing, where some of the complexities of chert and barite veining can be observed (Fig. 37). Of particular interest is the development of two textural types of pseudoconglomeratic hydrothermal breccias that are the result of discordant chert veining. Also of particular interest are discordant barite dykes containing textures ranging from massive coarse

Figure 34. Geological sketch map of the Dresser Formation in the Barite Range of the North Pole Dome, showing chert-filled listric normal faults, depositional chert–barite horizons, and radiating sets of hydrothermal chert–barite feeder dykes; unpatterned areas are dominantly pillow basalt

crystalline barite characteristic of the barite dykes to wrinkle-laminated textures typical of bedded, stromatolitic rocks seen in the previous outcrop and in the southeastern part of this outcrop. This raises the question as to whether or not stromatolite communities may have inhabited warm hydrothermal conduits in the subsurface. Note that the barite veins do not cut the overlying sandstone–conglomerate unit.

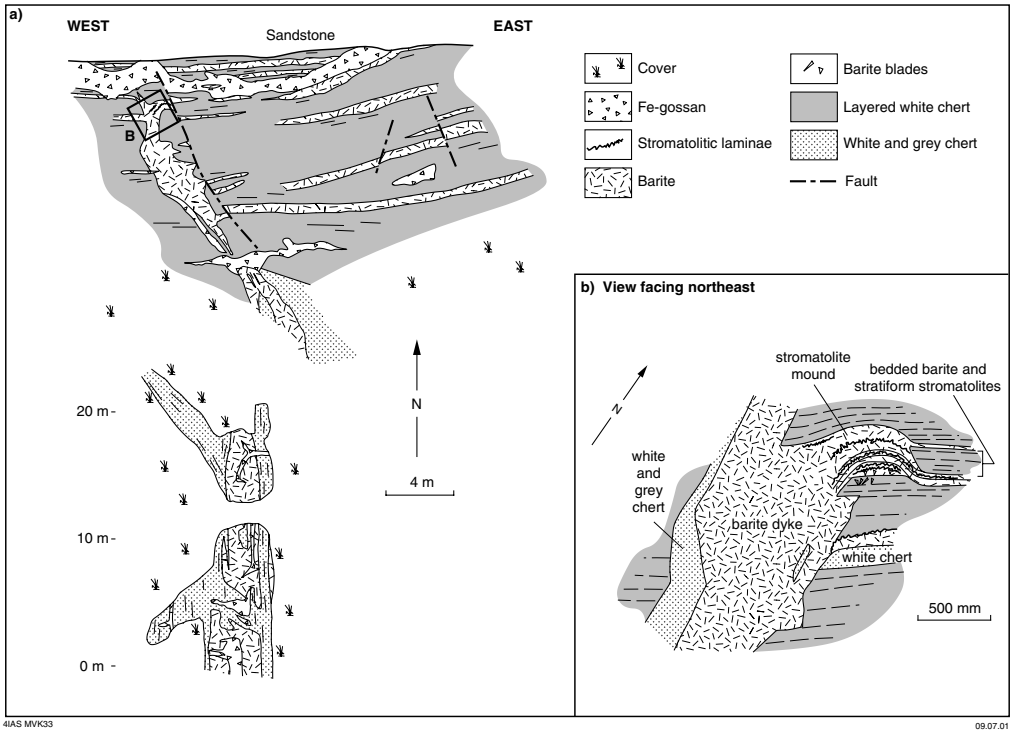

Figure 35. a) Geological sketch of a zoned chert–barite–Fe-gossan dyke and its penetration up into, and termination within, depositional chert–barite–Fe-gossan (locality is shown on Fig. 34); b) close-up of the dyke termination shown in (a). Note the growth of a stromatolite mound adjacent to the mouth of the dyke, and the development of stromatolitic laminations near the top of the dyke, contrasting with the massive nature of the barite in the core of the dyke

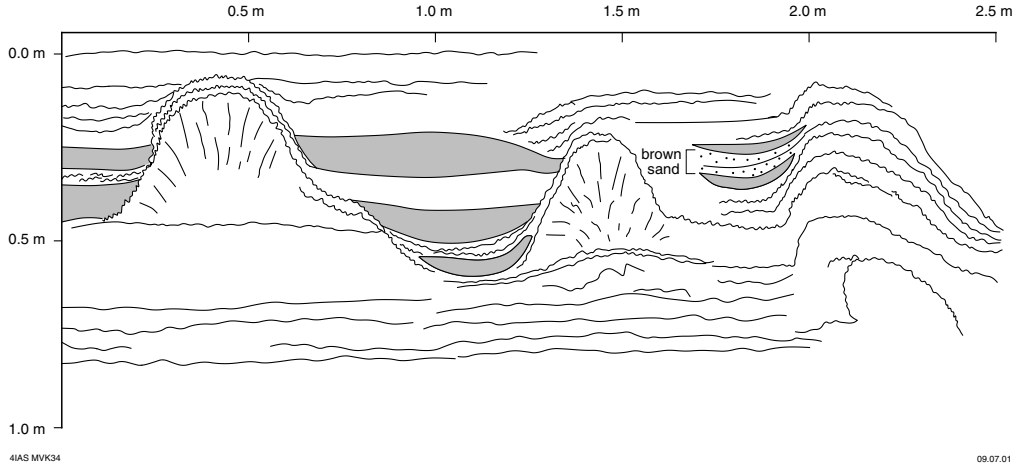

Figure 36. Cross sectional sketch of three domical wrinkle-laminated stromatolites in the Dresser Formation, from 5 m east of Figure 35. Note the sand wedges in between the stromatolites, showing that the domes were present during sedimentation

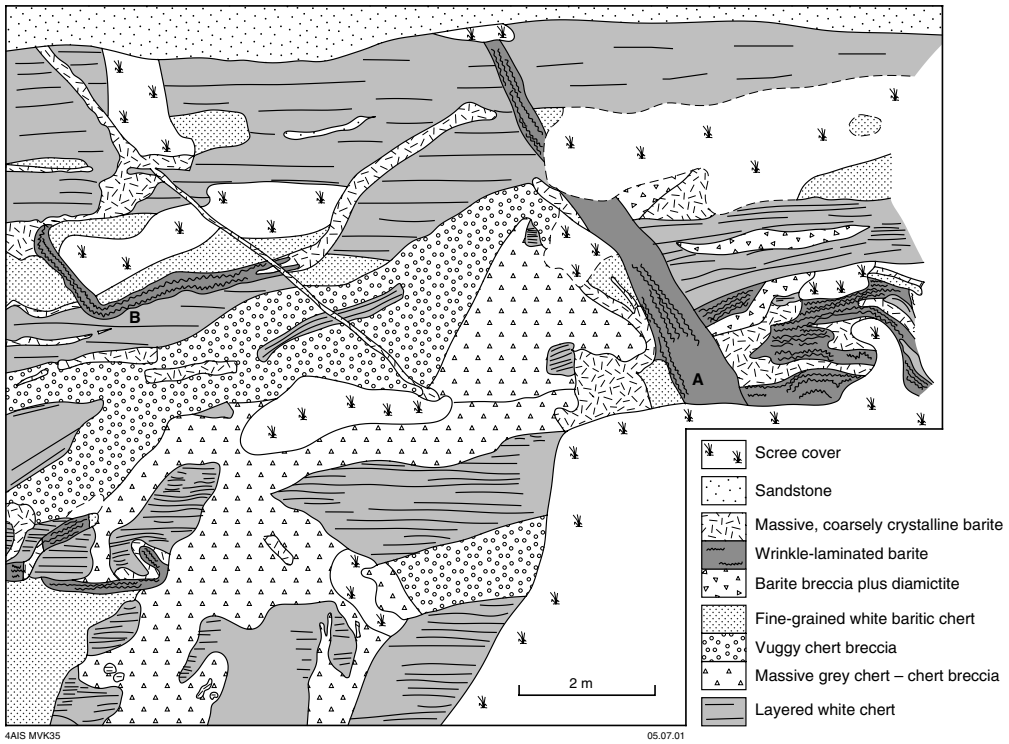

Figure 37. Geological sketch of a section through the lower part of the Dresser Formation chert (locality shown on Fig. 34). Note the extensive hydrothermal chert breccias and the distinctive, wrinkle-laminated barite in dykes (A) and sills (B), suggesting that microbial life may have flourished within hydrothermal fluids in the subsurface

Locality 2.4: Earth's oldest stromatolites, North Pole Dome

Note: This locality of major geological significance lies within a proposed Geological Monument area, and hammering or sample collection are not permitted.

Bedding in this outcrop near the top of the Dresser Formation dips 34° to the east and is broadly warped on east-northeasterly plunging axes. Otherwise these rocks are unaffected by penetrative deformation. The stromatolites here form black-weathering wrinkled mats, smooth broad domes, elliptical low-amplitude domes, small individual columns, and mounds of wrinkle-laminated barite. In addition, blades of diagenetic barite can be seen to push up what was still wet sedimentary bedding in silicified ?carbonates, and asymmetric ripples are at the top of thin sandstone beds. Massive barite veins are also present. Explore and enjoy.

Locality 2.5: Barite mound and diamictite

Synsedimentary listric growth faults in the Dresser Formation relate to roughly north–south tension, but are unrelated to the formation of the North Pole Dome. The fault set controlled:

- the thickness of the chert members and intercalated basalts of the Dresser Formation;
- the formation of black-chert veins in fault-related fractures that arose from growth faults and terminated in the cherts;
- the barite along chert veins and in large mounds in about 50 m water depth.

The data support a sedimentary model with primary hydrothermal barium and silica emanation (?white smokers) into a stratified water body with a barium-sulfate-saturated

brine containing silica gel below wave base, and a more-normal estuarine–lagoonal littoral circulation above that (Fig. 38). The sedimentary model implies repeated uplift probably coeval with felsic volcanism elsewhere and subsidence with development of faults and fractures, the intensity of which diminished from the deposition of the lowermost chert–barite unit to that of the uppermost, fifth chert unit of the Dresser Formation.

In the hangingwall of one of the leading growth faults of the Dresser Formation, barite forms a number of mounds that were built convex-upward from a bedding plane. The large barite mound at this locality (Fig. 39) is at least 20 m high, with a minimum diameter along the base of about 50 m. The mound includes several smaller hemispherical mounds of barite, crystallized in palisades of up to 10 cm-long, bladed crystals. Thin chert and iron-oxide laminae often separate successive barite layers, and lenses of black-and-white banded chert and silicified sandstone are enclosed by the barite (Fig. 39). The mound stands on a base of diamictite (Fig. 40) over basalt, exposed in the creek bed.

Uplapping against the mound are evenly bedded, black-and-white layered chert (basin centre facies, Fig. 38), coarsening upward into silicified sandstone (littoral–tidal channel facies). The contact shows pinch-outs and internal discordances where overlapping beds truncate layers that have been warped upward by crystallization (Fig. 39). This is interpreted to prove the synsedimentary nature of the barite growth. In places, the chert beds contain sinter layers of light-grey, fine-grained barite crystals, stratiform barite with large, dark-grey crystals, and diamictite beds containing barite clasts. Separated from the main body of the mound are several minor, isolated barite mounds that are associated with synsedimentary deformation of the flanking sediment.

Chert–barite veins intersect the underlying basalt and terminate in the mound (Figs 39 and 40). We relate the formation and deposition of the barite and the high silica content of the sediments to growth-fault-controlled hydrothermal systems (Fig. 38).

Locality 2.6: Barite dykes and altered pillow basalts, Dresser mining centre (North Shaw, AMG 752600N 7659400N)

Return to vehicles, and continue south along the track for 3.75 km, turning right at 3.3 km. The track leads back to the North Pole Road. Turn left (south) and continue for 2.9 km, following the swing of the road around to the left into the abandoned Dresser mining centre, where 129 505 t of barite was mined between 1970 and 1990. Drive past the ore stockpile and the ruined sorter apparatus, and up the deeply eroded second track on the right, driving farther into the mining centre. Take extreme care up the first part of this small track as boulders and washouts are present! Drive right to the end of the straight section, for about 800 m, leave the vehicle and head over the small tailings pile into the openpit.

This locality is the smaller of two mining pits (Fig. 41), the larger one to the west having been effectively mined out. On the eastern wall of the smaller pit there is a 15–20 m-wide, subvertical barite dyke intersecting highly altered, pillowed basalts. The dyke is a multiple structure with distinct partings separating horizontal barite crystals up to 40 cm long, indicating a multiple crack-seal origin. The dyke tapers out rapidly at this point and this apparently discouraged further mining. The northeastern wall of the pit has perfectly preserved pillow shapes, but the rocks have been totally altered to fine-grained, soft, white rock composed entirely of (?)kaolinite — a style of alteration consistent with high-sulfur epithermal systems.

Return down the rough track and back to the flat area just past the decrepit sorter, where we will camp for the night.

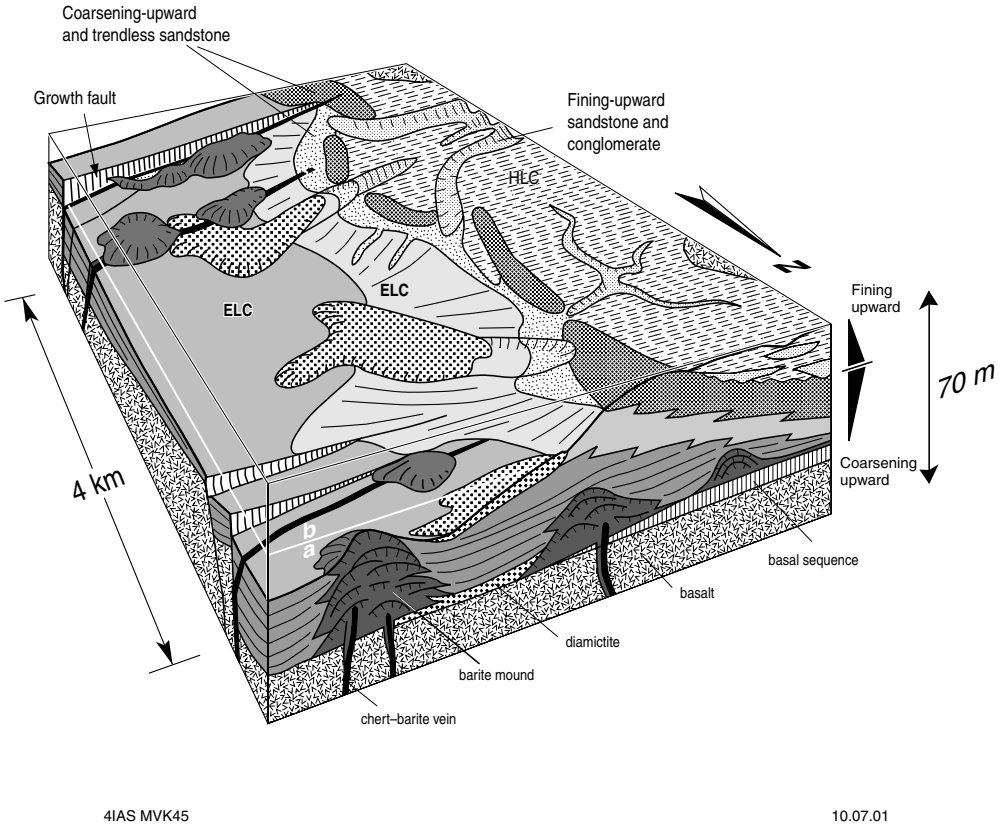

Figure 38. Tectono-sedimentary model of the Dresser Formation chert–barite unit (ELC = even-laminated chert, HLC = heterolithic chert; 'a' and 'b' refer to the stratified structure of the water body; modified from Nijman et al., 1998a, 1999a, fig. 14)

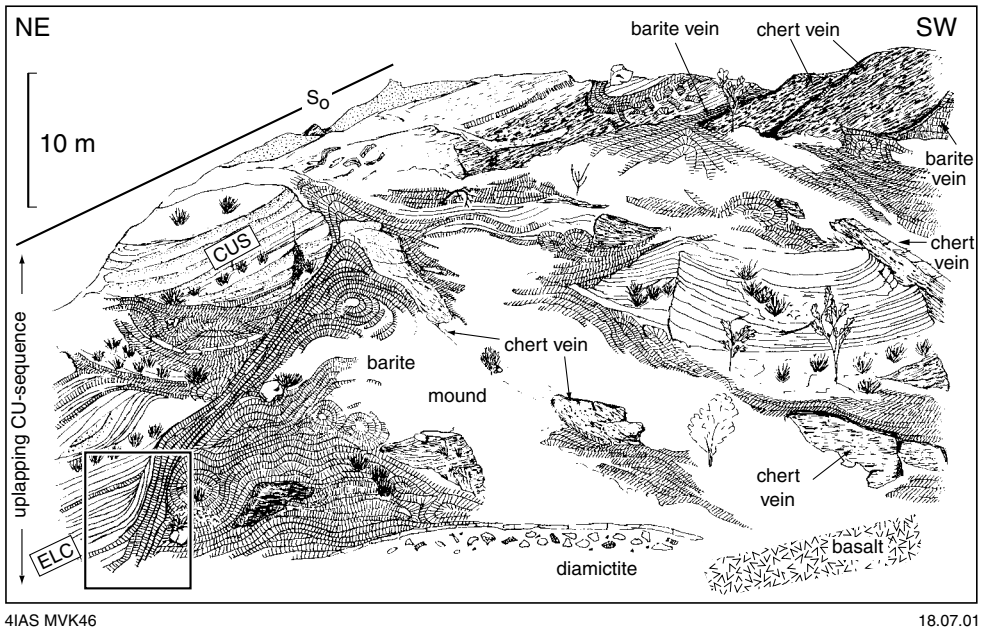

Figure 39. Detailed field sketch of a barite mound outcrop at the crossing of a fault and fracture-bound chert–barite veins (by C. H. de Bruijne). Barite-lined black chert veins are subvertical and form resistant walls in the mound. The frame on the left-hand side shows uplap and minor disconformities in even-laminated chert (ELC) overlain by sandstone in a coarsening-up sequence (CUS) along the flank of the mound (modified from Nijman et al., 1998a, 1999a, fig. 11)

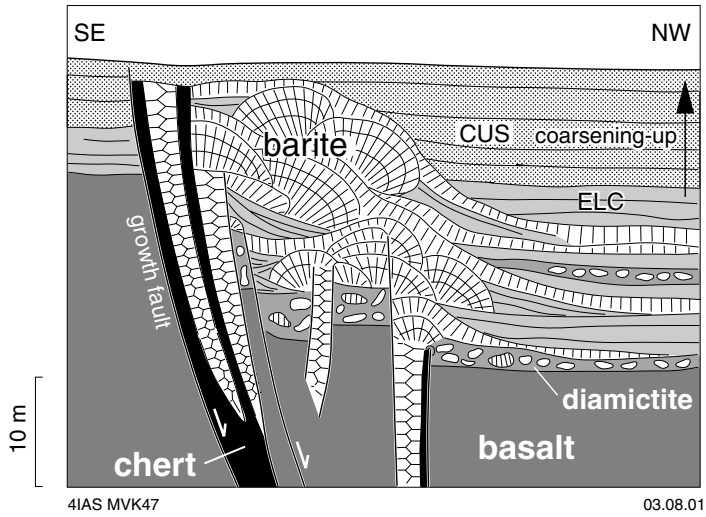

Figure 40. Schematic cross section of a barite mound at right angles to the exposure of Figure 39, illustrating the close relationship between faults, chert veins, barite in the veins, the barite mound and uplapping coarsening-up basin fill with diamictite (modified from Nijman et al., 1998a, 1999a, fig. 13). ELC = even-laminated chert; CUS = coarsening-up sequence

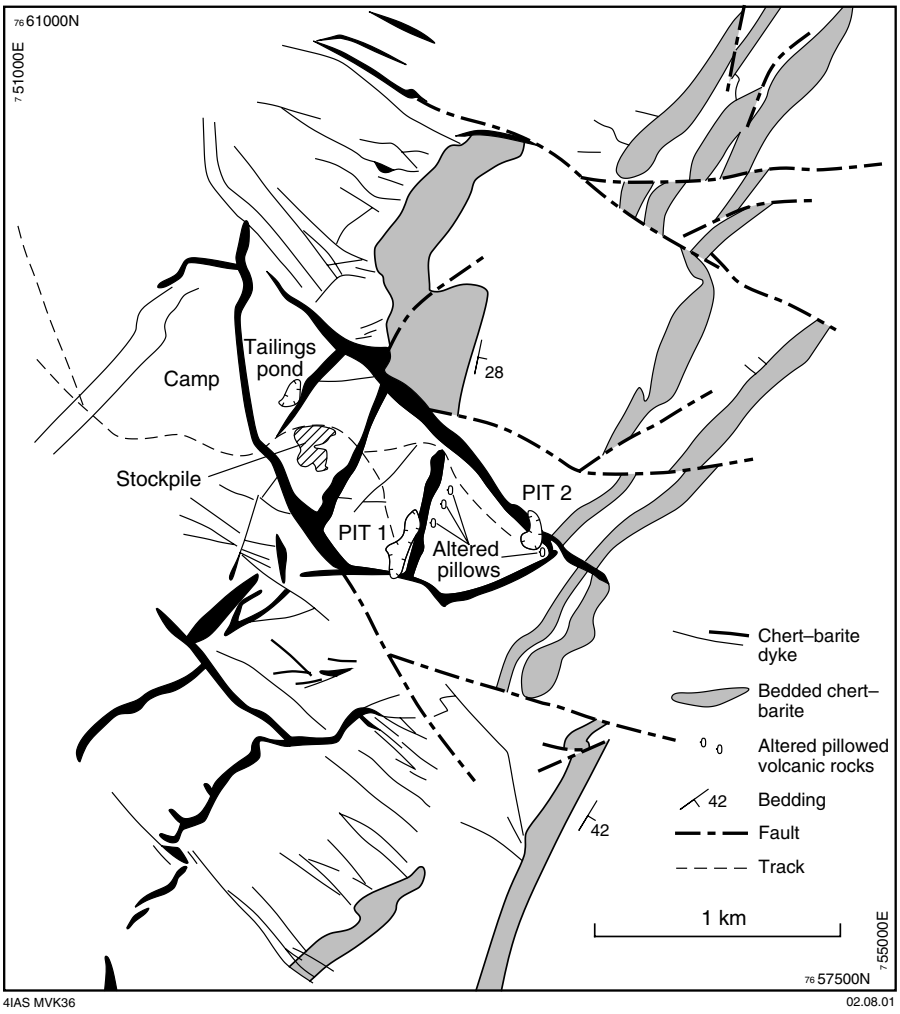

Figure 41. Geology of the Dresser mine at Locality 2.6

Day 3: The c. 3.45 Ga Panorama Formation

This day is divided into two parts. In the morning, M. Van Kranendonk will guide us through the last two localities in the North Pole Dome, in the vent and volcaniclastic ejecta apron of the felsic Panorama volcano (Panorama Formation). In the afternoon, W. Nijman of the University of Utrecht will lead us through another part of the Panorama Formation, but 70 km away in the Coppin Gap greenstone belt, where we will undertake a walking traverse through a synvolcanic growth-fault array.

Locality 3.1: Carbonate-bearing felsic volcaniclastic rocks of the Panorama Formation, North Pole Dome (North Shaw, AMG 747700E 7672900N)

Head out of the Dresser mining centre (to the west) and rejoin the main track, keeping right. Follow the track north for about 15 km to a high chert ridge on the right and park the vehicles. This locality involves a 700 m walk over low, rubbly outcrops.

The Panorama volcano includes a vent preserved in plan view between splays of a fault system (see **Locality 3.2** below), and an adjacent apron of volcaniclastic ejecta up to 1600 m thick, that has been deformed into a steeply plunging, east-facing anticline by sinistral transpression at c. 2940 Ma (Fig. 42). At the base of the ejecta apron near the vent is about 50 m of decimetre- to centimetre-scale interbedded carbonate, jasper chert, and felsic tuff. Overlying this, in turn, is the first of several fining-upward eruptive cycles, at the base of which is 50–100 m of densely welded rhyolitic ignimbrite with eutaxitic texture, and massive felsic volcanic rocks. Rocks of the volcaniclastic apron proximal to the volcanic vent contain abundant carbonate in the matrix, whereas in the more distal parts along strike to the north and northwest (Fig. 42), a similar sequence of rocks lacks the matrix carbonate and has a white-weathering surface appearance. The significance of this will be discussed at the next locality.

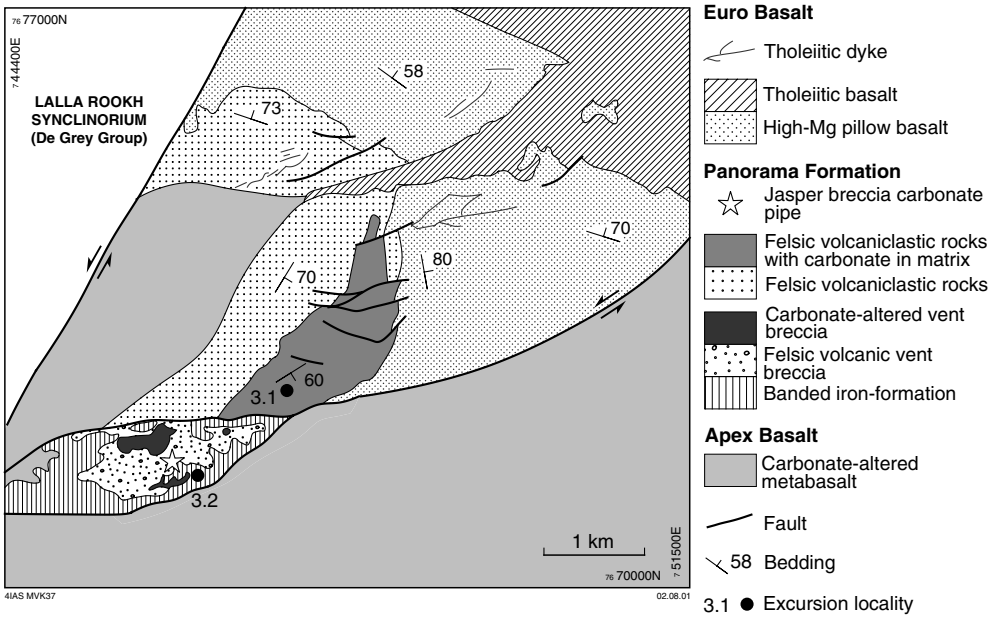

Figure 42. Simplified geological map of the 3.45 Ga Panorama volcano in the North Pole Dome, showing Localities 3.1 and 3.2

The transect through the volcaniclastic apron commences near the top of a 30–40 m-thick chert, about a third of the way up the section, adjacent to the volcanic vent breccia. The chert is characterized by 5–50 cm-scale layering defined by alternating layers of red hematitic chert and white chert, with less common dark-blue chert layers and thin intervening volcaniclastic beds. Above this, felsic volcaniclastic rocks proximal to the vent are predominantly dark brown weathering and a matrix consisting of a microgranular, granophyric intergrowth of quartz and feldspar (devitrified rhyolitic glass) together with carbonate (ferroan dolomite or ankerite).

A section through this part of the sequence shows that it is composed of nine fining-upward cycles, each with distinct textures and compositions (Fig. 43). At the base there are two fining-up cycles that contain interbedded carbonate-bearing and carbonate-free volcaniclastic rocks, including a unit of millimetre-bedded porcelainite. Petrographic studies reveal that the amount and grain size of carbonate varies across bedding in accordance with the size of clastic detritus. These cycles are overlain by poorly bedded volcaniclastic rocks characterized by subrounded clasts of white, fine-grained felsic volcanic rock and chert up to 10 cm in diameter, in a medium-grained equigranular matrix of carbonate and granophyric quartz–feldspar that hosts equant quartz phenocrysts. This unit is similar in texture and composition to the vent-facies breccia of the Panorama volcano. Above these rocks lies a unit packed with angular jasper fragments in a dark-brown carbonate-bearing matrix with quartz phenocrysts. At Locality 3.2 it will be seen that this unit was fed by a small diatreme from the vent of the volcano that cut up through the basal BIF. This and other coarse jasper-fragment debris flows are crudely bedded on a 1–4 m scale and display symmetrical, reverse, or normal grading.

Locality 3.2: The vent of the Panorama volcano (North Shaw, AMG 746300E 7671400N)

Return to the vehicles, turn them around, and drive south for about 1.3 km along the North Pole Road and then turn right into the bush. Follow the faint track for about 1.2 km down a small stream. Park the vehicles and walk for about 500 m northwest through a low saddle into the bed of a stream to outcrops of jaspilitic BIF. Continue for 250 m north along the western bank of the creek, from high jasper ridges to the first low outcrops of felsic volcaniclastic rocks.

The vent facies of the Panorama volcano includes a rim unit of jasper–siderite BIF, up to 150 m thick, which everywhere dips moderately inwards towards the vent. It is cut by coarse, unsorted volcanic breccia in the core of the vent, which contains local fumaroles and several small diatremes. The iron-formation consists of centimetre- to decimetre-thick alternations of jasper and brown carbonate (probably siderite or ferroan dolomite), with subordinate beds of iron-chlorite. South of the high cliff, and in places within the cliff, are large-scale folds of bedding that verge towards the core of the vent to the north. These folds are interpreted to represent synsedimentary slump folds, as equivalent folds on the northern rim of the vent are cut by undeformed vent breccia.

Past the BIF, downstream to the north, there is a poorly sorted, coarse volcanic breccia interpreted to represent the vent facies of the Panorama volcano. The breccia consists of weakly quartz- and feldspar-phyric felsic volcanic rock with 5–10% of angular fragments (less than or equal to 40 cm across) of fine-grained felsic volcanic rock and less common jasper.

Cutting the vent facies breccia in two places are small circular breccia pipes (Fig. 42). These contain fragments of felsic volcanic rocks or jasper (or both) in a matrix composed of a microgranular, granophyric intergrowth of quartz and feldspar

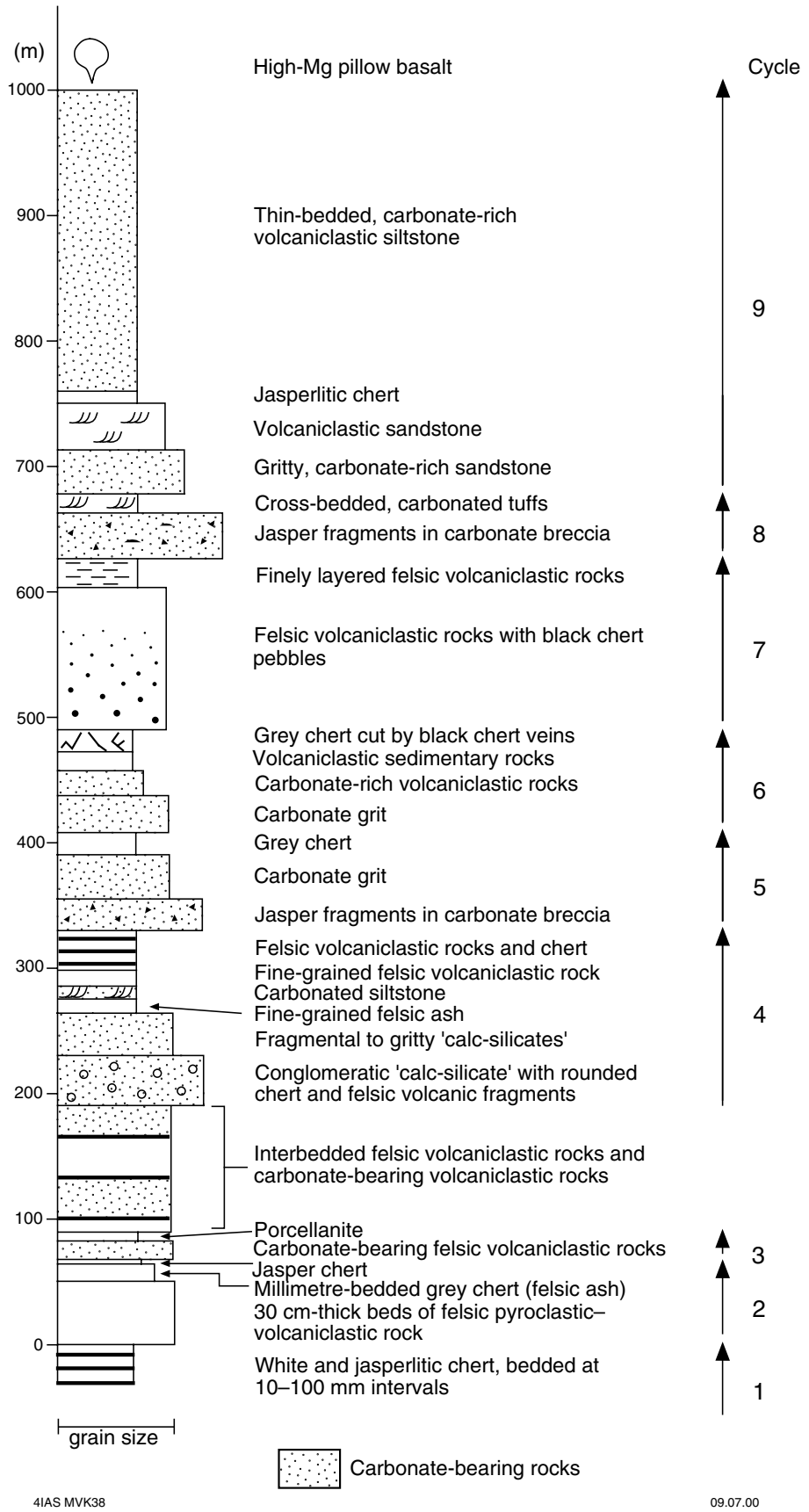

Figure 43. Stratigraphic section through the carbonate-bearing, volcaniclastic ejecta apron of the Panorama Formation, proximal to the vent of the Panorama volcano at Locality 3.1, showing nine fining-upward eruptive cycles

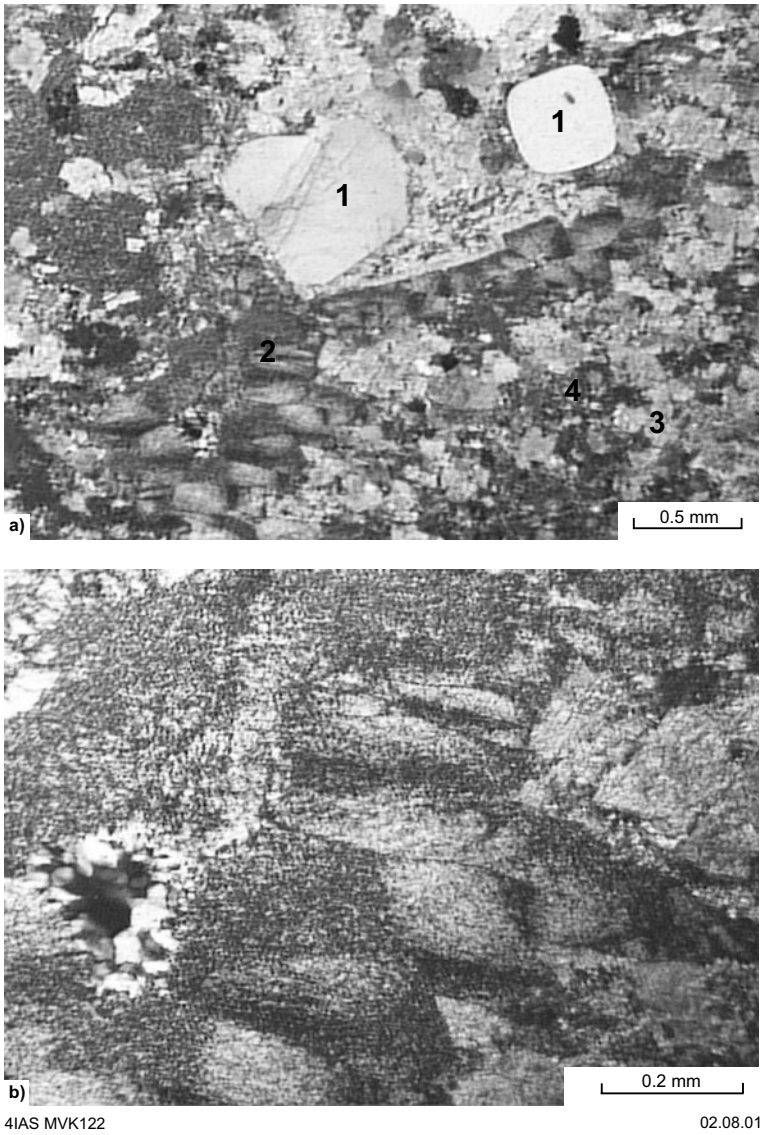

Figure 44. Thin sections of the matrix of the jasper-fragment breccia pipe in the vent of the Panorama volcano (cross polarized light):
a) subhedral quartz phenocrysts (1) and a sharp-edged domain of pure quartz (2) in a matrix containing scattered carbonate rhombs (3) in devitrified rhyolite glass (4);
b) detail of the pure quartz domain, showing that it is composed of radiating sheaths of fibre bunches nucleated on the prismatic terminations of carbonate rhombs and an inner core of coarser textured, granoblastic quartz. The fibre bunches are characteristic textures of precipitation from boiling fluids. The fact that the quartz fibres nucleate on carbonate rhombs indicates that carbonate was of magmatic origin

(devitrified rhyolitic glass) and abundant carbonate (ankerite, ferroan dolomite, or siderite). The largest of these, east of this area, is 20 m in diameter and dark chocolate-brown in colour, containing sparse and irregular fragments of fine-grained felsic volcanic rock up to 35 cm in size. The smaller pipe, seen at this locality, is 1 m in diameter and packed with angular jasper and subordinate felsic volcanic fragments in a carbonate-bearing matrix of devitrified rhyolite glass. The fragments display a vertical flow alignment. The jasper breccia pipe is identical in appearance to the basal debris flows of fining-upward cycles 5 and 8 in the proximal volcaniclastic apron, and it is

interpreted to be a feeder vent to the eruptive material deposited on the flanks of the volcano.

Petrographic studies of the jasper breccia pipe show that the matrix consists of granophyric quartz–feldspar and intergrown carbonate, with subordinate, irregular-shaped, sharp-walled domains of pure quartz (Fig. 44a). The pure quartz domains contain an outer margin of radial quartz-fibre bundles that passes inwards to medium-grained cores with unstrained, polygonal textures (Fig. 44b). These textures indicate primary crystallization of quartz into a supersaturated magmatic fluid (cf. Craig and Vaughan, 1981, p. 116). Significantly, the radial quartz-fibre bundles nucleated on the prismatic terminations of carbonate rhombs (Fig. 44b), thereby indicating that the carbonate was present as a magmatic component of the matrix in the jasper breccia pipe. This is used to infer that the carbonate deposited in the conformably overlying Strelley Pool Chert was ultimately derived from a volcanic source.

The new evidence for a magmatic origin of carbonate in the Panorama Formation may have important implications for the sources of sulfates and carbonates in fossiliferous cherts of the Warrawoona Group and for the development of early life on Earth (Van Kranendonk, 1999b). The reason is that the Strelley Pool Chert lies everywhere conformably above volcaniclastic rocks of the Panorama Formation, except above the area of its greatest thickness around the stratigraphically thickest (topographically highest) part of the volcanic vent (cf. DiMarco and Lowe, 1989). This indicates that the chert represents the final silicified emissions of the felsic volcanic event, in much the same way as the marker chert at the top of the Sulphur Springs Group marks the end of that volcanic episode. The presence of jasper, carbonates, and sulfates in the fossiliferous chert horizons is in stark contrast to the commonly accepted hypothesis that the Archaean hydrosphere and atmosphere were anoxic. The evidence for a magmatic source for the carbonate in the Panorama volcano suggests a possible explanation for the presence of the highly oxygenic minerals whereby locally oxygenating conditions in seawater were caused by emissions of oxygenic volcanic gasses (CO_2, SO_4, FeO) from degassing magma chambers (e.g. Fig. 32b: Van Kranendonk, in prep. c).

Locality 3.3: Synsedimentary collapse structures in the Warrawoona Group, Coppin Gap greenstone belt (Muccan, AMG 195200E 7687200N)

by W. Nijman, S. T. de Vries, I. Vos, and K. Louzada (Institute of Earth Sciences, Utrecht University, The Netherlands)

The outcrops to be visited at this locality are located south of Kittys Gap in the Coppin Gap greenstone belt (Plate 1; for overviews of the local geology, see Nijman et al., 1998b, 1999b, and Williams, 1999). Here, a weakly metamorphosed stratigraphic sequence of basalt, felsic volcanic rocks, and siliceous sedimentary rocks are offset by an array of normal faults (Fig. 45). The felsic volcanic rocks belong to the Panorama Formation of the Salgash Subgroup (3454 ± 1 Ma, Thorpe et al., 1992a; 3458 ± 2 Ma, R. Thorpe in Williams, 1999; 3445.7 ± 2.0 Ma, J. Wijbrans and W. Nijman, unpublished data), and represent an extension of the rocks from the type area in the North Pole Dome. Note that some data presented in this section are preliminary results of current research.

Significance of growth faults

Nijman et al. (1998b, 1999b) described the structures south of Kittys Gap as an example of growth-fault extension, similar to those in the felsic to intermediate volcanic Duffer

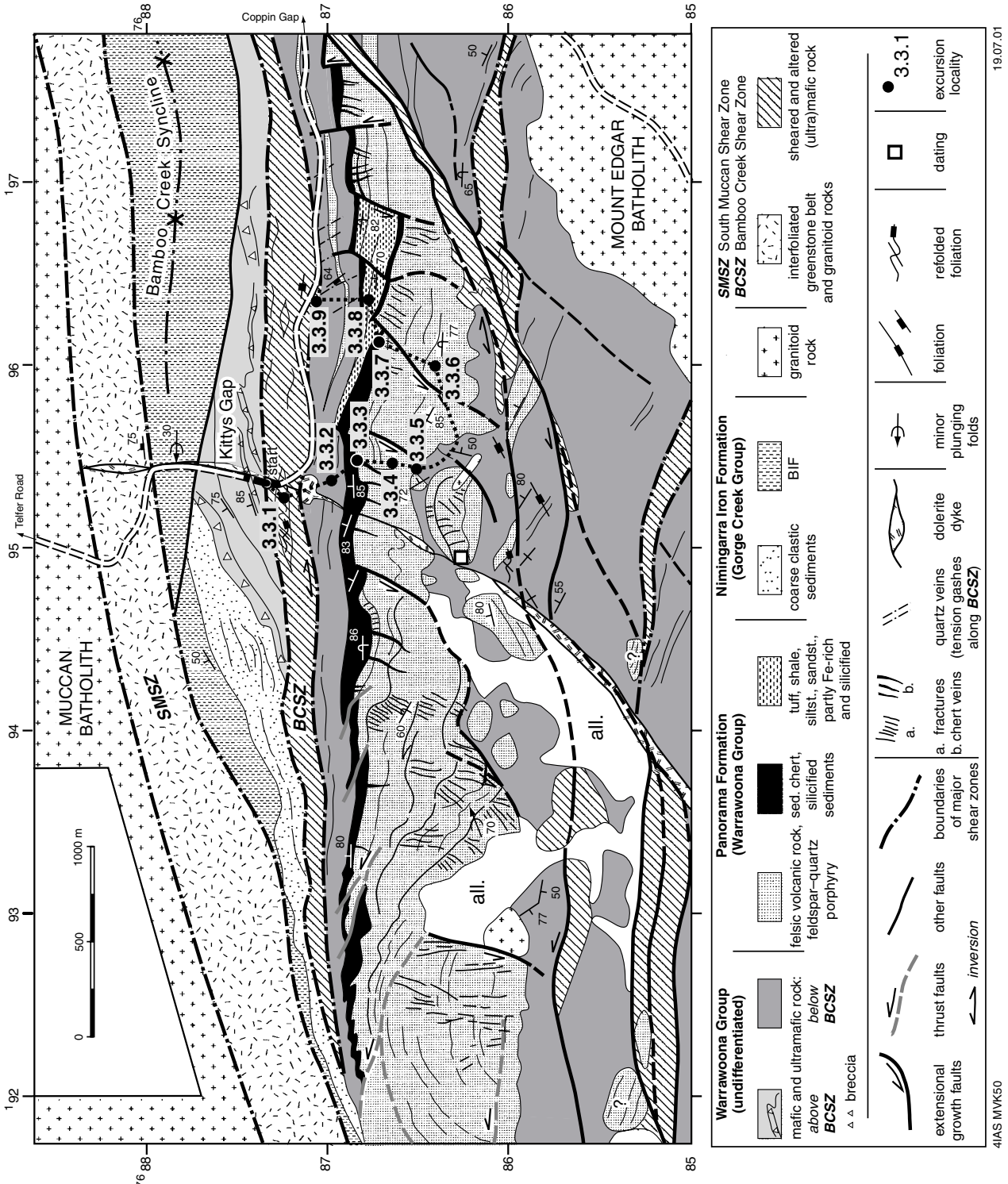
MUCCAN BATHOLITH
MOUNT EDGAR BATHOLITH
Bamboo Creek Syncline
Coppin Gap
Kittys Gap
Telfer Road
start
SMSZ
BCSZ
3.3.1
3.3.2
3.3.3
3.3.4
3.3.5
3.3.6
3.3.7
3.3.8
3.3.9
all.
0
500
1000 m
Warrawoona Group (undifferentiated)
mafic and ultramafic rock: above BCSZ / below BCSZ
breccia
Panorama Formation (Warrawoona Group)
felsic volcanic rock, feldspar–quartz porphyry
sed. chert, silicified sediments
tuff, shale, siltst., sandst., partly Fe-rich and silicified
Nimingarra Iron Formation (Gorge Creek Group)
coarse clastic sediments
BIF
granitoid rock
SMSZ South Muccan Shear Zone
BCSZ Bamboo Creek Shear Zone
interfoliated greenstone belt and granitoid rocks
sheared and altered (ultra)mafic rock
extensional growth faults
thrust faults
other faults
boundaries of major shear zones
inversion
a. fractures
b. chert veins
quartz veins (tension gashes along BCSZ)
dolerite dyke
minor plunging folds
foliation
refolded foliation
dating
excursion locality
4IAS MVK50
19.07.01

Formation of the same belt (cf. DiMarco and Lowe, 1989). These structures are similar to those found in the Dresser Formation of the North Pole Dome (Nijman et al., 1998a, 1999a; Van Kranendonk, 2000a; see **Locality 2.5**) and in the Coongan greenstone belt (Zegers et al., 1996). The same type of kilometre-scale growth faults also form the major control on the distribution of felsic volcanic rocks, volcaniclastic sedimentary rocks, and shallow-level tonalite intrusions in the otherwise mafic to ultramafic volcanic Onverwacht Group of the contemporaneous South African Barberton greenstone belt, Kaapvaal Craton (de Vries, 1999; Nijman, 1999; Lowe and Fisher Worrell, 1999).

Extensional faulting is the earliest deformation identified in the East Pilbara Granite–Greenstone Terrane by Zegers et al. (1996) and Kloppenburg et al. (in press), who stress a unidirectional pattern of extension. This may point to a phenomenon at the scale of an orogen or plate margin, for example, orogenic collapse, rifting, or the formation of core complexes.

Alternatively, where the fault arrays can be proven to have been concurrent with sedimentation and therefore active at the Earth's surface, their orientation does not support such unidirectionality of extension; nor are these structures related to the presently preserved distribution of granitoid domes as one would expect in a model of granitoid diapirism (Collins et al., 1998). Rather, as a working hypothesis currently under investigation, we suggest that the extensional growth faults may represent major scoop-shaped or circular gravitational collapse patterns with a diameter estimated to be 100 km. These periods of gravitational collapse might be related to episodic and local magmatic differentiation at deeper crustal levels (cf. Cullers et al., 1993; Vlaar et al., 1994) responsible for the concurrence of basaltic and felsic igneous rocks. The tensile structures are throughout the Warrawoona Group in the Dresser, Duffer, and Panorama Formations, and often coincide with places where hydrothermal siliceous fluids largely influenced sedimentation and early diagenesis. Felsic volcanism and high-level intrusion are absent (?not exposed) from some of these growth-fault arrays (e.g. Dresser Formation), but are intimately associated with them elsewhere. The depositional basins, rimmed by the extensional fault systems, appear to be generated by uplift from the subaqueous level of pillowed flood basalts, rather than by subsidence. Although the collapse structures resemble calderas, their size and deep derivation of contained felsic volcanic component makes them comparable to the corona structures on Venus (Philips and Hansen, 1994; Nijman and de Vries, 2001).

Stratigraphic continuity or not?

Nijman et al. (1998b, 1999b) described shear zones (sub)parallel to bedding in the more than 10 km-thick Warrawoona Group of the Coppin Gap greenstone belt south of Kittys Gap. These zones commonly descend through the stratigraphy westward along the belt, and these authors proposed that tectonic slicing had influenced the stratigraphic thickness of the belt, as has been observed in other belts of the EPGGT as well as in the Barberton greenstone belt of the Kaapvaal Craton, South Africa (Zegers, 1996; van Haaften and White, 1998).

Figure 45. Geological map of the Kittys Gap growth-fault array, showing Localities 3.3.1 – 3.3.9. The map reads as a cross section due to the subvertical orientation of the bedding. The listric growth-fault array back-steps to the east (to the right). During this process, hangingwall blocks at the western end of the fault array have been progressively backrotated and deformed into rollover anticlines. The updip-tapering wedges of hangingwall blocks onlap the previous ones and are slightly thrust over each other. The base of the structure is modified by a megabreccia of rotated, detached blocks of felsic volcanic rock within deformed metabasalt. This is only possible at a relatively low geostatic pressure (i.e. under restricted overburden). The combination of compressive and extensional deformation under low overburden is interpreted as clear evidence of the synsedimentary, surficial gravitational collapse character of the fault structure

Van Haaften and White (1998) suggested that tectonic shortening may have transported crustal slices over long flats and short ramps, and such a geometry was inferred for the hangingwall of the Bamboo Creek Shear Zone from Kittys Gap to beyond the Bamboo Creek mining centre (Nijman et al., 1998b, 1999b). This transport may have been accomplished on largely unspectacular faults, as , for example, in gravitational sliding. Characteristically, in gravitational collapse, tensile faults at the rear of a fault array are broadly contemporaneous with compressive features at the front. Evidence from the Kittys Gap area (Locality 3.3) and the Barberton greenstone belt of the Kaapvaal Craton shows this combination, and thus implies gravitational collapse as an important surficial deformation mechanism (see also de Wit, 1982). In this respect, we (Nijman and colleagues) suggest that the recumbent folds described by Collins (1989) in the McPhee Reward section of the Marble Bar greenstone belt may also represent toe-structures of large tensile fault arrays.

Alternatively, recent dates obtained by the Geological Survey of Western Australia (Williams, 1999) confirm an upward-younging of the stratigraphic sequence and are used as an argument for stratigraphic continuity within the belt, as elsewhere across the EPGGT (e.g. Van Kranendonk, 2000b; Van Kranendonk et al., 2001). However, since it is known (for instance from Alpine-type collisional orogens) that tectonic juxtaposition through shortening may involve stratigraphic sequences comprising only a few million years duration, the density of dating in greenstone belts of the EPGGT is still considered far from sufficient to permit a good evaluation of the arguments for or against tectonic duplication of stratigraphy.

Repeated action along shear zones appears to imply inversion from extension to compression wherever the original detachments were properly oriented to accommodate the later east-facing thrusting (Zegers, 1996; Nijman et al., 1998b, 1999b). The compressive structures are interpreted to have formed during deposition of the Gorge Creek Group at about 3240 Ma.

Excursion localities

Return to the vehicles, turn around and drive back out to the North Pole Road. Turn left, and follow the track for 39 km to Highway 138 and turn right. Proceed southeast along the highway for about 58 km and turn left onto the Woodie Woodie Road. Proceed for 24 km and continue past the turn on the left for a further 6 km and turn right down a track towards a range of hills for 4.5 km to Kittys Gap. The excursion will follow a semi-circular trace passing southwards to near the base of the South Kittys Gap growth-fault structure and then northeastward to end 1 km to the east of the departure point along the same track (Fig. 45).

Locality 3.3.1

Carbonate-altered, bladed olivine-komatiite flows are preserved in a deformed lens between anastomosing shear bands of the Bamboo Creek Shear Zone (Fig. 45: see also **Locality 3.3.9**). Relics of bedding and earlier shear foliations are refolded asymmetrically. This sort of observation forms the basis for the interpretation of inversion along some of the major shear zones.

Locality 3.3.2

Stacked basalt flows with brecciated, hyaloclastic bases indicative of lava flowing in shallow water, are overlain by columnar-jointed basalt. These are all part of the Euro Basalt, which forms the reference horizon for the observation of differential thickness in the growth-fault structure of the Panorama Formation. In places, the basalt contains

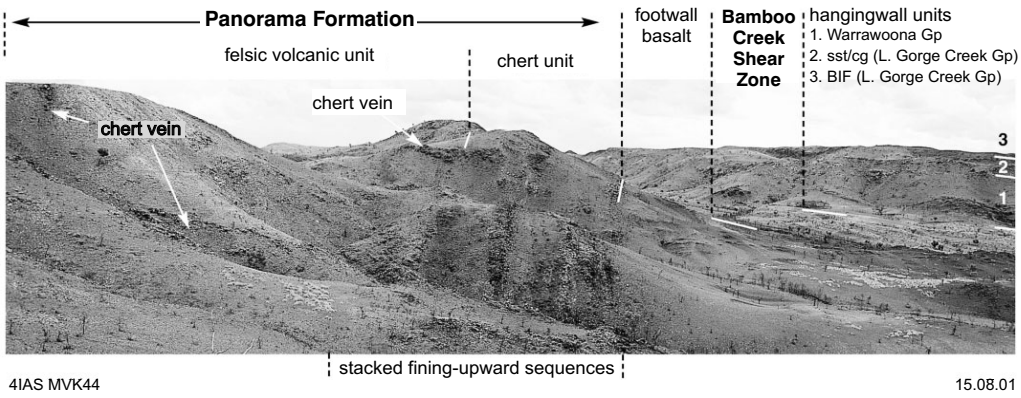

Figure 46. Westward view from Locality 3.3.3, strike-parallel to the top of the Panorama Formation (BIF = banded iron-formation, cg = conglomerate, sst = sandstone, L. Gorge Creek Gr = Lower Gorge Creek Group)

lenses of silicified sandstone or is itself silicified. Both the Euro Basalt and the top of the Panorama Formation are interpreted to have been deposited at sea level.

Locality 3.3.3

Bedded cherty rocks at the top of the Panorama Formation (Williams, 1999) display repeated, 10 m-scale, fining-upward (from conglomerate or sandstone, or both, to dense chert) cycles of silicified volcaniclastic sedimentary rocks (Fig. 46). Lateral-accretionary bedding, mega-cross-bedding and small-scale heterolithic sedimentary rocks are probably of tidal origin (Fig. 47). Metre-thick black chert veins terminate in the lowermost chert unit, and hydrothermal breccia pods (cf. Nijman et al., 1998b, 1999b) are in this sedimentary rock (Fig. 46).

Material from this site is currently being investigated by F. Westall (Lunar and Planetary Science Institute, Houston). who has found biofilm, coccoidal, and filamentous microbial remains in the laminated sediment.

Locality 3.3.4

From Locality 3.3.3 we head due south, following one of the major black-chert veins that traverses the felsic volcanic host rock, in a direction opposite to the younging direction of the rocks. Immediately eastwards, one of the growth faults is visible in the offset of the contact between the bedded chert and felsic lavas.

A network of black chert veinlets at the lower end of the chert vein extending from Locality 3.3.3 fills in situ breccia of felsic lava (cf. Nijman et al., 1998b, 1999b, fig. 11a). The subvertically dipping lavas consist of very poorly bedded quartz- and feldspar-phyric rhyolites, in places with flow banding. The outcrop illustrates the probable exhalative character of the brecciation of the host rock and concurrent infill with chert, precipitating rapidly from upward-moving fluids. In the North Pole Dome, chert seems to fill surficial conjugate fracture patterns, related to the growth fault geometry. Also in the Kittys Gap example, fractures also seem to cluster in the hangingwall next to the major growth faults (Fig. 45), and some of them develop into chert-bearing vein systems. Electron microscopy of the black chert reveals an isometrical, almost 100% pure, microquartz fabric without biofilm or carbonaceous matter.

Figure 47. Detail of the heterolithic cherty sediment capping the growth-fault structure at Locality 3.3.3, showing, from base to top: 1 = small-scale heterolithic ripple-laminated chert with paleocurrent dominantly to the left; 2 = wrinkly laminated 'ministromatolites', containing dispersed filamentous coccoidal microbia, and biofilm; 3 = flat to low-angle laminated chert deposited mainly through suspension settling; 4 = undulous stratification transitional into ?wave-ripple lamination

Locality 3.3.5

Locality 3.3.5 is the southernmost point of our excursion through the Kittys Gap growth-fault structure. The valley running parallel to the base of the rhyolite body is interpreted to be the basal detachment of the normal fault array.

Flow-banded rhyolite is disoriented with respect to the overall strike of the felsic volcanic unit. Disorientation is associated with mega-brecciation, sliding and rotation along the base of the felsic unit, causing irregular juxtaposition of the rhyolite blocks with the underlying basalt in the hangingwall of the basal detachment surface of the growth-fault structure.

Locality 3.3.6

From Locality 3.3.5 the excursion heads north-eastward.

Here we can observe a felsic agglomerate of quartz-porphyritic lava with a fine-grained matrix, interpreted to be a lahar-type volcanic deposit. The rocks show strong fracture cleavage which we relate to the proximity of one of the normal faults.

Locality 3.3.7

An overview of the local geologic setting shows that the entire rock sequence of the Coppin Gap belt to the north of the Bamboo Creek Shear Zone (Fig. 48), including the shear zone, is deformed into the Bamboo Creek Syncline with an easterly plunging axis parallel to the belt (Nijman et al., 1998b, 1999b; Figs 45 and Plate 1). The axis of the syncline is situated in the Nimingarra Iron Formation and growth strata of clastic sedimentary rocks (Cundaline Formation) of the Gorge Creek Group that form the range of hills in the hanging (northern) wall of the shear zone. Behind the hills lies a plain

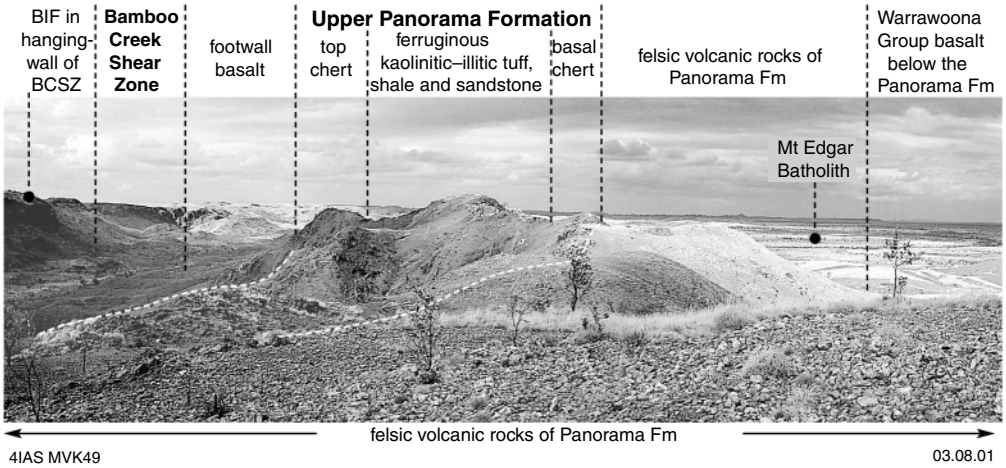

Figure 48. Eastward view from Locality 3.3.7 along the strike of the Panorama Formation. The upper Panorama Formation consists of a sedimentary wedge, tapering towards the viewer, that forms the terminal stage of growth-fault infilling and is composed of chert, tuff, and shale (see Locality 3.3.8)

underlain by the Muccan Granitoid Complex. Notice the difference in style of deformation between the hangingwall and footwall of the shear zone: en echelon east-northeast-striking slabs of silicified and brecciated mafic and ultramafic rock characterize the combined Warrawoona Group and Gorge Creek Group of the hangingwall along the north side of the shear zone, whereas bedding in the footwall tends to bend into an east-southeast strike against the faults of the south Kittys Gap growth-fault array. The latest stage of sedimentary infill consists of the shaley — in places silicified — volcanic sedimentary rock of Locality 3.3.8.

The plain to the southeast is underlain by the 3314 ± 13 Ma Coppin Gap Granodiorite (Williams and Collins, 1990) of the Mount Edgar Granitoid Complex. Due south and closer by, an east–west valley hosts the main detachment below the growth-fault array. Further south, the bulk of the Warrawoona Group is exposed.

Locality 3.3.8

The last-stage hangingwall infilling wedge of the leading growth fault consists of kaolinitic–illitic, partly to completely silicified shale or tuff, in places transitional into BIF, which is well exposed along steep gullies. Such a unit is also present 15 km east along strike (5 km southeast of the Bamboo Creek mining centre) where there is another growth-fault array (Plate 1).

Locality 3.3.9

Quartz-filled tension gashes tens of metres long, striking 232° and dipping 64° to the southwest are related to late oblique dextral slip along the Bamboo Creek Shear Zone. East-striking vertical shear foliations around lenses of altered komatiite are comparable to those at Locality 3.3.1.

Day 4: Geology of the Muccan and Warrawagine 1:100 000 map sheets

by I. R. Williams (Geological Survey of Western Australia)

On this day, we will visit a number of outcrops of granitoid rocks of different age in the Muccan and Warrawagine Granitoid Complexes on the Muccan, Warrawagine, and Cooragoora 1:100 000 sheet areas (Fig. 49; Williams, 1999, 2000, 2001). The granitoid rocks show a decrease in strain and complexity with decreasing age.

In addition we will see the well-preserved unconformity between the Nimingarra Iron Formation and Muccan Granitoid Complex, and the Nimingarra Iron Formation in a much more severely deformed state in the Coppin Gap Syncline between the Muccan and Mount Edgar Granitoid Complexes. The excursion localities were previously described, together with several additional localities, by Williams and Hickman (2000).

Locality 4.1: Coppin Gap copper–molybdenum prospect (Muccan, AMG 199100E 7687300N)

Continue 5 km east along the track to Coppin Gap Creek, and Locality 4.1.

The Coppin Gap copper–molybdenum prospect has inferred resources estimated at 102 Mt at 0.105% Mo and 0.152% Cu, which ranks it as one of the largest undeveloped molybdenum deposits in the world (Jones, 1990).

The host rocks for the copper–molybdenum mineralization are altered and metamorphosed, porphyritic to fine-grained dacite and rhyodacite, which form subconcordant, lenticular bodies and dykes in pillowed high-Mg basalt, sheared serpentinized peridotite, and talc–chlorite schist of the Euro Basalt.

The deposit is a multiple-phase stockwork of quartz–carbonate veins that carry up to 2% chalcopyrite, molybdenite, pyrite, pyrrhotite, scheelite, and rare sphalerite. The stockwork is best developed in the silicified contact zone of the intrusive porphyritic dacite and rhyodacite (Marston, 1979).

The felsic bodies are interpreted to be apophyses of the 3314 ± 13 Ma Coppin Gap Granodiorite (Williams and Collins, 1990), about 1 km to the south (Jones, 1990). A conventional titanite U–Pb date of 3317 ± 1 Ma was obtained from a porphyritic rhyolite body (Thorpe, R. I., 1992, written comm. in Williams, 1999). This is interpreted as the date of hydrothermal activity related to the magmatic emplacement of the porphyry.

Locality 4.2: Nimingarra Iron Formation of the Gorge Creek Group, Coppin Gap Syncline (Muccan, AMG 200000E 7688000N)

Continue along the track for 1 km to Coppin Gap and Locality 4.2.

This spectacular gorge provides superb exposures of red and black jaspilite, banded chert, and BIF of the Nimingarra Iron Formation in the tight, east-plunging Coppin Gap Syncline. The northern limb of the fold is locally overturned and separated from the Muccan Granitoid Complex to the north by the South Muccan Shear Zone. Remnants of the basal epiclastic unit of the Nimingarra Iron Formation can be found on both sides of the syncline. The Nimingarra Iron Formation on the southern limb, at this locality, is in sheared contact with talc–chlorite schist and sheared serpentinite of the Euro Basalt.

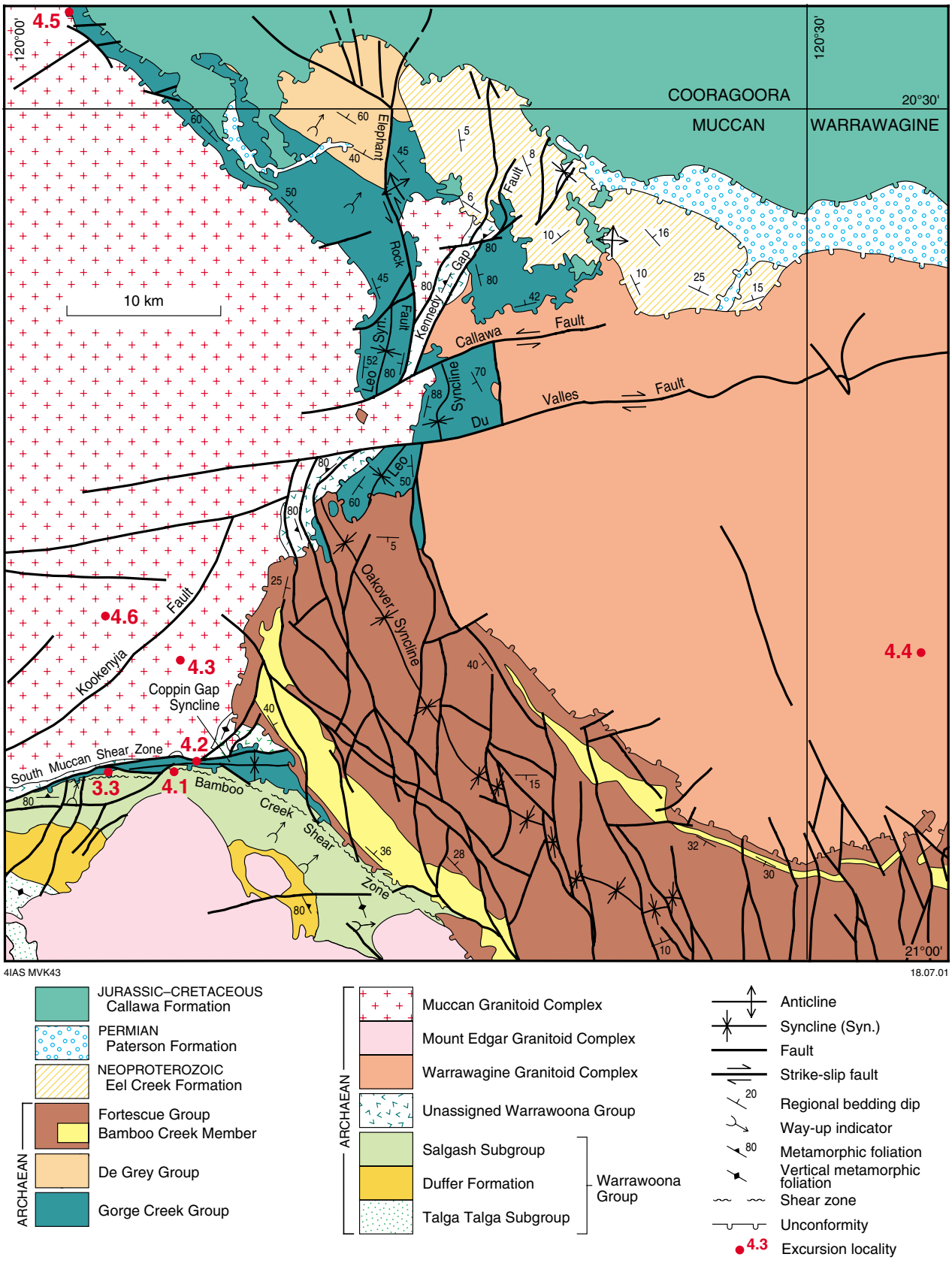

Figure 49. Regional geology of the Muccan 1:100 000 sheet and adjacent areas, showing excursion localities for part of Day 3 and Day 4 (modified from Williams and Hickman, 2000)

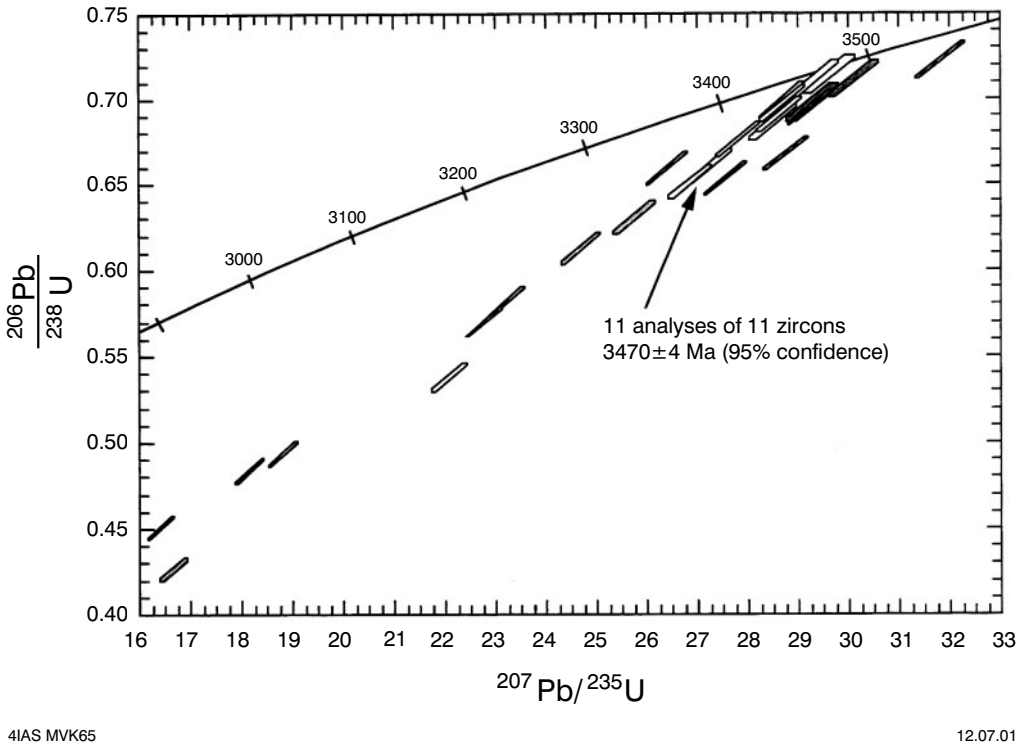

Figure 50. Concordia plot of analysed zircons from the heterogeneous granodiorite gneiss at Locality 4.3 (after Nelson, 1998)

Locality 4.3: Granodiorite gneiss, Fred Well area (Muccan, AMG 199100E 7694800N)

Turn vehicles around and return to Kittys Gap (~5.5 km) and out to the main road (~6 km). Turn right and proceed for 3.5 km (to AMG 199000E 7695100N), then turn right and proceed for 500 m cross-country to Locality 4.3.

This locality contains small, low outcrops of heterogeneous granodiorite gneiss that has yielded the oldest date so far obtained from the Muccan Granitoid Complex, at 3470 ± 4 Ma (Fig. 50; Nelson, 1998). It contains several xenocrystic zircons dated at between c. 3574 and 3506 Ma, around the age of the Coonterunah Group. The gneissosity here is extremely schlieric and possibly inherited from whole-scale melting and remobilization of older (Coonterunah Group age) granitoid rocks. This differs from the type of gneissic layering in much of the Shaw Granitoid Complex (see **Day 7**), which was largely generated by leucogranite injection and in situ leucosome generation.

Locality 4.4: Ancient gneisses of the Warrawagine Granitoid Complex (Warrawagine, AMG 246800E 7696600N)

Return to the Warrawagine Road, turn right and drive for 17.5 km. Turn right and proceed for 45 km (to AMG 247100E 7695400N). Turn north off the road and continue for 1.2 km to a low ridge at Locality 4.4.

This locality is an example of the complexity encountered in some areas of the Warrawagine Granitoid Complex. The rocks record several events ranging from a young crosscutting porphyritic biotite granodiorite dyke, dated at 3244 ± 3 Ma (Nelson, 1999), to xenoliths of folded tonalite gneiss, one of which has yielded xenocrystic zircon

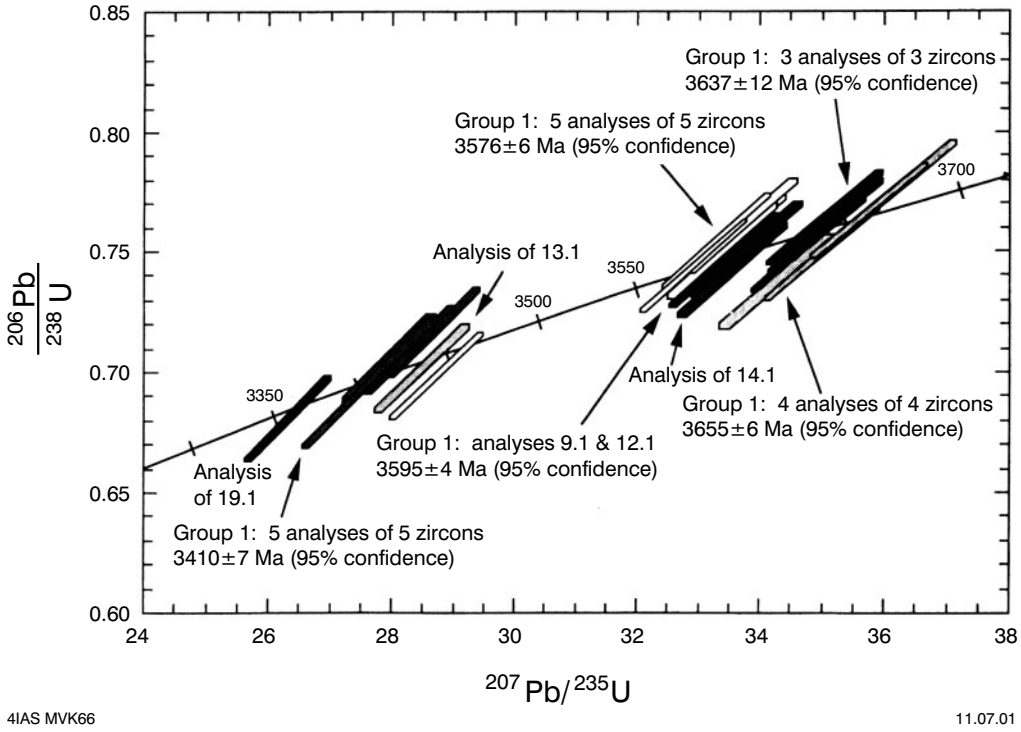

Figure 51. Concordia plot of analysed zircons from the tonalite gneiss inclusion at Locality 4.4 (after Nelson, 1999)

populations of 3576 ± 6, 3595 ± 4, 3637 ± 12, and 3655 ± 6 Ma (Fig. 51; Nelson, 1999). The 3655 ± 6 Ma zircon population is the oldest zircon date yet determined from Pilbara granitoid complexes, using the SHRIMP U–Pb zircon method. A 3410 ± 7 Ma population of zircons from the tonalite gneiss is interpreted as the date for the deformation and metamorphism which produced the gneiss (Nelson, 1999). The c. 3655–3576 Ma ages of protoliths are extremely significant as they indicate the existence of crustal material older than any rocks yet identified in the greenstone succession (oldest age 3515 Ma; Buick et al., 1995) and thus suggest that the greenstone succession may have been deposited on a sialic substrate. This result supports geochemical studies on the oldest greenstones showing that they have been affected by significant crustal contamination during eruption (Green et al., 2000).

The foliated biotite granodiorite host at this locality did not yield a definitive date. However, the poor-quality data suggest an affinity with the c. 3300 Ma plutons, which are found elsewhere in the Warrawagine Granitoid Complex. The c. 3240 Ma age from the granodiorite dyke is interesting in that it extends the effects of the Sulphur Springs Group event over a much wider area than covered simply by associated greenstones.

Locality 4.5: Sunrise Hill unconformity between BIF of the Gorge Creek Group (Nimingarra Iron Formation) and the Muccan Granitoid Complex (Cooragoora, AMG 190900E 7736100N)

Return to the Warrawagine road and turn right. Proceed for 45 km and turn hard right at a Y-junction. Proceed 1 km and turn left. Proceed for 14.5 km and turn right at a

T-junction onto the Muccan – Shay Gap road. Proceed 15.5 km, crossing the De Grey River, to the Nimingarra mine turnoff. Turn left across the Port Hedland – Yarrie iron mine railway (BHP owned). ***Caution: Stop sign for rail crossing****. Continue 15 km along graded road to Locality 4.5.*

The Sunrise Hill West 4 openpit (abandoned) lies on the southwestern side of the Shay Gap – Sunrise Hill ridge. This location is the site of the first published account (Dawes et al, 1995) of the regional unconformity between the basal unit of the Gorge Creek Group — the newly named Nimingarra Iron Formation (Williams, 1999) — and the Muccan Granitoid Complex. A detailed account of the local mine geology is given in Podmore (1990).

In the openpit, the unconformable contact trends east-southeasterly and dips steeply to the north. The unconformity is folded and sheared in places. Although the underlying foliated biotite granodiorite is weathered, it can be seen to be a medium-grained granitoid, a sample of which yielded an age of 3443 ± 6 Ma (Nelson, 1996). The basal unit of the overlying succession comprises polymictic conglomerate containing rounded quartz pebbles and subrounded granitoid boulders up to 40 cm across. The conglomerate is between 0.5 and 1.5 m thick and overlain by about 6 m of highly sheared, ferruginous sandstone, siltstone, and shale. Banded iron-formation lies conformably on the shale unit. All rocks are of low metamorphic grade. The unconformity has been traced southeasterly and easterly across MUCCAN, where it separates the Gorge Creek Group from the Muccan and Warrawagine Granitoid Complexes, and southward to the Coppin Gap Syncline where it separates the Gorge Creek Group from the Warrawoona Group.

Locality 4.6: Wolline Monzogranite, Muccan Granitoid Complex (MUCCAN, AMG 194400E 7697700N)

Return to vehicles, turn around and drive back out the way we came in, 15.5 km east, over the railway tracks, and turn right. Proceed for 32.3 km south along the track and turn left off the road and drive 700 m cross-country (four-wheel drive) to prominent granitoid tors.

The weakly foliated biotite-phyric Wolline Monzogranite is an example of the youngest plutons identified in the Muccan Granitoid Complex, dated at 3244 ± 3 Ma (Nelson, 1998). The principal minerals include K-feldspar (microcline), with abundant quartz

and plagioclase, minor biotite, and accessory chlorite, epidote, muscovite, opaque minerals, apatite, allanite, and carbonate. This monzogranite intrudes c. 3470 Ma gneissic granitoids such as viewed at Locality 4.3.

Day 5: Geology of the Marble Bar greenstone belt

by A. H. Hickman and M. J. Van Kranendonk (Geological Survey of Western Australia)

Days 5 and 6 involve examination of the outcrop data behind the competing hypotheses for the origin of the prominent dome-and-syncline geometry of the EPGGT in the type areas of the Marble Bar greenstone belt (Day 5) and Warrawoona Syncline (Day 6; Fig. 52).

The Marble Bar greenstone belt on the northwestern flank of the Mount Edgar Granitoid Complex contains a succession, up to 12 km thick, of mafic and felsic volcanic rocks, chert, and subordinate metasedimentary rock of the lower Warrawoona Group (Fig. 53; Talga Talga Subgroup and Duffer Formation of Hickman, 1983). Stratigraphically overlying the Duffer Formation, the upper part of the Warrawoona Group (Salgash Subgroup) has a total thickness of more than 5 km, this being a minimum estimate because the uppermost components are obscured by unconformably overlying rocks of the Fortescue Group. All volcanic and sedimentary strata of the belt young consistently northwestward. At the base of the succession, closest to the centre of the dome, strata dip about 20° to the northwest. However, farther northwestward, towards the centre of the greenstone syncline, dips progressively increase until near the top of the Duffer Formation strata pass through vertical to become overturned (dipping steeply southeast, but still younging to the northwest). Overturning of the upper Duffer Formation and the Towers Formation is well displayed at Marble Bar Pool (**Locality 5.8**).

Although previous models suggested that the Marble Bar greenstone belt contains a coherent stratigraphic section tilted on edge by diapiric doming of the Mount Edgar Granitoid Complex (Fig. 54; Hickman, 1983, 1984; Collins, 1989), the total thickness of the Warrawoona Group, combined with the presence of local bedding-parallel shears in this area, led van Haaften and White (1998) to propose that regional northeasterly directed thrusting produced a tectono-stratigraphic assemblage of inverted greenstones deformed in a thrust-stack culmination into which granitoid rocks of the Mount Edgar Granitoid Complex were later emplaced (Fig. 55).

For several reasons, Van Kranendonk et al. (2001) rejected the structural arguments behind the thrust culmination model, although van Haaften and White (2001) defended the model. At the centre of the debate is the relative importance of shear-related structures along the boundaries of some formations, the presence or absence of radial lineation patterns, and geochronology.

On Day 5 we will undertake a transect through the Marble Bar greenstone belt and present data from geological mapping (Hickman and Lipple, 1978; Hickman, A. H., unpublished data), geochemical sampling traverses (Glikson and Hickman, 1981), and U–Pb zircon geochronology (Thorpe et al., 1992a; Nelson, 1999, 2000) that precludes tectonic inversion of the Marble Bar belt by thrusting or folding. Rather, we will provide evidence to suggest that rocks of the Marble Bar greenstone belt are stratigraphic components of a coherent volcanic pile unaffected by duplication, the least competent horizons of which have been affected by a minor component of bedding-parallel shear during doming.

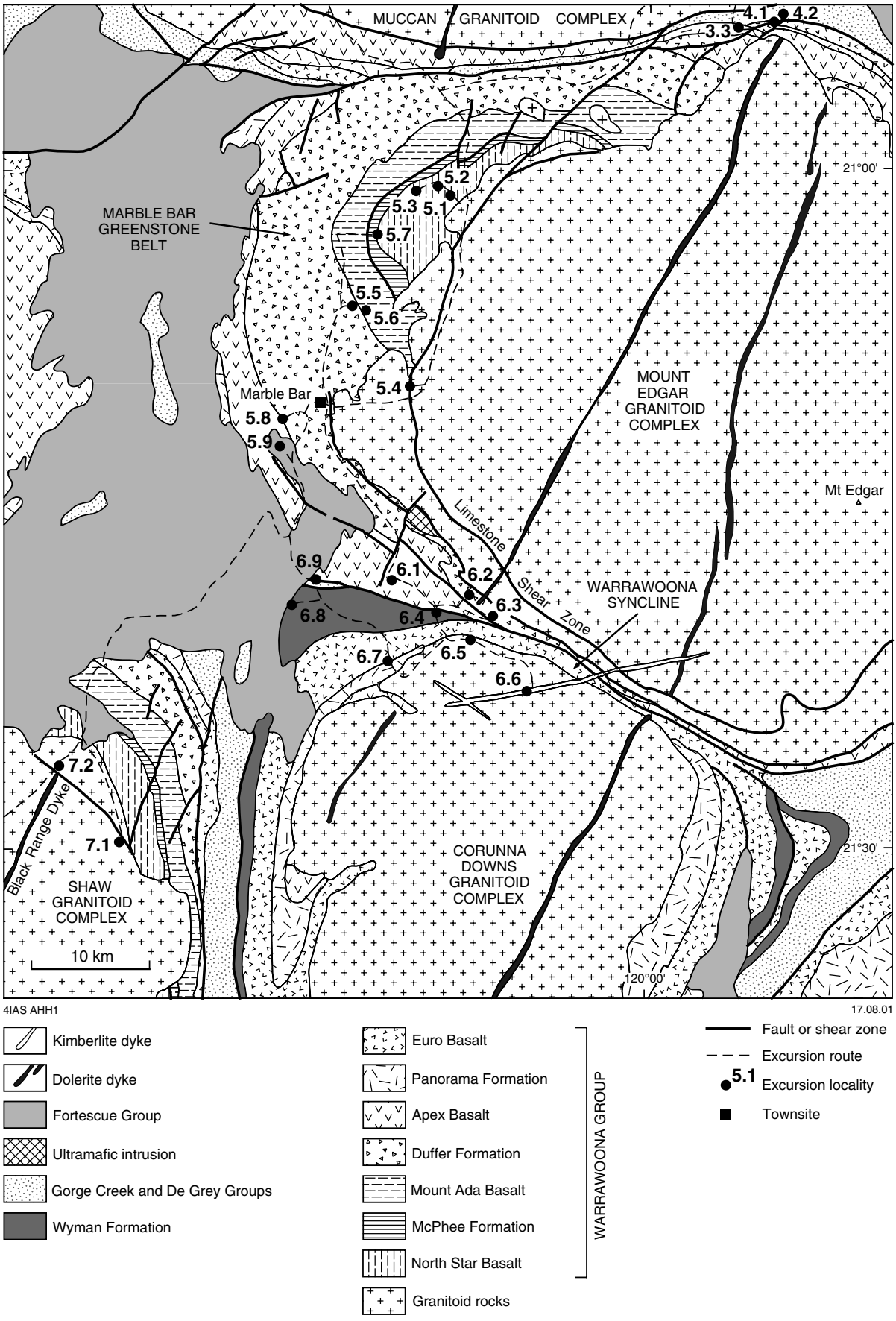

Figure 52. Geological map of the Marble Bar greenstone belt and Warrawoona Syncline, showing excursion localities for Day 5 and Day 6

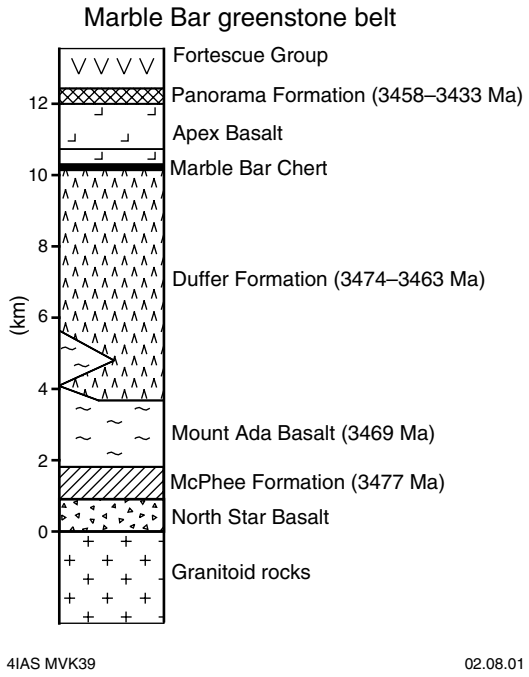

Figure 53. Simplified stratigraphic section of the Marble Bar greenstone belt, showing geochronological data

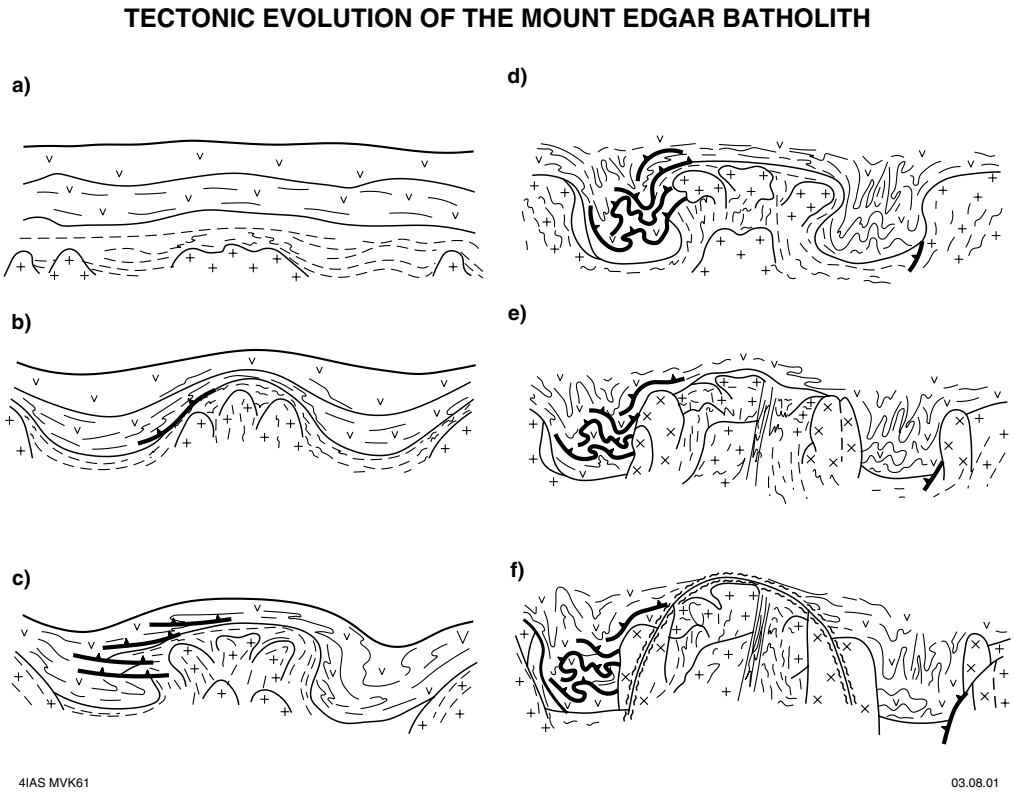

Figure 54. Proposed geological model of the diapiric evolution of the Mount Edgar Granitoid Complex and structures in adjacent greenstones (after Collins, 1989)

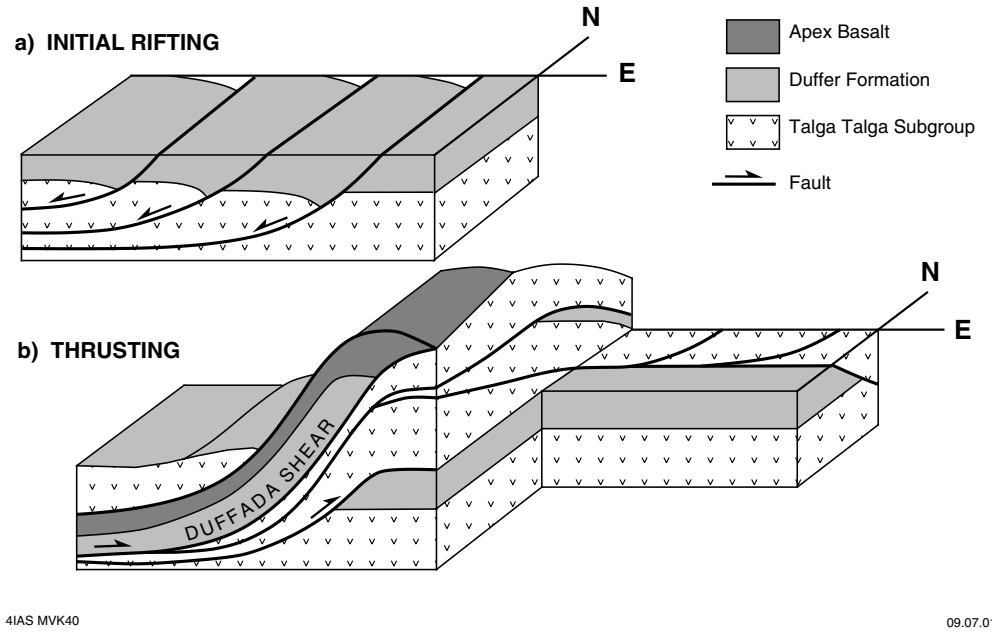

Figure 55. Proposed model for construction of the Marble Bar greenstone belt, through easterly directed thrusting (modified from van Haaften and White, 1998)

During Day 6, we will visit some of the major lithological units in the Warrawoona Syncline, and a post-tectonic, diamondiferous kimberlite dyke, and examine the classic structural fabric elements described by Collins (1989) and Collins et al. (1998) associated with a zone of sinking during granitoid diapirism.

The Warrawoona Syncline is between the Mount Edgar Granitoid Complex to the north and the Corunna Downs Granitoid Complex to the south (Fig. 52). Greenstones that underlie the northern limb of the syncline include the southward continuation of the lower part of the Warrawoona Group in the Marble Bar belt (Mount Ada Basalt to Apex Basalt). These are separated from greenstones belonging to the upper part of the Warrawoona Group (Panorama Formation and Euro Basalt) and to the Wyman Formation on the southern limb of the syncline by faulting in the core of the syncline (**Locality 6.10**). The rocks are weakly deformed in the western part of the syncline where it is 12.5 km wide, but become more highly strained to the east where the greenstone assemblage narrows to 1 km in width.

As the rocks become more intensely transposed from west to east into the core of the syncline, metamorphic foliations are accompanied by the progressive development of mineral elongation lineations that gradually change orientation from moderately east plunging to vertical in the core of the syncline and moderately west plunging out the eastern side of the syncline (Collins, 1989; Teyssier and Collins, 1990). Teyssier and Collins (1990) showed that in combination with the steepening of the lineations, fabric shape elements changed from S>L, to L>>S, to pure L-tectonites in a zone of sinking (Figs 56a,b), identical to the geometry predicted by centrifuge models of diapirs (Figs 56c,d). Collins et al. (1998) summarized this data and used it in support of partial crustal overturn, which previous geochronology showed occurred at c. 3300 Ma (Williams and Collins, 1990). As far as we are aware, no other mechanism has been proposed to explain these fabric elements, and they certainly cannot be explained by cross-folding.

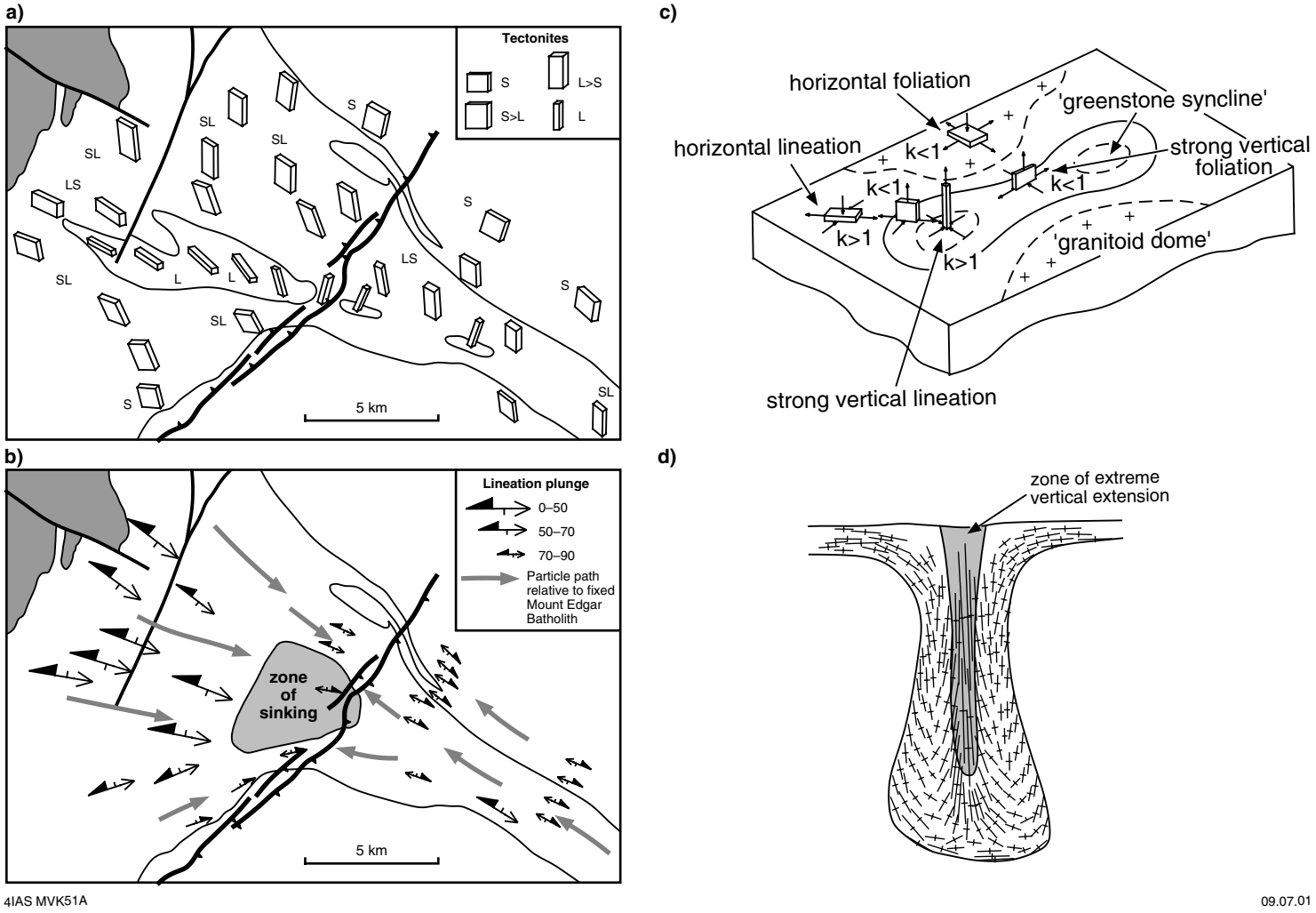

Figure 56. Strain patterns across the margin of the Mount Edgar Granitoid Complex and Warrawoona Syncline: a) strain pattern variation; b) lineation pattern showing convergence toward a central point along the synclinal axis. Combined with kinematic data, this indicates that the greenstones sunk through a zone of vertical constrictional strain in the axis of the Warrawoona Syncline; c) variation in strain across a modelled diapiric syncline. Note the identical nature of the modelled strain relative to that in the Warrawoona Syncline shown in (a); d) cross sectional profile showing a zone of extreme vertical extension in the core of a modelled diapiric syncline; (a) and (b) after Teyssier and Collins (1990); (c) and (d) modified from Dixon and Summers (1983)

a)

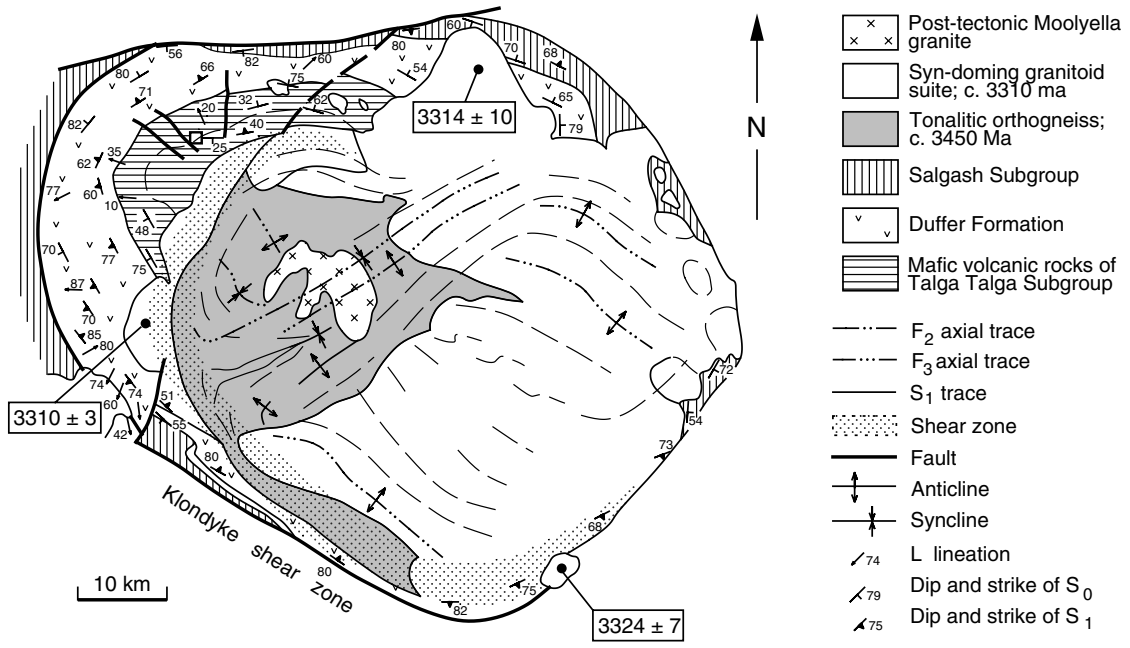

b)

4IAS MVK13

4IAS MVK13a

03.08.01

06.08.01

Figure 57. a) Generalized geological map of the Mount Edgar Granitoid Complex, showing the marginal limestone shear zone, Klondyke Shear Zone, and intrusive contacts in the northeastern part of the complex (after Williams and Collins, 1990). Note the similar ages of dated granitoid rocks that cut and are cut by the shear zone; b) aerial photograph of a salt diapir from Iran, showing similar features as the Mount Edgar Granitoid Complex, including a horseshoe-shaped ring fault at lower left and an intrusive contact with tilted overburden in the top right (modified from Jackson et al., 1990)

The Klondyke Shear Zone is related to ring faults that encircle the Mount Edgar and Corunna Downs Granitoid Complexes (Fig. 8), but the most recent mapping (Hickman, 2001) has shown it to be discontinuous northward (Fig. 57). The shear zone is host to numerous gold deposits mined at the turn of the century, and similar mineralized shear zones are present in other greenstone belts of the east Pilbara region. There is a wedge of kyanite-bearing schists is between the Klondyke Shear Zone and the Limestone Shear Zone developed along the margin of the Mount Edgar Granitoid Complex. Pressure–temperature estimates of 5.5 – 6 kb and 500–600°C have been obtained from the schists and associated metabasites (Delor et al., 1991) that indicate initial burial to depths of about 25 km. Collins and Van Kranendonk (1999) showed that these deeply buried rocks were exhumed within the kyanite stability field, and that this was consistent with heating along the side of a rising diapir as indicated by numerical modelling (Mareschal and West, 1980).

A ring fault that encircles the Corunna Downs Granitoid Complex (Fig. 9)

4IAS MVK80 03.08.01

Figure 58. Aerial photograph of a salt diapir from Iran, showing similar features as the Corunna Downs Granitoid Complex (cf. Fig. 9), including hook-shaped folds in the top right and top left, and a bounding ring fault (modified from Jackson et al., 1990)

bounds hook-shaped folds that formed during granite intrusion. Hook-shaped folds are also characteristic of salt diapirs (Fig. 58: Jackson et al., 1990), and these geometrical features led Van Kranendonk and Collins (in prep.) to support Hickman's (1984) original model of diapiric emplacement of granitoid complexes through a punctuated, multistage intrusion history over the 700 m.y. history of the east Pilbara region.

Locality 5.1: Serpentinite and metabasalt in the lower North Star Basalt (MARBLE BAR, MGA 795650E 7673000N)

From the previous locality, return to the track, turn left and proceed for 9 km to a T-junction. Turn right and proceed for 24 km to a T-junction with Highway 138, the road from Marble Bar to Port Hedland. Turn left toward Marble Bar and proceed for about 9 km to a gate on the western side of Highway 138. Once through the gate, follow the track

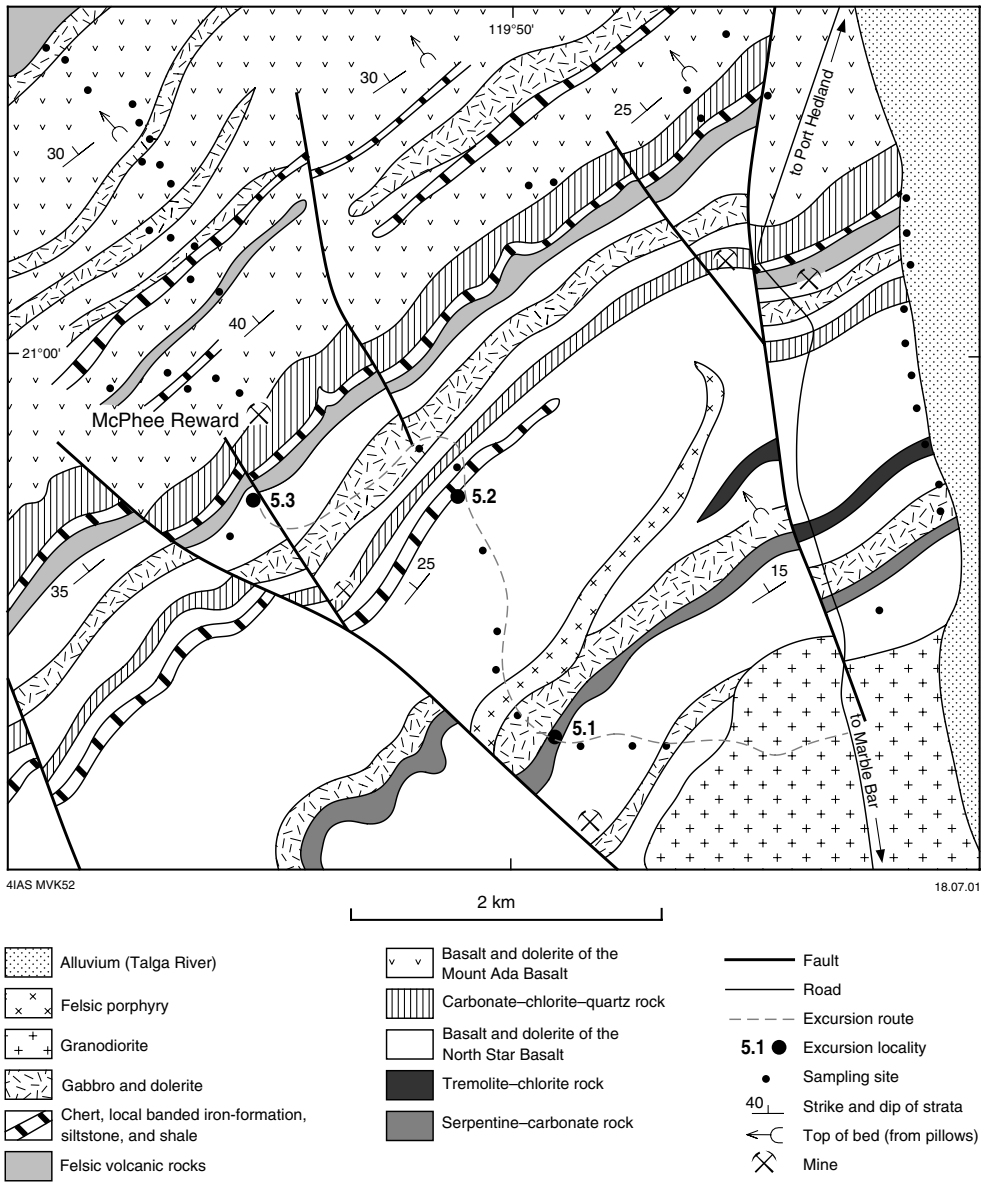

Figure 59. Geological map of the Talga Talga Subgroup in the McPhee Reward area, showing excursion localities and geochemical sample sites used in Figure 60 (after Hickman, 1980)

westward, keeping to the right at a fork, and drive for 1.5 km to Locality 5.1. Here the track runs along a rocky creek bed for about 100 m.

The track from Highway 138 to the abandoned McPhee Reward gold mine (Fig. 59) was used in one of the geochemical traverses undertaken by Glikson and Hickman (1981). Sampling sites on this traverse are shown in Figure 59, and some of the geochemical data are summarized in Figure 60.

The North Star Basalt is the basal formation of the Warrawoona Group, and older than 3477 Ma (see **Locality 5.6**). A sample (GSWA 45066) collected at Locality 5.1 is chemically tholeiitic, but has relatively high contents of Zr (151 ppm), Nb (7 ppm), and Y, La, and Ce (29, 10, and 32 ppm respectively). Figure 60 shows that two other basalts and a dolerite from the lowest part of the North Star Basalt have similar compositions. The chemistry of these basaltic rocks suggests contamination, either related to intrusion of granodiorite about 1 km to the east or as a result of crustal contamination during volcanism, as suggested independently for rocks of the Coonterunah and upper Warrawoona Groups farther west (Green et al., 2000). The metamorphic grade of the North Star Basalt in this

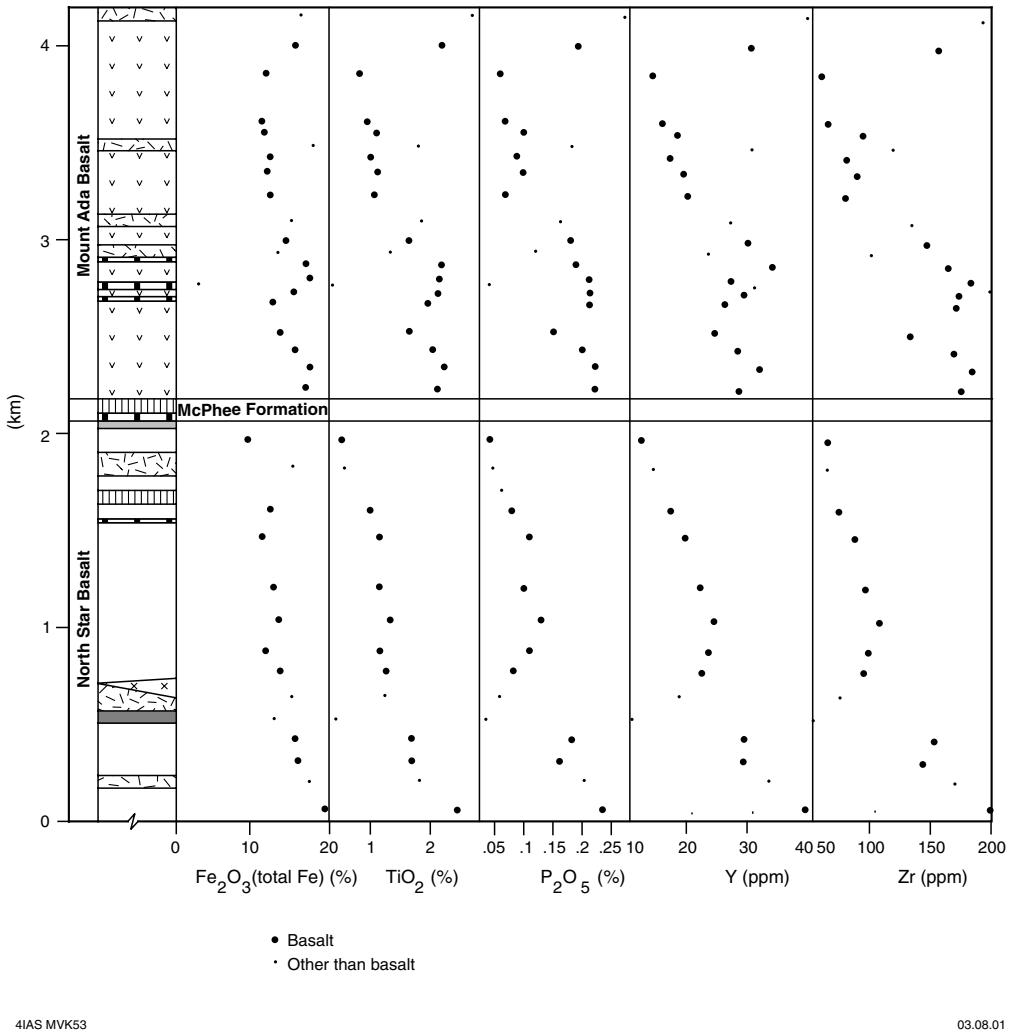

Figure 60. Geochemical trends in the McPhee Reward section (after Hickman, 1980)

area is lower amphibolite facies.

Metamorphosed basalt is exposed on high ground south of the track, together with carbonated serpentinized olivine-cumulate textured peridotite. Views to the north provide good examples of dip slopes, with the basaltic flows inclined at about 20° to the northwest. The basalt is overlain by a variably carbonated talc–chlorite–serpentine rock that is exposed on both sides of the track. The carbonated serpentinite is stratiform, and overlain by metapyroxenite and metadolerite. Its composition (sample GSWA 45065) includes: 40.30% SiO_2, 33.58% MgO, 2.31% H_2O, 3.75% CO_2, 4280 ppm Cr, and 2214 ppm Ni. Some parts of the rock preserve relict olivine-cumulate texture. Figure 59 indicates that the serpentinite may be the basal component of a volcanic sequence that overlies the sequence containing the pillow basalt.

Locality 5.2: Pillow basalt, chert, and carbonated ultramafic rock in the upper North Star Basalt (Marble Bar, MGA 794200E 7674150N)

Follow the McPhee Reward track westward for 2 km to the top of a ridge containing chert.

Locality 5.2 is situated at the top of a thick succession of pillow basalt and dolerite, and is of interest because it contains the lowest chert identified in the North Star Basalt. The chert includes banded iron-formation and silicified fine-grained clastic metasedimentary rock. It is immediately underlain by pillow basalt, and overlain by carbonated ultramafic rock. The basalt at Locality 5.2 contains vesicles infilled by quartz, feldspar, chlorite, and rare amphibole. Like the serpentinite at Locality 5.1, the ultramafic rock above the chert is probably an altered extrusive unit, and is interpreted to mark the base of a third package of flows within the formation. The bulk of this upper package consists of flows of high-Mg basalt intruded by dolerite and gabbro.

Locality 5.3: McPhee Formation (Marble Bar, MGA 793100E 7674150N)

Continue westward on the McPhee Reward mine track for 1.5 km as far as the entrance to a gorge.

The type section of the McPhee Formation (Hickman, 1977) is exposed in the gorge at Locality 5.3 (Fig. 61). Entering the gorge from the southeast, the basal member of the formation is a 25 m-thick grey and white banded chert. The chert stratigraphically overlies silicified high-Mg basalt at the top of the North Star Basalt. The high-Mg basalt shows relict clinopyroxene-spinifex texture, and is intruded by dykes and veins of chert immediately beneath the banded chert. At Locality 5.6, 6 km to the southwest, a silicified fine-grained tuff that locally overlies the high-Mg basalt is assigned to the base of the McPhee Formation, and was dated at 3477 ± 2 Ma (Nelson, 2000). The McPhee Formation is stratigraphically overlain by the Mount Ada Basalt, and about 2 km north of the gorge, the lower part of this formation contains a thin felsic tuff dated at 3469 ± 3 Ma (Nelson, 1999).

The grey-and-white banded chert at this locality is stratigraphically overlain by a 50 m-thick succession of carbonate–chlorite–quartz schist, ferruginous chert, and altered metabasalt. High nickel (about 1000 ppm) and chromium (about 2000 ppm) contents in the carbonate–chlorite–quartz schist indicate that it is a deformed ultramafic rock, and interlayering with thin beds of ferruginous chert suggest that it originated as lava or tuff. This is supported by the regional extent of the carbonate–chlorite–quartz schist

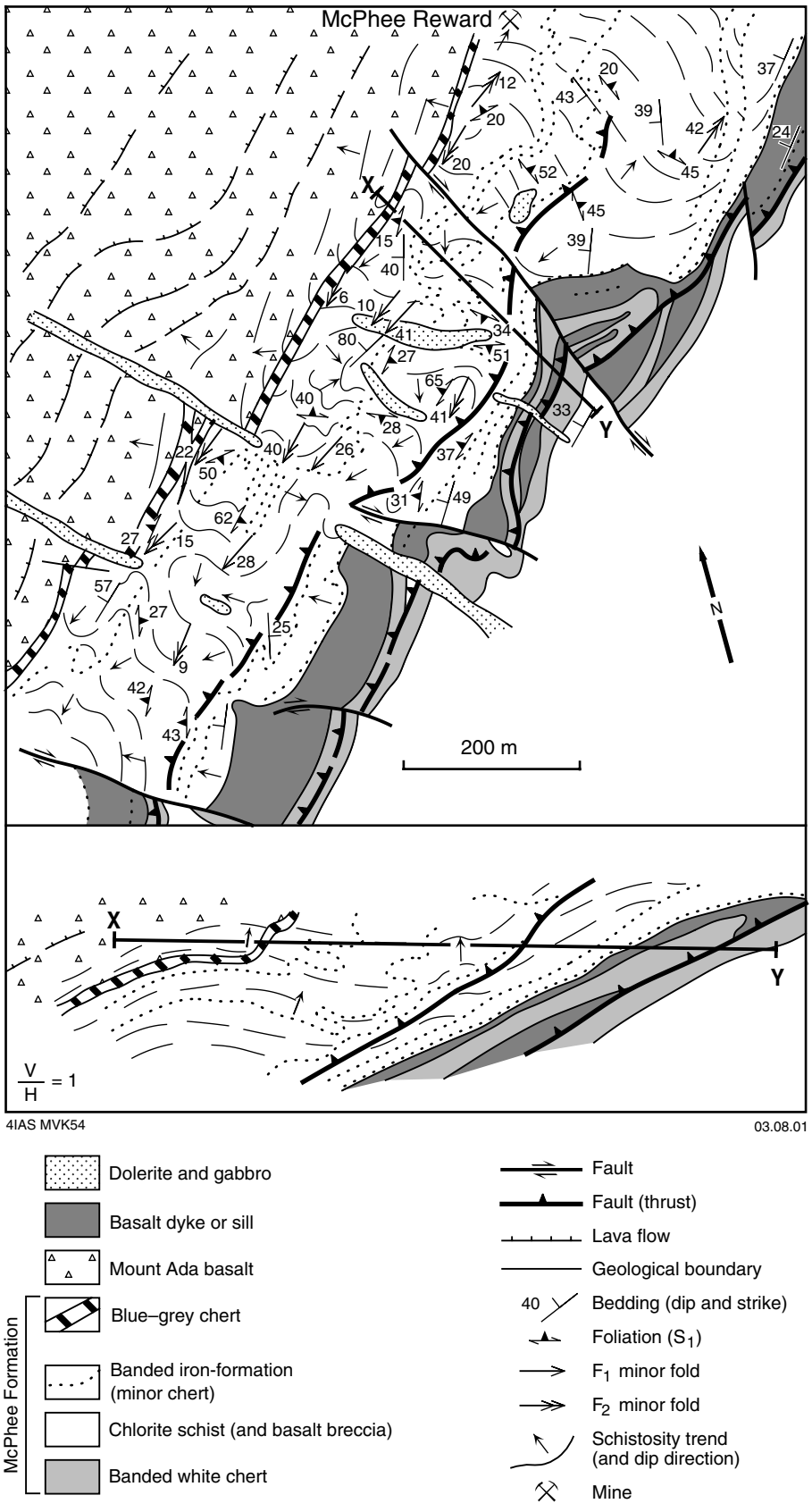

Figure 61. Structural geology of the McPhee Formation at Locality 5.3. Note the vergence of folds away from the Mount Edgar Granitoid Complex, and the later reverse faults that displace greenstones up and to the east, towards the granitoid complex (after Collins, 1989)

at this stratigraphic position, not only within the Marble Bar greenstone belt, but also 50 km to the southwest in the Coongan greenstone belt. This stratigraphic correlation to the succession of the Shark Gully area of the Coongan belt has recently been supported by SHRIMP U–Pb zircon geochronology. Nelson (2000) dated a granophyre sill in the Mount Ada Basalt of the Coongan belt at 3469 ± 3 Ma, and the overlying Duffer Formation at 3474 ± 7 Ma. Three other samples of the Duffer Formation from the Shark Gully succession have been dated at between 3470 and 3467 Ma (Nelson, in prep.).

In a disputed structural interpretation, van Haaften and White (1998) claimed that the McPhee Formation is not a stratigraphic unit, but represents a mylonitic shear zone between the Mount Ada and North Star Basalts. They interpreted this shear zone to mark a major thrust that involved tectonic stacking of material from the west. This thrust was interpreted to have reactivated an earlier, syndepositional normal fault. Most prominent lineations in the sheared rocks of the McPhee Formation plunge west-northwesterly in the direction of dip and, in combination with other kinematic indicators, are reported to indicate west-side-up movement (van Haaften and White, 1998). Thus, van Haaften and White (1998) suggested that the Mount Ada Basalt (west of the shear zone) is older than the North Star Basalt to the east. Recent geochronology (see above) has established that this is not the situation (see **Locality 5.7**).

The present interpretation is that the McPhee Formation is, as originally stated (Hickman, 1980), a well-defined stratigraphic unit of regional extent, and that the shear zone along its upper contact is relatively minor and has not changed the primary stratigraphic succession. The apparent thrust movement described by van Haaften and White (1998) is consistent with layer-parallel shear related to bed-length shortening of greenstones within diapiric synclines that formed during doming of the Mount Edgar Granitoid Complex (Van Kranendonk et al., 2001; Hickman, 2001). The earlier, normal sense of movement recognized by van Haaften and White (1998) is consistent with gravity sliding during the early stages of doming (Collins, 1989). Accordingly, this area does not provide convincing evidence of the syndepositional extension proposed by van Haaften and White (1998).

Above the McPhee Formation, the basal part of the Mount Ada Basalt displays well-preserved pillow structures confirming that the northwesterly dipping succession is right way up.

Locality 5.4: Marginal shear zone at the contact of the Mount Edgar Granitoid Complex (Marble Bar, MGA 793500E 7661220N)

Return to Highway 138, turn right and head towards Marble Bar. Follow the road for 11.5 km and turn right at a gate on a small track heading west. Follow the track for about 1 km to low outcrops at Locality 5.4.

At this outcrop can be seen the penetrative subvertical foliations and southwesterly plunging mineral elongation lineations developed in the marginal shear zone that bounds the southern three-quarters of the Mount Edgar Granitoid Complex (Fig. 57a; Collins, 1989). The fabric elements are developed in mesocratic quartz diorite and leucogranite of the 3310 ± 3 Ma (Nelson, 2000) Warrulinya Suite, a correlative of the pretectonic to syntectonic Boodallana Suite emplaced east of the shear zone (3304 ± 10 Ma) and the undeformed Coppin Gap Granodiorite farther north (3314 ± 13 Ma: suite nomenclature and age data from Williams and Collins, 1990). These data show that the bulk of shearing was developed during granite emplacement, at c. 3310 Ma, and Collins (1989) showed that kinematic data from around the shear zone indicated granite-side-up displacement.

Further evidence that shearing occurred at this time was presented in Collins and Van Kranendonk (1999) who quoted an age of 3324 ± 7 Ma for the Wilina Pluton that cuts the shear zone in the southeast (MOUNT EDGAR, AMG 211300E 7634800N).

The foliations in this zone extend along strike farther north along the contact of the Duffer Formation and Mount Ada Basalt in the area discussed at Locality 5.6.

Locality 5.5: Duffer Formation (MARBLE BAR, MGA 788200E 7664280N)

Return to Highway 138, turn right and head to Marble Bar. About 500 m east of Marble Bar, opposite the turnoff to Corunna Downs, turn right. Follow the track northward for about 8 km to the crossing at Duffer Creek. This crossing requires use of four-wheel drive vehicles. North of the crossing, continue on the track for 500 m northward, and turn right on a minor track leading eastwards. This track terminates after 100 m, but continue eastward across open country for 1.4 km to Locality 5.5.

Locality 5.5 has good outcrops of felsic pyroclastic rocks and reworked tuff in the lower part of the Duffer Formation. A sample (GSWA 148509) collected at this locality was dated (SHRIMP U–Pb zircon geochronology) at 3468 ± 2 Ma (Nelson, 2000). A foot traverse eastward from the sampling site reveals felsic tuff that includes 2–5 m-thick units of fine-grained chloritic tuff containing thin beds of chert and ferruginous chert. Sheets of dolerite have locally intruded this succession, and the fine-grained tuffaceous units contain a schistosity that dips 85° towards 230°. Lineations on this foliation plunge 80° towards 210°. Evidence for the origin of this lineation is better preserved at Locality 5.6.

Locality 5.6: Duffer Formation – Mount Ada Basalt contact (MARBLE BAR, MGA 788850E 7664180N)

Drive eastward about 650 m to Locality 5.6 located on low outcrops of chert on the western side of a small creek.

The purpose of visiting this locality is to examine the interpretation by van Haaften and White (1998) that a major thrust fault ('Duffada Shear') separates, and has tectonically inverted, the Mount Ada Basalt and Duffer Formation.

This contact had previously been mapped as a primary stratigraphic contact (Hickman and Lipple, 1978; Hickman, 1983), partly because a major shear zone is not present, and partly because the same lithostratigraphic succession is recognized over a wide area of the east Pilbara. Geochemical data (Glikson and Hickman, 1981; Hickman, 1980) also provide no evidence of tectonic duplication in the Marble Bar greenstone belt (Figs 60 and 62). However, from their studies in the Talga Talga area, van Haaften and White (1998) concluded that the c. 3470–3463 Ma Duffer Formation was thrust over 'younger' strata of the Mount Ada and North Star Basalts across the Duffada Shear, which is developed along this contact. Combined with their interpretation of the McPhee Formation as a thrust zone (see **Locality 5.3**), they asserted that 'the formations in the lower Warrawoona Group in the Marble Bar belt constitute a lithotectonic complex, and therefore this area is not a suitable type area of the Warrawoona Group'. They also commented that 'this is likely to be the case for almost all stratigraphic units in the structurally complex zones throughout the entire Pilbara Block'. These conclusions challenged the credibility of a stratigraphic interpretation, based on seven years of geological mapping in the east Pilbara, that

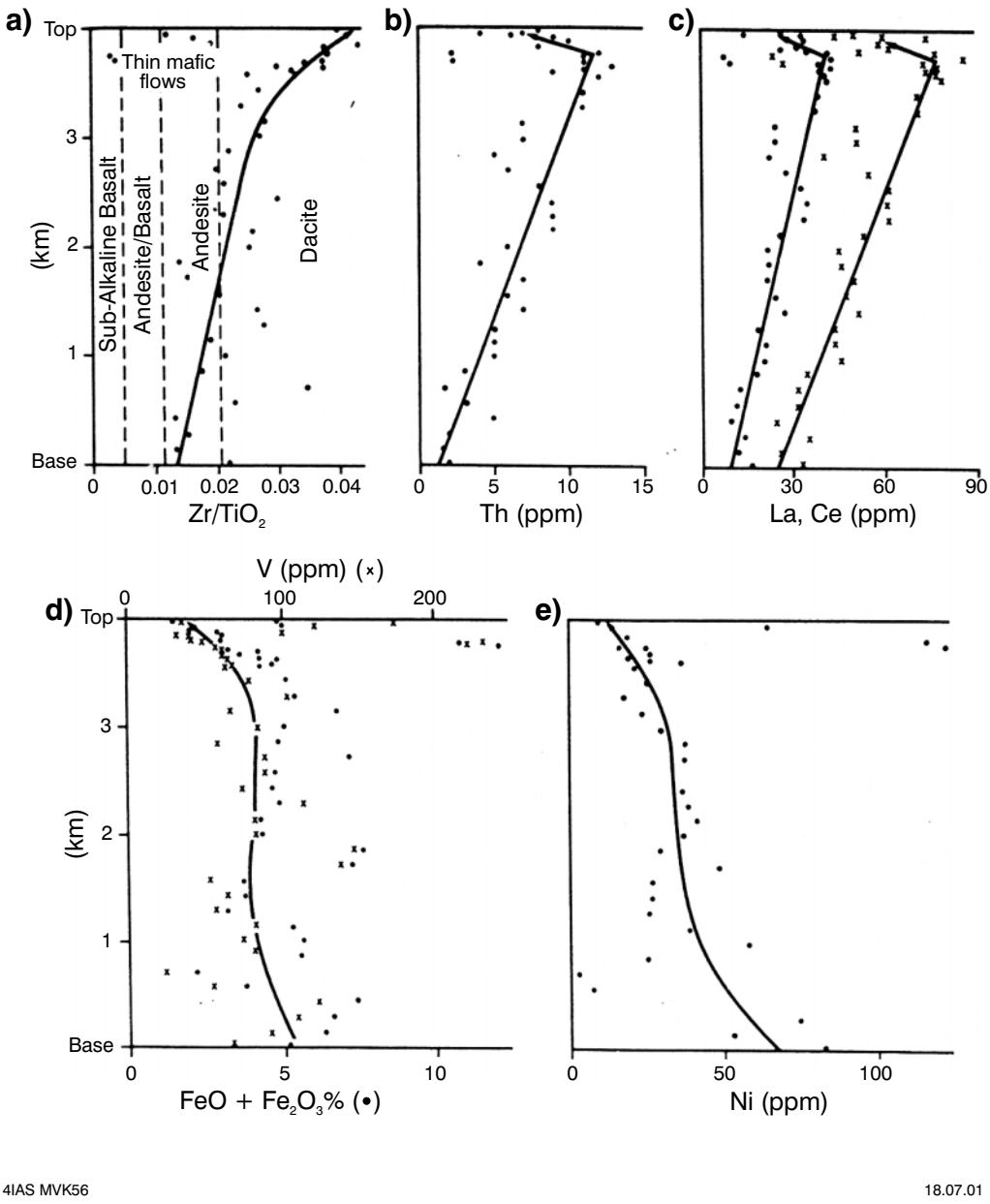

Figure 62. Differentiation trends in the Duffer Formation (after Hickman, 1983)

had been accepted, with minor modifications, for over 15 years, and which has provided a stratigraphic framework for numerous specialized studies during the 1980s and 1990s.

The interpretations of van Haaften and White (1998) are based on extremely limited and localized structural observations; in the case of the 'Duffada Shear', only data from the southern 2 km of the 50 km-long contact between the Duffer Formation and Mount Ada Basalt from Marble Bar to Coppin Gap was presented. They attempted to support their interpreted model of tectonic inversion by a reinterpretation of previously published geochronological data.

van Haaften and White (1998) justified their recognition of the 'Duffada Shear' from observations about 5 km southeast of Locality 5.6. This southeastern area is situated on the western margin of the Mount Edgar Granitoid Complex, where

the Duffer Formation – Mount Ada Basalt contact has been partly obliterated by intrusion of a c. 3310 ± 3 Ma hornblende granodiorite (Nelson, 1999, p. 152–155). In this area, shearing of the Mount Ada Basalt and Duffer Formation is related to a general tectonic attenuation of the succession on the western margin of the Mount Edgar Granitoid Complex (Fig. 52). It is situated at the northern end of mixed zone of sheared granitoids and amphibolite, which extends southward and eastward around the southern margin of the granitoid complex. A major component of the deformation in the area studied by van Haaften and White (1998) is therefore related to shear associated with doming of the Mount Edgar Granitoid Complex at about 3300 Ma.

Locality 5.6 is well removed from most of this deformation, and is not complicated by major granitoid intrusion. Thus, it provides more typical and less complicated exposures close to the Duffer Formation – Mount Ada Basalt contact. Three units of ferruginous chert and phyllite outcrop at 30–50 m intervals within metabasalt close to the top of the Mount Ada Basalt. To the east, this sequence of flows and interflow sedimentary rocks is separated from more massive outcrops of metabasalt by a zone of mafic schist containing lenticular quartz veins. This schist unit is a shear zone, and coincides with the structure that van Haaften and White (1998) named the 'Duffada Shear'. Mapping along strike has shown that the zone is between 1 and 5 m thick, veined by quartz, and locally contains deformed units of chert. It commonly dips steeply southwestward, but at Locality 5.6 it is almost vertical. Lineations measured at Locality 5.5 plunge steeply down-dip towards the southwest. However, in the chert units these lineations are seen to be intersection lineations between a bedding-parallel foliation and a cleavage parallel to the axial planes of steeply plunging tight to isoclinal folds. Fold geometry indicates strike-slip shear instead of up-dip thrust movement expected from van Haaften and White's (1998) interpretation of the 'Duffada Shear'. At Locality 5.6 this strike-slip movement was dominantly sinistral, although localities to the southeast also show evidence of dextral movement. The present interpretation is that the contact between the Duffer Formation and the Mount Ada Basalt has been sheared during several events, but that the displacements are minor.

Van Kranendonk et al. (2001) presented many lines of evidence to categorically reject the interpretations and conclusions of van Haaften and White (1998). New SHRIMP U–Pb zircon geochronology (Nelson, 1999, 2000) indicates that the Mount Ada Basalt is slightly older than the Duffer Formation, and that the McPhee Formation is older still. These new data are consistent with the original interpretation of a coherent, right-way-up stratigraphy (Fig. 53) and are summarized as follows:

- Duffer Formation (tuff): 3468 ± 2 Ma (Nelson, 2000), Locality 5.5;
- Mount Ada Basalt (tuff): 3469 ± 3 Ma (Nelson, 1999), near Locality 5.3;
- McPhee Formation (silicified tuff): 3477 ± 2 Ma (Nelson, 2000), Locality 5.6.

Additional SHRIMP U–Pb zircon data have been obtained from the Duffer Formation and Mount Ada Basalt in the Coongan greenstone belt, 30 km south-southwest of Marble Bar, that confirm the intact nature of the stratigraphic succession over this distance. There, three samples of the Duffer Formation were dated at 3467 ± 5, 3468 ± 5, 3470 ± 5, and 3474 ± 7 Ma, and an intrusive granophyre from the Mount Ada Basalt was dated at 3469 ± 3 Ma (Nelson, 2000, in prep.). These data support the interpretation, based on regional geological mapping, that the lower Warrawoona Group has the same stratigraphic succession, and age, in both greenstone belts (Hickman, 1983). The new geochronological information from the Marble Bar and Coongan belts precludes the tectonic stacking model of van Haaften and White (1998), and supports the Marble Bar belt as a fitting type area for the Warrawoona Group.

Locality 5.7: McPhee Formation geochronology site (Marble Bar, MGA 789500E 7669530N)

Backtrack westward about 2.5 km (to MGA 786600E 7664250N), turn right and follow the track northward for 6 km (to MGA 786800E 7669750N). Turn right on a minor track to the east, and follow this for 3 km to a gap through a ridge composed of the McPhee Formation (MGA 789300E 7669800N). Follow the track through the gap, crossing the creek at the eastern side, and drive about 200 m south (no track) to outcrops of chert on the eastern side of a small creek. Walk about 100 m south along the creek to Locality 5.7.

Grey-green, weakly banded chert outcrops in the bed of the creek at Locality 5.7 and dips westwards at about 40° (Fig. 52). The chert is situated 10 m above the base of the McPhee Formation, and contains silty, tuffaceous layers. A SHRIMP U–Pb zircon date of 3477 ± 2 Ma was obtained on the chert (Nelson, 2000), which is the oldest U–Pb date so far obtained from the Warrawoona Group. The chert is stratigraphically underlain by silicified tremolitic basalt at the top of the North Star Basalt. Pillow structures in this basalt establish that the succession youngs westward. At the eastern entrance to the gap, the chert is interbedded with finely laminated carbonate rocks and metamorphosed siltstone that contain pale-grey nodules of chert.

This sedimentary unit is overlain by basalt, but the upper part of the McPhee Formation is composed of carbonated ultramafic rock similar to that at Locality 5.3. A thin sheet of microgranite is present immediately above the lower sedimentary unit.

Locality 5.8: Transect across the upper contact of the Duffer Formation, through the Towers Formation including the Marble Bar Chert, and into the Apex Basalt (Marble Bar, MGA 781600E 7655400N to 781400E 7654400N)

Return to the main track, turn left and return to Marble Bar. Proceed through town and from the Government offices, head west for 400 m, and turn left onto the Marble Bar – Hillside track. After 750 m, turn right at the signposts to Chinaman and Marble Bar Pools. Proceed 2 km and turn right to Chinaman Pool, (MGA 781600E 7655400N).

This short traverse upstream along the east bank of the Coongan River starts in felsic agglomerate or volcaniclastic conglomerate (or both) at the upper contact of the Duffer Formation (Fig. 63, Locality 5.8a). The volcaniclastic rock is conformably overlain by a discontinuous unit, about 3 m thick, of centimetre-layered blue, white, and red chert of the Chinaman Pool Chert Member of the Towers Formation. Both of these rocks are cut by dolerite sills that have sheared margins. The chert dips 80° towards the east-northeast and, as seen from pillow structures in overlying basalt, is overturned.

Continuing up through the Towers Formation, one passes through a thin unit of komatiitic basalt (Locality 5.8b) up into variolitic pillow basalts (Locality 5.8c) that have well-preserved textures, including small vesicles around pillow margins, crackle rinds, and interpillow hyaloclastite, and way-up structures despite minor to moderate flattening. The pillows are slightly overturned to the east-northeast, but face west. Continuing south, the pillows become increasingly altered, with bleached pillow rinds and gas cavities in pillows filled by carbonate and quartz. At the southern end of the platform is a thick, almost undeformed dolerite sill.

Across the parking lot at Marble Bar Pool is the well-known, water-polished outcrop of blue, white, and red layered chert known as The Marble Bar (Locality 5.8d). The name comes from the mistaken identity of the rock as marble, and the word bar refers

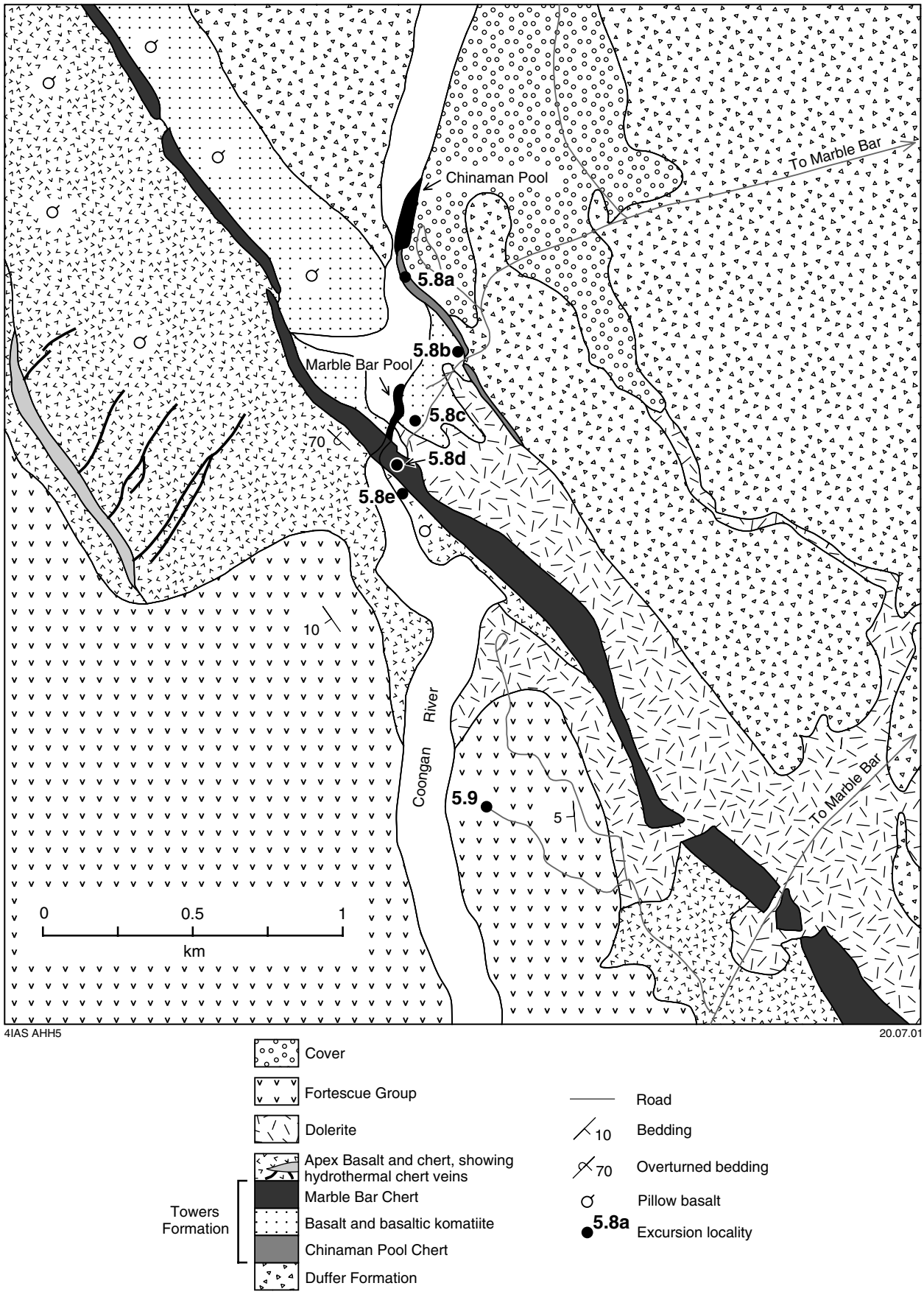

Figure 63. Geological map of the Marble Bar and Chinaman Pool area, showing excursion localities

to the point of rock that extends out across the river, partly barring the flow of water.

At the basal contact of the chert, altered massive volcanic rocks are cut by an anastomosing network of weakly folded, massive blue-black chert veins. Near the basal contact of the chert, the veins contain numerous fragments of the country rock, many with a jigsaw-fit, indicative of phreatic brecciation. Some of these veins extend up into the layered chert as breccia dykes, some of which become quite large, up to 12.5 m wide.

The Marble Bar Chert Member is composed of three distinct colour varieties that are interlayered at a centimetre to decimetre scale: thinly bedded jasper, milky-white chert, and blue-black chert. At Marble Bar Pool, jasper is only present in the top third of the unit (Plate 2). The lower parts of the chert are composed of more massive white and blue-black chert. Jasper is bedded at a millimetre scale, defined by slight changes in colour and the degree of faint granularity. The fine layering of the jasper indicates deposition under quiet-water conditions, and the presence of pillowed basalts above and below suggests that this was probably in a deep-marine setting. In some outcrops, veins of pyrite cut the bedded jasper, indicating that the hematite was a primary precipitate and not a late oxidation of sulfide. There is no textural evidence that the jasper replaced original carbonate.

The white chert forms centimetre-thick layers spaced at irregular intervals through the jasper, but is not bedded. Characteristically, the white chert forms lenses in the jasper, often with pinch-and-swell, or 'ball-and-pillow' load structures, but in many places it may be observed that bedded jasper strikes directly into, and is replaced by, white chert. Bedding-subparallel breccia horizons in the layered white and jasper chert are composed of elongate, angular fragments of white chert within a homogeneous matrix of remobilized, homogeneous jasper or blue-grey chert.

In stark contrast to the thinly bedded jasper are wide, branching veins of blue-black chert and chert breccia that cut up through the underlying, silicified, and altered basalts in areas of high vein density, and across most of the bedded chert (Plate 2). Blue-black chert also forms layers parallel to bedding throughout the chert, but predominantly in the lower third. Breccia veins contain numerous fragments of layered jasper and white chert, the shape of which varies from angular to round with decreasing size, indicating mechanical milling or thermal erosion (or both) processes. Black chert veins are almost entirely absent from the top 20% of the chert as well as from the conformably overlying pillow basalts, indicating that they were emplaced during chert formation and not as the result of later events. Blue-black chert veins feed sills injected laterally into the pre-existing layering. Locally, the force of emplacement of these sills formed layers of pseudoconglomerate comprising a matrix of blue-black chert and imbricated fragments of dismembered white-chert layers. The greater volume of black chert towards the bottom of the member, combined with its intrusive origin, indicates that the Marble Bar Chert Member thickened downward through intraplating and underplating of chert.

Although the origin of the jasper is unequivocally depositional and that of the blue-black chert is clearly intrusive, the origin of the white chert is more complex. A depositional origin for the white chert is superficially suggested by the fact that it is interlayered with jasper at such a regular spacing, lies in contact with jasper across contacts deformed by pinch-and-swell structures, and forms shingled, dismembered fragments within jasper in some bed-parallel breccia layers. However, several other features suggest that the white chert was intrusive. First, the white chert displays no bedding, except where inherited through replacement of bedded

jasper (see below). Second, veins of white chert commonly truncate bedded jasper and link up with bedding-parallel sills of white chert. Where intrusion of white chert is extensive, it replaces bedded jasper at the grain scale, replacing the jasper, but retaining the bedding characteristics of the host and pushing the finely disseminated hematite of the precursor into diffuse, colloform bands along replacement fronts whose margins may be 90° to bedding. The presence of pinch-and-swell and load structures between the jasper and white chert sills indicates that intrusion of the white chert occurred while the jasper was probably unlithified.

Thus the sequence of events that formed the Marble Bar Chert Member included deposition of finely bedded jasper during hydrothermal emanations (Sigutani, 1992), subsurface intrusion of white chert as sills and veins, to final intrusion of blue-black chert veins. As with the other chert horizons visited in this excursion, the original material deposited was an oxidized species, namely hematitic jasper, although in this case deposition occurred in quiet water.

The top contact of the chert is exposed to within 1 or 2 cm with overlying, beautifully preserved pillow basalt of the Apex Basalt (Locality 5.8e). Pillows commonly contain one or multiple pillow shelves. No chert veins extend up through the chert into the pillow basalt, indicating that deposition of the basalt was after chert veining.

Locality 5.9: Basal unconformity of the Fortescue Group (MARBLE BAR, MGA 781700E 7653300N)

Head back out the main track for about 2.6 km and turn right at the T-junction, heading south. Proceed for 3.4 km, turn right at the Flying Fox Lookout sign and follow the track for about 1 km to the parking area overlooking the Coongan River.

The Flying Fox Lookout provides an excellent view of the basal contact of the Fortescue Group south of Marble Bar Pool. The view northward from the lookout shows the c. 3460 Ma Marble Bar Chert forming a high ridge that strikes to the north-northwest. West of this ridge, the valley of the Coongan River, and particularly the rocky bed of

the river, contains exposures of gently dipping basalt lava flows of the c. 2770 Ma Mount Roe Basalt. This basalt is exposed at the lookout and in the cliffs on the opposite bank of the river, but the best exposures are available in the river immediately below the lookout. About 700 m to the north, the Mount Roe Basalt unconformably overlies steeply inclined pillow basalt of the Apex Basalt, although no actual exposures of the contact have been observed in the river bed. About 2 km northwest of the lookout, high ground west of the ridge of chert is composed of the Apex Basalt, and 1.5 km to the southwest the Mount Roe Basalt is in faulted contact with the Apex Basalt. These relationships, and the view from the lookout, indicate that the topography of the Marble Bar Chert Member, and parts of the Apex Basalt, at c. 2770 Ma ago was much as it is today. The Mount Roe Basalt was deposited on a very uneven land surface of chert ridges and metabasalt valleys.

River exposures below the Flying Fox Lookout show flows of the Mount Roe Basalt that contain thin interflow sediments, and exhibit irregular subhorizontal structures that may be lava tubes filled with litharenite (Blake, T. S., 1989, written comm.). Other features include vertical lava pipes, typically 10 cm in diameter and up to 50 cm long, that probably represent volatile conduits.

Day 6: Geology of the Warrawoona Syncline

by A. H. Hickman and M. J. Van Kranendonk (Geological Survey of Western Australia)

Locality 6.1: Moderately east plunging L–S fabric elements in the Warrawoona Syncline (Marble Bar, MGA 790500E 7641800N)

From Marble Bar Roadhouse, head east for about 200 m, then turn right. Proceed for 16.5 km, stopping the vehicles about 500 m past the sharp left bend in the road (at MGA 790500 7641800).

The steep hill on the south side of the track contains a thin chert unit in metamorphosed schistose metabasalts. The rocks show well-developed elongation lineations plunging moderately to the east-southeast, parallel in trend to the axis of the Warrawoona Syncline and plunging towards the zone of vertical L-tectonites in the centre of the zone of sinking farther along strike to the east (see **Locality 6.3**; Collins, 1989; Collins et al., 1998). Note that at the top of the hill is a set of en echelon quartz veins in tension gashes that are oriented at 90° to the lineation direction; these are interpreted as having formed during a late component of the stretching during sinking of the greenstones.

Locality 6.2: Steeply plunging L–S tectonites at the margin of the Warrawoona Syncline (Marble Bar, MGA 796650E 7640750N)

Continue along the track for 4.5 km and turn left onto a smaller track. Proceed for 1.6 km and turn sharply left. Continue along the track, in and out of a creekbed, for about 2.1 km to the base of a small but steep hill at Locality 6.2.

This locality is near the northern margin of the Warrawoona Syncline, in sheared greenstones within 1 km of the contact with the Mount Edgar Granitoid Complex, which is exposed in the flats to the north. Here, fabric elements related to doming include a penetrative foliation in addition to a strong, subvertical elongation lineation as defined by clasts in felsic agglomerate of the c. 3467 Ma Duffer Formation. The stretched clasts are important to keep in mind when we visit Locality 6.4 and discuss the origin of vertical lineations in chert.

Locality 6.3: Lineated fuchsitic chert in the Klondyke Shear Zone (MARBLE BAR, MGA 798450E 7638250N)

Return along the track for about 2.1 km and join the track, heading west. Proceed for about 4 km to the abandoned Klondyke Boulder gold mine.

This exposure of strongly lineated fuchsitic chert lies within the Klondyke Shear Zone, which is a steeply dipping, curviplanar zone of very high shear strain that encircles the southern part of the Mount Edgar Granitoid Complex and is interpreted as one of the ring faults that facilitated the diapiric rise of the complex. Farther along strike to the east-southeast, the zone truncates a significant amount of the stratigraphy on the southern limb of the syncline that wraps around the Corunna Downs Granitoid Complex.

The rocks are typically recrystallized, with moderately to steeply plunging mineral elongation lineations and penetrative foliations. Adjacent rocks within the zone include talc–carbonate schists that are typical of sheared and recrystallized ultramafic rocks (lavas or intrusions) that have been highly altered, indicating that a large volume of metamorphic fluids have passed through the rocks. This high fluid flow has resulted in the formation of several small, but rich, quartz-vein hosted gold deposits that were mined principally at the turn of the century, although some have been mined and explored until very recently.

The Klondyke Shear Zone is interpreted as a relatively late zone in the history of uplift of the Mount Edgar Granitoid Complex, as it was responsible for the exhumation of kyanite-bearing schists adjacent to the complex (Collins and Van Kranendonk, 1999). In this model, initial uplift of the Mount Edgar Granitoid Complex was accommodated by the marginal shear zone at the granite–greenstone contact. Uplift of the complex across this zone resulted in deep burial of axial greenstones, to depths of about 25 km (Delor et al., 1991). Subsequently, the kyanite-bearing schists and associated metabasites were exhumed to the current levels of exposure across the Klondyke Shear Zone, entirely within the kyanite stability field (Collins and Van Kranendonk, 1999). In this scenario, marginal greenstones that were initially buried and then largely dehydrated as a result of high-T metamorphism, became plastered onto the side of the rising granitoid complex and exhumed. Rubidium–strontium data from the Warrawoona Syncline indicate that this exhumation was essentially complete by c. 3200 Ma (Collins and Gray, 1990).

Locality 6.4: Steeply plunging L-tectonites in the core of the Warrawoona Syncline (MARBLE BAR, MGA 794480E 7639020N)

Return to the track, turn left, and backtrack for about 1.1 km. Turn right and proceed for 1.6 km to the main track. Turn left and proceed for about 500 m to the base of a small, rounded hill on your left at the curve of the road, and park the vehicles. Walk up to the top of the hill.

This locality is in the core of the Warrawoona Syncline in the centre of the zone of sinking of the greenstones (see Fig. 56a) and is characterized by vertical L-tectonite fabrics in chert. Although cleavages are visible cutting relict, highly transposed (millimetre-scale) bedding in the chert, the cleavages are in all directions and reflect equal compression from all directions during vertical stretching of the rock into the zone of sinking of the greenstones.

Locality 6.5: Corunna Downs Granitoid Complex (MARBLE BAR, MGA 796000E 7637000N)

Continue southward on the track for 2.5 km, then turn left just past the gate. Proceed for about 2 km to low outcrops of granite.

These outcrops of almost undeformed coarse-grained monzogranite are characteristic of much of the Corunna Downs Granitoid Complex and have been dated in several places at between c. 3317 (Barley and Pickard, 1999) and c. 3307 Ma (Nelson, 2000). The granitoid rocks have weakly deformed to locally sheared intrusive contacts with little-deformed metavolcanic rocks of the Warrawoona Syncline (e.g. Locality 6.7). The low strain state of the granitoid rocks and their envelope of greenstones contrasts sharply with the southern margin of the Mount Edgar Granitoid Complex, which is strongly deformed and composed of reworked, c. 3450 Ma orthogneisses (Williams and Collins, 1990).

Locality 6.6: Post-tectonic, diamondiferous kimberlite dyke (Marble Bar, MGA 801300E 7632100N)

Continue east along the track for about 6 km to a low exposure of brown-weathering rock at Locality 6.6.

This exposure is on the western section of the east-northeasterly striking, post-tectonic Brockman Dyke, which is a diamondiferous kimberlite dyke discovered in 1999 by Stockdale Prospecting Ltd (a subsidiary of De Beers) that extends for at least 20 km across the northern edge of the Corunna Downs Granitoid Complex, across the Warrawoona Syncline, and into the southern edge of the Mount Edgar Granitoid Complex. It occupies a fault that cuts and offsets by 30–50 m the dolerite dykes of the c. 2772 Ma Black Range Suite, and is thus younger than the Fortescue Group; otherwise its age is unknown.

The rock is composed of closely packed, rounded, and serpentinized olivine crystals, up to 1 cm in diameter, in a fine-grained green matrix. Less common xenocrysts of ilmenite have also been observed. Granitoid rocks marginal to most sections of the dyke have been affected by potassic alteration and are brick red in colour. Some outcrops along strike contain coarse crystalline patches of calcite containing fragments of carbonated kimberlite.

The dyke was reported to contain macrodiamonds (>0.4 mm) and microdiamonds that have been located in drilling. During 2000, Stockdale Prospecting (in joint venture with Haoma Mining NL) reported the recovery of 10 diamonds from 4 mini-bulk samples.

Locality 6.7: Southern limb of Warrawoona Syncline (Marble Bar, MGA 794450E 7639000N)

Return bout 8 km to the gate on the Corunna Downs road, turn left and drive 4.5 km to a sign for the Corunna Downs Airstrip. Turn right, following this track for 1 km, then turn right on a minor track to the north. Follow this track for 1.5 km to a gate adjacent to a high ridge of chert.

Until recently, the grey-and-white banded chert at Locality 6.7 was correlated with the Marble Bar Chert Member, and the overlying succession of ultramafic and mafic lavas was assigned to the Apex Basalt (Hickman, 1990, p. 34–35). SHRIMP U–Pb zircon geochronology (Nelson, 1999, 2000) dates the felsic formation immediately underlying the chert at c. 3430 Ma, suggesting that this felsic formation is the Panorama Formation (and not the Duffer Formation as previously interpreted), and that the chert is the Strelley Pool Chert. The thick succession of ultramafic and mafic volcanic rocks above

the chert is now correlated with the Euro Basalt.

The chert is about 30 m thick and dips steeply to the north-northwest. Along strike to the east, up to four separate units of chert can be distinguished, and are separated by poorly exposed quartz–sericite schist. Although the chert lithologically resembles parts of the Marble Bar Chert Member, it lacks red-and-white banding. Pale-grey chert and brown-and-white banded chert are also present along strike. A short traverse northward along the track provides exposures of serpentinized extrusive peridotite. A geochemical traverse (Glikson and Hickman, 1981) revealed that the succession of peridotite flows is about 400 m thick, and overlain by high-Mg basalt that passes up into a thicker succession of tholeiite and high-Mg basalt. The metaperidotite contains serpentinized cumulate-olivine crystals set in a matrix of tremolite, chlorite, clinozoisite, carbonate, and opaque minerals. Some surface exposures show poorly preserved bladed spinifex texture. The total thickness of the Euro Basalt in this area is about 4000 m. Felsic volcanic rocks are almost entirely absent from the succession, but several thin chert units in the central and upper parts of the formation are interpreted to be silicified tuffs, probably of intermediate composition.

Felsic and mafic volcanic rocks of the c. 3325 Ma Wyman Formation overlie the Euro Basalt.

Locality 6.8: Debris flow in rhyolitic Wyman Formation, Warrawoona Syncline, and Fortescue Group unconformity (Marble Bar, MGA 782150E 7639850N)

Follow the track for 8.3 km northward to Camel Creek, and turn left on a four-wheel drive track that joins the main track immediately south of the creek. Follow this track westward for 2.7 km to a low outcrop at the base of hills of the Fortescue Group.

Locality 6.8 shows two features of interest: old gold workings at the unconformity between the Mount Roe Basalt (Fortescue Group) and the Wyman Formation, and debris-flow deposits in the Wyman Formation. In several areas in the east Pilbara region, gold has been obtained from c. 2770–2760 Ma conglomerate and sandstone lenses (channel-fill deposits) at the base of the Fortescue Group. Production from this locality is not recorded, but was probably small. However, the workings do expose the unconformity between gently dipping basalt and steeply inclined altered felsic volcanic rocks.

About 100 m to the south there are excellent exposures of fragmental rhyolite and rhyolite-boulder conglomerate interpreted to represent a debris-flow deposit. SHRIMP U–Pb zircon geochronology is being undertaken on a sample of rhyolite from this locality.

Locality 6.9: Fieldings Gully Shear Zone: recognition of an important type of faulting in the hinges of greenstone synclines (Marble Bar, MGA 783700E 7641450N)

Return to the main track, turn left and cross Camel Creek. Drive northward for about 2 km to a point where a track can be seen crossing the ridge to the north (MGA 790400E 7635000N). Follow this track to the crest where it crosses the ridge. Examine exposures on the ridge to the east of the track.

Late in 2000, field observations in the area of Locality 6.9 led Hickman (2001) to recognize an important type of geological structure that may be unique to early to

middle Archaean crustal evolution. This type of structure provides some of the strongest evidence yet that the dome and synclines of the east Pilbara region were formed by diapirism.

Previous work in the east Pilbara region had identified that although many greenstone belts between granitoid domes were broadly synclinal, the stratigraphy on either limb did not always match and that the hinge region of a greenstone synclines is commonly occupied by a major fault generated by the differential diapiric rise of flanking granitoid complexes (Van Kranendonk, 1998). Collins et al. (1998) recognized such a fault (Fieldings Gully Shear Zone) in the core of the Warrawoona Syncline, but the 2000 mapping established that this wide shear zone is not a single fault, but actually two parallel faults defining a graben-like structure. Hickman (2001) subsequently demonstrated that similar fault pairs occupy the hinge regions of all greenstone synclines in the Marble Bar area. This suggests that such faulting may be an intrinsic feature of most early to middle Archaean greenstone synclines.

Locality 6.9 contains the most westerly outcrops of the Fieldings Gully Shear Zone, which can be traced eastward for at least 15 km. Recent geochronology has established that this major shear zone separates different stratigraphic sections of the Warrawoona Group, and must therefore involve relative vertical movement of several kilometres. Way-up indicators and stratigraphy confirm that the Warrawoona structure is a syncline, but that its hinge region is a major fault zone.

At Locality 6.9 the Fieldings Gully Shear Zone is about 700 m wide, but to the east it becomes progressively attenuated. The north–south sequence of units across the shear zone at Locality 6.9 therefore provides the most complete section available. The ridge, which strikes east–west, is composed of ultramafic caprock developed on sheared and mylonitized peridotite. Remnants of talc–carbonate schist form some outcrops. The tectonic foliation dips 80° to the north, and contains a lineation plunging 45° towards the east. This orientation is similar to that of the elongation lineation at Locality 6.1. Between the ridge and the track are outcrops of strongly sheared talc–chlorite schist and serpentinite. On the southern side of the track there are low, rubbly outcrops of platy (ex-olivine) spinifex-textured ultramafic rock. Farther south this unit is separated from a low ridge containing outcrops of rhyolite (Wyman Formation) by a zone of carbonated

mafic schist. North of the ridge, a 150 m-wide belt of metasedimentary rock includes quartzite and semipelitic schist. Along strike to the east this belt also contains metamorphosed wacke and pelite. The northern contact of this metasedimentary unit is a silicified mylonite, now represented by a chert-like unit. North of this mylonite is a thick succession of relatively massive metabasalt (Apex Basalt).

The ultramafic rocks in the Fieldings Gully Shear Zone are strongly deformed and could have originated as either intrusive or extrusive units. More important is the presence of two mylonite units separated by a central slice of clastic metasedimentary rocks. The latter are correlated with metasedimentary rocks of either the Gorge Creek Group or De Grey Group, which implies a axial sinking or down-drag of up to 10 km. Hickman (2001) recognized this possibility and re-examined the fault patterns of all greenstone belts in the Marble Bar area, concluding that all have fault-bounded zones of sinking in their hinge regions. This conclusion is consistent with centrifuged models that predict extreme vertical extension, and down-dragging of material, in the centres of synclines between rising diapirs. On a regional scale, the pattern of axial faulting is polygonal between the 30–100 km-wide domes, and could only have been produced by vertical deformation.

Return to the main track in the valley south of the ridge, turn right and drive about 6 km to the Marble Bar – Hillside road. Turn left and drive for about 30 km. Turn left onto a medium-sized dirt track and drive south for about 2.8 km, taking the right fork near the flats on the banks of a small stream where we will camp for the night.

Day 7: Geology of the Shaw Granitoid Complex and Tambourah Dome

by M. J. Van Kranendonk

On this day we will examine the relationships between various components of the Shaw Granitoid Complex, contacts of the complex with flanking greenstones, and then look at the processes of dome formation in the nose of the Tambourah Dome of the Yule Granitoid Complex.

As discussed in the geological overview at the start of this guidebook, the Shaw Granitoid Complex has been the subject of much research that has resulted in four different models of evolution:

- The first interpretation is that the Shaw Granitoid Complex represents a solid-state diapir that evolved over the entire geological history of the east Pilbara region, and is part of the regional model presented by Hickman (1983, 1984).
- A second model suggests that a period of horizontal thrusting preceded doming, and that the early deformation was responsible for high-grade metamorphic assemblages and complex folds with overturned greenstone stratigraphy in the northwestern Shaw area (Bickle et al., 1985).
- A third model suggests that the Shaw Granitoid Complex represents a metamorphic core complex formed during regional extension and granite intrusion at c. 3467 Ma (Zegers et al., 1996), following an episode of thrusting as suggested by these authors.
- A fourth model, presented herein, suggests that doming initiated at c. 3440 Ma, independent of thrusting, and that the complex was reactivated at c. 2940 Ma, at which time the folds of the northwestern Shaw area were formed as a result of localized compression within a restraining bend of the Mulgandinnah Shear Zone during regional sinistral transpression.

On this day we will visit the critical locations in these models and (superficially)

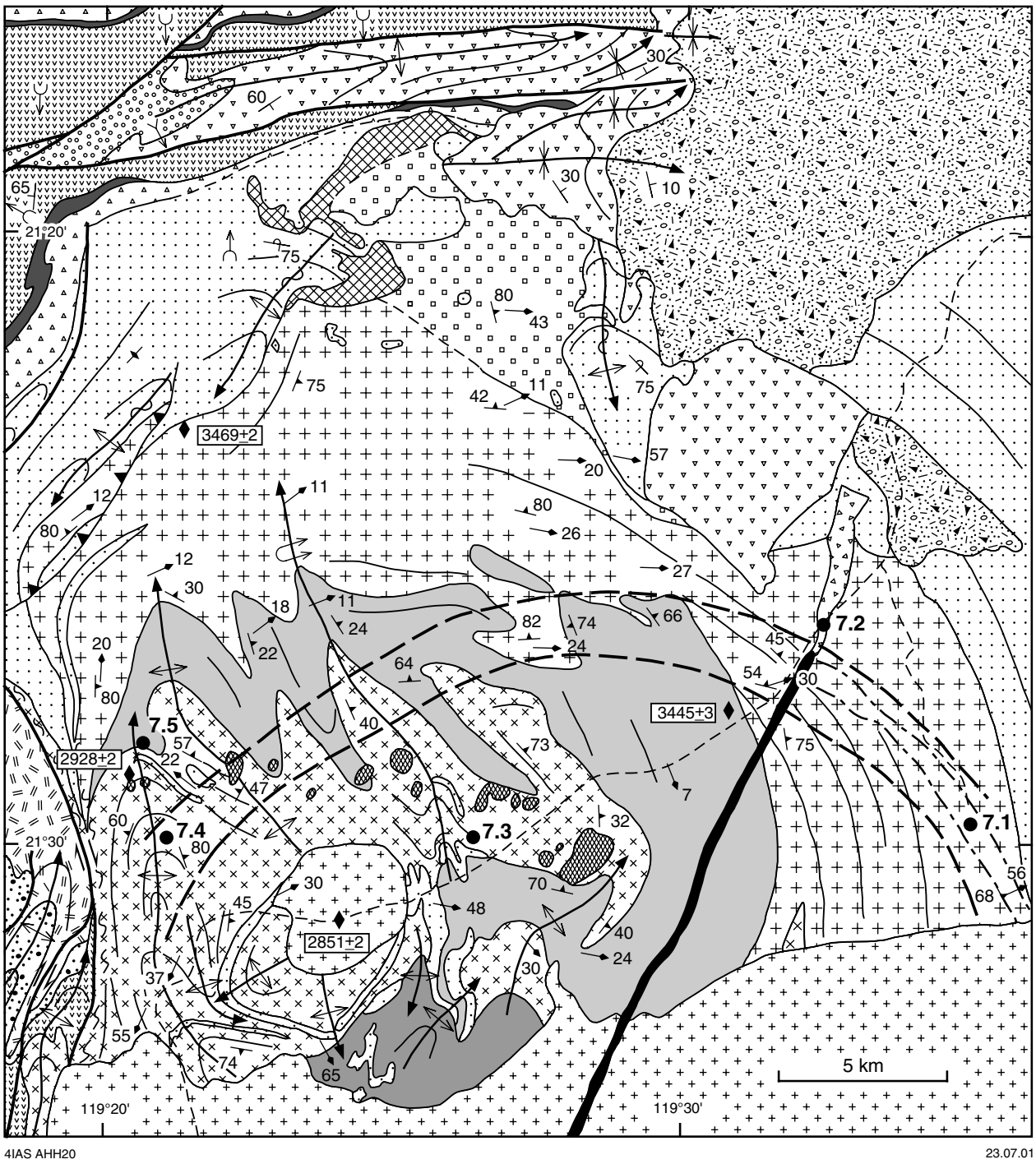

Figure 64. Simplified geological map of the northern part of the Shaw Granitoid Complex, showing excursion localities for part of Day 7 and geochronology sample sites. Note the contradiction between the proposed westerly continuation of the Split Rock Shear Zone suggested by Zegers et al. (1996) and the actual geology

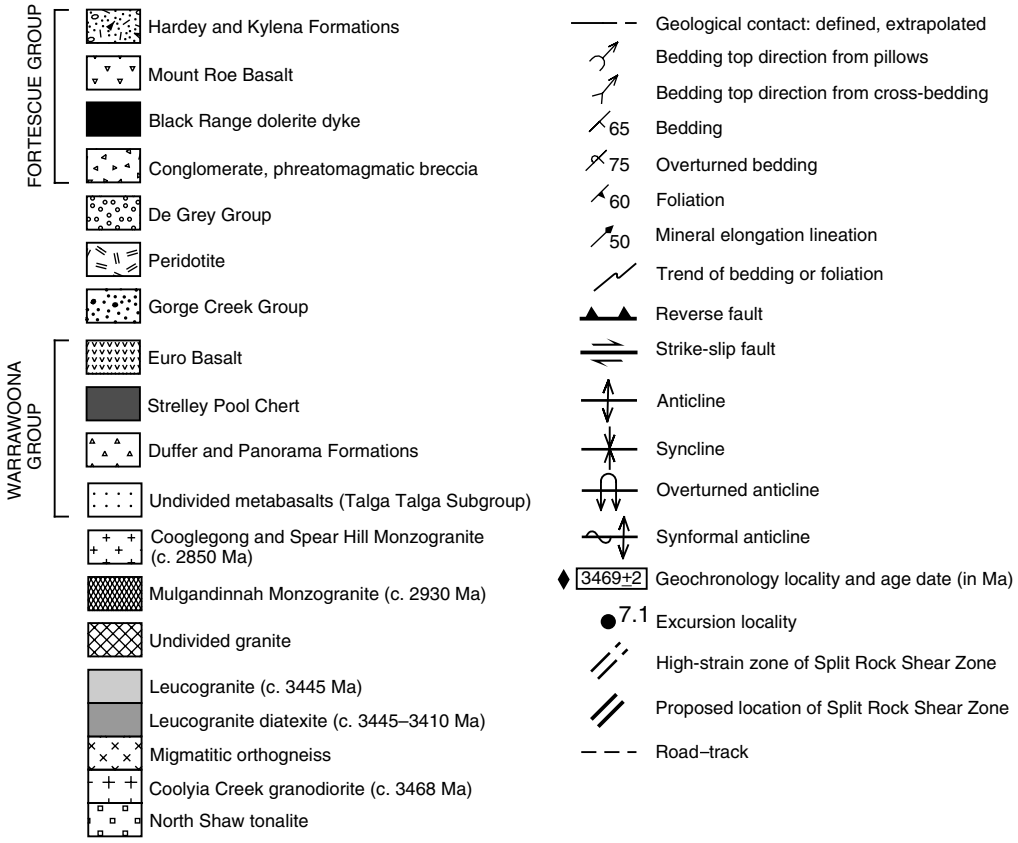

Figure 64. Legend

examine some of the evidence used in their construction (Fig. 64). In particular, we will examine the Split Rock Shear Zone — the proposed detachment zone in the metamorphic core-complex model — in two places: one where it does exist, and another where it does not (Localities 7.1 and 7.4 respectively). We will also examine the area of folds referred to in the Alpine thrusting model and discuss the timing and kinematics of this deformation (Localities 7.6 and 7.7). At other stops we will examine granite melting textures and intrusion features (Localities 7.3, 7.5, 7.6, 7.8) and discuss how they relate to doming.

Locality 7.1: The Split Rock Shear Zone — an enigma (MARBLE BAR, MGA 767800E 7621200N)

Continue across the stream for about 6.3 km and park the vehicles. Walk towards the outcrops on the right.

Here we will undertake a short transect through the highly strained rocks in the type area of the Split Rock Shear Zone described by Zegers et al. (1996). The shearing is developed in the c. 3467 Ma Coolyia Creek Granodiorite, which at this locality is veined by pegmatitic leucogranite. Penetrative foliations dip 65° to the east and contain downdip lineations defined by elongate mafic-mineral aggregates and feldspars. Zegers et al. (1996) described reverse kinematic indicators in this northerly–southerly striking part of the shear zone, but the most obvious shear sense indicators are visible on horizontal outcrop surfaces and indicate a dominantly sinistral component of shearing. On vertical outcrop surfaces, both

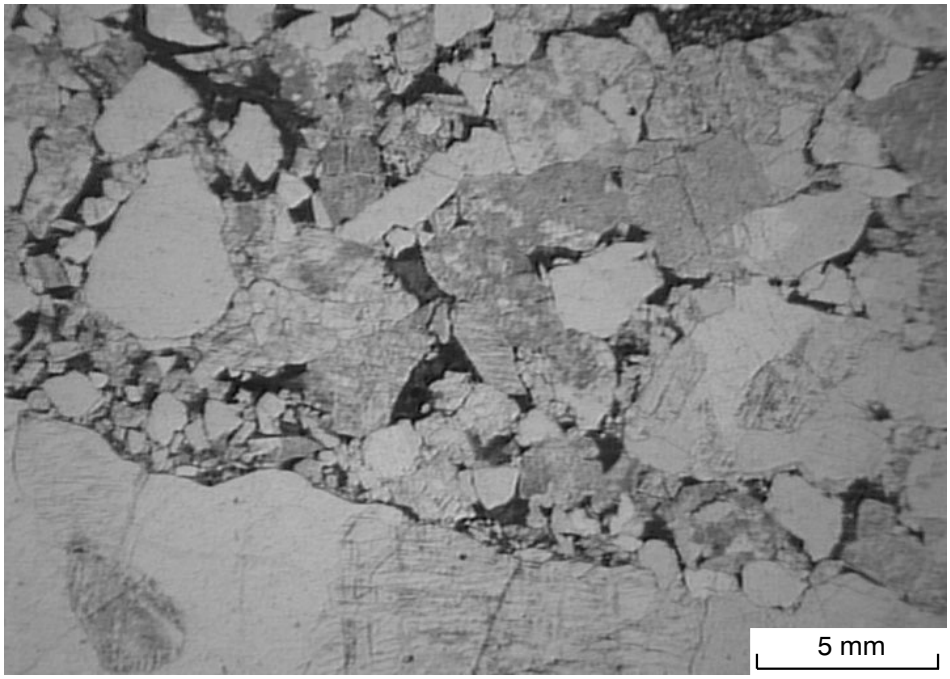

Figure 65. Thin section of the phreatomagmatic breccia at the tip of the Black Range dolerite dyke, Locality 7.2 (plane polarized light). Note the angular and cuspate edges of the fragments, giving the rock a shattered appearance. The dark matrix is largely greenish biotite

normal and reverse kinematic indicators have been observed, but the dominant impression is of pure shear-flattening across the foliation. Participants are encouraged to look for kinematic indicators on both vertical and horizontal surfaces and to discuss the apparent kinematics with respect to the well-developed lineations.

Locality 7.2: 'Conglomeratic' phreatomagmatic breccia dyke at the northern end of the Black Range dolerite dyke (Marble Bar, MGA 763200E 7627150N)

Backtrack to the Hillside Track (about 9.1 km) and turn left, heading west. Proceed for 2.5 km into the bed of Coolyia Creek, park the vehicles and walk 30 m to a low outcrop on the right side of the road in the stream bed.

This water-polished outcrop shows large, rounded boulders of a variety of granitoid gneisses in a fine- to medium-grained black, 'sandy' matrix. This rock occupies a 4 km-long area along the northern continuation of the c. 2772 Ma (Wingate, 1999) Black Range dolerite dyke (Fig. 64), which is the main feeder to basaltic lavas of the Mount Roe Basalt of the Fortescue Group. Although a cursory inspection of the macroscopic textures suggests that this may be a coarse-grained sedimentary rock, no bedding is present in this or any other outcrop of the unit. Instead, thin-section petrography shows in situ disintegration of granitoid clasts at grain and subgrain scale, set within a matrix of green chlorite (Fig. 65). These textures, combined with the position of the unit at the tip of the Black Range dyke, suggest that it is a phreatomagmatic breccia, formed in the propagating tip of the fracture into which the Black Range dolerite was emplaced.

Locality 7.3: Leucogranite sills in orthogneiss (North Shaw, AMG 752700E 7620700N)

Continue along the track for 12.6 km and turn right at a low angle onto a small track, following this for about 500 m. Turn right off the track and proceed cross-country for about 500 m to the north-northeast. Walk across the stream to the washed outcrop on the north bank.

This outcrop shows a leucogranite dyke–sill complex in tonalitic orthogneiss. Geochronology of leucogranite from a nearby outcrop returned an age of 3445 ± 3 Ma (Fig. 64; Nelson, 1998), and the grey tonalite is identical to unmigmatized protoliths dated in a number of places at c. 3467 Ma. This outcrop shows in smaller scale how the main leucogranite in the northern part of the Shaw Granitoid Complex was emplaced as a large sill. Although largely forming an intrusive network at this outcrop, much of the tonalitic gneiss host contains leucogranite leucosome, as we will be able to observe more dramatically at Locality 7.5. Intrusion of leucogranite is interpreted to have accompanied an early phase of doming of the Shaw Granitoid Complex, as further discussed at Locality 7.5.

Locality 7.4: Northwest-striking orthogneiss in the proposed extension of the Split Rock Shear Zone (North Shaw, AMG 743500E 7620800N)

Backtrack to the Hillside Track and turn right (west). Proceed for 7.3 km and turn right at a low angle, onto a smaller track. Follow the track for about 600 m onto a wide, abandoned, dirt airstrip and drive down it, veering left at the end onto a small track, following this for about 500 m for 3.5 km. Park the vehicles and walk over a small rise to a large platform exposure of red-weathering granitoid rocks.

This outcrop of moderately strained tonalitic orthogneiss contains a northwesterly–southeasterly striking gneissosity and is located on the eastern limb of a large-scale fold associated with regional D_3 shearing at c. 2940 Ma along the western margin of the Shaw Granitoid Complex (Fig. 64). The purpose of visiting this locality is threefold.

First, make a mental note of the rather simple, 'normal'-looking migmatitic texture of the gneiss, which consists of a foliated medium-grained tonalite and sheeted leucosome veins, in order to compare it with the gneisses in the next locality which have undergone a significantly higher degree of partial melting. Note the lack of K-feldspar in the gneiss and the presence of biotite in the tonalite, which defines the foliation.

The second purpose of this stop is to show that the proposed westerly, sinistral extension of the Split Rock Shear Zone, as described by Zegers et al. (1996), does not exist and that a core-complex model for the formation of the Shaw Granitoid Complex is thus invalid. This locality is only one of several where foliations have been measured that are oriented 90° to the proposed shear direction and axial planar to a train of north-northwesterly trending regional D_2 folds defined by lithology and gneissosity trends (see Fig. 64: Van Kranendonk, 1999a). These folds affect 3445 Ma leucogranite and thus shearing — were it present and folded (a possibility not presented by Zegers et al., 1996) — would have to be younger than 3445 Ma and could not have occurred at 3467 Ma as proposed by these authors.

The third feature of this outcrop is the recent fault that has offset the weathered surface of the outcrop by 30–40 cm and has a reverse sense of displacement. The fault has thrown out blocks of fresh granite, up to 60 cm long, a distance of 40 cm or more. The strike of the fault and sense of displacement is granite-side-up relative to

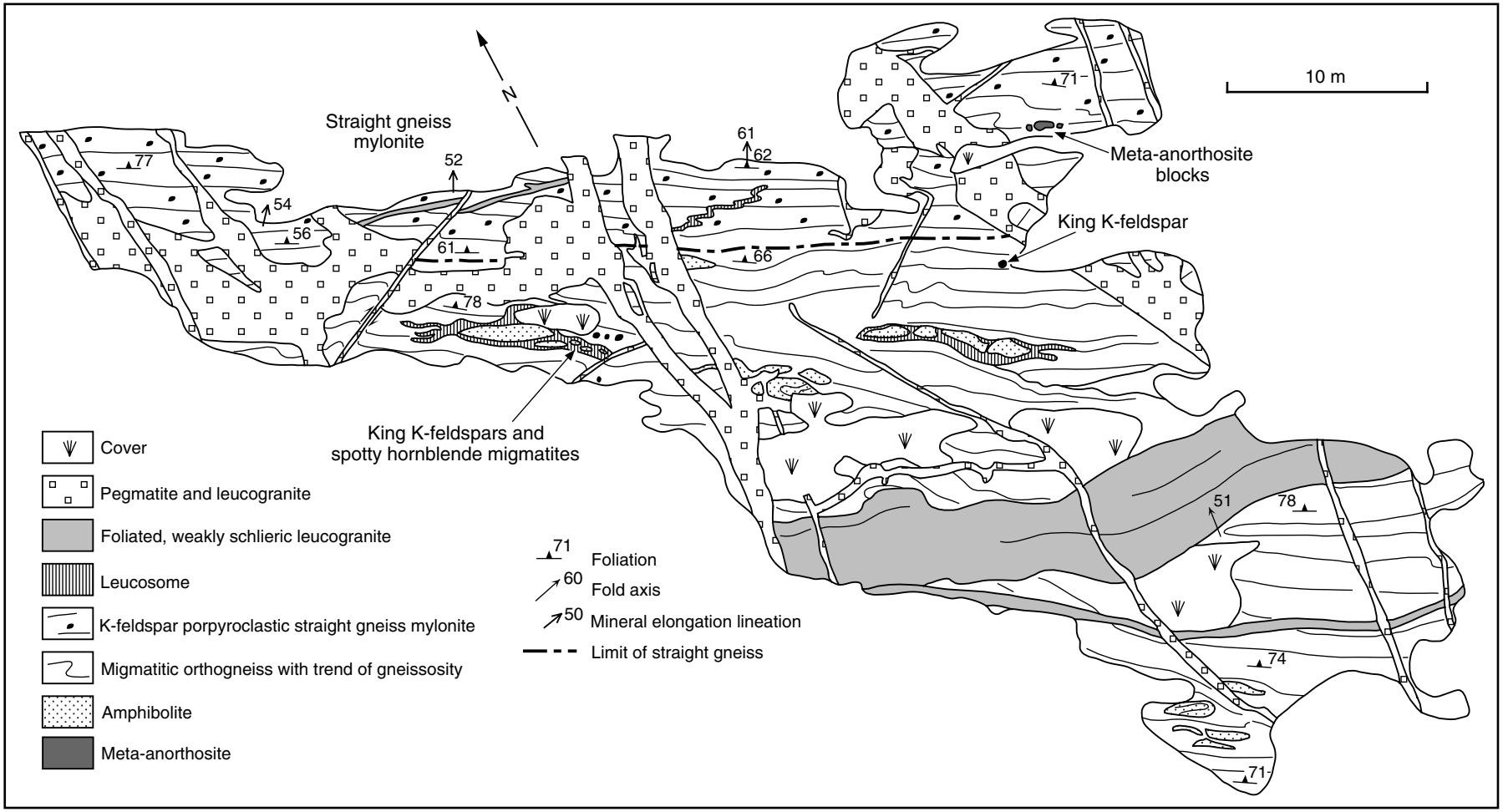

Figure 66. Sketch map of the southern gneissic outcrop at Locality 7.5 (adapted from a more detailed map by M. Pawley, University of Newcastle)

greenstones, which underlie the low hills to the west, 2 km away.

Locality 7.5: Leucogranite diatexite (North Shaw, AMG 742800E 7623700N)

Continue north along the track for about 500 m and turn right into the bush, following tyre tracks through the spinifex grass. Proceed for 2 km north, joining a track along the way, then turn left off the track, downhill, following tyre tracks once more for about 600 m to Locality 7.6.

A pair of outcrops here on the eastern bank of the Shaw River show the contact between migmatitic orthogneiss, with evidence of in situ partial diatexis, and leucogranite diatexite. The first, southerly outcrop where the vehicles are parked (Fig. 66), is a heterogeneous, migmatitic orthogneiss consisting predominantly of a partly melted tonalitic precursor. The tonalite contains inclusions of amphibolite, quartzite, and anorthositic host rocks, the latter preserved as a train of small blocks in the southeastern part of the outcrop. These are probably part of the 3578 ± 4 Ma suite dated by McNaughton et al. (1988) elsewhere in the Shaw Granitoid Complex. In the southern part of the outcrop, the tonalitic protolith is shot through with veins and dykes of leucogranite and is characterized by two textures that distinguish it from the more characteristic biotite tonalite orthogneiss of the last locality. This includes a spotty hornblende texture and numerous large, ovoid K-feldspar crystals up to 15 cm in diameter. These textures are interpreted to be the result of an increased amount of partial melting of the tonalite, whereby biotite and plagioclase are transformed into hornblende and K-feldspar during high-temperature metamorphism following the (unbalanced) reaction:

$$2CaAl_2Si_2O_8 \text{ (plagioclase)} + K_2Fe_6\ Si_6Al_2O_{20}(OH)_4 \text{ (biotite)} \rightarrow$$
$$2KAlSi_3O_8 \text{ (K-feldspar)} + Ca_32(Mg, Fe)_5Si_6Al_2O_{22}\ (OH)_2 \text{ (hornblende)} + \text{melt}$$

At the northern margin of the outcrop is a 70° north-dipping zone of porphyroclastic straight gneiss mylonite, which contains down-dip, amphibolite-facies mineral-elongation lineations and rare kinematic indicators of north-side-down displacement. The north-side-down kinematics is consistent with the geometry of southerly plunging synformal anticlines on either side of the northern tip of the Shaw Granitoid Complex (Fig. 64). These features suggest northerly displacement of supracrustal rocks, together with the little-deformed top part of the Shaw Granitoid Complex (North Shaw Suite of Bickle et al., 1983, 1993), as shown in Figure 67.

The zone of dislocation between the relatively rigid hangingwall (including the North Shaw Suite and attached greenstones) and the more-ductile granitoid core in the footwall occurred across the transition from migmatitic orthogneiss into leucogranite diatexite, as exemplified in the second outcrop, about 100 m to the north (Fig. 68). At this locality, remnants of migmatitic orthogneiss are swamped by new melt, which is present as dykes, patches, and blobs of pegmatitic granite, single K-feldspar porphyroblasts, and discordant, zoned dykes of leucogranite (Fig. 69). Significantly, the undeformed, discordant leucogranite dykes are parallel to the shear zone in the last outcrop, suggesting that a component of shearing and diatexis were coeval. The zoned dykes display asymmetrical textural features that can be used as way-up indicators, consistent with top to the north (Fig. 69b). SHRIMP dating of this outcrop indicates melting at 3410–3400 Ma (age of zircon rims) of a c. 3450 Ma protolith (zircon cores; Nelson, D. R., 2001, written comm.).

Locality 7.6: Sheeted granite intrusion into amphibolites

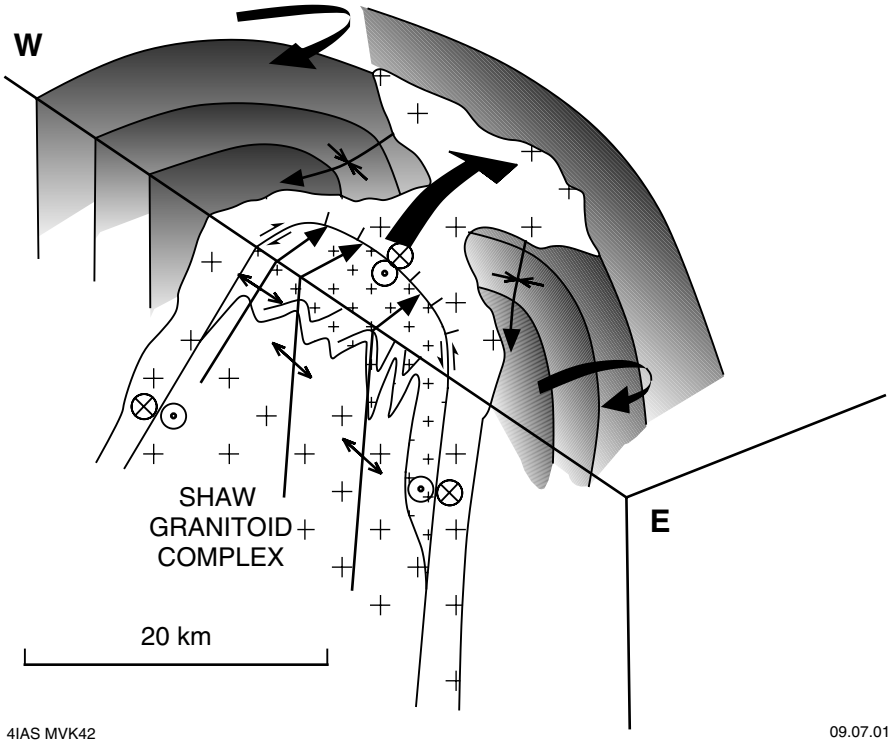

Figure 67. Schematic tectonic model showing an early component of doming of the Shaw Granitoid Complex. In this model, doming occurred during intrusion of leucogranite and downward displacement to the north of the North Shaw Suite and attached greenstones of the North Shaw greenstone belt

(TAMBOURAH, MGA 735400E 7613700N)

Backtrack to the Hillside Track, turning right at the end of the airstrip. Continue west and south along the Hillside Track for 2.9 km, turning right at the fork in the main road. Follow the track across the Shaw River for about 9 km and take the right turn. Then proceed for about 4 km along a small track heading northwest.

This locality is at the northern contact of folded granitoid lobes in the area described by Bickle et al. (1985) as having been affected by Alpine-style thrusting (Fig. 12a). These authors suggested that the granitoid lobes and surrounding supracrustal rocks had been intercalated by thrusting and folded during a period of Alpine-style thrusting prior to granitoid doming. They described a distinctive unit of calc-silicate rocks outlining isoclinal folds around the margins of some granitoid lobes, that they interpreted as having formed as recumbent structures during the thrusting. Zegers et al. (1996) suggested that this episode of compressional deformation pre-dated extensional core-complex formation at c. 3467 Ma, despite the fact that the dated South Daltons Pluton is affected by these folds and is c. 3430 Ma old (McNaughton et al., 1993).

An alternative interpretation was presented by Van Kranendonk (1997), who suggested that much of the folding occurred at c. 2940 Ma, during regional sinistral transpression (see also Collins and Van Kranendonk, 1999). At this and the next locality, we will superficially examine the possible evidence for these competing hypotheses.

The main lithology of the granitoid lobe is a homogeneous, grey, medium-grained biotite granitoid that is weakly strained and contains xenoliths of strongly deformed migmatitic tonalitic orthogneiss (Fig. 70a). Dating of the homogeneous granitoids at

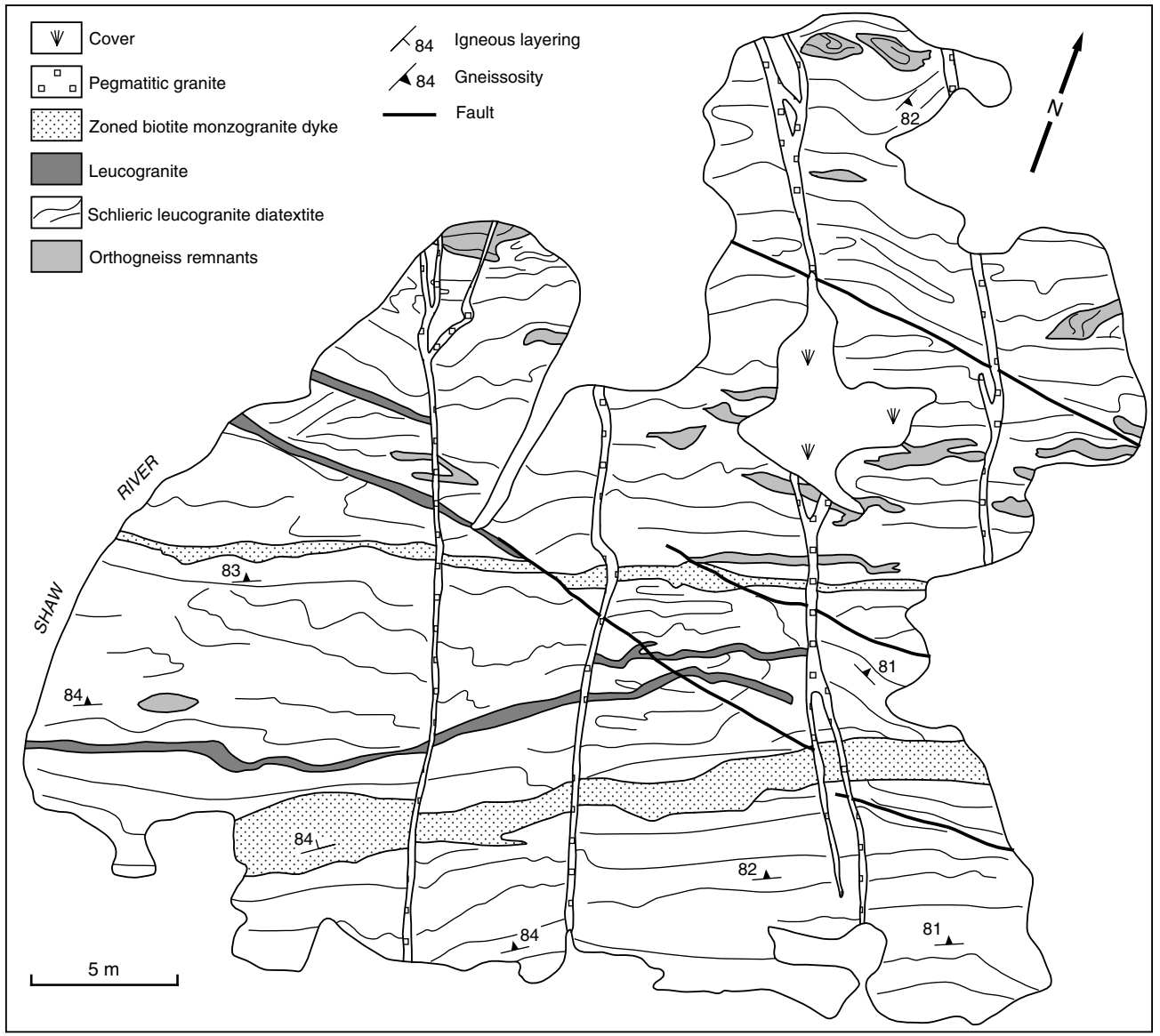

Figure 68. Sketch map of the northern gneissic outcrop at Locality 7.5 (adapted from a more detailed map by M. Pawley, University of Newcastle)

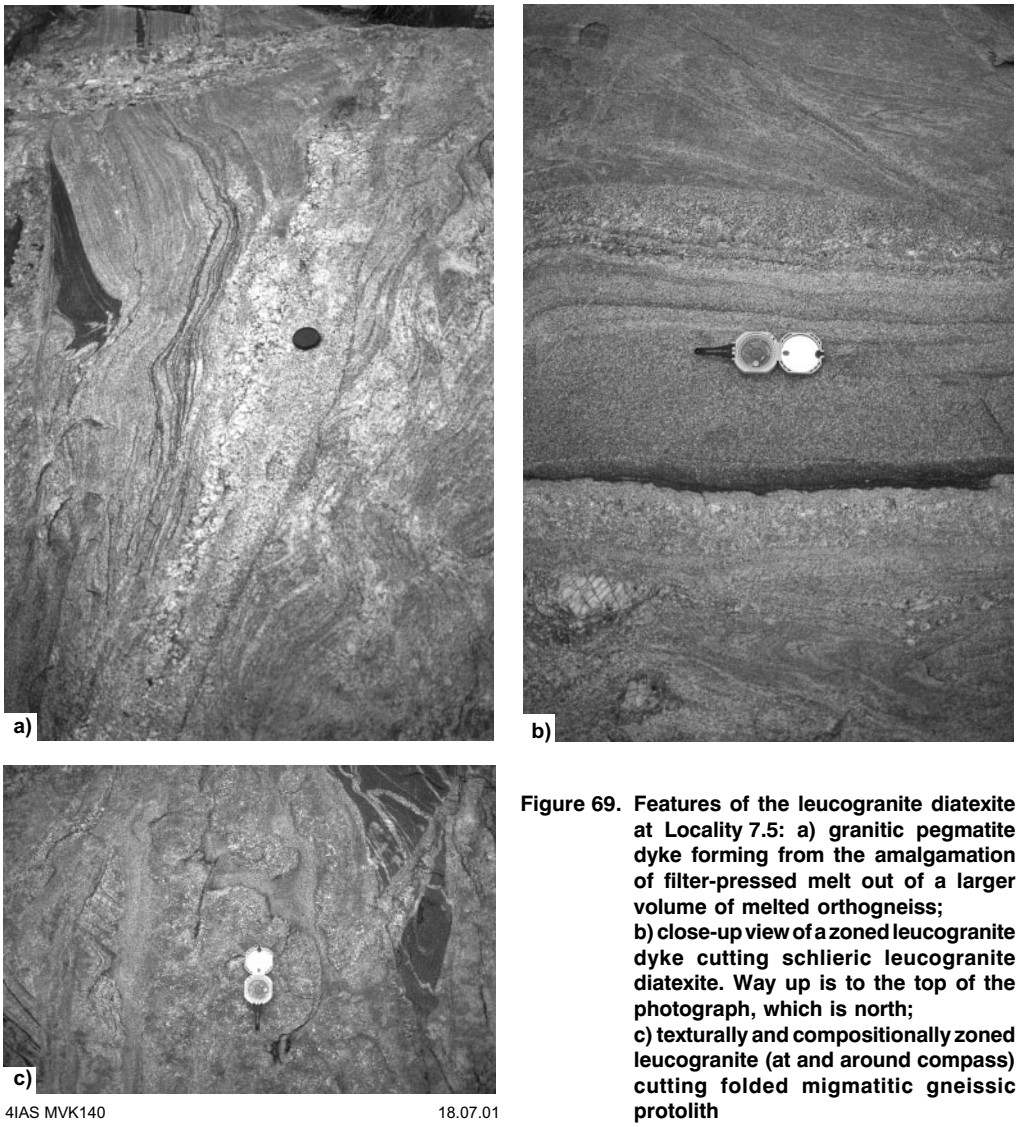

Figure 69. Features of the leucogranite diatexite at Locality 7.5: a) granitic pegmatite dyke forming from the amalgamation of filter-pressed melt out of a larger volume of melted orthogneiss; b) close-up view of a zoned leucogranite dyke cutting schlieric leucogranite diatexite. Way up is to the top of the photograph, which is north; c) texturally and compositionally zoned leucogranite (at and around compass) cutting folded migmatitic gneissic protolith

various places along the western margin of the Shaw Granitoid Complex (e.g. Locality 7.9) has returned ages of between 3435 and 3425 Ma, whereas the protolith of the gneisses is c. 3467 Ma, indicating significant local deformation between these ages as suggested by the features described at Locality 7.5.

North of the homogeneous granitoid rocks is a flat area of outcrop that consists of sheeted granitoid sills in amphibolites; these are the so-called calc-silicate rocks of Bickle et al. (1985). The sheeted granitoid sills are medium grained and thoroughly recrystallized. Together with the intervening screens of amphibolite, they are strongly foliated and contain downdip lineations. These amphibolite-grade tectonites are cut by swarms of undeformed tourmaline veins, and the rocks have been strongly altered by metasomatic fluids associated with granitoid intrusion; thus the granitoid sheets in amphibolites must belong to the c. 3467 Ma suite, and much of the deformation must have occurred prior to, or during, intrusion of the homogeneous granitoids at c. 3430 Ma. Amphibolites become progressively more leucocratic towards the granitoid contact and display a change in mineralogy from hornblende–plagioclase – opaque minerals to tremolite–actinolite–epidote–titanite – saussuritized plagioclase. In contrast, granitoid sills become more mafic away

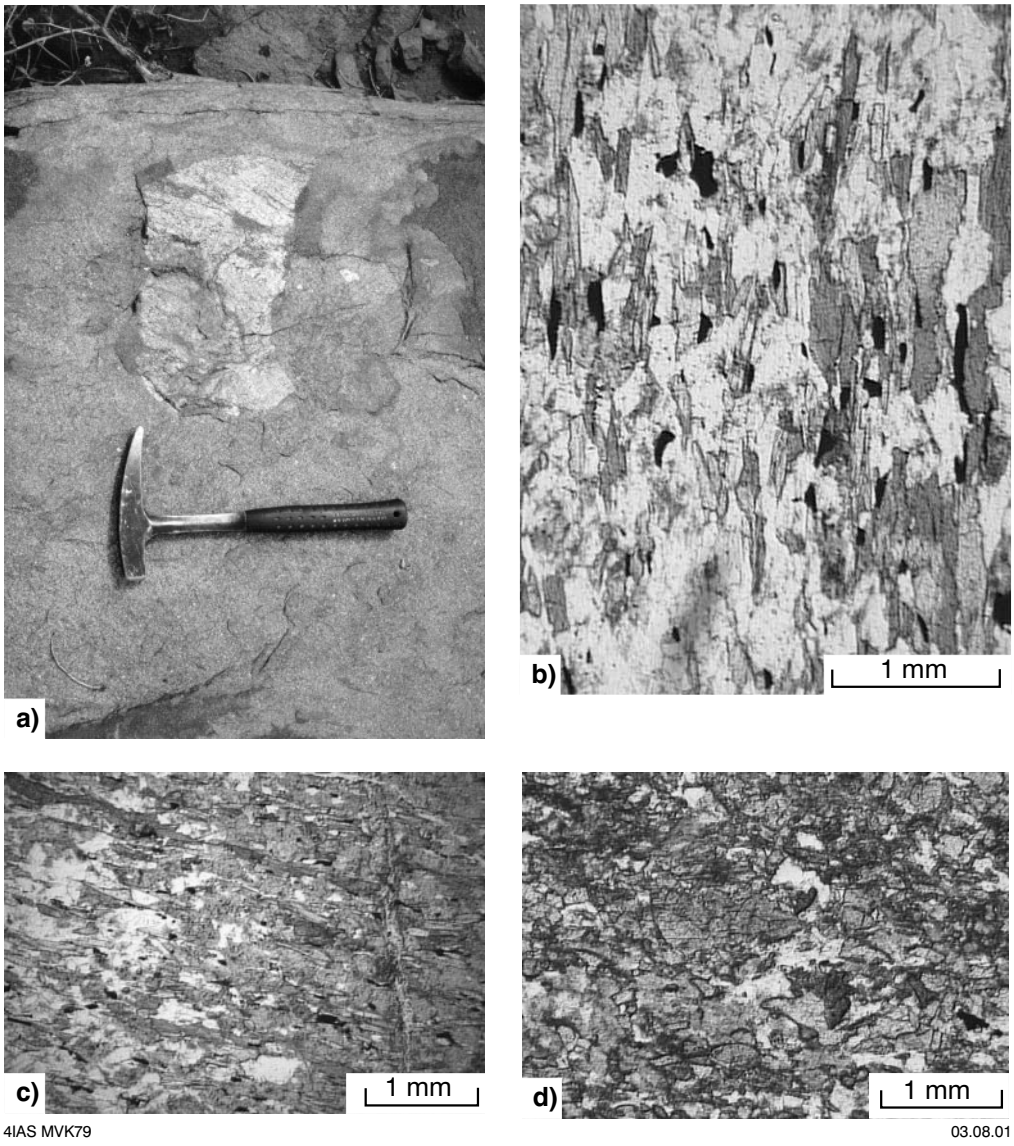

Figure 70. Features of the contact of the folded granitoid lobe at Locality 7.6 in the northwestern Shaw Granitoid Complex: a) homogeneous grey granodiorite with a xenolith of migmatitic orthogneiss; b) thin section of a granitoid sheet proximal to the main body of the folded granitoid lobe, showing aligned, acicular actinolite (dark) and tremolite (light), and opaque minerals in a matrix of fresh plagioclase and quartz (plane polarized light); c) thin section of another granitoid sheet (slightly more distal from the main body and past some amphibolite rafts) that has the same mineralogy as (b), but has been altered by a post-tectonic vein cutting across the foliation to the right, causing alteration of adjacent matrix feldspars (plane polarized light); d) thin section of a distal granitoid sheet with coarse epidote–actinolite–titanite (T) mineralogy as a result of interaction with, and partial assimilation of, entrained peels of amphibolite (plane polarized light). This rock had been interpreted as a calc-silicate by Bickle et al. (1985)

from the granitoid contact, probably due to assimilation of amphibolite or possibly as a result of metasomatic exchange of components with amphibolite. The least altered granitoid sills adjacent to the granitoid contact contain fresh plagioclase, quartz, actinolite, tremolite, and opaque minerals and are well foliated (Fig. 70b). Farther away, feldspars are saussuritized by fluids introduced by thin greisen veins (Fig. 70c), whereas the most distal sheets have been completely recrystallized to a granoblastic assemblage of epidote, actinolite, and titanite (Fig. 70d).

Despite the evidence for early deformation, the regional fold geometry of rocks in this area must have formed after deposition of the Gorge Creek Group (less than 3240 Ma), as these rocks have also been affected by the folding. Regional considerations suggest that this folding occurred at c. 2940 Ma, during regional sinistral transpression, as discussed in more detail at the next locality.

Locality 7.7: Folded dextral ultramylonite (Tambourah, MGA 740500E 7614950N)

Backtrack for 4 km, rejoining the major track, and follow this track back for about 5.9 km towards the Hillside Track. Park the vehicles here and walk north up a small creek bed for about 500 m.

This locality is in the easternmost of the five folded granitoid lobes of the northwestern Shaw area (Fig. 12a). Here, one may observe dextral ultramylonite fabrics in migmatitic orthogneiss that have been folded by the main set of north-northeasterly trending folds in this area. The dextral fabrics here contrast with the symmetrical structural fabric elements in the central granitoid lobes and with folded sinistral mylonites in the westernmost granitoid lobes.

The northwestern Shaw area of folded granitoid lobes and attached supracrustal rocks is in between stepped kilometre-wide strands of the Mulgandinnah Shear Zone. Van Kranendonk (1997) suggested that the folds and associated shear asymmetries were consistent with formation as a result of localized compression within a restraining bend between the shear strands (Fig. 12b). This is consistent with the fact that the folds are co-linear with mineral elongation lineations in the Mulgandinnah Shear Zone and that the complex folding and shearing in this area is atypical of the rest of the east Pilbara region. The restraining bend model also accounts for the preservation of medium-pressure metamorphic mineral assemblages in this area, and for the thermal anomaly associated with proximity to the granitoid complex that was otherwise unexplained by the Alpine thrusting model of Bickle et al. (1985), as described by Collins and Van Kranendonk (1999).

Locality 7.8: Flat intrusive contact of the Cooglegong Monzogranite (Tambourah, MGA 747100E 7598750N)

Return to the Hillside Track, a distance of 3.6 km, and turn right (south).Proceed for 18.8 km and turn right into the bush, heading west along the northern bank of a small stream for about 850 m to the edge of a small cliff over the Shaw River. Park the vehicles and walk south (left) for about 200 m across a small creek, and along the base of the small cliff.

Here, on the east bank of the Shaw River, is a beautiful vertical exposure through the lower, flat contact of the Cooglegong Monzogranite, which cuts through subvertical migmatitic orthogneiss. This, and evidence through a large part of this western contact area of a flat contact, shows that the Cooglegong Monzogranite is a flat sheet, emplaced into the crest of the Shaw Dome. As with older intrusive phases elsewhere (e.g. Localities 7.3 and 7.5), intrusion was probably coeval with, or caused (or both), a component of doming of the Shaw Granitoid Complex prior to deposition of the Fortescue Group. Such punctuated uplift was accompanied by basin development in adjacent greenstones, as represented by successive generations of unconformities between groups of supracrustal rocks.

Locality 7.9: Tonalite orthogneiss in the c. 2940 Ma Mulgandinnah

Shear Zone (TAMBOURAH, MGA 731500E 7592500N)

Return to the vehicles and drive back to the Hillside Track. Turn right (south) and follow the track across the Shaw River, past the turnoff to Hillside Station and farther for a total distance of 20 km until just past a small gully. Turn right (north) onto a small track and proceed for about 200 m and park the vehicles. Walk down to the streambed and the water-polished outcrop about 250 m to the west.

This stream exposure of orthogneiss is located within 1 km of the western contact of the Shaw Granitoid Complex with the Western Shaw greenstone belt. The outcrop is at the eastern margin of the sinistral, c. 2940 Ma Mulgandinnah Shear Zone (Zegers et al., 1998), which forms the eastern boundary to the Lalla Rook – Western Shaw structural corridor (renamed from the Central Pilbara structural corridor of Van Kranendonk and Collins, 1998), which is a late-tectonic zone of sinistral transpression that represents the farthest east manifestation of events affecting the West Pilbara Granite–Greenstone Terrane, Mallina Basin, and Yule Granitoid Complex (see Fig. 10).

The outcrop displays an increase in strain from east to west across the outcrop, from sheeted tonalite intrusions (c. 3430 Ma: Nelson, 2000) cut by metre-wide, little-deformed net-vein pegmatite dykes to sinistral straight gneiss mylonite. In the more highly strained rocks, synkinematic pegmatite dykes occupy the hinge zones of S-asymmetric shear folds, and K-feldspar porphyroclasts display textbook examples of sinistral rotational asymmetry. The age of shearing has been determined from a nearby synkinematic granite pegmatite (c. 2936 Ma; Van Kranendonk, M., unpublished data) and from a synkinematic granite pegmatite farther north in the eastern splay of the zone (2934 ± 2 Ma; Zegers, 1996). An earlier phase of leucosome veins intruded the blue-grey tonalite host prior to emplacement of the synkinematic pegmatitic granitoid dykes, and are shredded out in this outcrop. Dating attempts on these earlier veins have been unsuccessful. In the far southwestern corner of the outcrop is a discordant dyke of the Cooglegong Monzogranite.

Locality 7.10: Chlorite mylonite schist and vein quartz in the western boundary fault of the Lalla Rookh – Western Shaw structural corridor (TAMBOURAH, MGA 729000E 7591800N)

Return to the Hillside Track and turn right. Proceed west and notice the contact between the Shaw Granitoid Complex and the Western Shaw greenstone belt. After 2.2 km, park the vehicles on the side of the road.

This small outcrop on the north side of the road is a chlorite schist with classic 'S–C–C' textures indicative of sinistral transcurrent shear. This high strain zone marks the western boundary fault of the Lalla Rook – Western Shaw structural corridor and separates amphibolite-facies S–L pillow basalts to the west from greenschist facies heterolithic greenstones, cherts, and subordinate BIF to the east. The high strain zone is characterized by carbonate alteration and quartz veining — characteristic features associated with gold mineralization found along strike of this zone both to the north and south.

Locality 7.11: Granite emplacement during doming in the nose of the Tambourah Dome (TAMBOURAH, MGA 717500E 7591800N)

Return to the Hillside Track and turn right. Drive for 13.5 km and turn right at the top of a small rise onto a smaller track marked by a tin can on a post. Follow this

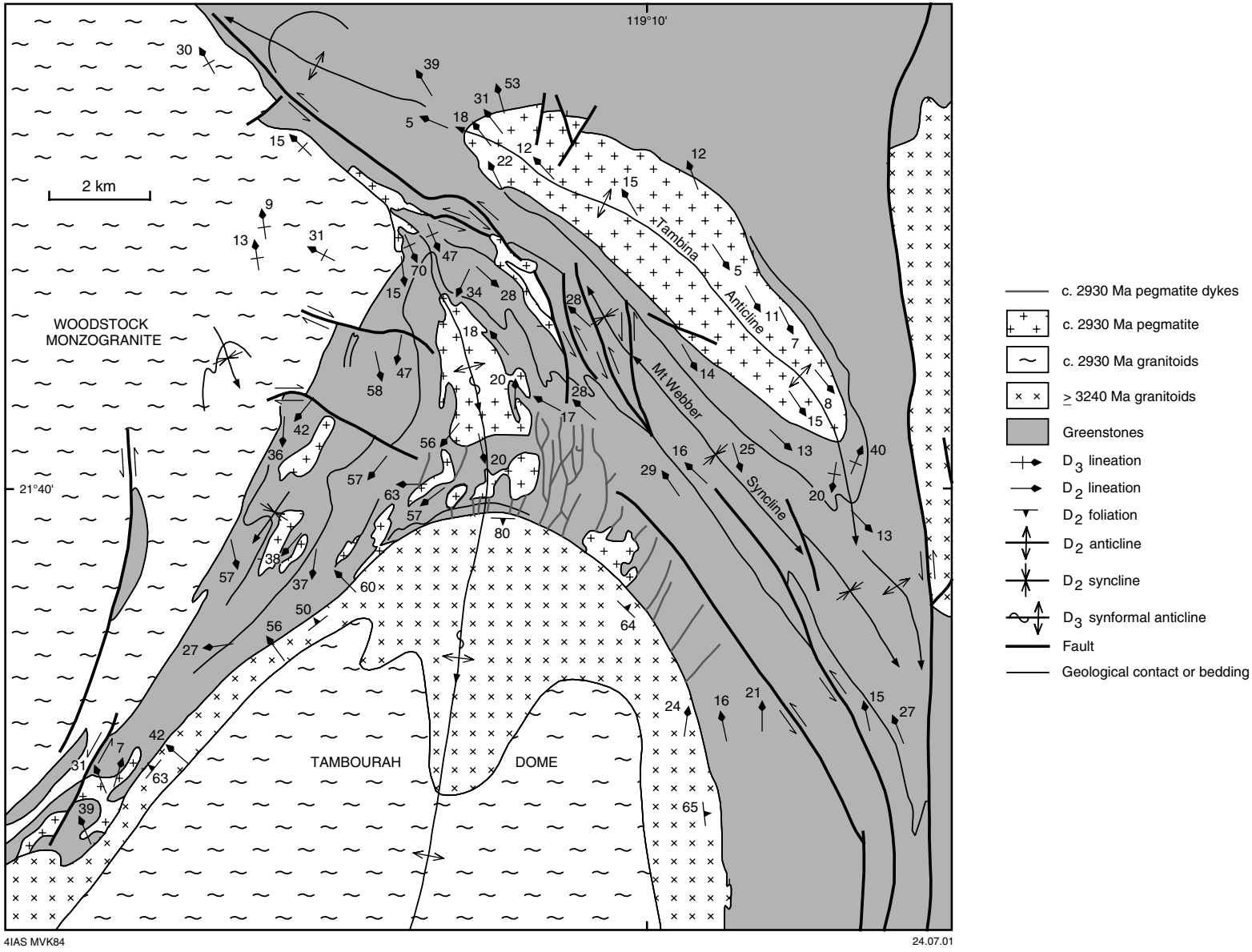

Figure 71. Structural geology around the hinge region of the Tambourah Dome

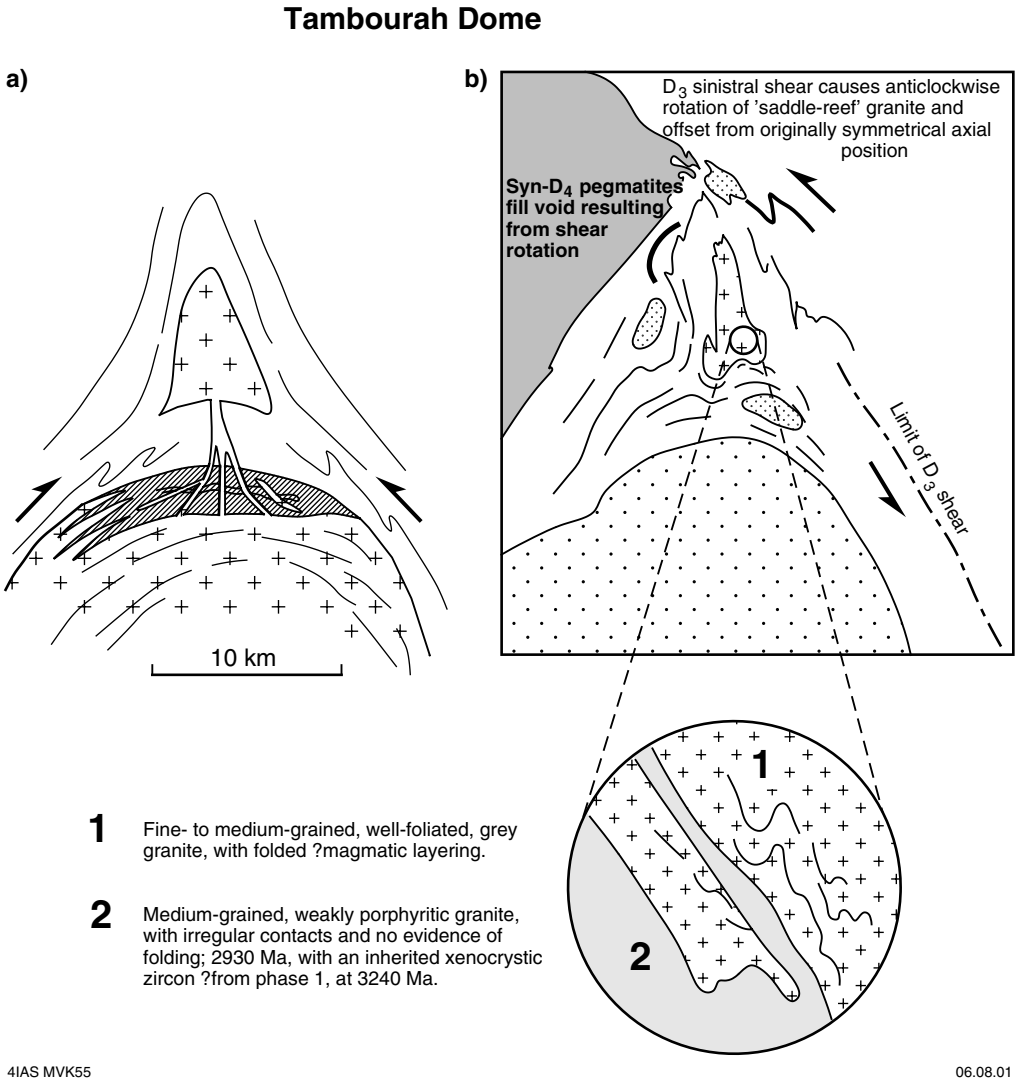

Figure 72. Structures associated with formation of the Tambourah Dome at c. 2930 Ma: a) folding of greenstones around the nose of the dome and synkinematic intrusion of the saddle-reef granite that was fed by granite dykes along the axial plane of the dome. Enlarged sketch shows relationships between two phases of the saddle-reef granite, both of which have identical ages of c. 2933 Ma; b) schematic geological sketch showing the intrusion of small pegmatitic granitoid bodies into dilatational gaps formed as a result of rotation of the saddle-reef granite due to a late component of sinistral shear along the Pulcunnah Shear Zone

track for 4.9 km, park the vehicles and walk south of the track for about 150 m to a low outcrop.

The Tambourah Dome forms the eastern lobe of the Yule Granitoid Complex, from which it is separated by a train of greenstone xenoliths. The dome is primarily composed of undeformed, late, very coarse grained, but irregular, granite pegmatite, which was intrusive into fine- to medium-grained grey granite and gneiss. However, at this locality in the nose of the dome, the relationships between earlier phases of granitoid rocks are preserved.

At this locality, three phases of granitoid rocks may be observed (Fig. 71). The oldest is a migmatitic, weakly porphyritic quartz diorite whose gneissosity parallels a sheeted

intrusive contact with amphibolite-facies metabasalts. The gneisses from this locality have been dated at c. 3420 Ma (Van Kranendonk, M., unpublished data). The second phase is a foliated, medium-grained grey granite that intrudes the gneisses as a series of subparallel, sheeted sills. One of the sheets from this locality was dated at c. 3240 Ma, the same age as the Strelley Granite and upper part of the Sulphur Springs Group (Van Kranendonk, M., unpublished data). These foliated granite sheets cut across the gneissosity in the older rocks at a progressively higher angle approaching the nose of the dome, suggesting emplacement during an early component of doming (Fig. 71).

A north-trending subvertical granite dyke cuts across both earlier phases in the nose of the dome at the western end of the platform, and represents one of a swarm of feeder dykes to a triangular-shaped granite occupying the saddle-reef position in the hinge of folded greenstones around the nose of the Tambourah Dome (Fig. 72). Two dates on distinctive phases of the saddle-reef granite returned ages of c. 2933 ± 3 Ma (Nelson, 1998; Van Kranendonk, M., unpublished data), with inherited cores dated at 3240, c. 3310, and c. 3400 Ma, and some older than 3500 Ma.

Thus, in this outcrop, we see evidence for the progressive formation of a dome, through three stages:

- Stage 1: intrusion of TTG as sills into greenstones.
- Stage 2: partial doming during granitoid intrusion (at c. 3240 Ma).
- Stage 3: amplification of the dome during regional compression at c. 2930 Ma.

Backtrack the 4.9 km to the Hillside Track and turn right. Drive for 31.8 km to the BHP iron ore railway and cross over it, continuing west for another 8.5 km to the Great Northern Highway. Take out the hubs and put the vehicles into two-wheel drive, increasing tyre pressure if necessary. Turn right and drive to Port Hedland, a distance of 156 km.

References

AMELIN, Y., LEE, D.-C., and HALLIDAY, A. N., 2000, Early–middle Archaean crustal evolution deduced from Lu–Hf and U–Pb isotopic studies of single zircon grains: Geochimica et Cosmochimica Acta, v. 64, p. 4205–4225.

ARNDT, N. T., KERR, A. C., and TARNEY, J., 1997, Dynamic melting in plume heads: the formation of Gorgona komatiites and basalts: Earth and Planetary Science Letters, v. 146, p. 289–301.

ARNDT, N. T., NELSON, D. R., COMPSTON, W., TRENDALL, A. F., and THORNE, A. M., 1991, The age of the Fortescue Group, Hamersley Basin, Western Australia, from ion microprobe zircon U–Pb results: Australian Journal of Earth Sciences, v. 38, p. 261–281.

BARLEY, M. E., 1981, Relations between volcanic rocks in the Warrawoona Group: continuous or cyclic evolution?: Geological Society of Australia, Special Publication 7, p. 263–273.

BARLEY, M. E., 1997, The Pilbara Craton, *in* Greenstone belts *edited by* M. J. de WIT and L. ASHWAL: Clarendon Press, Oxford University Monographs on Geology and Geophysics, no. 35, p. 657–664.

BARLEY, M. E., DUNLOP, J. S. R., GLOVER, J. E., and GROVES, D. I., 1979, Sedimentary evidence for Archaean shallow-water volcanic-sedimentary facies, eastern Pilbara Block, Western Australia: Earth and Planetary Science Letters, v. 43, p. 74–84.

BARLEY, M. E., LOADER, S. E., and McNAUGHTON, N. J., 1998, 3430 to 3417 Ma calc-alkaline volcanism in the McPhee Dome and Kelley Belt, and growth of the eastern Pilbara Craton: Precambrian Research, v. 88, p. 3–24.

BARLEY, M. E., and PICKARD, A. L., 1999, An extensive, crustally-derived, 3325 to 3310 Ma silicic volcanoplutonic suite in the eastern Pilbara Craton: evidence from the Kelley Belt, McPhee Dome and Corunna Downs Batholith: Precambrian Research, v. 96, p. 41–62.

BICKLE, M. J., BETTENAY, L. F., BARLEY, M. E., CHAPMAN, H. J., GROVES, D. I., CAMPBELL, I. H., and de LAETER, J. R., 1983, A 3500 Ma plutonic and volcanic calc-alkaline province in the Archaean East Pilbara Block: Contributions to Mineralogy and Petrology, v. 84, p. 25–35.

BICKLE, M. J., BETTENAY, L. F., BOULTER, C. A., GROVES, D. I., and MORANT, P., 1980, Horizontal tectonic intercalation of an Archaean gneiss belt and greenstones, Pilbara Block, Western Australia: Geology, v. 8, p. 525–529.

BICKLE, M. J., BETTENAY, L. F., CHAPMAN, H. J, GROVES, D. I., McNAUGHTON, N. J., CAMPBELL, I. H., and de LAETER, J. R., 1989, The age and origin of younger granitic plutons of the Shaw batholith in the Archaean Pilbara Block, Western Australia: Contributions to Mineralogy and Petrology, v. 101, p. 361–376.

BICKLE, M. J., BETTENAY, L. F., CHAPMAN, H. J, GROVES, D. I., McNAUGHTON, N. J., CAMPBELL, I. H., and de LAETER, J. R., 1993, Origin of the 3500–3300 Ma calc-alkaline rocks in the Pilbara Archaean: isotopic and geochemical constraints from the Shaw Batholith. Precambrian Research, v. 60, p. 117–149.

BICKLE, M. J., MORANT, P., BETTENAY, L. F., BOULTER, C. A., BLAKE, T. S., and GROVES, D. I., 1985, Archaean tectonics of the Shaw Batholith, Pilbara Block, Western Australia: structural and metamorphic tests of the batholith concept, *in* Evolution of Archean Supracrustal Sequences *edited by* L. D. AYERS, P. C. THURSTON, K. D. CARD, and W. WEBER: Geological Association of Canada, Special Paper 28, p. 325–341.

BLAKE, T. S., 1993, Late Archaean crustal extension, sedimentary basin formation, flood basalt volcanism and continental rifting: the Nullagine and Mount Jope supersequences, Western Australia: Precambrian Research, v. 60, p. 185–241.

BLEWETT, R. S., 2000, North Pilbara 'Virtual' structural field trip: Australian Geological Survey Organisation, Record 2000/45.

BOULTER, C. A., BICKLE, M. J., GIBSON, B., and WRIGHT, R. K., 1987, Horizontal tectonics pre-dating upper Gorge Creek Group sedimentation, Pilbara Block, Western Australia: Precambrian Research, v. 36, p. 241–258.

BRAUHART, C., 1999, Regional alteration systems associated with Archean volcanogenic massive sulphide deposits at Panorama, Pilbara, Western Australia: University of Western Australia, PhD thesis (unpublished).

BRAUHART, C., GROVES, D. I., and MORANT, P., 1998, Regional alteration systems associated with volcanogenic massive sulphide mineralisation at Panorama, Pilbara, Western Australia: Economic Geology, v. 93, p. 292–302.

BUICK, R., and BARNES, K. R., 1984, Cherts in the Warrawoona Group: Early Archaean silicified sediments deposited in shallow-water environments, *in* Archaean and Proterozoic basins of the Pilbara, Western Australia: evolution and mineralization potential *edited by* J. R. MUHLING, D. I. GROVES, and T. S. BLAKE: University of Western Australia, Geology Department and University Extension, Publication no. 9, p. 37–53.

BUICK, R., and DOEPEL, M. G., 1999, Panorama VMS zinc–copper prospects, *in* Lead, zinc and silver deposits of Western Australia *compiled by* K. M. FERGUSON: Western Australia Geological Survey, Mineral Resources Bulletin 15, p. 80–86.

BUICK, R., and DUNLOP, J., 1990, Evaporitic sediments of early Archaean age from the Warrawoona Group, North Pole, Western Australia: Sedimentology, v. 37, p. 247–277.

BUICK, R., THORNETT, J. R., McNAUGHTON, N. J., SMITH, J. B., BARLEY, M. E., and SAVAGE, M., 1995, Record of emergent continental crust ~3.5 billion years ago in the Pilbara Craton of Australia: Nature, v. 375, p. 574–577.

CAMPBELL, I. H., GRIFFITHS, R. W., and HILL, R. I., 1989, Melting in an Archean mantle plume: heads it's basalts, tails it's komatiites: Nature, v. 339, p. 697–699.

CASANOVA, J., 1986, Les stromatolites continentaux: Paleoecologie, paleohydrologie, paleoclimatologie application au rift Gregory: Université d'aix-Marseilles, PhD thesis, (unpublished).

CHAMPION, D. C., and SMITHIES, R. H., 2000, The geochemistry of the Yule Granitoid Complex, East Pilbara Granite–Greenstone Terrane; evidence for early felsic crust; Western Australia Geological Survey, Annual Review 1999–2000, p. 42–48.

CHARDON, D., CHOUKROUNE, P., and JAYANANDA, M., 1996, Strain patterns, décollement and incipient sagducted greenstone terrains in the Archaean Dharwar craton (south India): Journal of Structural Geology, v. 18, p. 991–1004.

COLLINS, W. J., 1989, Polydiapirism of the Archaean Mt Edgar batholith, Pilbara Block, Western Australia: Precambrian Research, v. 43, p. 41–62.

COLLINS, W. J., 1993, Melting of Archaean sialic crust under high a_{H2O} conditions: genesis of 3300 Ma Na-rich granitoids in the Mount Edgar Batholith, Pilbara Block, Western Australia: Precambrian Research, v. 60, p. 151–174.

COLLINS, W. J., and GRAY, C. M., 1990, Rb–Sr isotopic systematics of an Archaean granite–gneiss terrain: The Mount Edgar batholith, Pilbara Block, Western Australia: Australian Journal of Earth Sciences, v. 37, p. 9–22.

COLLINS, W. J., and VAN KRANENDONK, M. J., 1999, Model for the development of kyanite during partial convective overturn of Archaean granite–greenstone terranes: the Pilbara Craton, Australia: Journal of Metamorphic Geology, v. 17, no. 2, p. 145–156.

COLLINS, W. J., VAN KRANENDONK, M. J., and TEYSSIER, C., 1998, Partial convective overturn of Archaean crust in the east Pilbara Craton, Western Australia: driving mechanisms and tectonic implications: Journal of Structural Geology, v. 20, p. 1405–1424.

COOPER, J. A., JAMES, P. R., and RUTLAND, R. W. R., 1982, Isotopic dating and structural relationships of granitoids and greenstones in the eastern Pilbara, Western Australia: Precambrian Research, v. 18, p. 199–236.

CRAIG, J. R., and VAUGHAN, D. J., 1981, Ore microscopy and ore petrography: John Wiley and Sons, 406p.

CULLERS, R. L., DiMARCO, M. J., LOWE, D. R., and STONE, J., 1993, Geochemistry of a silicified, felsic volcaniclastic suite from the early Archaean Panorama Formation, Pilbara Block, Western Australia: an evaluation of depositional

and post-depositional processes with special emphasis on the rare-earth elements: Precambrian Research, v. 60, p. 99–116.

DAVIDS, C., WIJBRANS, J. R., and WHITE, S. H., 1997, $^{40}Ar/^{39}Ar$ laserprobe ages of metamorphic hornblendes from the Coongan Belt, Pilbara, Western Australia: Precambrian Research, v. 83, p. 221–242.

DAWES, P. R., SMITHIES, R. H., CENTOFANTI, J., and PODMORE, D. C., 1995, Sunrise Hill unconformity: a newly discovered regional hiatus between Archaean granites and greenstones in the northeastern Pilbara Craton: Australian Journal of Earth Sciences, v. 42, p. 635–639.

DELOR, C., BURG, J.-P., and CLARKE, G., 1991, Relations diapirisme–metamorphisme dans la Province du Pilbara (Australie-occidentale): implications pour les régimes thermiques et tectoniques à la Archéen: Comptes Rendus de l'Academie des Sciences Paris, v. 312, p. 257–263.

de VRIES, S. T., 1999, Sedimentology, deformation and felsic volcanism of the Early Archaean Buck Ridge Chert Complex, Upper Onverwacht Group, Barberton Greenstone Belt, South Africa: the Netherlands, Utrecht University, MSc thesis (unpublished).

De WIT, M. J., 1982, Gliding and overthrust nappe tectonics in the Barberton Greenstone Belt: Journal of Structural Geology, v. 4, p. 117–136.

De WIT, M. J., 1998, On Archean granites, greenstones, cratons and tectonics: does the evidence demand a verdict?: Precambrian Research, v. 91, p. 181–226.

De WIT, M. J., ROERING, C., HART, R. J., ARMSTRONG, R. A., de RONDE, C. E. J., GREEN, R. W. E., TREDOUX, M., PEBERDY, E., and HART, R. A., 1992, Formation of an Archaean continent: Nature, v. 357, p. 553–562.

DiMARCO, M. J., and LOWE, D. R., 1989, Stratigraphy and sedimentology of an Early Archean felsic volcanic sequence, Eastern Pilbara Block, Western Australia, with special reference to the Duffer Formation and implications for crustal evolution: Precambrian Research, v. 44, p. 147–169.

DIXON, J. M., and SUMMERS, J. M., 1983, Patterns of total and incremental strain in subsiding troughs: experimental centrifuged models of inter-diapir synclines: Canadian Journal of Earth Sciences, v. 20, p. 1843–1861.

DOSTAL, J., and MUELLER, W. U., 1997, Komatiite flooding of a rifted Archean rhyolitic arc complex: Geochemical signature and tectonic significance of the Stoughton-Roquemaure Group, Abitibi Greenstone Belt, Canada: Journal of Geology, v. 105, p. 545–563.

ERIKSSON, K. A., KRAPEZ, B., and FRALICK, P., 1994, Archean sedimentation: Earth-Science Reviews, v. 37, p. 1–88.

FARMER, J. D., 2000, Hydrothermal systems: Doorways to Early Biosphere Evolution: GSA Today, v. 10(7), p. 1–9.

GLIKSON, A. Y., and HICKMAN, A. H., 1981, Geochemistry of Archaean volcanic successions, eastern Pilbara Block, Western Australia: Australia BMR, Record 1981/36, 83p.

GLIKSON, A. Y., DAVY, R., and HICKMAN, A. H., 1986, Geochemical data files of Archaean volcanic rocks, Pilbara Craton, Western Australia: Australia BMR, Record 1986/14, 12p.

GLIKSON, A. Y., DAVY, R., HICKMAN, A. H., PRIDE, C., and JAHN, B., 1987, Trace elements geochemistry and petrogenesis of Archaean felsic igneous units, Pilbara Block, Western Australia: Australia BMR, Record 1987/30, 63p.

GREEN, M. G., SYLVESTER, P. J., and BUICK, R., 2000, Growth and recycling of early Archaean continental crust: geochemical evidence from the Coonterunah and Warrawoona Groups, Pilbara Craton, Australia: Tectonophysics, v. 322, p. 69–88.

GROVES, D. I., DUNLOP, J. S. R., and BUICK, R., 1981, An early habitat of life: Scientific American, v. 245, p. 64–73.

GRUAU, G., JAHN, B.-M., GLIKSON, A. Y., DAVY, R., HICKMAN, A. H., and CHAUVEL, C., 1987, Age of the Archaean Talga-Talga subgroup, Pilbara Block, Western Australia, and early evolution of the mantle: new Sm–Nd isotopic evidence: Earth and Planetary Science Letters, v. 85, p. 105–116.

GRIFFIN, T. J., 1990, North Pilbara granite–greenstone terrane, *in* Geology and mineral resources of Western Australia: Western Australia Geological Survey, Memoir 3, p. 128–158.

HAMILTON, P. J., EVENSEN, N. M., O'NIONS, R. K., GLIKSON, A. Y., and HICKMAN, A. H., 1981, Sm–Nd dating of the North Star basalt, Warrawoona Group, Pilbara Block, Western Australia: *in* Archaean geology *edited by* J. E. GLOVER and D. I. GROVES: Geological Society of Australia, Special Publication 7, p. 187–192.

HAMILTON, W. B., 1998, Archean magmatism and deformation were not products of plate tectonics: Precambrian Research, v. 91, p. 143–180.

HICKMAN, A. H., 1975, Precambrian structural geology of part of the Pilbara region: Western Australia Geological Survey, Annual Report 1974, p. 68–73.

HICKMAN, A. H., 1977, New and revised definitions of the Warrawoona Group, Pilbara Block: Western Australia Geological Survey, Annual Report 1976, p. 53.

HICKMAN, A. H., 1980. Excursion Guide — Archaean geology of the Pilbara Block: Geological Society of Australia (W.A. Division), Second International Archaean Symposium, 55p.

HICKMAN, A. H., 1983, Geology of the Pilbara Block and its environs: Western Australia Geological Survey, Bulletin 127, 268p.

HICKMAN, A. H., 1984, Archaean diapirism in the Pilbara Block, Western Australia, *in* Precambrian Tectonics Illustrated *edited by* A. KRÖNER and R. GREILING: Stuttgart, E. Schweizerbarts'che Verlagsbuchhandlung, p. 113–127.

HICKMAN, A. H., 1990, Geology of the Pilbara Craton, *in* Third International Archaean Symposium, Excursion Guidebook No. 5: Pilbara and Hamersley Basin *edited by* S. E. HO, J. E. GLOVER, J. S. MYERS, and J. R. MUHLING: University of Western Australia, Geology Department and University Extension, Publication no. 21, p. 2–13.

HICKMAN, A. H., 1997, A revision of the stratigraphy of Archaean greenstone successions in the Roebourne–Whundo area, west Pilbara: Western Australia Geological Survey, Annual Review 1996–97, p. 76–82.

HICKMAN, A. H., 2001, East Pilbara diapirism: new evidence from mapping, *in* GSWA extended abstracts: new data for WA explorers: Western Australia Geological Survey, Record 2001/5, p. 23–25.

HICKMAN, A. H., and LIPPLE, S. H., 1978, Marble Bar, W.A. Sheet SF 50-8: Western Australia Geological Survey, 1:250 000 Geological Series.

HICKMAN, A. H., SMITHIES, R. H., PIKE, G., FARRELL, T. R., and BEINTEMA, K. A., 2001, Evolution of the West Pilbara Granite–Greenstone Terrane and Mallina Basin, Western Australia — a field guide: Western Australia Geological Survey, Record 2001/16.

HILL, R. M., 1997, Stratigraphy, structure and alteration of hanging wall sedimentary rocks at the Sulphur Springs volcanogenic massive sulphide (VMS) prospect, east Pilbara Craton, Western Australia: University of Western Australia, BSc Honours thesis (unpublished).

HOFFMAN, H. J., GREY, K., HICKMAN, A. H., and THORPE, R., 1999, Origin of 3.45 Ga coniform stromatolites in Warrawoona Group, Western Australia: Geological Society of America, Bulletin, v. 111, p. 1256–1262.

HORWITZ, R. C., and KRAPEZ, B., 1991, A new proposal for subdivision of the pre- Mount Bruce Supergroup, Archaean supracrustal rocks of the Pilbara Craton: Australia CSIRO Division of Exploration Geoscience, Exploration Research News 5, p. 10–11.

HORWITZ, R., and PIDGEON, R. T., 1993, 3.1 Ga tuff from the Scholl Belt in the west Pilbara: further evidence for diachronous volcanism in the Pilbara Craton: Precambrian Research, v. 60, p. 175–183.

JACKSON, M. P. A., CORNELIUS, R. R., CRAIG, C. H., GANSSER, A., STOCKLIN, J., and TALBOT, C. J., 1990, Salt diapirs of the Great Kavir, Central Iran: Geological Society of America, Memoir 177, 139p.

JONES, C. B., 1990, Coppin Gap copper–molybdenum prospect, *in* Geology of the mineral deposits of Australia and Papua New Guinea, Volume 1 *edited by* F. E. HUGHES: Australasian Institute of Mining and Metallurgy, Monograph 14, p. 141–144.

JONES, B., and RENAUT, R. W., 1996, Morphology and growth of aragonite crystals in hot-spring travertines at Lake Bogoria, Kenya Rift Valley: Sedimentology, v. 43, p. 323–340.

JONES, B., RENAUT, R. W., and ROSEN, M. R., 1997, Vertical zonation of biota in microstromatolites with hot springs, North Island, New Zealand: Palaios, v. 12, p. 220–236.

KINNY, P. D., 2000, U–Pb dating of rare-metal (Sn–Ta–Li) mineralized pegmatites in Western Australia by SIMS analysis of tin and tantalum-bearing ore minerals: Beyond 2000, New Frontiers in Isotope Geoscience, Lorne, Victoria, 2000, Abstracts and Proceedings, p. 113–116.

KIYOKAWA, S., and TAIRA, A., 1998, The Cleaverville Group in the west Pilbara coastal granite–greenstone terrane of Western Australia: an example of a mid-Archaean immature oceanic island-arc succession: Precambrian Research, v. 88, p. 102-142.

KRAPEZ, B., 1984, Sedimentation in a small, fault-bounded basin: the Lalla Rookh sandstone, east Pilbara Block, *in* Archaean and Proterozoic basins of the Pilbara, Western Australia : evolution and mineralization potential *edited by* J. R. MUHLING, D. I. GROVES, and T. S. BLAKE: University of Western Australia, Geology Department and University Extension, Publication 9, p. 89–110.

KRAPEZ, B., 1993, Sequence stratigraphy of the Archaean supracrustal belts of the Pilbara Block, Western Australia: Precambrian Research, v. 60, p. 1–45.

KRAPEZ, B., and BARLEY, M. E., 1987, Archaean strike-slip faulting and related ensialic basins: evidence from the Pilbara Block, Australia: Geological Magazine, v. 124, p. 555–567.

KRAPEZ, B., and EISENLOHR, B., 1998, Tectonic settings of Archaean (3325-2775 Ma) crustal–supracrustal belts in the West Pilbara Block: Precambrian Research, v. 88, p. 173-205.

LOWE, D. R., 1983, Restricted shallow-water sedimentation of Early Archaean stromatolitic and evaporitic strata of the Strelley Pool Chert, Pilbara Block, Western Australia: Precambrian Research, v. 19, p. 239–283.

LOWE, D. R., 1994, Abiological origin of described stromatolites older than 3.2 Ga: Geology, v. 22, p. 387–390.

LOWE, D. R., and FISHER WORRELL, G., 1999, Sedimentology, mineralogy, and implications of silicified evaporites in the Kromberg Formation, Barberton Greenstone Belt, South Africa: *in* Geologic evolution of the Barberton Greenstone Belt, South Africa *edited by* D. R. LOWE and G. H. BYERLY: Geological Society of America, Special Paper 329, p. 167–188.

McNAUGHTON, N. J., COMPSTON, W., and BARLEY, M. E., 1993, Constraints on the age of the Warrawoona Gp, eastern Pilbara Block, Western Australia: Precambrian Research, v. 60, p. 69–98.

McNAUGHTON, N. J., GREEN, M. D., COMPSTON, W., and WILLIAMS, I. S., 1988, Are anorthositic rocks basement to the Pilbara Craton?; Geological Society of Australia, Abstracts v. 21, p. 272–273.

MARESCHAL, J.-C., and WEST, G. F., 1980, A model for Archean tectonism. Part 2. Numerical models of vertical tectonism in greenstone belts: Canadian Journal of Earth Sciences, v. 17, p. 60–71.

MARSTON, R. J., 1979, Copper mineralization in Western Australia: Western Australia Geological Survey, Mineral Resources Bulletin 13, p. 73.

MORANT, P., 1998, Panorama zinc–copper deposits: Australasian Institute of Mining and Metallurgy, Monograph 22, p. 287–292.

NELSON, D. R., 1996, Compilation of SHRIMP U–Pb zircon geochronology data, 1995: Western Australia Geological Survey, Record 1996/5, 168p.

NELSON, D. R., 1997, Compilation of SHRIMP U–Pb zircon geochronology data, 1996: Western Australia Geological Survey, Record 1997/2, 189p.

NELSON, D. R., 1998, Compilation of SHRIMP U–Pb zircon geochronology data, 1997: Western Australia Geological Survey, Record 1998/2, 242p.

NELSON, D. R., 1999, Compilation of geochronology data, 1998: Western Australia Geological Survey, Record 1999/2, 222p.

NELSON, D. R., 2000, Compilation of geochronology data, 1999: Western Australia Geological Survey, Record 2000/2, 251p.

NELSON, D. R., in prep., Compilation of geochronology data, 2000: Western Australia Geological Survey, Record 2001/2.

NEUMAYR, P., GROVES, D. I., RIDLEY, J. R., and KONING, C. D., 1993, Syn-amphibolite facies Archaean lode gold mineralisation in the Mt York District, Pilbara Block, Western Australia: Mineralium Deposita, v. 28, p. 457–468.

NIJMAN, W., 1999, Growth structures: examples of integrated sedimentological and structural–geological basin analysis: The Netherlands, Utrecht University, Geologica Ultraiectina, v. 173, 48p. and CD.

NIJMAN, W. and de VRIES, S. T., 2001, Collapse structures in the Early Earth and planetary equivalents, *in* Lunar and Planetary Science XXXII, Abstract 1289, Lunar and Planetary Institute, Houston (CD-ROM).

NIJMAN, W., de BRUIJNE, C. H., and VALKERING, M. E., 1998a, Growth fault control of Early Archaean cherts, barite mounds and chert–barite veins, North Pole Dome, Eastern Pilbara, Western Australia: Precambrian Research, v. 88, p. 25–52.

NIJMAN, W., de BRUIJNE, C. H., and VALKERING, M. E., 1999a, Growth fault control of Early Archaean cherts, barite mounds and chert–barite veins, North Pole Dome, Eastern Pilbara, Western Australia: (Erratum to article in Precambrian Research, v. 88, p. 25–52) Precambrian Research, v. 95, p. 247–274.

NIJMAN, W., WILLIGERS, B. A., and KRIKKE, A., 1998b, Tensile and compressive growth structures: relationships between sedimentation, deformation and granite intrusion in the Archaean Coppin Gap greenstone belt, Eastern Pilbara, Western Australia: Precambrian Research, v. 88, p. 83–107.

NIJMAN, W., WILLIGERS, B. A., and KRIKKE, A., 1999b, Tensile and compressive growth structures: relationships between sedimentation, deformation and granite intrusion in the Archaean Coppin Gap greenstone belt, Eastern Pilbara, Western Australia: (Erratum to article in Precambrian Research, v. 88, p. 83–107) Precambrian Research, v. 95, p. 277–302.

OHTA, H., MARUYAMA, S., TAKAHASHI, E., WATANABE, Y., and KATO, Y., 1996, Field occurrence, geochemistry and petrogenesis of the Archaean Mid-Oceanic Ridge Basalts (A-MORBs) of the Cleaverville area, Pilbara Craton, Western Australia: Lithos, v. 37, p. 199-221.

PHILIPS, R. J., and HANSEN, V. J., 1994, Tectonic and magmatic evolution of Venus: Annual Review of Earth and Planetary Sciences, v. 22, p. 597–654.

PIDGEON, R. T., 1978, 3450 M.y. old volcanics in the Archaean layered greenstone succession of the Pilbara Block, Western Australia: Earth and Planetary Science Letters, v. 37, p. 423–428.

PIDGEON, R. T., 1984, Geochronological constraints on early volcanic evolution of the Pilbara Block, Western Australia: Australian Journal of Earth Sciences, v. 31, p. 237–242.

PODMORE, D. C., 1990, Shay Gap – Sunrise Hill and Nimingarra iron ore deposits, *in* Geology of the mineral deposits of Australia and Papua New Guinea, Volume 1, *edited by* F. E. HUGHES: Australasian Institute of Mining and Metallurgy, Monograph 14, p.137–140.

RASMUSSEN, B., 2000, Filamentous microfossils in a 3,235-million-year-old volcanogenic massive sulphide deposit: Nature, v. 405, p. 676–679.

RENAUT, R. W., and JONES, B., 1997, Controls on aragonite and calcite precipitation in hot spring travertines at Chemurkeu, Lake Bogoria, Kenya: Canadian Journal of Earth Sciences, v. 34, p. 801–818.

SIGUTANI, K., 1992, Geochemical characteristics of Archean cherts and other sedimentary rocks in the Pilbara Block, Western Australia: evidence for Archean seawater enriched in hydrothermally derived iron and silica: Precambrian Research, v. 57, p. 21–47.

SMITH, J. B., BARLEY, M. E., GROVES, D. I., KRAPEZ, B., McNAUGHTON, N. J., BICKLE, M. J., and CHAPMAN, H. J., 1998, The Sholl Shear Zone, West Pilbara; evidence for a domain boundary structure from integrated

tectonostratigraphic analysis, SHRIMP U–Pb dating and isotopic and geochemical data of granitoids: Precambrian Research, v. 88, p. 143–172.

SMITHIES, R. H., 2000, The Archaean tonalite-trondhjemite-granodiorite (TTG) series is not an analogue of Cenozoic adakite: Earth and Planetary Science Letters, v. 182, p. 115–125.

SUN, S-S., and HICKMAN, A. H., 1998, New Nd-isotopic and geochemical data from the west Pilbara: implications for Archaean crustal accretion and shear zone development: Australian Geological Survey Organisation, Research Newsletter, no. 28, p. 25–29.

TEYSSIER, C., and COLLINS, W. J., 1990, Strain and kinematics during the emplacement of the Mount Edgar Batholith and Warrawoona Syncline, Pilbara Block, Western Australia, *in* Third International Archaean Symposium, Extended Abstracts Volume *compiled by* J. E. GLOVER, and S. E. HO: Perth, Western Australia, Geoconferences (W.A.) Inc., p. 481–483.

THORNE, A. M., and TRENDALL, A. F., 2001, The geology of the Fortescue Group, Hamersley Basin, Western Australia: Western Australia Geological Survey, Bulletin 144, 249p.

THORPE, R. I., HICKMAN, A. H., DAVIS, D. W., MORTENSEN, J. K., and TRENDALL, A. F., 1992a, U–Pb zircon geochronology of Archaean felsic units in the Marble Bar region, Pilbara Craton, Western Australia: Precambrian Research, v. 56, p. 169–189.

THORPE, R. I., HICKMAN, A. H., DAVIS, D. W., MORTENSEN, J. K., and TRENDALL, A. F., 1992b, Constraints to models for Archaean lead evolution from precise U–Pb geochronology from the Marble Bar region, Pilbara Craton, Western Australia, *in* The Archaean: Terrains, processes and metallogeny *edited by* J. E. GLOVER and S. E. HO: University of Western Australia, Geology Department and University Extension, Publication no. 22, p. 395–408.

TOMLINSON, K. Y., HUGHES, D. J., THURSTON, P. C., and HALL, R. P., 1999, Plume magmatism and crustal growth at 2.9 to 3.0 Ga in the Steep Rock and Lumby lake area, Western Superior Province: Lithos, v. 46, p. 103–136.

TYLER, I. M., FLETCHER, I. R., de LAETER, J. R., WILLIAMS, I. R., and LIBBY, W. G., 1992, Isotope and rare earth element evidence for a late Archaean terrane boundary in the southeastern Pilbara Craton, Western Australia: Precambrian Research, v. 54, p. 211–229.

van HAAFTEN, W. M., and WHITE, S. H., 1998, Evidence for multiphase deformation in the Archean basal Warrawoona Group in the Marble Bar area, East Pilbara, Western Australia: Precambrian Research v. 88, p. 53–66.

van HAAFTEN, W. M., and WHITE, S. H., 2001, Reply to comment on 'Evidence for multiphase deformation in the Archaean basal Warrawoona Group in the Marble Bar area, East Pilbara , Western Australia' by M. J. VAN KRANENDONK, A. H. HICKMAN, and W. J. COLLINS: Precambrian Research v. 105, p. 79–84.

VAN KRANENDONK, M. J., 1997, Results of field mapping, 1994–1996, in the North Shaw and Tambourah 1:100 000 sheet areas, eastern Pilbara Craton, northwestern Australia: Australian Geological Survey Organisation, Record 1997/23, 44p.

VAN KRANENDONK, M. J., 1998a, Spatially and temporally distinct episodes of vertical and horizontal tectonics in the evolution of the Archaean Pilbara Craton, Western Australia, *in* 14th International Conference on Basement Tectonics, Ouro Preto, Brazil, 1998, Abstracts volume, p. 145–148.

VAN KRANENDONK, M. J., 1998b, Litho-tectonic and structural map components of the North Shaw 1:100 000 sheet, Archaean Pilbara Craton: Western Australia Geological Survey, Annual Review 1997–98, p. 63–70.

VAN KRANENDONK, M. J., 1999a, North Shaw, W.A. Sheet 2755: Western Australia Geological Survey, 1:100 000 Geological Series.

VAN KRANENDONK, M. J., 1999b, Two-stage degassing of the Archaean mantle: evidence from the 3.46 Ga Panorama volcano, Pilbara Craton, Western Australia, *in* GSWA '99 extended abstracts: new geological data for WA explorers: Western Australia Geological Survey, Record 1999/6, p. 1–3.

VAN KRANENDONK, M. J., 2000a, Geology of the North Shaw 1:100 000 sheet: Western Australia Geological Survey, 1:100 000 Geological Series Explanatory Notes, 86p.

VAN KRANENDONK, M. J., 2000b, Evidence of thick Archaean crust in the East Pilbara, *in* GSWA 2000 extended abstracts: new geological data for WA explorers in the new millenium: Western Australia Geological Survey, Record 2000/8, p. 1–3.

VAN KRANENDONK, M. J., in prep. a, Volcanic degassing, hydrothermal circulation and the flourishing of life on Earth: New evidence from the c. 3.46 Ga Warrawoona Group, Pilbara Craton, Western Australia: Precambrian Research.

VAN KRANENDONK, M. J., in prep. b, A hydrothermal setting for Early Archaean (3.43 Ga) stromatolites of the Strelley Pool Chert, Pilbara Craton, Western Australia: Geological Society of America, Bulletin.

VAN KRANENDONK, M.J., in prep. c, Tambourah, W.A. Sheet 2754: Western Australia Geological Survey, 1:100 000 Geological Series.

VAN KRANENDONK, M. J., and COLLINS, W. J., 1995, Lateral escape tectonics during c. 3200 Ma collisional orogeny following 3300 Ma extensional core complex formation in the eastern part of the Archaean Pilbara Craton, NW Australia: Geological Society of Australia, Abstracts, no. 40, p. 166–167.

VAN KRANENDONK, M. J., and COLLINS, W. J., 1998, Timing and tectonic significance of Late Archaean, sinistral strike-slip deformation in the Central Pilbara Structural Corridor, Pilbara Craton, Western Australia: Precambrian Research, v. 88, p. 207–232.

VAN KRANENDONK, M. J., and COLLINS, W. J., in prep., Partial convective overturn of the eastern part of the Archaean Pilbara Craton, Western Australia: Field evidence for the diapiric emplacement of domical granitoid complexes: Precambrian Research.

VAN KRANENDONK, M. J., and HICKMAN, A. H., 2000, Archaean geology of the North Shaw region, East Pilbara Granite–Greenstone Terrain, Western Australia — a field guide: Western Australia Geological Survey, Record 2000/5, 64p.

VAN KRANENDONK, M. J., HICKMAN, A. H., and COLLINS, W. J., 2001, Evidence for multiphase deformation in the Archaean basal Warrawoona Group in the Marble Bar area, East Pilbara, Western Australia: Precambrian Research, v. 105, p. 73–78.

VAN KRANENDONK, M. J., HICKMAN, A. H., SMITHIES, R. H., NELSON, D. R., and PIKE, G., in prep., Geology and tectonic evolution of the Archaean North Pilbara Terrain, Pilbara Craton, Western Australia: Economic Geology.

VAN KRANENDONK, M. J., and MORANT, P., 1998, Revised Archaean stratigraphy of the North Shaw 1:100 000 sheet, Pilbara Craton: Western Australia Geological Survey, Annual Review 1997-98, p. 55–62.

VEARNCOMBE, S., 1996, Volcanogenic massive sulphide–sulphate mineralisation at Strelley, Pilbara Craton, Western Australia: University of Western Australia, PhD thesis (unpublished).

VEARNCOMBE, S., and KERRICH, R., 1999, Geochemistry and geodynamic setting of volcanic and plutonic rocks associated with Early Archaean volcanogenic massive sulphide mineralization, Pilbara Craton: Precambrian Research, v. 98, p. 243–270.

VEARNCOMBE, S., BARLEY, M. E., GROVES, D. I., McNAUGHTON, N. J., MIKUCKI, E. J., and VEARNCOMBE, J. R., 1995, 3.26 Ga black smoker-type mineralization in the Strelley Belt, Pilbara Craton, Western Australia: London, Journal of the Geological Society, v. 152, p. 587–590.

VEARNCOMBE, S., VEARNCOMBE, J. R., and BARLEY, M. E., 1998, Fault and stratigraphic controls on volcanogenic massive sulphide deposits in the Strelley Belt, Pilbara Craton, Western Australia: Precambrian Research, v. 88, p. 67–82.

VLAAR, N. J., VAN KEKEN, P. E., and VAN DEN BERG, A. P., 1994, Cooling of the Earth in the Archaean: Consequences of pressure-release melting in a hotter mantle: Earth and Planetary Science Letters, v. 121, p. 1–18

WELLMAN, P., 2000, Upper crust of the Pilbara Craton, Australia: 3D geometry of a granite–greenstone terrain: Precambrian Research, v. 104, p. 187–206.

WHITE, R. V., TARNEY, J., KERR, A. C., SAUNDERS, A. D., KEMPTON, P. D., PRINGLE, M. S., and KLAVER, G. T., 1999, Modification of an oceanic plateau, Aruba Dutch Caribbean: implications for the generation of continental crust: Lithos, v. 46, p. 43–68.

WIJBRANS, J. R., and McDOUGALL, I., 1987, On the metamorphic history of an Archaean granitoid greenstone terrane, East Pilbara, Western Australia, using the $^{40}Ar/^{39}Ar$ age spectrum technique: Earth and Planetary Science Letters, v. 84, p. 226–242.

WILHELMIJ, H. R., and DUNLOP, J. S. R., 1984, A genetic stratigraphic investigation of the Gorge Creek Group in the Pilgangoora syncline, *in* Archaean and Proterozoic Basins of the Pilbara, Western Australia: evolution and mineralisation potential *edited by* J. R. MUHLING, D. I. GROVES, and T. S. BLAKE: University of Western Australia, Geology Department and University Extension, Publication no. 9, p. 68–88.

WILLIAMS, I. R., 1999, Geology of the Muccan 1:100 000 sheet: Western Australia Geological Survey, 1:100 000 Geological Series Explanatory Notes, 39p.

WILLIAMS, I. R., 2000, Geology of the Cooragoora 1:100 000 sheet: Western Australia Geological Survey, 1:100 000 Geological Series Explanatory Notes, 23p.

WILLIAMS, I. R., 2001, Geology of the Warrawagine 1:100 000 sheet: Western Australia Geological Survey, 1:100 000 Geological Series Explanatory Notes, 34p.

WILLIAMS, I. R., and HICKMAN, A. H., 2000, Archaean geology of the Muccan region, East Pilbara Granite–Greenstone Terrane, Western Australia — a field guide: Western Australia Geological Survey, Record 2000/4, 30p.

WILLIAMS, I. S., and COLLINS, W. J., 1990, Granite–greenstone terranes in the Pilbara Block, Australia, as coeval volcano-plutonic complexes; evidence from U–Pb zircon dating of the Mount Edgar batholith: Earth and Planetary Science Letters, v. 97, p. 41–53.

WINGATE, M. T. D., 1999, Ion microprobe baddeleyite and zircon ages for Late Archaean mafic dykes of the Pilbara Craton, Western Australia: Australian Journal of Earth Sciences, v. 46, p. 493–500.

ZEGERS, T., 1996, Structural, kinematic and metallogenic evolution of selected domains of the Pilbara granitoid-greenstone terrain: Nederlands, Universiteit Utrecht, aculteit Aardwetenschappen, Geologica Ultraiectina 46.

ZEGERS, T. E., de KEIJZER, M., PASSCHIER, C. W., and WHITE, S. H., 1998, The Mulgandinnah shear zone; and Archean crustal-scale strike-slip zone, eastern Pilbara, Western Australia: Precambrian Research, v. 88, p. 233–248.

ZEGERS, T. E., WHITE, S. H., de KEIJZER, M., and DIRKS, P., 1996, Extensional structures during deposition of the 3460 Ma Warrawoona Group in the eastern Pilbara Craton, Western Australia: Precambrian Research, v. 80, p. 89–105.

ZEGERS, T. E., WIJBRANS, J., and WHITE, S. H., 1999, $^{40}Ar/^{39}Ar$ age constraints on tectonothermal events in the Shaw area of the eastern Pilbara granite–greenstone terrain (Western Australia): 700 Ma of Archaean tectonic evolution: Tectonophysics, v. 311, p. 45–81.

ZHOU, M.-F., ZHAO, T.-P., MALPAS, J., and SUN, M., 2000, Crustal-contaminated komatiitic basalts in Southern China: products of a Proterozoic mantle plume beneath the Yangtze Block: Precambrian Research, v. 103, p. 175–189.

VAN KRANENDONK et al.

Archaean geology of the East Pilbara Granite–Greenstone Terrane, Western Australia — a field guide

4IAS EXCURSION GUIDE

RECORD 2001/9

Further details of geological publications and maps produced by the Geological Survey of Western Australia can be obtained by contacting:

Information Centre
Department of Mineral and Petroleum Resources
100 Plain Street
East Perth WA 6004
Phone: (08) 9222 3459 Fax: (08) 9222 3444
www.dme.wa.gov.au

GSWA Record 2001/9, Plate 1
Geological map of the Coppin Gap greenstone belt

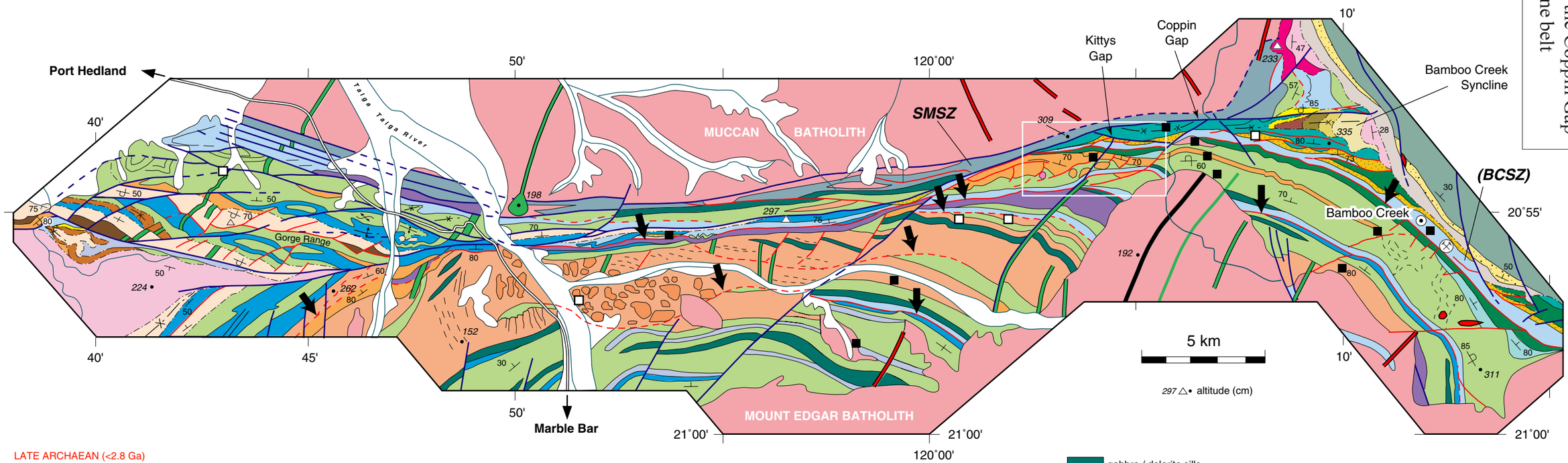

LATE ARCHAEAN (<2.8 Ga)

Fortescue Group

porphyry
basalts
sandstone
agglomerate

MIDDLE ARCHAEAN (2.8 - 3.3 Ga)

Gorge Creek Group (?): fill of Bamboo Creek Syncline

conglomerate
vesicular basalts

Gorge Creek Group: siliciclastic systems

IV black and white chert & conglomerate
III quartz / feldspathic arenite
II Fining-up fanglomerate and Fe-sandstone
I quartz arenite

LATE EARLY AND MIDDLE ARCHAEAN

Warrawoona Group and Gorge Creek Group in thrust-deformed hangingwall of BCSZ

BIF and siliciclastic base (Gorge Creek Group)

Interlayered, in places brecciated, silicified basalt with minor komatiite, chert, sandstone, and minor felsic volcanic rock, including slices of Wyman Formation age, (mainly upper Warrawoona Group)

silicified basalt (Warrawoona Group)

EARLY ARCHAEAN (> 3.3 Ga.)

Warrawoona Group

tuff, shale & ferruginous sst
sedimentary chert & silicified sst.
felsic volcanic rock, quartz-porphyry, & minor sst.
Panorama Formation

intermediate to felsic volcanic complex of Duffer Subgroup; in the central part, agglomerate, and *megabreccia of collapse or hydrothermal origin

(ferruginous) chert

basalt (predominant)

gabbro / dolerite sills
peridotite / serpentinite sills
ultramafic rocks, komatiite
intensly sheared, folded, and chemically altered (ultra)mafics: e.g. Bamboo Creek shear zone **(BCSZ)**

batholiths

Muccan and Mount Edgar batholiths
South Muccan shear zone **(SMSZ)**

dykes

2.8 Ga dolerite dykes
<2.8 Ga hornblende porphyry

fault systems

pre-2.8 Ga
syn- to post- 2.8 Ga

unconformities

tectonic discontinuities

White frame: Growth-fault structure of Figure 46
Available datings
U-Pb zircon datings in preparation

4IAS MVK57

19.07.01

Plate 1. **Geological map of the Coppin Gap greenstone belt (modified from Nijman et al., 1998a, 1999b). The greenstone belt is an asymmetrical synclinorium widening at both ends, with a well-preserved southern limb, but a severely sheared and reduced northern limb. The white frame indicates the growth-fault structure south of Kittys Gap (Locality 3.3). Black arrows indicate the anomalous stratigraphic and sheared contacts in the Warrawoona Group. The Kittys Gap growth structure is along the top of an intermediate to felsic volcanic complex with interlayered basalts, the bulk of which belongs to the Duffer Formation. Over the entire eastern and central part of the belt, this formation appears to have undergone early west-facing extension. Parts of these structures have been reactivated and inverted into east-facing thrusts during Gorge Creek Group deposition**

GSWA Record 2001/9, Plate 2
The Marble Bar Chert on the Coongan River

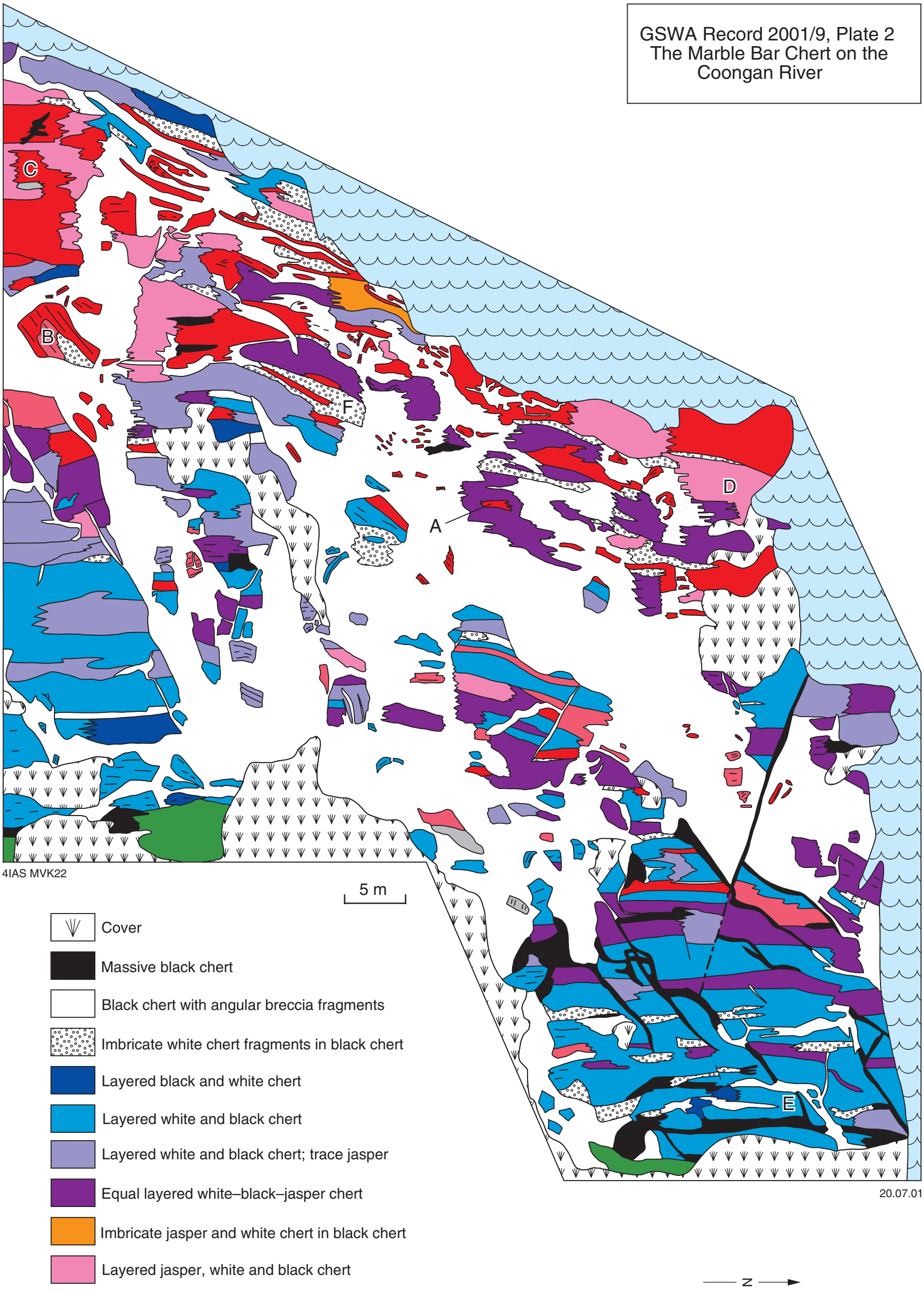

Plate 2. **Geological map of the Marble Bar Chert at Marble Bar Pool. Note the predominance of jasper in the top third of the unit, the extensive vein network of black hydrothermal-chert breccia, and the offset of the lower contact across a zone of massive black-chert breccia. Specific features of interest marked by circled letters: A = a relict core of layered jasper and white chert surrounded by white-and-red layered chert that has been invaded from all sides by black-chert sills; B = lateral invasion of jasper and white layered chert by black-chert sills emplaced from right to left; C = jagged contacts (at a high angle to bedding) between layered jasper – white chert and jasper – white-and-black chert as a result of invasion by black chert sills; D = progressive downward replacement of jasper by white-and-black chert, the latter emplaced by sideways intrusion of sills; E = a dense vein–sill complex of black chert with local development of imbricate structures, previously interpreted as conglomerates; F = imbricate white-chert fragments in black chert 'pseudoconglomerate' that passes along strike into black-chert breccia.**